BMR JOURNAL
OF AUSTRALIAN GEOLOGY & GEOPHYSICS

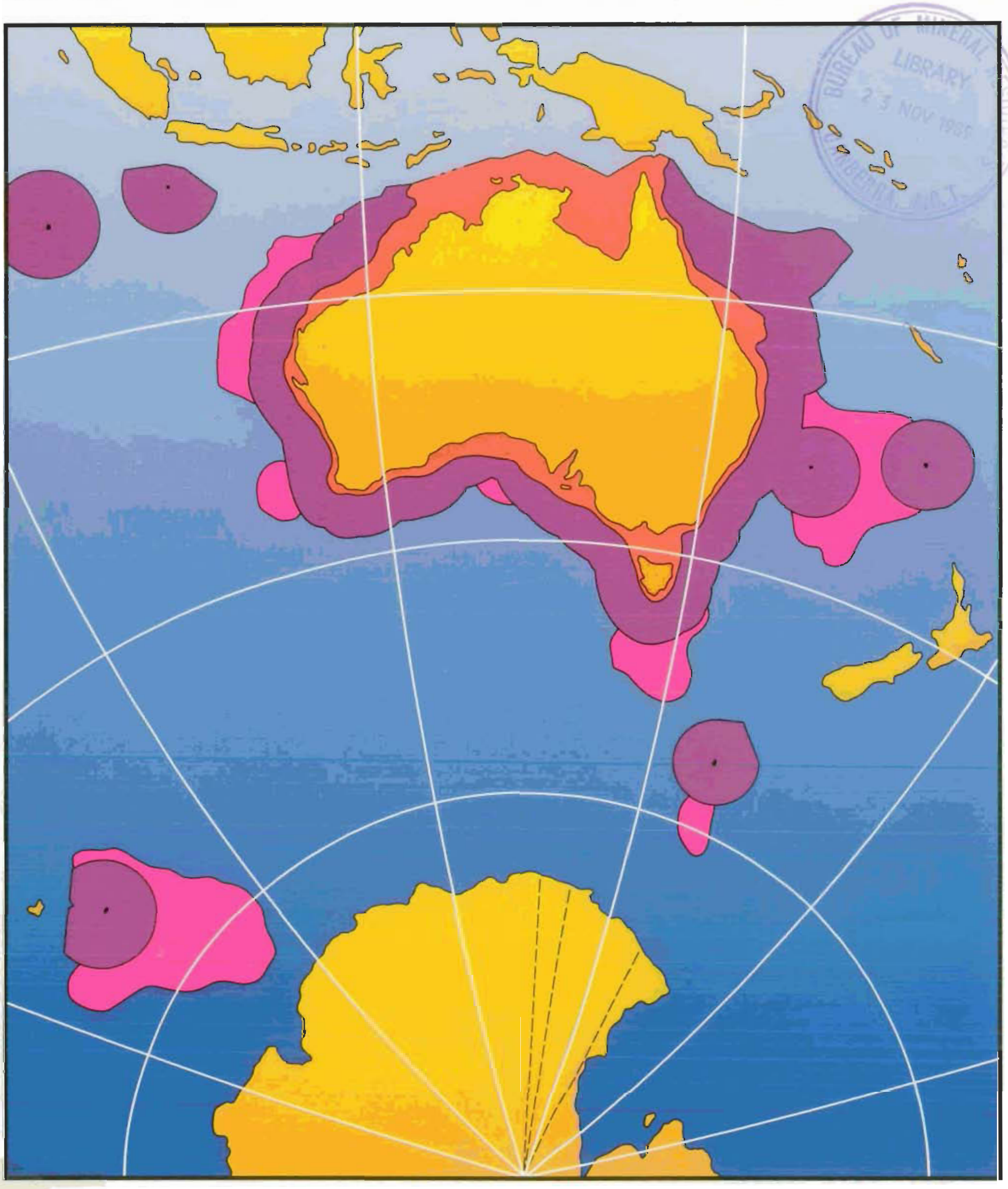

VOLUME 11 NUMBER 1

BMR JOURNAL

OF AUSTRALIAN GEOLOGY & GEOPHYSICS

VOLUME 11 NUMBER 1

CONTENTS

Front cover: Approximate limits of a 200 nautical mile Exclusive Economic Zone (EEZ) and a Legal Continental Shelf around Australia and its island territories, as defined by the United Nations Convention on the Law of the Sea.

The geomorphic shelf (<200 m water depth) is shown in red (approximately 2.0 million km^2); the area of an EEZ beyond the geomorphic shelf of Australia and its island territories is shown in purple (8.6 million km^2); the area of a Legal Continental Shelf beyond an EEZ is shown in pink (approximately 3.7 million km^2). The area of the landmass of continental Australia is approximately 7.8 million km^2. Regions beyond EEZ are discussed in Symonds & Willcox (this issue).

AUSTRALIAN GOVERNMENT PUBLISHING SERVICE CANBERRA 1989

ISSN 0312-9608

Month of issue: September

Subscriptions to the BMR Journal are managed by the Australian Government Publishing Service (Mail Order Sales, GPO Box 84, Canberra, ACT 2601; telephone (062) 95 4485), to which enquiries should be directed.

Other matters concerning the Journal should be sent to the Director, marked for the attention of the Editor, BMR Journal.

Printed in Australia by Pirie Printers Sales Pty Ltd

A century of earthquakes in the Dalton-Gunning region of New South Wales

K.McCue[1], B.L.N. Kennett[3], B.A. Gaull[2], M.O. Michael-Leiba[1], J. Weekes[3], & C. Krayshek[3]

The Dalton-Gunning region of New South Wales (34.5–35.0°S, 148.5–149.5°E) is one of the more seismically active areas in Australia. Reports of felt earthquakes which occurred there in 1888, 1934 and 1984 were used to draw up isoseismal maps using the Modified Mercalli Scale (MM) of intensity. Magnitudes of 5.3, 5.6 and 4.4 were computed from the radius of perceptibility of each earthquake, and epicentral co-ordinates were assumed to be coincident with the centre of the highest isoseismals. These, and other earthquakes of magnitude 4.0 or greater that are known to have occurred since 1886, are tabulated to enable more accurate earthquake risk analyses to be undertaken for the region.
Extreme-value analysis of the hundred years of earthquake data yields magnitudes of 3.3, 4.6 and 5.8 for the 1, 10 and 100 year return periods in the region. These data are extrapolated to compute a return period of 120 years for a large, potentially damaging, earthquake of magnitude 6.0 or greater.

Introduction

The 9 August 1984 'Oolong' earthquake (Gaull & Michael-Leiba, 1985) was the latest in a series of damaging earthquakes in the Dalton-Gunning region of New South Wales during the last 100 years (Burke-Gaffney, 1952; Drake, 1974). Isoseismal maps have been compiled for seven of these earthquakes (Everingham & others, 1982; Rynn & others, 1986) and three more are presented here; one for the recent 9 August 1984 Oolong earthquake (Gaull & Michael-Leiba, 1985) and the others for the larger and earlier earthquakes of 18 November 1934 and 5 July 1888. The maps for the two earlier earthquakes are based solely on contemporary newspaper accounts as, in those days, seismographs were not widely established and the maps yield reasonable epicentres, magnitudes, and focal depth. The macroseismic epicentre is defined here as the centre of the highest isoseismal contour with an assumed epicentral uncertainty equal to the radius of that contour. These distances are 25 km and 20 km for the 1888 and 1934 earthquakes respectively. The radius of the circle equivalent in area to that enclosed by the MM III isoseismal line is defined after McCue (1980) as the radius of perceptibility. The magnitudes of these two earthquakes were determined from the radius of perceptibility with an uncertainty of ±0.3 (McCue, 1980) while the focal depths were assumed to be shallow as are those computed for recent earthquakes.

With this information these important early earthquakes can be incorporated into modern earthquake catalogues and, by greatly extending the sample period, they can be used for more meaningful earthquake risk analyses. Table 1 contains all known earthquakes of magnitude ML 4.0 or greater that have occurred in the Dalton-Gunning zone since 1886 and was compiled largely from the Bureau of Mineral Resources (BMR) data file, Drake (1974), Everingham & others (1982) and Rynn & others (1986). Intensities of MM VII or more have occurred four times and MM VIII on two occasions (in 1934 and 1949).

The computation of more accurate epicentres has only been possible since October 1958 (Cleary, 1967) when the Australian National University and Snowy Mountains Hydroelectric Authority commenced the installation of a nine station seismograph network to monitor seismic activity in the Snowy Mountains. Currently, with four portable seismographs operated by the Bureau of Mineral Resources (BMR) between Dalton and Gunning (inset Figure 6), uncertainties in epicentre, magnitude and depth are of the order of ±2.0 km, ±0.2 and ±5 km respectively; the big advance over the last three decades has been the reduction in the detection threshold from magnitude ML 4.5 to magnitude ML 1.0 or less.

Maps of epicentres within New South Wales published recently (Kennett, 1985) for each year since 1958, highlight the relatively high seismic activity in the Dalton–Gunning region compared with the general background activity of the eastern highlands.

There is as yet no obvious explanation for this spatial clustering of intraplate earthquakes; the three large north-west to north-north-west striking lineaments clearly visible on LANDSAT photographs appear to have no causal association with the seismicity. A seismic refraction survey through the zone (Finlayson & McCracken, 1981) found no anomalous velocities or variations in crustal thickness.

Isoseismal maps

The 5 July 1888 earthquake

Cleary (1967) followed Burke-Gaffney (1952) in assigning this earthquake to the Robertson-Bowral region of NSW though the limited number of newspaper reports, 22 in all, indisputably point to Yass and Gunning, 100 km to the west, as being the towns closest to the epicentral region.

The only damage report emanated from Yass, where the walls of a row of houses were reported to be split by the shock (The Yass Courier, 10 July, 1888), but the type and quality of building materials were not specified.

The earthquake was felt as far away as the northern suburbs of Sydney and at Orange, but not at Cooma or Wagga, so it was smaller than the 1886 earthquake (Rynn & others, 1986) and the later 1934 event discussed below. The isoseismal map presented here in Figure 1 is not well constrained but a magnitude of ML 5.3(I) has been derived from the radius of perceptibility (McCue, 1980).

The 18 November 1934 earthquake

The lead story in the Sydney Morning Herald of 20 November 1934 stated: 'Probably the severest earthquake recorded in New South Wales was experienced at 8 o'clock yesterday morning when a wide area of the state was shaken'.

[1]Division of Geophysics, Bureau of Mineral Resources, GPO Box 378, Canberra ACT 2601

[2]Mundaring Geophysical Observatory, Hodgson Street, Mundaring, WA 6073

[3]Research School of Earth Sciences, Australian National University, GPO Box 4, Canberra ACT 2601

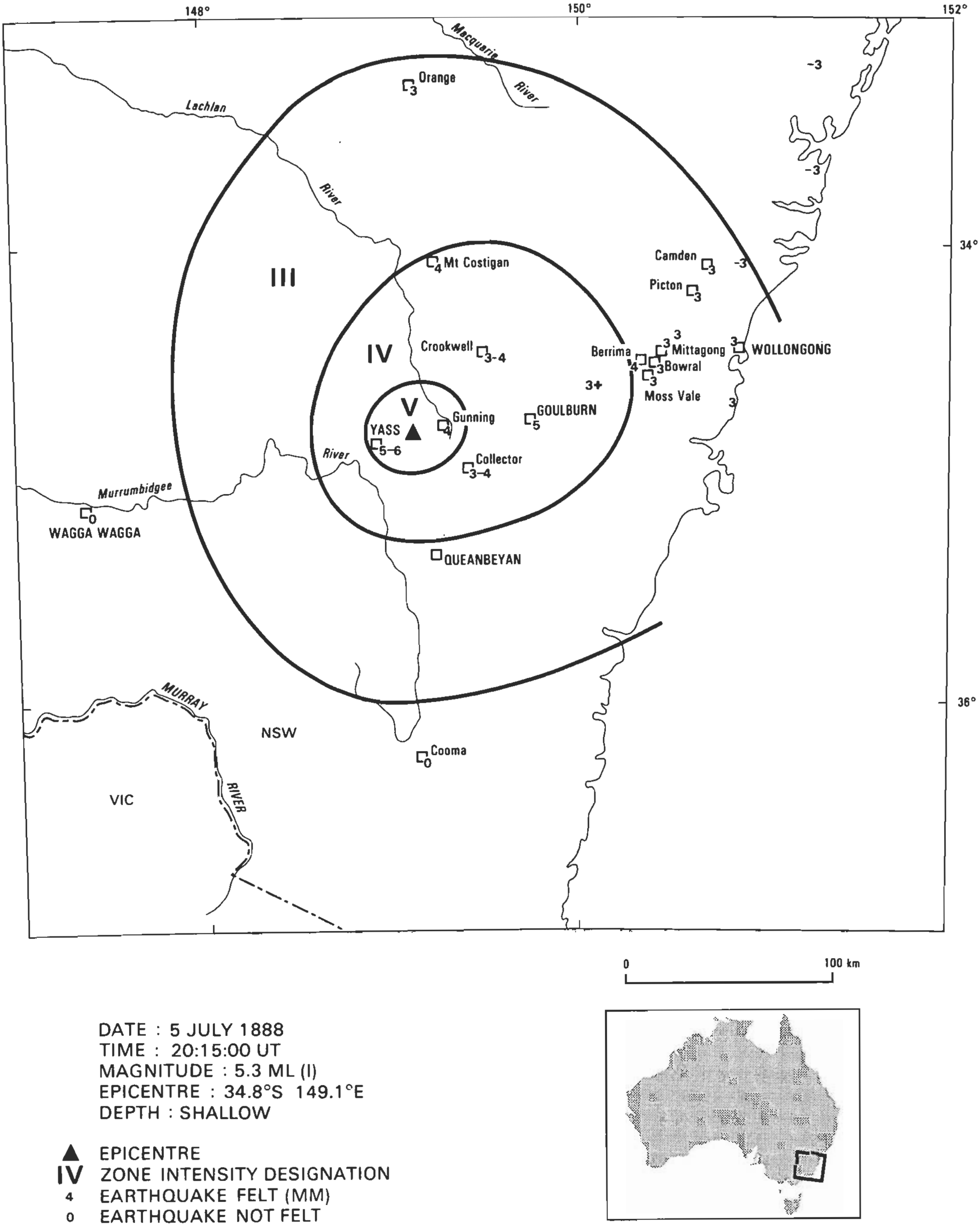

Figure 1. Isoseismal Map, 5 July 1888 Earthquake

It continued: 'The worst damage was reported from Gunning where practically every brick and stone building received damage in some form, huge rocks were split, trees were felled, and great fissures were opened in the ground.'

The earthquake was the culmination of a week-long series of foreshocks and was reported to be the worst shock in the history of Gunning. It was followed by a long series of aftershocks, one of which, on Sunday 25 November was felt at least as strongly in Cooma, 160 km distant, as was the main shock.

Several buildings in Gunning lost chimneys and one baker's oven was so badly cracked that it was rendered useless. In many houses the walls cracked and plaster fell from the ceilings. Pictures on walls were dislodged and in some

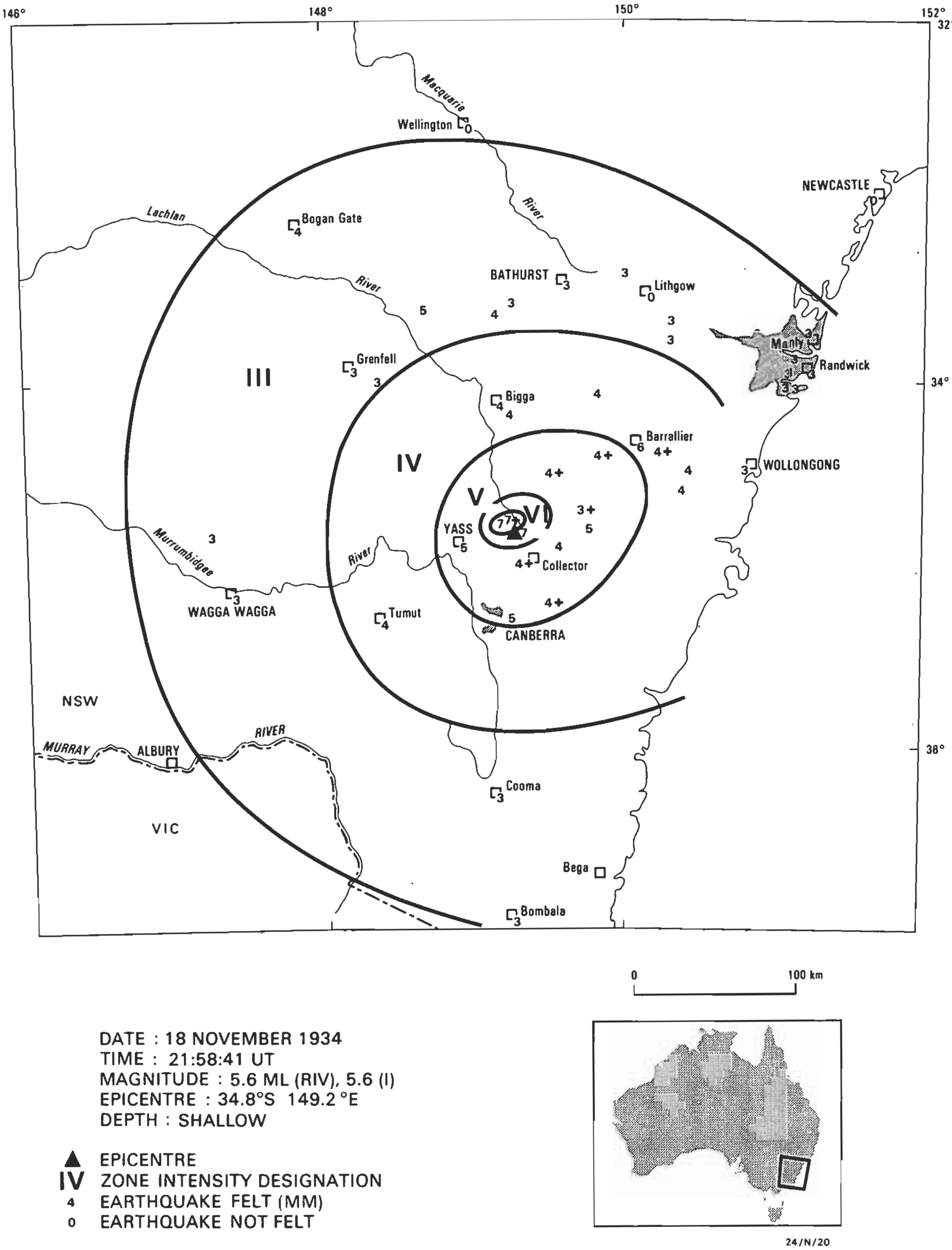

Figure 2. Isoseismal Map, 18 November 1934 Earthquake

instances turned right round. These reports are commensurate with an intensity of VIII on the Modified Mercalli Scale. At Dalton the damage was reported to have been extensive though no details were given.

According to the Canberra Times, the water in the Canberra swimming pool (at Manuka) was considerably agitated and in the pool office the telephone wobbled enough to tinkle the bell as if it were ringing. Early morning strollers reported that the road appeared to be undulating and trees vibrated violently.

The Sydney Morning Herald reported that: 'deep fissures appeared in the road between Dalton and Gunning in four places. The fissures apparently run for a considerable distance and although they are mere cracks in some places, they are several inches wide in others.' Cracks were also reported to have opened on a ridge 3 km west of Gunning but afterwards closed up. From this brief newspaper description it is impossible to determine whether these cracks are indicative of primary faulting or just secondary fractures caused by local settlement; undoubtedly the focus of the earthquake was very shallow.

Large granite boulders were reported to have split asunder just west of Gunning. P. Chopra suggested (personal communication) that these rocks had weathered completely through along frost and joint fractures and simply collapsed as a result of the intense shaking.

According to the Sydney Morning Herald, residents in practically all suburbs of Sydney felt the tremor. No mention was made in the Newcastle papers of the tremor being felt locally, nor was it felt at Wellington or Albury; yet at Bombala, a similar distance to the south, it was felt at intensity III. A smoothed isoseismal map was compiled from 43 reports in local newspapers including 'The Sydney Morning Herald', 'Canberra Times', 'Goulburn Penny Post', 'Lithgow Mercury',

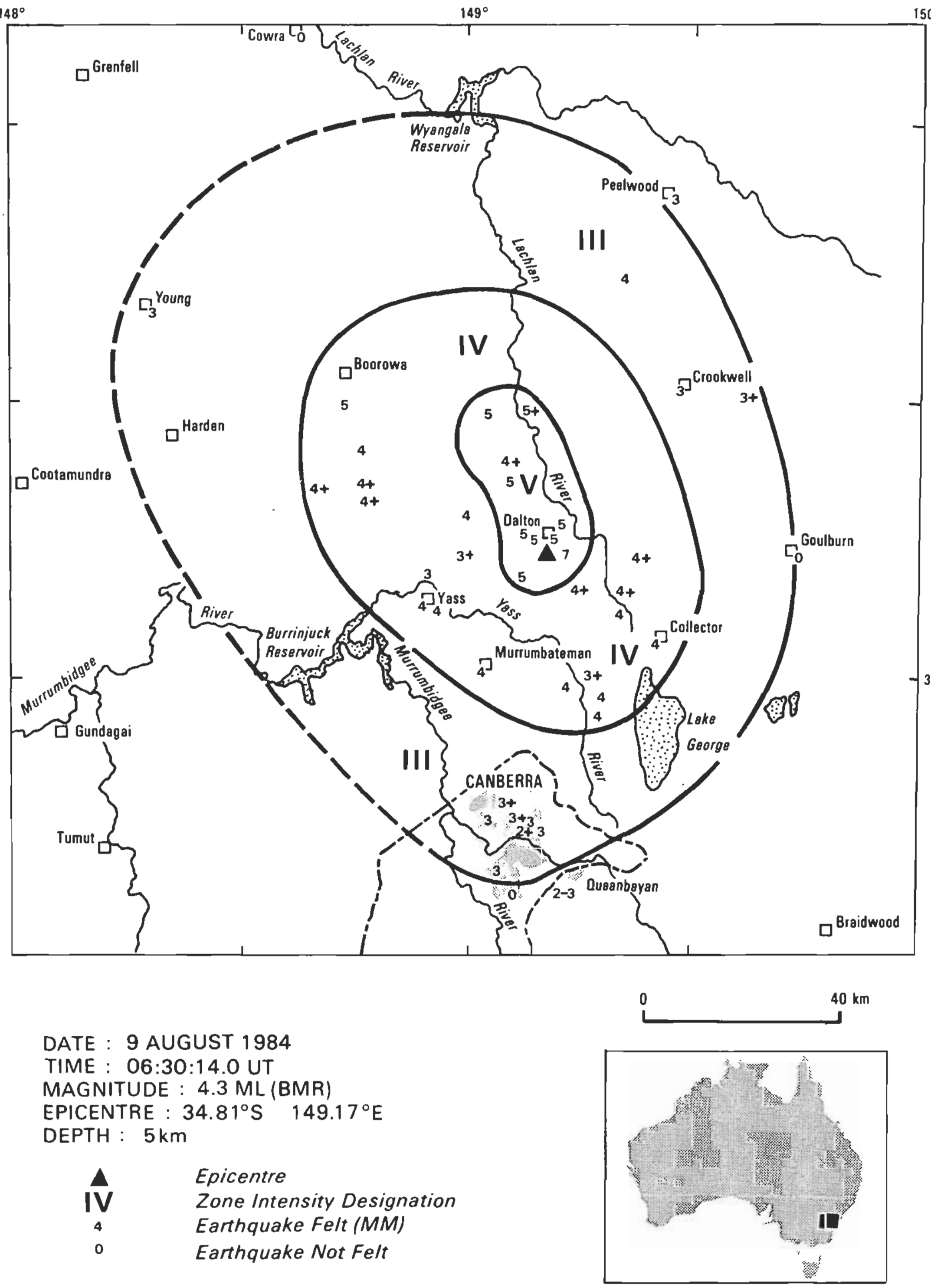

Figure 3. Isoseismal Map, 9 August 1984 Earthquake

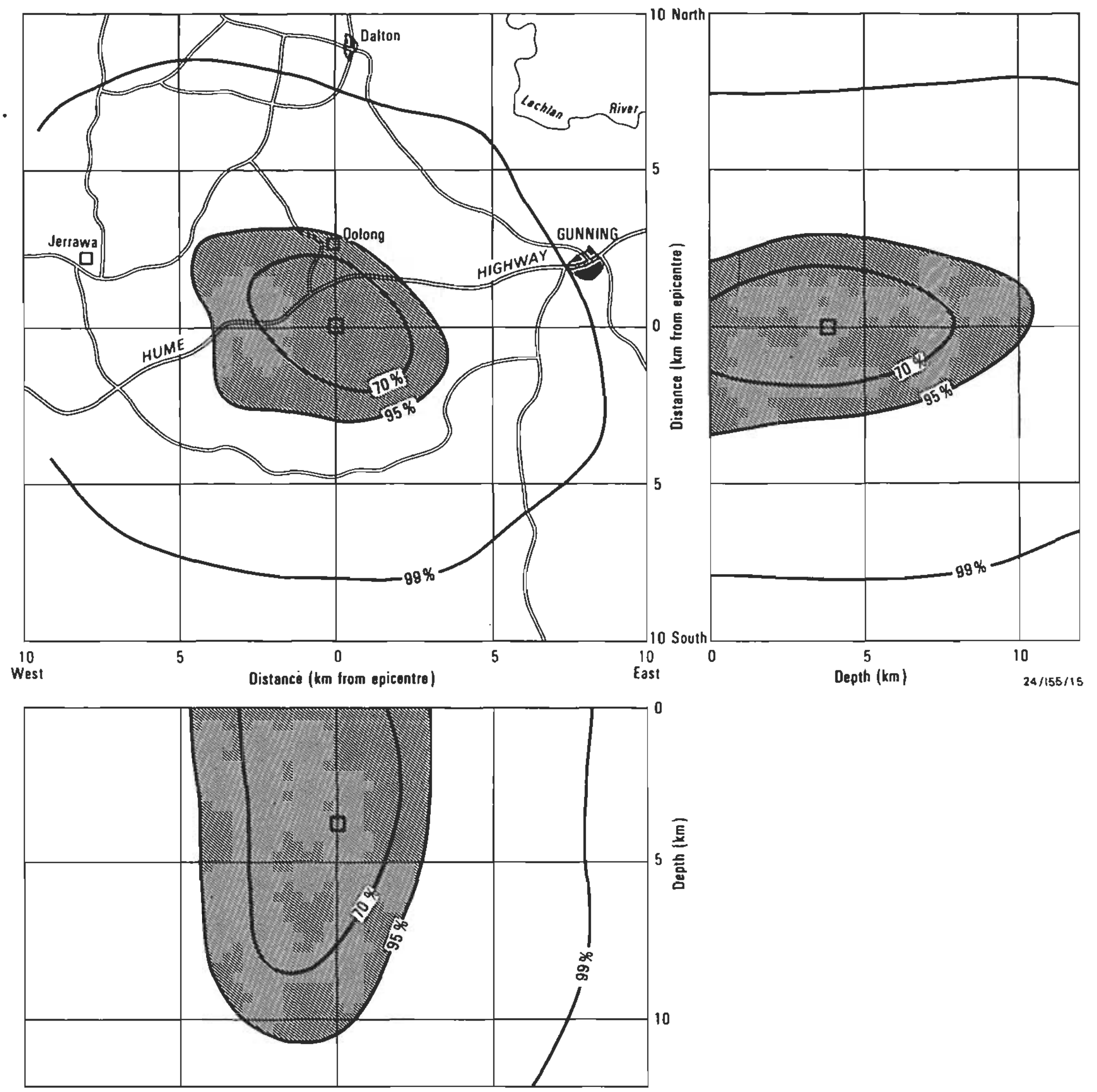

Figure 4. Confidence regions for the hypocentre of the 1984 August 9 event near Oolong determined by the method of Sambridge & Kennett (1986).

The contours enclose the regions in which the statistical confidence levels for the occurrence of the hypocentre are 70, 95 and 99 per cent, the 95 per cent region is shaded.

Table 1. Earthquakes in the Dalton–Gunning region 1886-1985, ML 3.9

Date	*Time (U.T.)*	*Lat (° S)*	*Long (° E)*	*ML**	*Maximum Intensity+*
1886 11 29	1700	34.8	148.8	5.5(I)	VII
1888 07 05	2015	34.9	148.8	5.3(I)	VI
1907 02 20	1730	34.8	149.2	4	IV
1924 03 06	2345	34.9	149.0	4.0(I)	V
1930 10 27	020351	34.5	149.0	5.0(RIV)	
1933 01 11	201051	34.8	149.2	4.8(RIV)	
1934 01 30	202754	34.8	149.5	4.7(RIV)	
1934 11 10	234740	34.8	149.2	4.8(RIV)	
1934 11 18	215841	34.8	149.2	5.6(RIV)	VIII
1934 11 21	063206	34.8	149.2	4.8(RIV)	
1947 05 05	094348	35.0	149.5	4.5(RIV	
1949 03 10	223033	34.8	149.2	5.5(RIV)	VIII
1952 09 07	054114	34.8	149.3	4.7(RIV)	
1952 11 18	100306	34.8	149.3	4.4(RIV)	
1952 11 19	015916	34.8	149.3	4.9(RIV)	V
1952 11 22	075720	34.8	149.3	4.6(RIV)	
1971 11 03	200536	34.78	149.17	4.3(RIV)	VI
1977 06 30	124822	34.67	148.87	4.2(BMR)	IV
1977 07 04	200520	34.65	148.89	5.0(CAN)	VI
1984 08 09	063013	34.80	149.17	4.4(BMR)	VII

* RIV Drake's (1974) reading of the Riverview Seismograms
CAN Australian National University
(I) Derived from intensity data.
\+ Modified Mercalli Scale

'Adelong and Tumut Express and Adelong Argus', 'Bombala Times', 'Cooma Express' and 'Queanbeyan Age'. The radius of perceptibility was about 250 km (Fig. 2) which converts empirically to a magnitude of ML 5.6(I) (McCue, 1980). This is identical to the Richter or local magnitude Drake (1974) measured from the Riverview seismograms. The locations of identified foreshocks and aftershocks in Table 1 have been set the same as the mainshock.

The 1984 Oolong earthquake

The earthquake struck at 4.30 pm on 9 August causing extensive cracking in a brick homestead at Oolong and the Anglican Church in Dalton, both of which had suffered previous damage during the 1949 earthquake (Table 1). Shaking was felt over an average radius of about 70 km (Fig. 3), which corresponds to a magnitude of ML 4.4(I). A similar magnitude of ML 4.3 was determined at the BMR from eastern Australian seismograms.

Using a simple model for the entire southeast Australian region (Doyle, & others, 1959), the preliminary location from the Australian National University (ANU) Bulletin No. 28/84 was determined at:

Latitude : 34.81° S
Longitude : 149.14° E
Depth : 10 km

For convenience in travel-time calculations, the BMR used an averaged model (Table 2) based on the Finlayson and McCracken (1981) data but without low velocity zones, and determined a hypocentre at:

Latitude : 34.81° S (±0.02)
Longitude : 149.17° E (±0.02)
Depth : 5.3 km (±5.2)

about 3 km away from the preliminary estimate. This estimate is in excellent agreement with that obtained using the direct search scheme of Sambridge & Kennett (1986):

Latitude : 34.81° S
Longitude : 149.18° E
Depth : 3.8 km

The 70, 95 and 99 per cent confidence regions associated with this solution are shown in Figure 4, by the shaded region in map view and in the north-south and east-west sections through the hypocentre.

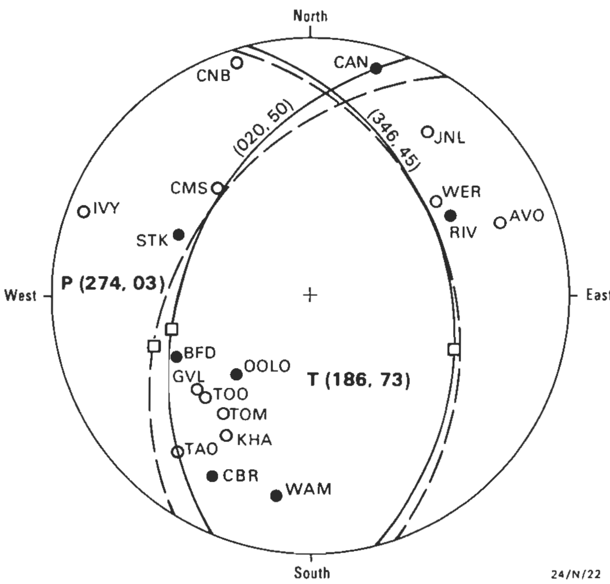

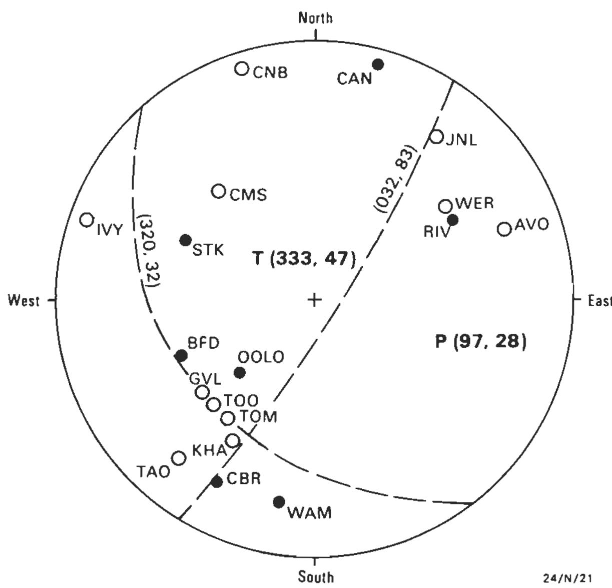

Figure 5. Focal mechanism solutions for the 9 August 1984 earthquake.

Open circles represent dilatations, full circles compressions and crosses emergent arrivals. P,T are the largest and smallest principal stress axes respectively.

Table 2. Crustal model in the Dalton-Gunning region

Depth km	Velocity km/s	
	Vp	Vs
0		
	5.80	3.35
10.5		
	6.30	3.64
26.5		
	6.90	3.98
31.0		
	7.35	4.24
50.0		
	8.08	4.66

An SMA-1 accelerograph at Oolong was triggered by the earthquake and by 20 of the aftershocks. Normally, the P-wave arrival on these instruments is lost because there is a start-up delay of at least 0.1 s so the data cannot be used for locating earthquakes. However, in this sequence, two of the aftershocks were only 5 seconds apart so the instrument was still operating from the first shock when the second began. A clear S-P time of 0.4 s was observed in this case corresponding to a slant distance of about 3 km from Oolong and in fair agreement with the computed distance.

The centre of the MM V isoseismal is at 34.66° S, 149.14° E, within 13 km of the computed epicentre which is within the estimated error of ±20 km quoted in the introduction.

In this case a unique focal mechanism solution could not be determined due to the small amplitude of the refracted (Pn) first arrivals on distant seismograph stations and, conversely, such a large, impulsive, direct P arrival on close stations; the photographic recording trace simply disappeared and no direction of motion could be read even under a microscope. The eighteen remaining first arrivals were plotted onto a lower hemisphere projection of the focal sphere and the plot indicates the two possible fault plane solutions illustrated in Figure 5. In each case, three of the eighteen polarites are incompatible with the solution; RIV, STK and KHA in the upper solution, and RIV, CNB and CMS in the lower one. There was no observed surface faulting to indicate which of the nodal planes was the fault plane. The only consistent features of these two focal mechanisms are the east-west direction of the principal stress and the compressive nature of the failure. This agrees with other focal mechanisms computed for Dalton-Gunning zone earthquakes (Denham & others, 1981) and downhole stress measurements in the region (Chopra, 1985).

Spatial extent of epicentres

The plot in Figure 6 shows that epicentres located between 1960 and 1984 are scattered over two distinct zones of spatial extent 10 km, one north of the Castle Hill (CAH) seismograph station, the other south of Dalton. The southern zone is the more active of the two. It will be interesting to see whether the gap between the two zones is still evident through the next decade or so.

Focal depth distribution

During 1985/86 up to four additional seismographs were deployed by BMR in the Dalton region (inset Fig. 6). Using data from these seismographs to supplement the Australian National University data and using a local crustal model

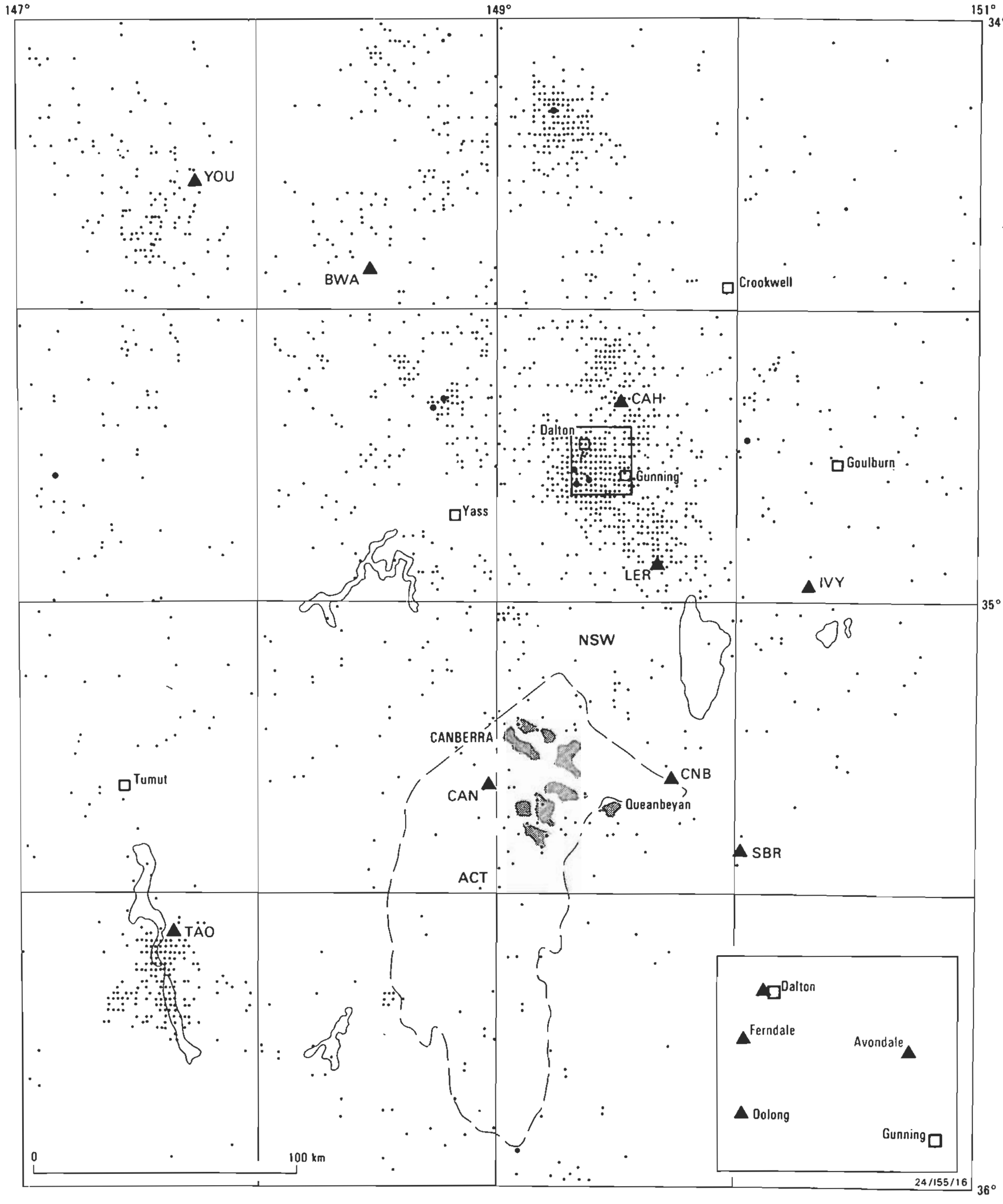

Figure 6. Plot of epicentres in the Dalton-Gunning Region (34-36° S, 148-150° E), 1950-1984.
Triangles represent seismographic stations operated by the Australian National University, except CNB which is operated by BMR. The inset shows the location of four temporary seismographs operated by the BMR during 1986.

(Finlayson & McCracken, 1981) in the computer location program, better focal depth control has been achieved. The histogram of Figure 7 summarises focal depths of 53 microearthquakes which occurred in the Dalton area during the period 1 April 1986 to 30 November 1986 and which are located by at least 5 stations. Focal depths ranged from 0 to 11 km with a mean of 1 km and most (64%) had a very near surface depth (0 to 1 km).

The shallowness of these small events is attested by the fact that at least 24 of them were felt by Dalton residents, 14 with intensities of MM IV, and another two (one of which had a magnitude of only ML 1.5) with an intensity of MM V! The smallest felt event had a magnitude of ML 1.0.

Records from portable digital recorders deployed by the Australian National University in November/December 1984

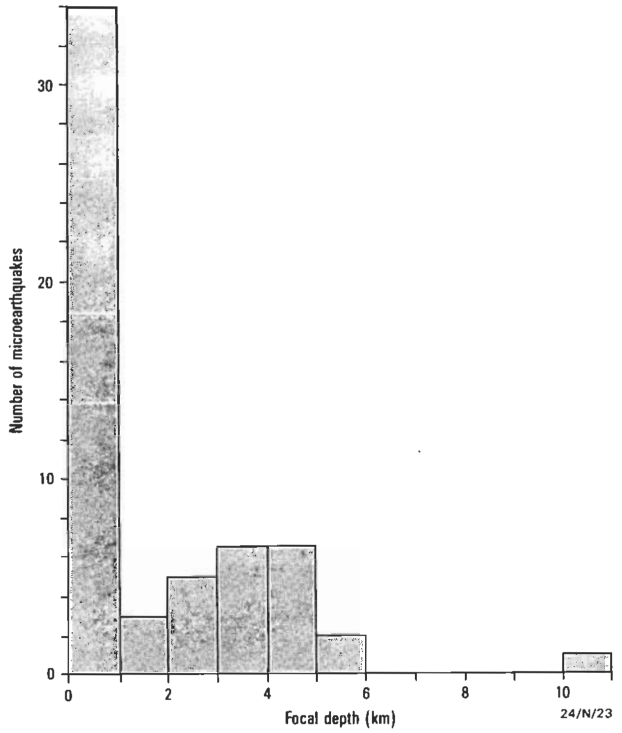

Figure 7. Histogram of focal depths for 25 microearthquakes located in 1986 using additional data from the four-station microearthquake network shown in Figure 6.

showed then that these small events were shallower than 2 km depth. Furthermore, the ML 3.1 earthquake which occurred on 7 January 1986 at 34.76°S, 149.18°E (4 km south of Dalton) had a computed depth of 2(±3) km. It was felt with a maximum intensity of MM IV-V at Dalton, and it dislodged plaster in the Anglican Church from cracks caused by the 1984 Oolong earthquake. A similar intensity was experienced at Oolong, 2 km to the southwest of the epicentre.

Apparent frequency of earthquake recurrence

The earthquake history of the Dalton/Gunning zone is probably complete for the following time-magnitude sets: ML>4.9 since 1886, ML>4.4 since 1909, when seismographs were installed at Riverview, and ML>1.9 since 1961, when a seismograph was installed at Dalton. The completeness of the two larger magnitude sets over the stated time periods was confirmed using the test devised by Stepp (1972).

Excluding aftershocks, there have been six earthquakes of at least magnitude ML 5.0; the largest at magnitude ML 5.6 was that of 1934 which caused considerable damage to domestic structures in Gunning and Dalton. From Table 1 and the post-1958 ANU data file, the set of largest annual earthquakes was compiled and fitted, using least squares, by a Gumbel (1958) Type 1 extreme-value distribution which is plotted in Figure 8. The equation of the line of best fit is:

$$-\ln(-\ln P) = \beta M - \ln\alpha$$

where P is the probability that the largest earthquake in any year is less than M and α and β are constants. The left hand side of this equation is termed the reduced probability. The slope of the curve 'β' is b ln 10 where 'b' is the slope of the familiar recurrence relation, relating the number of large to small earthquakes. A b-value of 0.81 (±0.02) was obtained which is not significantly different from the value

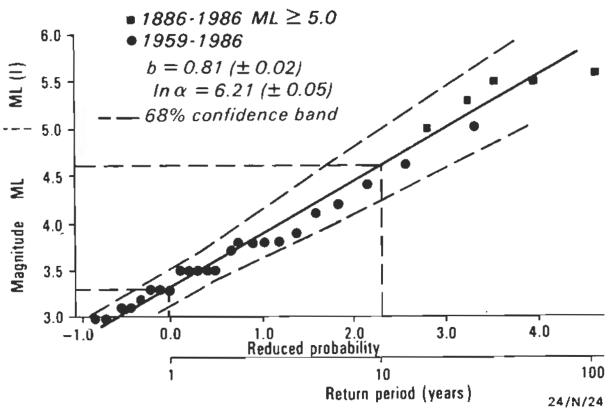

Figure 8. Gumbel type 1 extreme-magnitude distribution of the set of largest annual earthquakes in the Dalton-Gunning region, 1886–1985.

of 0.80 found by Gaull & Michael-Leiba (personal communication) during a new study of the seismic risk in the region. With this 'b' value and a value of lnα of 6.21 (±0.05), return periods of 1, 10 and 100 years were computed for magnitudes of 3.3, 4.6 and 5.8 respectively. Extrapolation of the 100 year data set indicates that an earthquake of magnitude 6.0 has an estimated return period of 120 ±12 years.

Large earthquakes are not unknown in eastern Australia; they have occurred in Bass Strait, in 1885 and 1892, and in Queensland in 1918 (Everingham & others, 1982).

The 100 year earthquake has not occurred in the Dalton-Gunning region in the last century; by definition there is a 37 per cent chance that an earthquake will not occur in any time interval equal to its return period and a 13.5 per cent chance that it will not occur in a time interval double the return period. Likewise, in three of the last ten decades, no earthquake has exceeded magnitude 4.0 though the computed return period for an earthquake of this size is 3.5 years.

Maximum magnitude

There is no clear increase in 'b' with magnitude in Figure 8, showing that the sample period is too short to compute a maximum magnitude but there is also no indication that it is likely to be less than magnitude ML 6.0. An earthquake of this size would cause considerable damage to domestic dwellings in nearby Dalton and Gunning where old masonry homes have already been repeatedly damaged by past earthquakes. Because the focal depths are so shallow, surface faulting would be expected to accompany such a large earthquake thereby endangering other facilities which traverse the zone such as the Moomba–Sydney gas pipeline and the Sydney to Melbourne railway.

Discussion

It is rare indeed to have in Australia as extensive an earthquake data set as the one hundred year sample in the Dalton-Gunning region. It should be possible to push the earthquake history back another 30 years or so by doing a more extensive literature search to check the stationarity of 'b' with time and magnitude.

Analysis of the data shows that the earthquakes are localised in a very small source area which has an earthquake risk comparable to that of the Southwest Seismic Zone of Western Australia (Gaull & Michael-Leiba, 1987) where earthquakes up to magnitude MS 6.8 have occurred in the last century. No earthquake has exceeded magnitude ML 5.6 in the Dalton–Gunning region since 1886 and probably not since June 1788 when the European colonisers of New South Wales felt their first earthquake at Port Jackson. However, there is no reason to suppose that an earthquake exceeding magnitude ML 6.0 is an impossible or even unlikely event.

Conclusions

Analysis of historical documents and of modern instrumental data has led to the compilation of the most comprehensive list yet published of earthquakes of magnitude ML 4.0 or more in the Dalton–Gunning region of New South Wales during the past 100 years. The list is only complete for earthquakes above magnitude ML 4.9 for the whole period, although this threshold drops to 4.4 from 1909, and 1.9 from 1960.

Macroseismic epicentres and magnitudes were calculated from intensity information based on the Modified Mercalli scale and the three new isoseismal maps bring to eleven the number so far compiled for the Dalton region.

With the aid of a four-station microearthquake network accurate focal depths of 53 microearthquakes have been determined of which 64 per cent occurred within 1 km of the surface.

Using extreme-value statistics we found the slope 'b' of the magnitude-frequency relationship to be 0.81 (±0.02) and the return period of a large magnitude ML 6.0 earthquake to be 120 (±12) years.

The largest earthquake near Dalton in the period studied occurred on 18 November 1934 and had a magnitude of ML 5.6.

Previous measurements of the regional crustal stress are supported by a fault-plane solution for the 9 August 1984 earthquake which indicates that the upper crust, at least, is under horizontal compression in an east-west direction.

References

Burke-Gaffney, T.N., 1952 — The seismicity of Australia. *Journal and Proceedings of the Royal Society of New South Wales*, 85, 47–52.

Chopra, P., 1985 — In-situ crustal stress measurements using a new hydrofracture system. *In* Rheology of the Lithosphere & Australian Earthquakes. Compiled by B. Drummond, M.O. Michael-Leiba, D. Denham & C. Collins, *Bureau of Mineral Resources, Australia, Record* 1985/31.

Cleary, J., 1967 — The seismicity of the Gunning and surrounding areas, 1958–1961. *Journal of the Geological Society of Australia*, 14(1), 23–29.

Denham, D., Weekes, J., & Krayshek, C., 1981 — Earthquake evidence for compressive stress in the southeast Australian crust. *Journal of the Geological Society of Australia*, 28, 323–332.

Doyle, H.A., Everingham, I.B., & Hogan, T.K., 1959 — Seismic recordings of large explosions in south-eastern Australia. *Australian Journal of Physics*, 13, 222–230.

Drake, L., 1974 — The seismicity of New South Wales. *Journal and Proceedings of the Royal Society of New South Wales*, 107, 35–40.

Everingham, I.B., McEwin, A., & Denham, D., 1982 — Atlas of Isoseismal Maps of Australian Earthquakes. *Bureau of Mineral Resources, Australia, Bulletin* 214.

Finlayson, D.M., & McCracken, H.M., 1981 — Crustal structure under the Sydney Basin and Lachlan Fold Belt, determined from explosion seismic studies. *Journal of the Geological Society of Australia*, 28, 177–190.

Gaull, B.A., & Michael-Leiba, M., 1985 — Oolong earthquake series, August-December 1984. *Bureau of Mineral Resources, Australia, Research Newsletter* (unpublished).

Gaull, B.A., & Michael-Leiba, M., 1987 — Probabilistic earthquake risk maps of southwest Western Australia. *BMR Journal of Australian Geology & Geophysics*, 10, 145–151.

Gumbel, E.J., 1958 — Statistics of Extremes. *Columbia University Press. New York*. 375 pp.

Joklik, G.F., 1951 — Dalton Gunning area, NSW., Earth Tremors of March, 1949. *Journal and Proceedings of the Royal Society of New South Wales*, 84, 17–27.

Kennett, B.L.N., 1985 — Seismicity of southeastern Australia 1959–1984. *Research School of Earth Sciences, Australian National University, Canberra.*

McCue, K.F., 1980 — Magnitude of some early earthquakes in southeastern Australia. *Search*, 11(3), 78–80.

Rynn, J., Denham, D., Greenhalgh, S., Jones, T., McCue, K.F., & Smith, R.S., 1986 — Atlas of isoseismal maps of Australian earthquakes. *Bureau of Mineral Resources, Australia, Bulletin* 222.

Sambridge, M.S., & Kennett, B.L.N., 1986 — A novel method of hypocentre location. *Geophysical Journal of the Royal Astronomical Society*, 87, 679–697.

Stepp, J.C., 1972 — Analysis of completeness of the earthquake sample in the Puget Sound area and its effect on statistical estimates of earthquake hazard. *National Oceanic & Atmospheric Administration, Environmental Research Laboratories, Boulder, Colorado.*

Australia's petroleum potential in areas beyond an Exclusive Economic Zone

P.A. Symonds[1] & J.B. Willcox[1]

The United Nations Convention on the Law of the Sea gives Australia the option of proclaiming a Legal Continental Shelf around both the continent and its island territories, over which it would control exploration and exploitation of the natural resources of the seabed and subsoil. A Legal Continental Shelf is considered to extend throughout the natural prolongation of the land territory to the outer edge of the continental margin, which, where it extends beyond the 200 nautical mile limit (Exclusive Economic Zone — EEZ), is defined by a two-part formula based on measurements from 'foot of continental slope' reference points. To fully use this formula, both bathymetric and sediment thickness information are required.

The area of a Legal Continental Shelf around Australia and its territories would be approximately 12 million km^2 (about 1.5 times the area of the continent itself), which would be one of the largest Legal Continental Shelves in the world. Eight regions of this shelf, totalling more than 3 million km^2, would extend beyond an EEZ. Sediment thicknesses greater than 2000 m — sufficient to have generated hydrocarbons from any potential source rocks — occur in six of these regions: Lord Howe Rise/Norfolk Ridge, South Tasman Rise, Great Australian Bight, Naturaliste Plateau, Exmouth/Wallaby Plateaus and Kerguelen Plateau. Most of the remote parts of the Australian margin with possible resource potential would lie within a Legal Continental Shelf.

Our relative rating of petroleum potential of regions beyond an EEZ is based on both a qualitative and quantitative assessment. The potential petroleum recovery estimates are greatest for western Lord Howe Rise and the southern Kerguelen Plateau, but relatively high values were also obtained for the South Tasman Rise and the eastern flank of Lord Howe Rise. Of the deepwater ocean basin areas, the New Caledonia Basin has the greatest potential recovery, although the estimates are clearly unrealistically large. Small but potentially high-yielding basins, such as the Taranui Sea Valley on the Norfolk Ridge, are also of interest.

Over all, the assessment indicates that the western flank of Lord Howe Rise has the greatest petroleum potential, even though the relatively small size of some of its individual basins tends to downgrade the chance of finding 'giant' and thus economically viable fields. However, this part of Lord Howe Rise appears more promising when the equivalent area and potential within an EEZ around Lord Howe Island are considered. The southern Kerguelen Plateau produced the largest potential petroleum recovery estimates of any of the moderate water depth regions; however, its real potential will remain unknown until its origin (continental or oceanic) and volcanic history are better understood.

Although the regions discussed are in relatively deep water (generally over 1000 m), they are not consistently any deeper than areas of plateaus and slopes within an EEZ, such as the Exmouth Plateau, which has been explored and drilled. Since areas with petroleum potential beyond an EEZ are remote, and in some cases in hostile environments, their exploration is unlikely to be economically viable in the near future; however, they may well provide Australia with a strategic resource into the next century. In the light of Australia's dwindling petroleum resources, these regions should not be overlooked in long-term planning by government and industry.

Introduction

The mineral resources of the oceans, especially oil and gas, have assumed increasing importance in the last 20 years. At present, about 20 per cent of the world's petroleum supply comes from submerged areas, generally from shelfward extensions of known structures and from producing fields onshore. Gradual depletion of these areas and any accompanying escalation in oil prices will undoubtedly entice explorers into the more remote and deepwater regions. Such a situation is particularly relevant to Australia, with its vast area of continental shelf and marginal plateaus (Fig. 1), particularly if the declining resources of the Gippsland Basin fields are not rapidly offset by new discoveries in the onshore and nearshore basins. The importance of establishing a legal regime which would allow Australia to explore and exploit its deepwater mineral resources has been emphasised by Prescott (1979, 1985).

The 200 nautical mile (n.m.) line, which defines Australia's Fisheries Zone and lies beyond areas covered by most oil exploration surveys, is frequently taken to be the limit of national interest. However, significant areas of continental margin, and related legal continental shelf, lie beyond an EEZ, and may have mineral potential which could be exploited into the next century. Although those areas are remote, their water depth in many places is no greater than that of the marginal plateaus and slopes within the 200 n.m. limit.

This study has three components: the delimitation of seabed boundaries around Australia to identify regions of the continental margin which extend beyond an EEZ; a review of regional setting, basin development, and aspects of petroleum geology; and a brief discussion of methodology leading to estimates of petroleum potential, which serve as a guide to the relative importance of these regions.

[1]Division of Marine Geosciences & Petroleum Geology, Bureau of Mineral Resources, GPO Box 378, Canberra, ACT 2601

Seabed boundaries

An Australian Exclusive Economic Zone

In 1982, international agreement was reached on jurisdiction of over 100 million square kilometres of ocean. The Convention on the Law of the Sea was adopted at the eleventh session of the Third United Nations Conference on the Law of the Sea, after deliberation in a series of Law of the Sea Conferences, initiated in 1973, but stemming from the Truman Proclamation of 1945 (Ross, 1979). Australia has since signed but not ratified the Convention.

In accord with the Law of the Sea Convention (Articles 55–57) (United Nations, 1983), Australia could proclaim an 'Exclusive Economic Zone' (EEZ) over which it has the right to explore and exploit living and non-living resources of the seabed, subsoil and superjacent waters. An EEZ extends for 200 nautical miles from the baseline from which the breadth of the territorial sea is measured (Fig. 2). The Australian EEZ delimitation is essentially formed by a suite of arcs of 200 n.m. radius around Australia and its island territories. The total area enclosed would be about 8.6 million km^2 (Table 1). Where the EEZs (and Legal Continental Shelves) of adjacent states overlap, the seabed boundary is subject to negotiation[2].

[2]A negotiated seabed boundary separates Australia (and/or territories) from Indonesia (except for East Timor, the Ashmore Reef area and Christmas Island), Papua New Guinea, and the French territories of the New Caledonia region and Kerguelen Island. Negotiations are under way with New Zealand and Indonesia.

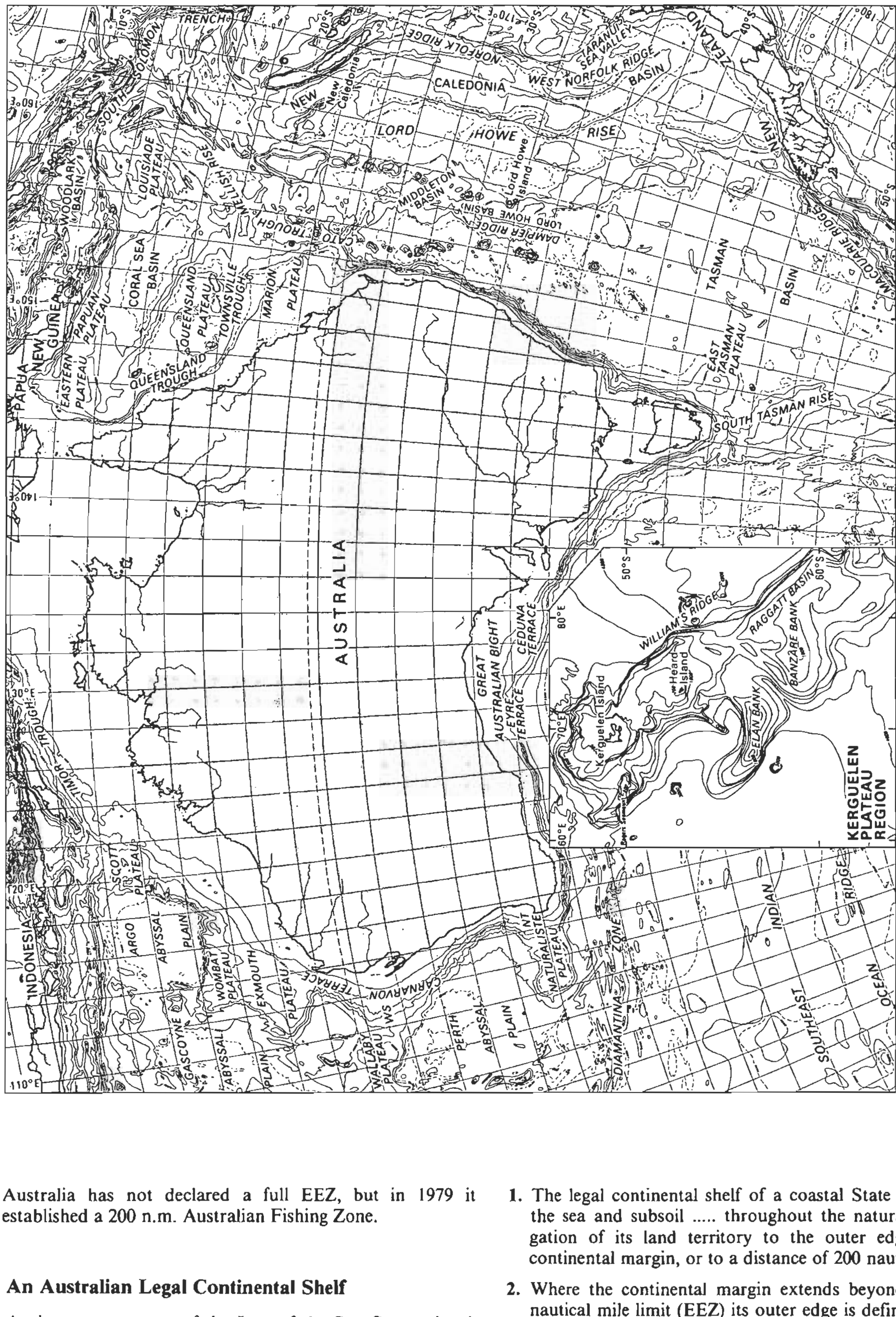

Figure 1. Bathymetry of the Australian region and Kerguelen Plateau region (inset) showing the main physiographic features.
Isobaths around Australia are 200 m, then 1000 m intervals (solid line), and in places the intermediate 500 m levels (dashed line). Isobaths on the Kerguelen Plateau are 200 m, then 500 m, intervals. Based on Plate Tectonic Map of the Circum-Pacific Region, Southwest Quadrant, Base Map (AAPG, 1978); Houtz & others (1977); Ramsay & others (1986b). NT = Naturaliste Trough, WS = Wallaby Saddle.

Australia has not declared a full EEZ, but in 1979 it established a 200 n.m. Australian Fishing Zone.

An Australian Legal Continental Shelf

An important aspect of the Law of the Sea Convention is the definition of a 'Legal Continental Shelf' (Article 76 of the Convention), which is quite distinct from the morphological continental shelf. A coastal state has sovereign rights over its 'legal' shelf for the purposes of exploring and exploiting the natural resources of its seabed and subsoil. The main points of Article 76 are that

1. The legal continental shelf of a coastal State comprises the sea and subsoil ..... throughout the natural prolongation of its land territory to the outer edge of the continental margin, or to a distance of 200 nautical miles
2. Where the continental margin extends beyond the 200 nautical mile limit (EEZ) its outer edge is defined by the so-called Irish Formula, which is in two parts:

   (i) A line delineated by the outermost fixed points at which the thickness of sedimentary rocks is at least 1 per cent of the shortest distance from the foot of the continental slope (sediment thickness formula, Fig. 3a), and

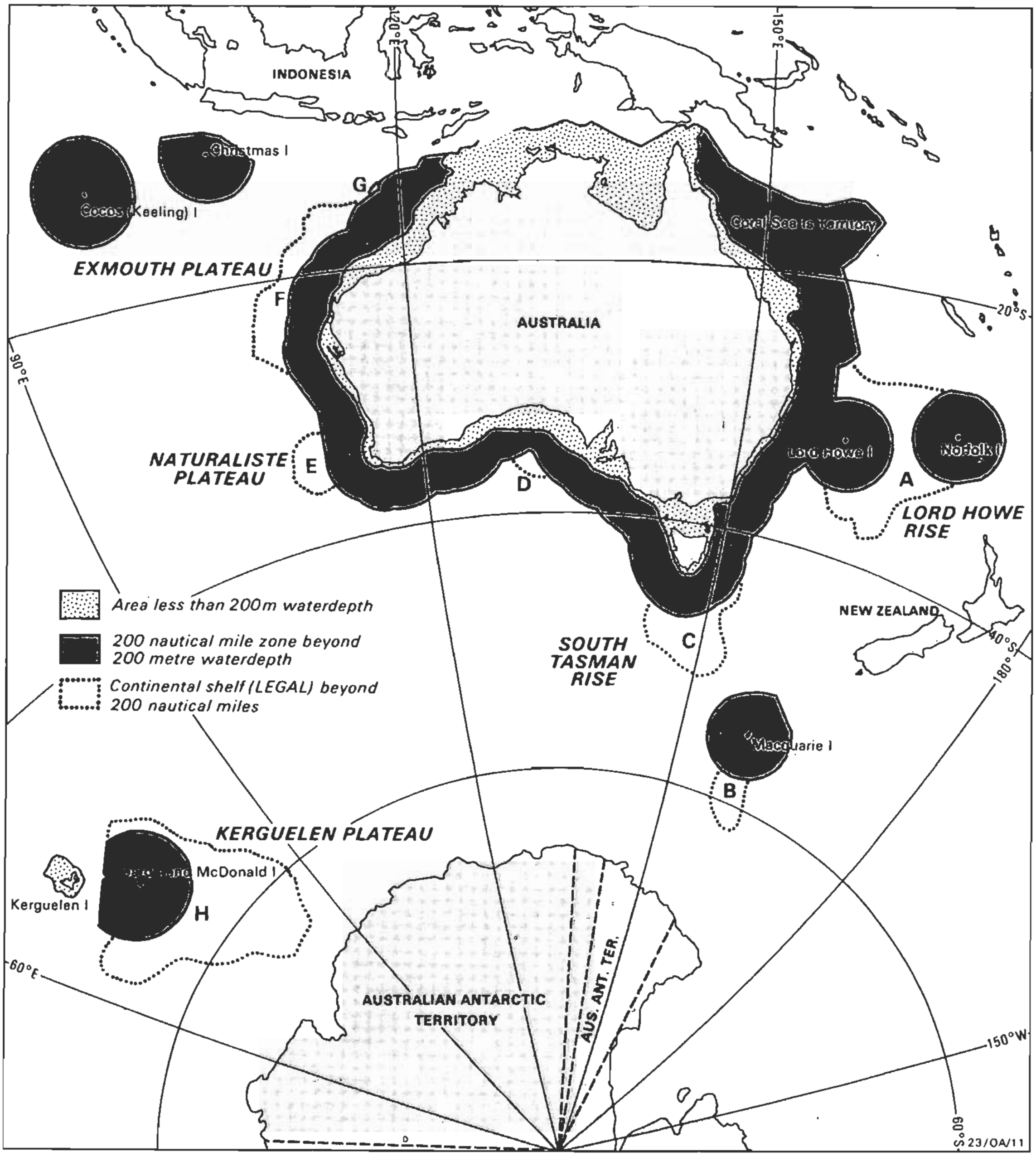

Figure 2. Approximate limits of a 200 nautical mile Exclusive Economic Zone (EEZ) and Legal Continental Shelf around Australia and its island territories.
The geomorphic shelf (<200 m water depth) is stippled; the area of an EEZ beyond the geomorphic shelf is screened; the limit of a Legal Continental Shelf beyond an EEZ is indicated by dotted line. Also shown are regions of the Legal Continental Shelf beyond an EEZ (A to H) discussed in the text.

(ii) A line not more than 60 nautical miles from the foot of the continental slope (Hedberg Line, Fig. 3b).

The legally defined outer edge of the continental margin is cut back by a formula, which is also in two parts, to give the outer limits of the Legal Continental Shelf beyond the EEZ. It consists of:

(i) A line not exceeding 350 nautical miles from the territorial sea baselines (Fig. 3c), and

(ii) a line not exceeding 100 nautical miles from the 2500 m isobath.

The limits of a Legal Continental Shelf are positioned by a combination of the various criteria contained in Article 76. The criteria that would be currently used to define a legal shelf over the parts of the Australian margin extending beyond an EEZ are indicated in Figures 4, 7 and 12 by E — 200 n.m. line, EEZ; H — Hedberg line; X — 350 n.m. cutoff; and Y — 2500 m isobath + 100 n.m. cutoff. N and M indicate where the legal shelf is, or may be defined by negotiated or median line boundaries with adjacent coastal states.

Because there is sporadic coverage and poor quality of seismic data beyond the foot of the slope, it is only possible to construct a sediment thickness line around approximately 15 per cent of the Australian margin. The application of the Irish Formula to define the outer edge of the continental margin around Australia is thus at present dependent mainly on the Hedberg Line.

Table 1. Approximate area statistics ($10^6 km^2$)

Australian landmass		7.8
Continental shelf (geomorphological)		2.0
EEZ	Australia + Lord Howe overlap	6.7
	Australia + island territories[1]	8.6
	Australia + island territories + AAT[2]	11.1
Legal Continental Shelf beyond EEZ	South to AAT	3.3
	South to EEZ around AAT	3.7
Total Legal Continental Shelf	Australia + territories, south to AAT	11.9
	Australia + territories, south to EEZ around AAT	12.3
	Australia + territories + EEZ around AAT	14.8

[1]Norfolk, Macquarie, Christmas, Cocos and Heard Islands
[2]Australian Antarctic Territory

Symonds & Willcox (1988) present basic data maps around Australia and over the Kerguelen Plateau, which show the detailed application of parts of Article 76, and include the positions of the 'foot of continental slope' reference points, the 'edge of continental rise' and the 'edge of the continental margin' as defined by the Hedberg line and sediment thickness formula.

The area of a Legal Continental Shelf around Australia and its territories (Fig. 2) would be approximately 11.9 million km^2 (about 1.5 times the area of the continent itself, and one of the largest in the world), or approximately 14.8 million km^2 if the Australian Antarctic Territory is included (Table 1).

Regions beyond an EEZ

Eight regions of a Legal Continental Shelf of Australia and its territories would lie beyond an EEZ (Figs 1 & 2), and cover a total area of more than 3 million km^2 (Table 1). These regions and their approximate areas are as follows:

A — Lord Howe Rise/Norfolk Ridge	0.87 million km^2
B — Macquarie Ridge	0.11
C — South Tasman Rise	0.54
D — Great Australian Bight	0.09
E — Naturaliste Plateau	0.19
F — Exmouth/Wallaby Plateaus	0.60
G — Argo Abyssal Plain	0.02
H — Kerguelen Plateau	0.91 (to AAT) 1.24 (to EEZ around AAT)

Although seismic data over most of these regions are sparse and of varied quality, it is apparent that areas of relatively thick sediment, which have at least some petroleum potential, occur in all regions except Macquarie Ridge and the Argo Abyssal Plain. Macquarie Ridge and the Argo Abyssal Plain are oceanic crust and have only a thin sediment cover, from which petroleum is unlikely to have been generated; these two regions do not warrant further consideration here.

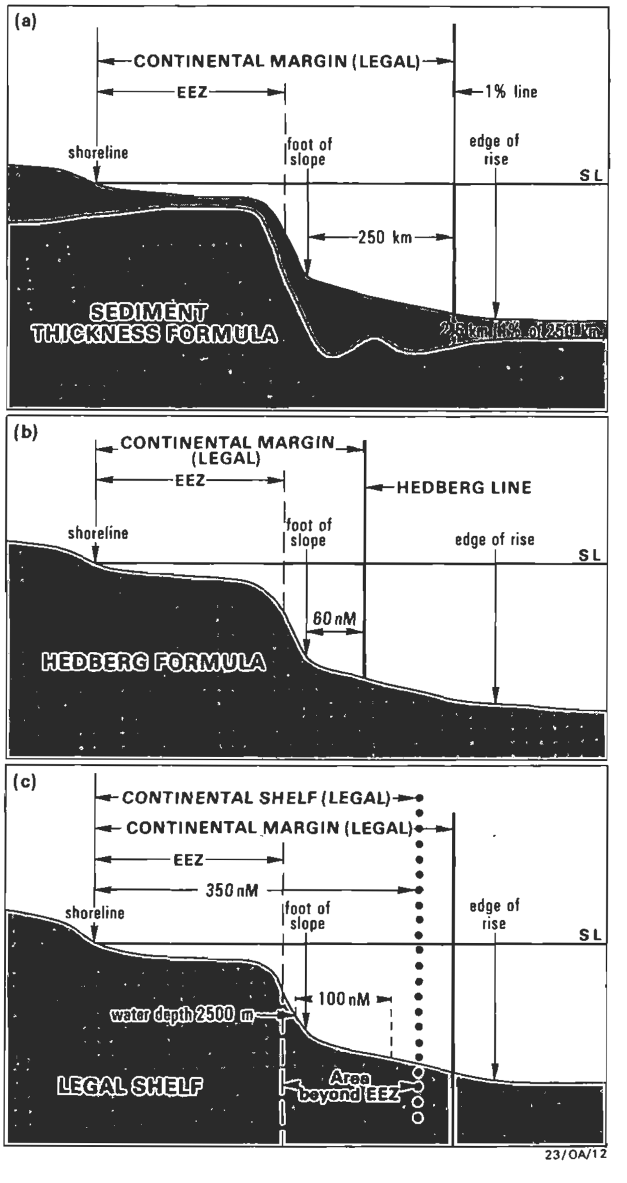

Figure 3. United Nations Convention on the Law of the Sea (Article 76) — procedures to determine seabed boundaries.
Definition of a Continental *Margin*, **(a)** using Sediment Thickness Formula (ie. thickness equal to 1 per cent of distance from foot of slope), and **(b)** Hedberg Line (60 nautical miles beyond foot of slope). **(c)** Definition of a Legal Continental *Shelf* using cutoff formula (a maximum of 350 nautical miles from the shoreline (actually baselines) or 100 nautical miles beyond the 2500 m isobath, whichever is the greater). Also shown is the area of a Legal Continental Shelf beyond an EEZ under consideration in this paper.

Owing to a lack of deep drilling in all eight regions, our understanding of the lithologies and depositional environments has to be inferred from seismic stratigraphy, and by analogy either with better known areas of similar geological style, or, in places, with contiguous areas within an EEZ.

The prospective areas within each region beyond an EEZ are labelled A1, A2, A3, etc., in Figures 4, 7 and 12.

Geology of regions beyond an EEZ

Lord Howe Rise (Region A)

Australia's seabed claim in this region stems from the presence of Lord Howe and Norfolk Islands, which are Australian territory and would both generate EEZs.

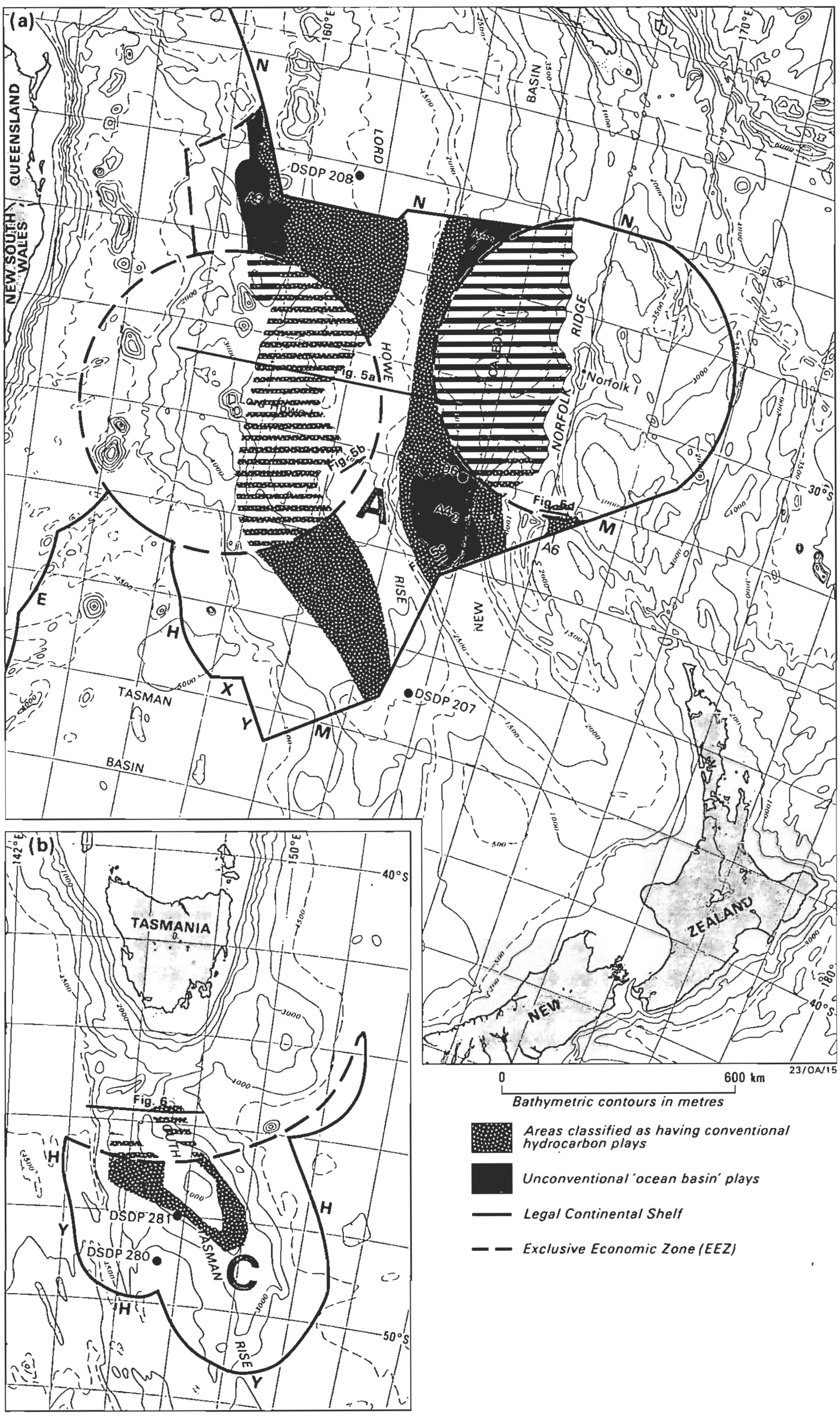

Figure 4. An EEZ and Legal Continental Shelf in (a) Lord Howe Rise/Norfolk Ridge Region (A), and (b) South Tasman Rise Region (C).

The criteria used to define a Legal Continental Shelf are: E = EEZ, H = Hedberg Line, X = 350 nautical mile cutoff, Y = 100 nautical mile beyond 2500 m isobath cutoff; N = negotiated boundary, M = median line with the adjacent coastal state. Isobaths are in metres. Shading shows areas of 'conventional' and 'unconventional' petroleum plays (see text), with $A1_1$, A_2, etc., being the areas referred to in Tables 3, 4 & 5. DSDP 206, 207, 208, 280 & 281 are Deep Sea Drilling Project drill sites. Heavy lines show location of seismic profiles and cross-sections presented in Figs 5 & 6.

Petroleum potential ratings: western LHR ($A1_1$ & $A1_2$)– fair; eastern LHR (A2)– fair/poor; Middleton Basin (A3)– unknown; New Caledonia Basin ($A4_1$ & $A4_2$)– unknown; West Norfolk Ridge (A5)– fair/poor; Taranui Sea Valley (A6)– fair; South Tasman Rise ($C1_1$ & $C1_2$)– fair/poor.

Regional physiography The major submarine feature in the region, the Lord Howe Rise (Figs 1 & 4a), extends north—northwest from the south island of New Zealand to Lord Howe Island and then north to the Chesterfield Island group at about 20° S. Lord Howe Rise is a plateau-like feature, which is most clearly defined by the 2000 m isobath — the crest of the rise is generally 750 to 1200 m below sea level. Lord Howe Rise is separated from the Norfolk Ridge by the New Caledonia Basin, which is an ocean basin with a relatively flat floor 3000–3500 m deep.

The Norfolk Ridge system is a steep-sided feature about 75 km wide, which extends from New Zealand to New Caledonia. The southern part of the ridge is offset to the west and forms a double-ridge system. The western part of the ridge is generally referred to as the West Norfolk Ridge; and the eastern part, as the Norfolk Ridge or, sometimes, the Wanganella Ridge (Eade, 1984). The crestal relief of the Norfolk/West Norfolk Ridge is more rugged than that of the Lord Howe Rise, and the depth ranges generally from about 500 to 1000 m. The two parts of the double-ridge system are separated by a narrow bathymetric trough, the Wanganella Trough. A significant bathymetric trough — the Taranui Sea Valley — lies on the eastern flank of the double-ridge system, near its point of offset.

Between 26° S and 34°, the small Middleton and Lord Howe Basins separate Lord Howe Rise from the Dampier Ridge to the west. Beyond this, the 4500 m deep Tasman Basin extends to the narrow continental margin of eastern Australia.

Regional geology The crustal structure of the Tasman Sea Basin, as interpreted from seismic refraction and gravity anomaly measurements (Officer, 1955; Dooley, 1963; Shor & others, 1971; Woodward & Hunt, 1971), and confirmed by identifiable seafloor spreading magnetic anomalies (Ringis, 1972; Weissel & Hayes, 1977), indicates that it is a normal oceanic basin. The crust beneath the New Caledonia, Middleton and Lord Howe Basins is commonly considered to be oceanic, though it is slightly thicker than typical oceanic crust.
Seismic refraction surveys and gravity modelling over Lord Howe Rise (Shor & others, 1971) indicate a crust 26 km thick and of continental origin. The rise is largely composed of crust with a P-wave velocity of 6.0 km/s, which is similar to values found for the Australian continent (Shor & others, 1971). Thus the Lord Howe Rise is a fragment of continental crust, seismically indistinguishable from the Australian continent. The complex nature of basement rocks beneath Lord Howe Rise, as shown by their seismic character and magnetic response, indicates that these rocks may once have formed part of the similarly complex Tasman Fold Belt of eastern Australia.

The Dampier Ridge is thought to be a continental fragment altered by rifting and igneous intrusions, and this theory seems to be confirmed by samples dredged by R/V *Sonne*, which has recovered granite, microdiorite and feldspathic sandstone (Roeser & others, 1985). The Lord Howe Rise and Dampier Ridge were detached from Australia during seafloor spreading, which commenced some 80 Ma ago and formed the Tasman, Middleton and Lord Howe Basins.

There is general agreement that at least part of the Norfolk Ridge system was rifted and separated from Gondwanaland, probably during the Late Cretaceous (Willcox & others, 1980; Kroenke, 1984), but several hypotheses have been advanced to explain the Tertiary development of New Caledonia and the Norfolk Ridge, and the adjacent New Caledonia Basin. These include the evolution of a complex arc system (Dubois & others, 1974; Kroenke, 1984), arc migration and marginal basin development (Karig, 1971; Packham & Falvey, 1971). The pre-Permian metamorphic and sedimentary rocks forming the core of New Caledonia were once part of the ancient Australian (Gondwanaland) continent, so it is most probable that the core of the Norfolk Ridge is also continental.

The plate tectonic model for the evolution of this part of the southwest Pacific appears to have been one of progressive rifting of the eastern margin of the Australia–Antarctic supercontinent (Gondwanaland), followed by continental break-up and seafloor spreading, island arc development and the creation of new ocean basins by further seafloor spreading. The fragments of continental crust that were rifted, thinned and left stranded between the Tasman Basin and the New Caledonia Basin during this process subsided to form a complex zone of troughs and plateaus, extending from New Zealand in the south, through Lord Howe Rise, to the Queensland Plateau in the north.

Recently, the region has been interpreted in terms of a detachment model (Lister & others, in press; Etheridge & others, in press) in which southeastern Australia is an underplated upper plate margin, with the Lord Howe Rise/Norfolk Ridge region being its complementary lower plate margin. This implies that a detachment system underlies the whole region, and that the Lord Howe Rise and Norfolk Ridge are composed of extended upper continental crust, whereas the small intervening ocean basins (except for the Tasman Basin) may be floored by highly thinned lower continental crust.

Western Lord Howe Rise (Areas A1_1 & A1_2, Fig. 4a; Fig. 5a,b) The general absence of Cretaceous extensional (rift) basins on the eastern seaboard of Australia has led to speculation that the basins may have become detached, and are now located beneath the western flank of Lord Howe Rise (Jongsma & Mutter, 1978). A zone of horst and graben structures, probably of this age and some 200 km wide, has been described (Fig. 5a; Willcox & others, 1980). The grabens are up to 50 km wide, several tens of kilometres long, and trend north–northwesterly. They terminate abruptly at transfer-like faults (Gibbs, 1984); the oblique angle that these faults make with the normal extensional faults suggests that the grabens formed within a 'transtensional zone'. These grabens are best developed on the western half of Lord Howe Rise north of Lord Howe Island, where their sediment fill is up to 4500 m thick in places (Roeser & others, 1985). Extensional basins south of Lord Howe Island appear to be less complex. Recent work (Whitworth & Willcox, 1985) has indicated that some fault blocks in the southern area may contain dipping sedimentary strata of Mesozoic age, rather than solely Tasman Fold Belt rocks, as previously believed (Fig. 5b). These sediments may be age equivalent to the older (Strzelecki) sequences in the Gippsland Basin.

The nature of the sediment fill within the Lord Howe Rise basins is a matter for conjecture. It is generally assumed to be of Late Mesozoic age, but correlation with older eastern Australian basins — such as the Permo-Triassic Sydney Basin and Esk Trough, and the Triassic–Jurassic Clarence Morton Basin — cannot be completely dismissed. There are, for example, strong similarities between some seismic profiles on Lord Howe Rise and profiles in the Esk Trough region (BMR *Geotraverse* 16, Korsch & others, 1989), which warrant closer scrutiny.

If, however, the Lord Howe Rise basins formed according to classical models for development of Atlantic-type passive

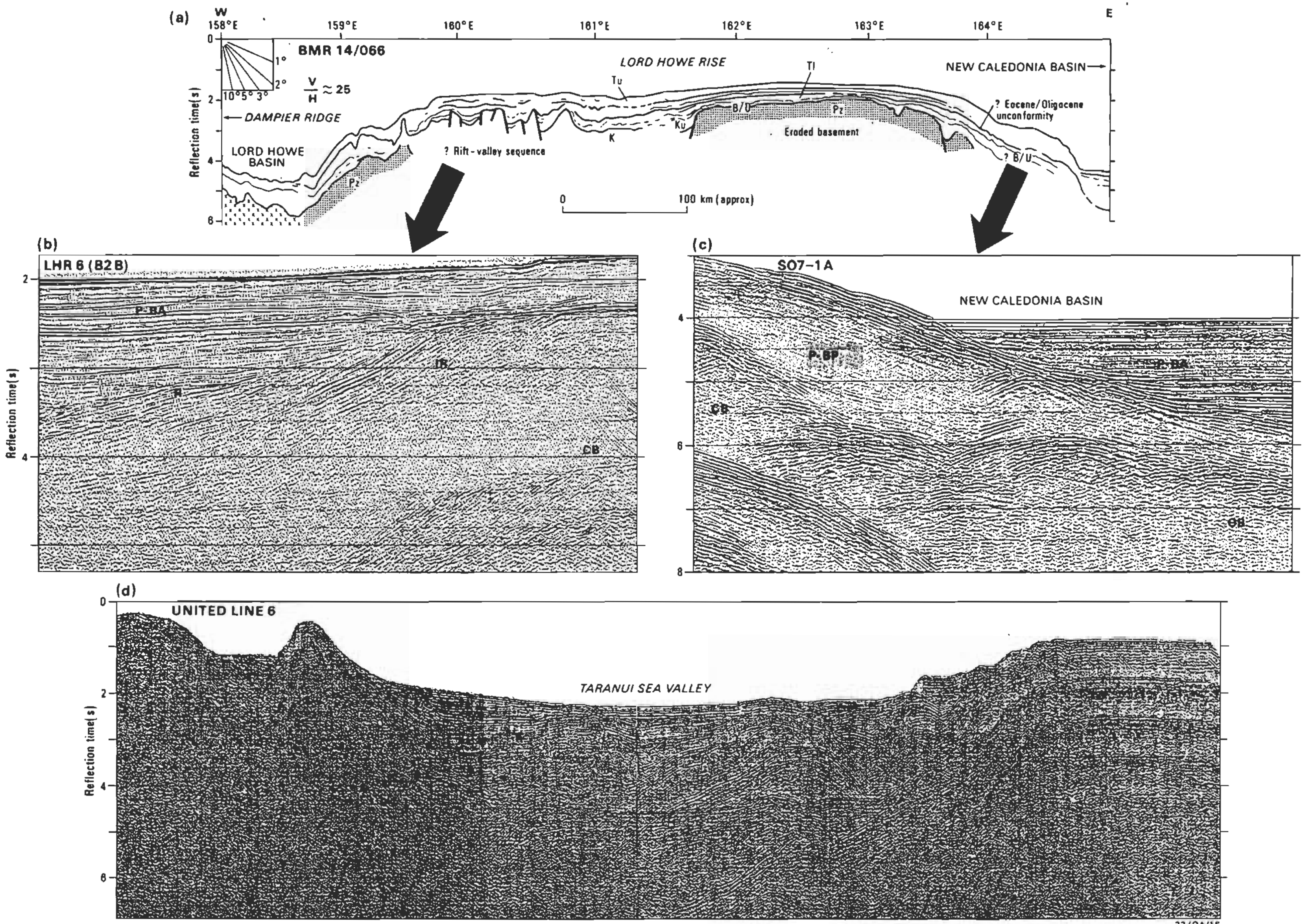

Figure 5. Cross-section and sesmic profiles from Lord Howe Rise (lHR) Region (A) (locations given in Fig. 4).

(a) Cross-sections of **LHR** based on **BMR** Line 14/066 (after Willcox, 1981). Tu = Miocene—Recent, Tl = Paleocene—Oligocene, **K** = Late Cretaceous, Pz = Palaeozoic, **B/U** = breakup unconformity, crosses = basement of unknown origin (possibly oceanic). Arrows show approximate structural location of seismic details below. **(b)** Seismic details from **BMR** *Rig Seismic* Line **LHR6** (width ~ 11 km) showing a sediment-filled graben on the Western flank of **LHR.** **(c)** Seismic detials from **BGR** *Sonne* Line S07-1A (width ~ 25 km), showing a wedge of pre-Maastrichtian sediment on the anicent on the ancient continental margin, now the eastern edge of **LHR. CB** =continental basement, **OB** =? **oceanic basement, IR** = infrarift (pre-rift) section, **R** = rift-fill sediments, **P—BA** = post-breakup (aggradation), **P-BP** = post-breakup (progradtion). **(d)** Seismic profile, United Line 6 (width ~ 65 km), from West Norfolk Ridge (left) to Norfolk Ridge (right), showing thick folded and faulted sediments in the intervening taraning Sea Valley, continental margins, much of the earliest sediment fill would have been of fluvial-lacustrine origin, which could contain a high proportion of humic source material. During recent surveys, diapiric structures were identified which suggest the movement of shale, or possibly salt, within the basins (Roeser & others, 1985). In the overlying section, there is evidence that wave-base erosion has planated several of the horst blocks, and it can be inferred that a shallow (?anaerobic) sea, which would be expected to favour the deposition of oil-prone source rocks, may have occupied the intervening grabens during the Late Cretaceous. Results from the Deep Sea Drilling Project (DSDP) Site 207 (Burns & others, 1973) confirm that restricted shallow marine silts and clays of Maastrichtian age overlie the horst blocks of the southern Lord Howe Rise. Rocks of similar age and depositional environment were recently dredged from the deep continental slope off southern New South Wales (Packham, University of Sydney, personal communication, 1985). Hence, up to 3000 m of sediment containing potential petroleum source rocks may occur in the basins of the western Lord Howe Rise. Interbedded sandstone in the fluviatile and shallow marine sequences is the most likely potential reservoir rock, and pelagic ooze could provide a regional seal. Lord Howe Rise has been subjected to several periods of volcanism, but it is not known whether this had any adverse affect on the reservoir potential of rocks within the basins.

In most places on Lord Howe Rise, the Maastrichtian shallow marine sequence is overlain by less than 1000 m of overburden, which is probably an insufficient thermal blanket for petroleum generation, unless heat flow was abnormally high. Thus, in these areas, petroleum generation may only have taken place at depth within the grabens. On the eastern flank of the Lord Howe and Middleton Basins (Figs 1, 4a), however, the sedimentary overburden may be thick enough (up to 2000 m) for any source material within the Maastrichtian sediments to have matured.

The rift basins of the Lord Howe Rise might be expected to have had high geothermal gradients at the inception of seafloor spreading, and source rocks might well have matured with less overburden than would normally be required. There are some indications that heat flow is anomalously high. The only heat-flow measurement on the Lord Howe Rise, recorded on its western margin, gave a value of 100 mW/m^2 (Grim, 1969), which is about twice normal. It has also been suggested that the Tertiary volcanism in the region is related to northward drift over a mantle hot-spot (Vogt & Conolly, 1971), implying that a zone of high heat flow associated with the Lord Howe seamount chain might be present on the western Lord Howe Rise.

Reconstruction of the Australian region in the Cretaceous brings the central area of the Lord Howe Rise (just south of the Dampier Ridge) against the Gippsland Basin (Jongsma & Mutter, 1978; Shaw, 1978). It has been suggested that the Gippsland Basin formed within the failed-arm of a three-branched rift system (Burke & Dewey, 1973), and this implies that dissected remnants of the other arms should occur beneath Lord Howe Rise. According to Threlfall & others (1976), the non-marine shales and coals of the uppermost Cretaceous and Palaeocene Latrobe Group are the source of the oil and gas in the Gippsland Basin. The petroleum is most commonly trapped at the Eocene/Oligocene unconformity, which lies at the top of the Latrobe Group. The development of successive shorelines and palaeoslopes in the eastern part of the Gippsland Basin, and the dredging of shallow marine ?Latrobe Group from deep on the continental slope (Packham, University of Sydney, personal communication, 1985) strongly suggest that parts of the Latrobe Group have had a laterally equivalent marine section to the east, that is, now on Lord Howe Rise. In addition, the transition from predominantly continental to predominantly marine deposition is thought to have occurred earlier in the east. Thus rocks of similar type to those producing hydrocarbons in the Gippsland Basin, but of somewhat greater age, may have been deposited deep within the grabens on Lord Howe Rise.

Eastern flank of Lord Howe Rise (Area A2, Fig.4a; Fig. 5a,c) The eastern flank of Lord Howe Rise might have formed an ancient seaboard of the Australian-Antarctic supercontinent (Willcox & others, 1980). A considerable thickness (about 2000 m) of clastic sediment was deposited across this margin during or before the Late Cretaceous (Fig. 5c). Most of this sediment was probably derived from the now planated basement blocks to the west. The sedimentary (?pelagic) overburden ranges from about 1000 m on the eastern edge of the Lord Howe Rise to more than 2000 m in the New Caledonia Basin.

Depositional environments favourable for both the production and preservation of oil-generating matter of aquatic origin may have occurred on this continental slope, as is thought to be the case on many other continental slopes around the world (Dow, 1979).

Faulting, and folding of the? Late Cretaceous sediment wedge, could provide structural traps for petroleum. The progradation observed on some profiles may give rise to stratigraphic traps (Fig. 5c). Petroleum migrating up dip could be trapped against the basement surface and at unconformities, and sealed by the overlying pelagic oozes.

Middleton Basin (Area A3, Fig. 4a) Considerable thicknesses of Late Cretaceous sediments, including potential source rocks, might occur in area A3 on the flanks of the Middleton Basin, in a similar manner to that previously described for the rift basins beneath the western Lord Howe Rise. During rifting and the earliest phase of seafloor spreading in the late Cretaceous, Lord Howe Rise was probably a trough-bounded marginal plateau with the trough centred on the Lord Howe and Middleton Basins (Willcox & others, 1980). This implies a stronger marine influence within the Middleton Basin than within the rift basins beneath the Lord Howe Rise. The latest Cretaceous rocks are probably carbonate and terrigenous sediments deposited in a restricted marine environment.

New Caledonia Basin (Areas $A4_1$, $A4_2$, Fig. 4a; Fig. 5c) The New Caledonia Basin may contain at least 4000 m of sediment (3 s of reflection time) in places and, near its margins, the basal 2000 m of this section probably consists of Cretaceous marginal and shallow marine terrigenous sediments. This sequence was gently folded throughout the basin during the Late Cretaceous and early Tertiary, perhaps in response to convergent tectonics to the east. The basal sequence is overlain by deep-sea biogenic ooze.

The prospectivity of the New Caledonia Basin is difficult to assess, as both its origin and the depositional environment of the deeper sediment are uncertain. In theory, small enclosed ocean basins are among the most promising areas for petroleum accumulation (Hedberg & others, 1979). Proximity to land and large rivers ensures deposition of thick sedimentary sections, where both terrestrial and marine organic matter accumulate, even in the centre of the basins. The restricted nature of the basins limits circulation and favours the preservation of organic matter, either under bottom-reducing conditions or as a result of relatively rapid burial by sediments. Favourable reservoirs are to be expected in deltaic and submarine fan sediments within these basins. Small ocean basins, such as the New Caledonia Basin, are often situated in tectonically mobile environments, where fold and fault structures and repeated unconformities provide numerous play types.

West Norfolk Ridge (Area A5, Fig. 4a) In area A5, the offset southern extension of the Norfolk Ridge is actually a double-ridge system consisting of the broad West Norfolk Ridge in the west and the narrow Norfolk Ridge in the east; the two ridges are separated by the Wanganella Trough. A significant bathymetric trough called the Taranui Sea Valley occurs on the eastern flank of the double-ridge system near the point of offset of the ridge (Fig. 1).

The western part of the West Norfolk Ridge is underlain by relatively planar basement, which has been downfaulted to form flanking grabens which, in places, contain up to 3000 m of sediment. The sediments in the grabens are probably very similar to those already described within the rift basins beneath the Lord Howe Rise; however, on the West Norfolk Ridge, the rift-fill sediments have been folded, resulting in a larger variety of structural petroleum plays than on the Lord Howe Rise. The northern end of the Wanganella Trough (between areas A5 and A6) is underlain by at least 1500 m of sediment containing mounded and progradative facies. This might be a deltaic sequence deposited along the trough during subaerial erosion and planation of the northern West Norfolk ridge. This sediment undoubtedly thickens to the south beyond Australia's putative Legal Continental Shelf.

Taranui Sea Valley (Area A6, Figs 4a, 5d) Up to 4000 m of faulted and folded sedimentary rocks occur in a graben-like feature beneath the head of the Taranui Sea Valley, in less than 2000 m of water (Fig. 5d). Several prominent angular unconformities occur throughout the sedimentary section, but both the nature and depositional environment of the sediments and the nature of the underlying basement are unknown.

The structural style of the basin suggests wrench tectonics, and could indicate that the sediments were deposited in a dextral strike-slip zone which was responsible for the offset of the Norfolk Ridge.

South Tasman Rise (Region C: Areas $C1_1$ & $C1_2$, Fig. 4b)

The South Tasman Rise lies in water about 1000–3000 m deep, and is separated from the Tasmanian continental slope by a bathymetric and structural saddle (Figs 1 & 4b). The area of the Rise is about 150 000 km², and 70 per cent of the feature lies beyond an EEZ. Its margins appear to be shear zones related to the dispersal of Australia and Antarctica during the Late Cretaceous to Eocene (Willcox, 1986).

The generalised structure of the South Tasman Rise was interpreted by Willcox (1981) from two BMR seismic profiles across its northern part (Fig. 6). More recent seismic and geological sampling cruises (R/V *Sonne*; Hinz & others, 1985) have provided sufficient information for a regional analysis of its structure and seismic stratigraphy. Deep Sea Drilling Project Sites (DSDP) 280 and 281 (Fig. 4b) are located on the deep ocean floor to the south and near the structural culmination of the rise, respectively.

A continental origin for the South Tasman Rise is deduced from its location in continental reconstructions, the drilling results at DSDP Site 281, and its relatively quiet gravity and magnetic signature. At drill site DSDP 281, basement is composed of mica-schist overlain by a basal angular agglomerate. This agglomerate is overlain by late Eocene detrital sediments deposited in a shallow marine, deepening to a marine, environment. The drillhole penetrated Miocene to Holocene ooze above the late Eocene to Oligocene unconformity, which is widespread in the Tasman and Coral Seas.

The seismic interpretation suggests that the South Tasman Rise consists of a central, probably Palaeozoic, core flanked by two northwesterly trending rift basin systems (Areas $C1_1$ & $C1_2$), which contain up to 4000 m of sediment. The sedimentary sequences have been correlated with the Cretaceous and Tertiary of the Otway Basin (Willcox, 1981; Hinz & others, 1985). The basins are structurally complex, and potential reservoir porosity has probably been down-graded by the inclusion of volcanics. Whiticar & others (1985) reported small yields of thermogenically derived hydrocarbons from geological samples dredged from the northern extremity of the plateau.

Great Australian Bight (Region D: Areas D1 & D2, Fig. 7a)

In the Great Australian Bight, approximately 25 000 km² of continental rise to the southwest of the Ceduna Terrace lies beyond the EEZ (Figs 1 & 7a). Tertiary and Cretaceous sediments, 4000–5000 m thick, overlie deeply subsided continental (Area D1) and oceanic basement (Area D2) (Fig. 8; Willcox, 1978; Fraser & Tilbury, 1979). Early Cretaceous sediments, probably deposited in continental to shallow marine environments, might have hydrocarbon potential. In the past, most authors have suggested that the Early Cretaceous deposits are of dominantly continental origin; however, this view needs some revision in the light of Potoroo-1 and Jerboa-1 wells, which intersected Aptian and Albian sediments of restricted and near-shore marine origin, respectively (Stagg & Willcox, 1988). Marine sedimentation was presumably a consequence of an incursion from the west along the subsiding rift system. If restricted marine deposition occurred on the northern margin of the rift valley, then it seems reasonable to suppose that deeper, and possibly more protracted, marine conditions prevailed

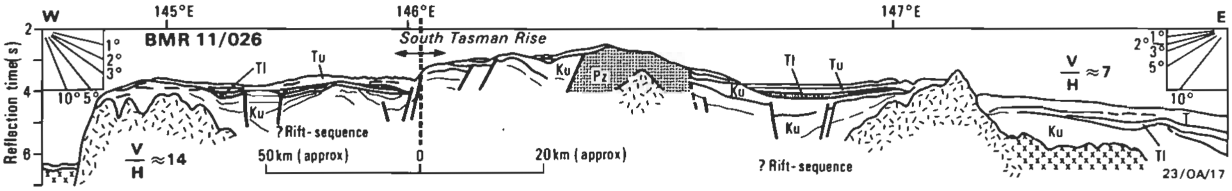

Figure 6. Cross-section of South Tasman Rise Region (C)
Based on BMR Line 11/026, showing rift basins developed on the flanks of the Rise (after Willcox, 1981). Note change in horizontal scale at about 146° E. Location given in Fig. 4.

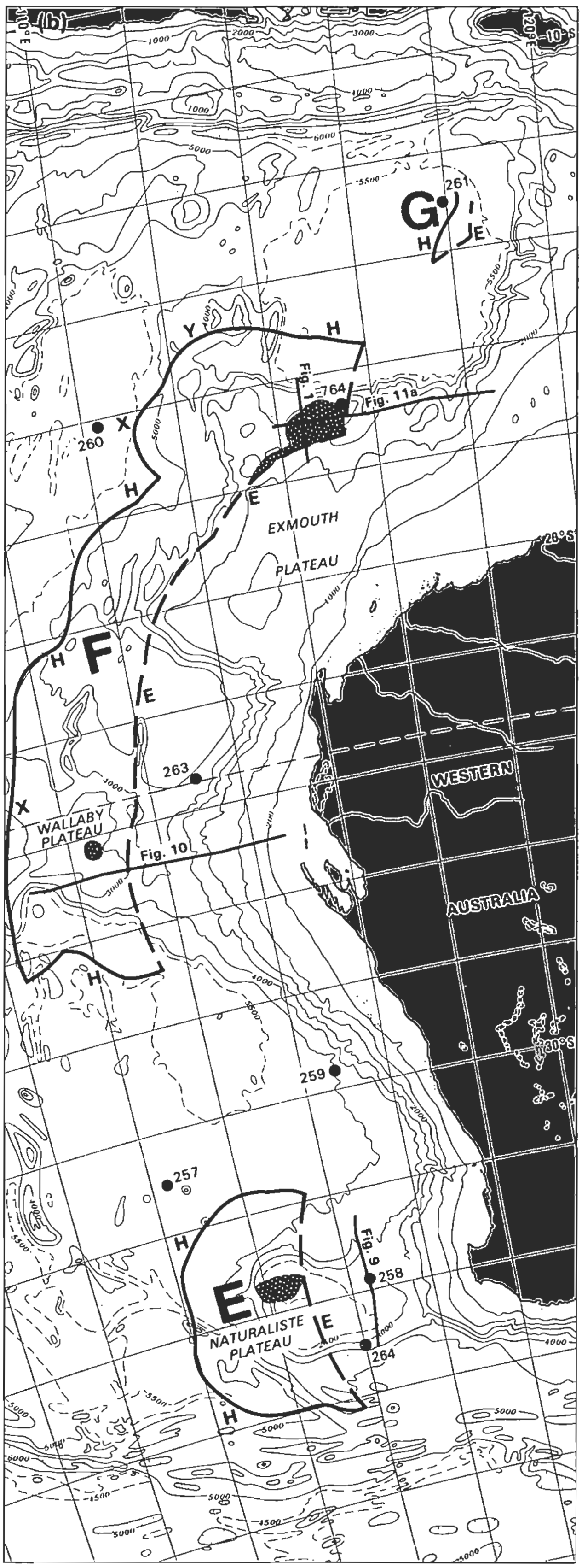

over the depressed valley floor in the Bight region to the south. The presence of marine source rocks beneath the deepwater part of the Great Australian Bight Basin would considerably enhance its prospectivity.

In this region the basin-forming faults within basement indicate northwest-southeast extension (Lister & others, in press; Willcox & others, in press). Also prominent are Cenomanian northwest-southeast-trending normal faults, which are synsedimentary and have produced some drape and rollover in the overlying section. In the deeper water part of the basin, close to the northern boundary of region D, faulted anticlines have resulted from relative movement and dip reversal in closely spaced fault blocks (Fig. 8a).

In the past, the main problems perceived for oil exploration within the Great Australian Bight Basin were considered to be an apparent dearth of marine source rocks and a lack of reservoir sands, together with the uneconomic size of the structural traps in relation to the considerable water depths. A greater volume of marine source rocks can be expected in the deeper part of the basin in region D, but the great water depths (3000–5500 m) will certainly discourage exploration.

Naturaliste Plateau (Region E: Area E1, Fig. 7b)

About 50 per cent of the Naturaliste Plateau lies beyond an EEZ, in water 2200–5000 m deep (Figs 1, 7b). The origin

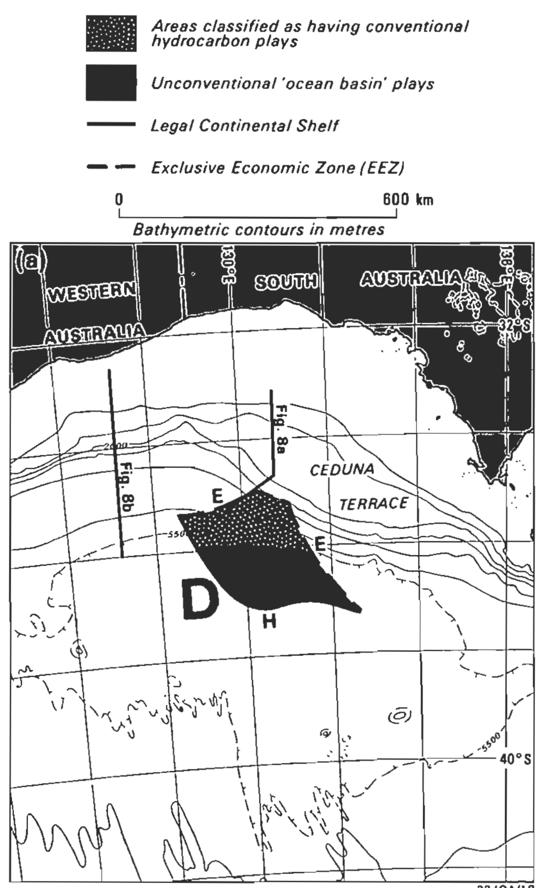

Figure 7. An EEZ and Legal Continental Shelf in (a) the Great Australian Bight Region (D), and (b) the Naturaliste Plateau Region (E), Wallaby/Exmouth Plateau Region (F) and Argo Abyssal Plain Region (G).

Criteria used to define a Legal Continental Shelf are: E = EEZ, H = Hedberg Line, X = 350 nautical mile cutoff, Y = 100 nautical mile beyond 2500 m isobath cutoff. Isobaths in metres. Shading shows areas of 'conventional' and 'unconventional' petroleum plays (see text), with D1, D2, etc., being the areas referred to in Tables 3, 4 & 5. 257, 258, 259, 260, 261, 263 and 264 are Deep Sea Drilling Project (DSDP) drill sites, and 764 is an Ocean Drilling Program (ODP) site. Heavy lines show the location of cross-sections presented in Figs 8, 9, 10 & 11.

Petroleum potential ratings: Great Australian Bight Region mid-slope (D1)- poor; lower slope and basin floor (D2)- unknown; Naturaliste Plateau (E)- poor; Wallaby Plateau (F1)- poor/nil; northwest Exmouth Plateau (F2)- fair/poor.

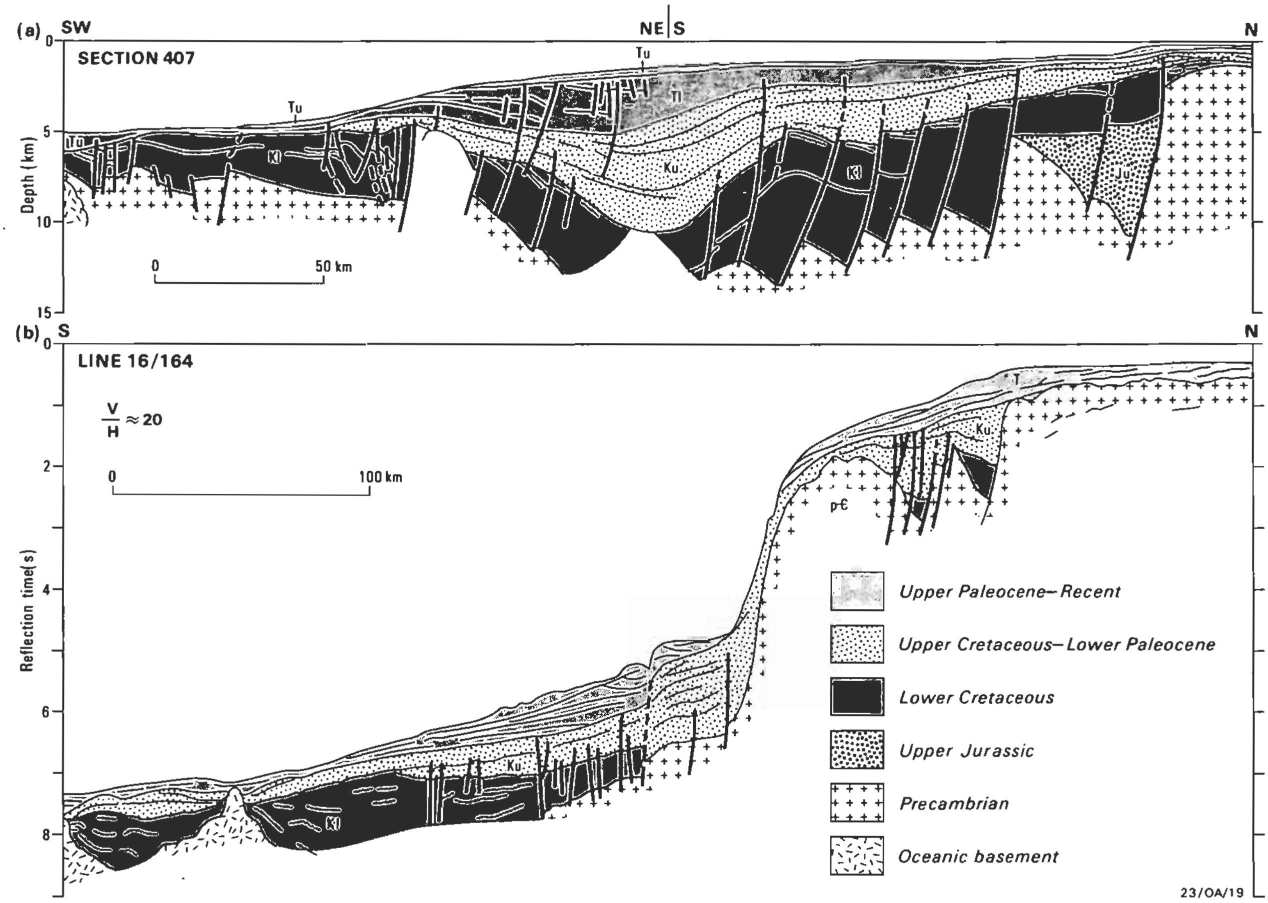

Figure 8. Cross-sections of the Great Australian Bight Region (D). Locations in Fig.7.
(a) Shell Line 407, across Ceduna Terrace area, showing the very thick (12+ km) sedimentary section in the Great Australian Bight Basin, extending under the continental rise beyond an EEZ (after Boeuf & Doust, 1975). **(b)** BMR Line 16/164, across the Eyre Terrace (Eyre Sub-basin) and continental rise, showing the thick sedimentary section in 3000+ m deep water (after Willcox, 1978). A similar section lies beyond an EEZ in the central Bight; opinion is divided as to whether the basement is oceanic (suggesting 'unconventional' play-types may be present) or of extended continental origin.

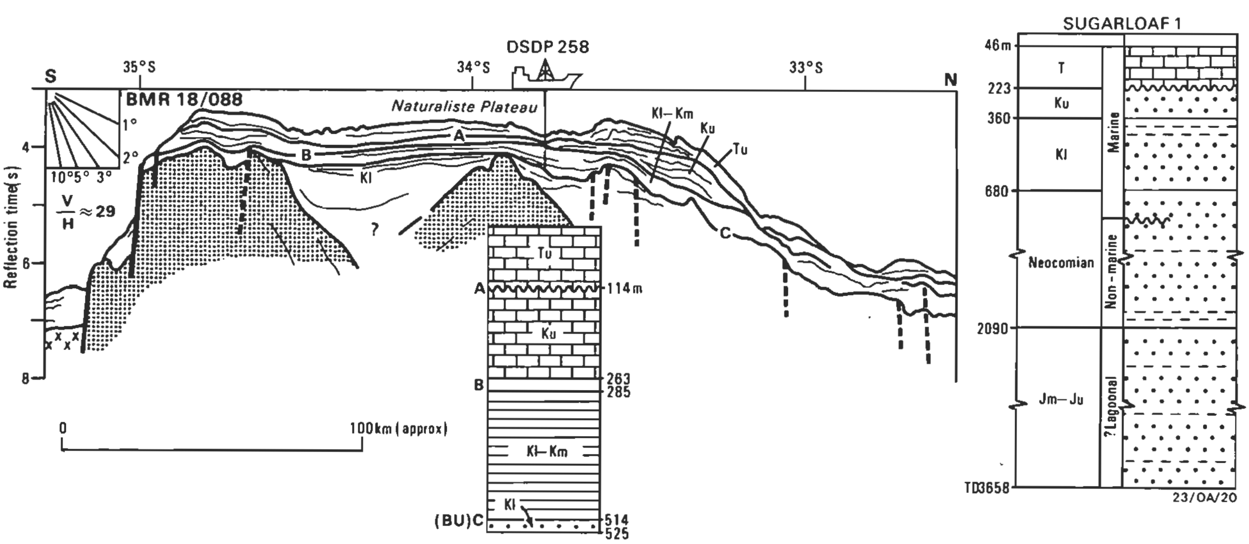

Figure 9. Cross-section of the Naturaliste Plateau Region (E), based on BMR Line 18/088 (after Willcox, 1981). Also shows stratigraphy for DSDP Site 258 and WAPET Sugarloaf No. 1 exploration well in the Perth Basin. Location in Fig. 7.

of the Naturaliste Plateau is uncertain, like that of the Wallaby Plateau (see later), but the weight of evidence tends to favour it being a continental feature (Jongsma & Petkovic, 1977).

The western part of the Naturaliste Plateau is similar to the Wallaby Plateau and contains few areas with thick sediment (Fig. 9). However, beneath the eastern part of the Plateau, within the EEZ, pre-breakup strata up to 2000 m thick lie between major crystalline basement blocks. Sonobuoy data show that these pre-breakup strata incorporate a refractor with a velocity of only 2.8 km/s, not uncommon for 'normal' rift-fill sediments. However, this velocity does not preclude volcanogenic sediments either. The post-breakup sediments are about 500 m thick over most of the area, but up to 2000 m thick in the Naturaliste Trough, which lies between the Plateau and the continental shelf.

The Naturaliste Plateau section can be dated by tying to an on-site sonobuoy profile recorded at DSDP Site 258, close to BMR Line 18/088 (Fig. 9). The tie indicates that the Horizon C unconformity is pre-middle Albian, the B reflector marks a contact of Albian detrital clay and Cenomanian chalk, and the A reflector lies within Miocene to Holocene foraminiferal ooze. The C unconformity can be dated more closely by making a tentative tie to Sugarloaf-1 well on the adjacent continental shelf (Willcox, 1981). It appears to correlate with the top of a Neocomian sandstone, and hence probably marks the onset of marine conditions and seafloor spreading in what is now the Perth Abyssal Plain. The sediments below this unconformity might have been deposited in marginal marine and continental environments and could have some petroleum prospectivity.

Two heat-flow measurements on the Naturaliste Plateau provide little information on source rock maturity. An extremely high value of about 220 mW/m^2 was obtained in the northwestern part of the Plateau (von Herzen & Langseth, 1965), but it is of doubtful accuracy. The other measurement, near DSDP Site 264, gave a near-average value of about 60 mW/m^2 (Jongsma & Petkovic, 1977).

The prospectivity of the Naturaliste Plateau beyond the EEZ is rated as poor.

Wallaby and Exmouth Plateaus (Region F)

Wallaby Plateau (Area F1; Fig. 7b) Nearly all the Wallaby Plateau lies in water 2200–4500 m deep beyond the EEZ (Figs 1, 7b). The Plateau appears to be formed by a thin sequence of post-breakup sediments draped over a folded and faulted, layered sequence, which in places resembles the pre-Jurassic sequence on the Exmouth Plateau (Fig. 10; Symonds & Cameron, 1977; von Stackelberg & others, 1980).

Until the late 1970s, the Wallaby Plateau was regarded as a thinned continental fragment (Symonds & Cameron, 1977). Veevers & Cotterill (1978) suggested that it is an accumulation of oceanic volcanics (an 'epilith') formed during the time of spreading in the Cuvier Abyssal Plain. A variety of volcanic and volcaniclastic rocks of unknown ages, obtained during dredging on the margins of the Plateau, led von Stackelberg & others (1980) to conclude that on the eastern and southern Wallaby Plateau 'the layered sequence beneath the main Neocomian unconformity consists of interbedded and weathered tholeiitic and differentiated alkali basalts, tuffs, basalt breccias and thick volcaniclastic sandstones and conglomerates'. A minimum mid-Cretaceous K/Ar age of 89 Ma was determined from an altered basalt from the southern Wallaby Plateau. Because the sequence sampled can be traced on seismic profiles from the margins to the centre of the Plateau, von Stackelberg & others (1980) suggested that intense volcanism and associated deposition of volcaniclastic debris flows formed the Plateau, during or after the Neocomian breakup of this region. They mentioned the alternative interpretation that a marginal intrusion or extrusive sequence had been sampled, and stated that 'whether continental crust lies below the layered volcanic material could be tested only by deep drilling in the centre of the plateau'. A seismic profile which passes through the middle of their sampled area indicates that there could well be a marginal intrusive body at this location, and thus the sequences sampled might not be representative of the rocks beneath the centre of the Plateau.

The origin of the Wallaby Plateau remains in doubt. If continental, the layered sequence beneath the intra-

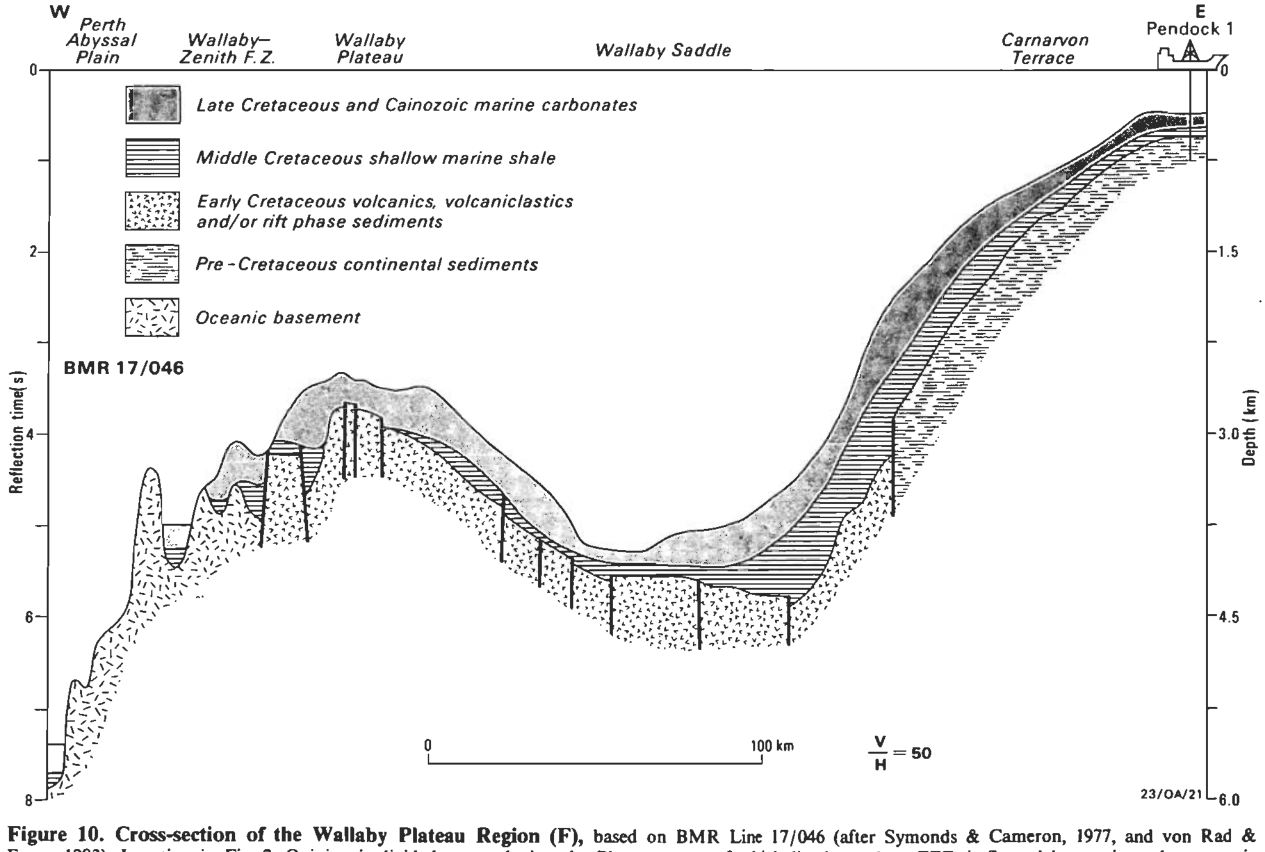

Figure 10. Cross-section of the Wallaby Plateau Region (F), based on BMR Line 17/046 (after Symonds & Cameron, 1977, and von Rad & Exon, 1983). Location in Fig. 7. Opinion is divided as to whether the Plateau, most of which lies beyond an EEZ, is floored by continental or oceanic basement.

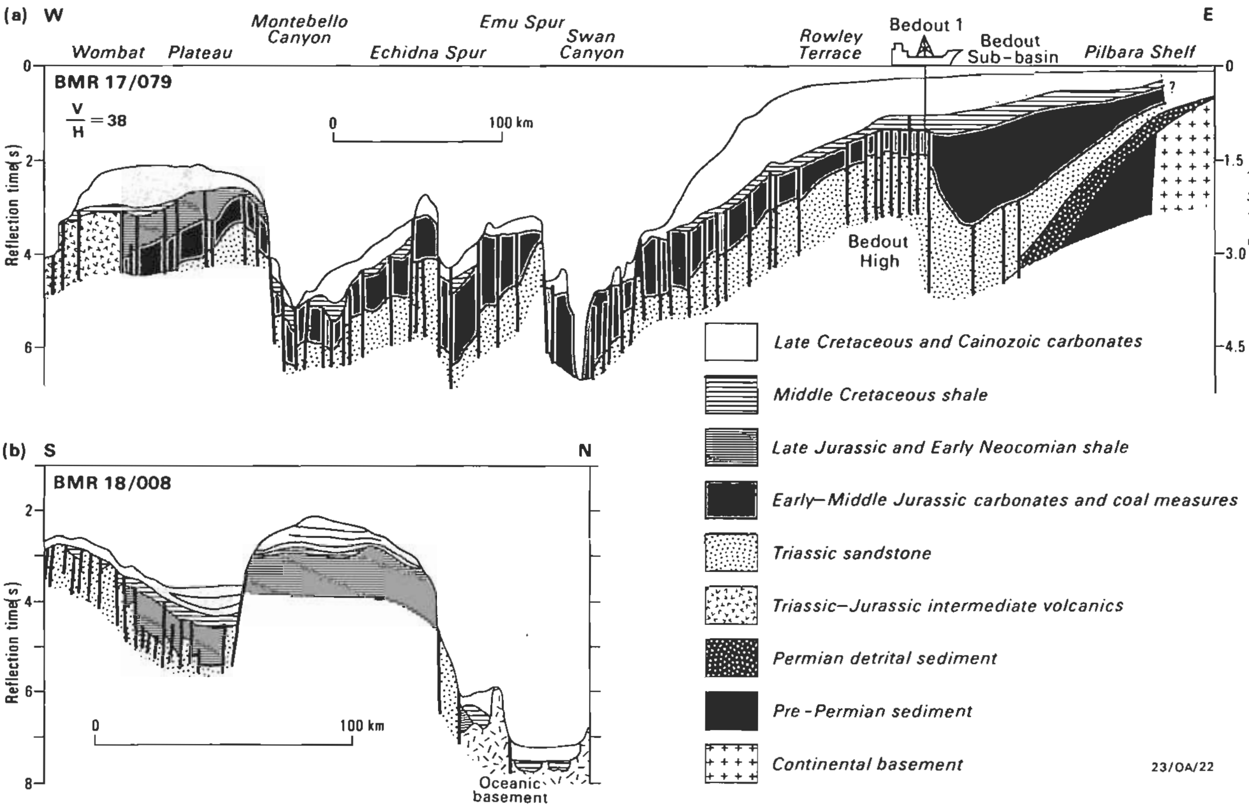

Figure 11. Cross-sections of the northern margin of the Exmouth Plateau Region (F), based on **(a)** BMR Line 17/079 from Wombat Plateau to Pilbara Shelf showing thick sediments on the numerous plateaus and spurs (after von Rad & Exon, 1983), and **(b)** BMR Line 18/008 showing prospective fault-block structures on the Wombat Plateau (after Exon & Willcox, 1980). Only the Wombat Plateau area lies beyond an EEZ. Locations given in Fig. 9.

Neocomian unconformity might consist of rift-phase sediments with some petroleum potential; however, if the sequence consists of volcaniclastics and lava flows, the Plateau would have no potential, owing to the absence of source and reservoir rocks.

Northwest Exmouth Plateau (Area F2, Fig. 7b) About 15 per cent of the area of prospective sediment on the Exmouth Plateau lies beyond the EEZ in water 1800–3000 m deep (Figs 1 & 7b). This includes the small Wombat Plateau (3000 km^2), from which samples of a Triassic to Middle Jurassic coal measure sequence have been dredged (von Rad & Exon, 1983). The northwest Exmouth Plateau is underlain by numerous fault blocks of probable Triassic age (Exon & Willcox, 1980) (Fig. 11). Although the Jurassic and younger strata are thinner in the northwest than elsewhere on the Plateau, this does not significantly affect the prospectivity of the Triassic blocks themselves, which still have ample overburden in places. Palaeogeographic considerations suggest that Triassic depositional environments might have been more marine in the north and northwest than elsewhere on the Plateau, thus favouring deposition of oil-prone aquatic kerogens (Willcox, 1981). Higher heat flow associated with intrusions, and proximity to ocean/continent boundary, might also be favourable factors. Recent drilling on the Wombat Plateau, as part of the Ocean Drilling Program (ODP), discovered a possible Triassic reef which could prove to be a significant new petroleum play in the region (Williamson & others, 1989).

Kerguelen Plateau (Region H: Areas H1 & H2, Fig. 12)

The Kerguelen Plateau is a major topographic high in the southern Indian Ocean adjacent to, but apparently structurally separate from, Antarctica (Fig. 1). The Plateau rises about 3700 m above the deep ocean floor and extends northwest for 2000 km. Australia's claim to the southern part of the Plateau stems from the presence of Heard and McDonald Islands which are Australian territory. About 70 per cent of the area to which Australia could lay claim lies beyond an EEZ, but this is complicated by the fact that about 40 per cent of this area overlaps with the Australian Antarctic Territory (AAT) beyond 60°S (Fig. 12). In this study, the areas of prospective sediment as far south as the saddle (Challenger Passage) between the Kerguelen Plateau and the margin of Antarctica are considered.

Heard, Kerguelen, and McDonald Islands consist of a series of Cainozoic volcanics overlying mid-Eocene-mid-Oligocene pelagic limestone (Nougier, 1969; Dosso & others, 1979; Clarke & others, 1983). The geology of the submerged part of the Plateau is poorly known. Geophysical surveys (Schlich & others, 1971; Houtz & others, 1977; Ramsay & others, 1986a,b) indicate that there are marked differences in the structure of the northern and southern parts of the Plateau. The northern sector includes the Plateau's islands and consists mainly of a series of igneous intrusions or basement horsts separated by basins. A major sedimentary basin lies immediately southeast of the Kerguelen Islands. By contrast, the southern sector shows evidence of intense block faulting (Ramsay & others, 1986b). The presence of a significant depocentre beneath the southeastern side of the Plateau was originally indicated by the study of Houtz & others (1977). A more recent BMR Rig Seismic survey in this area (Ramsay & others, 1986a) defined a large sedimentary basin (the Raggatt Basin), which occupies an area of about 50 000 km^2.

Any assessment of the petroleum potential of the Kerguelen Plateau is to some extent dependent on whether it has an

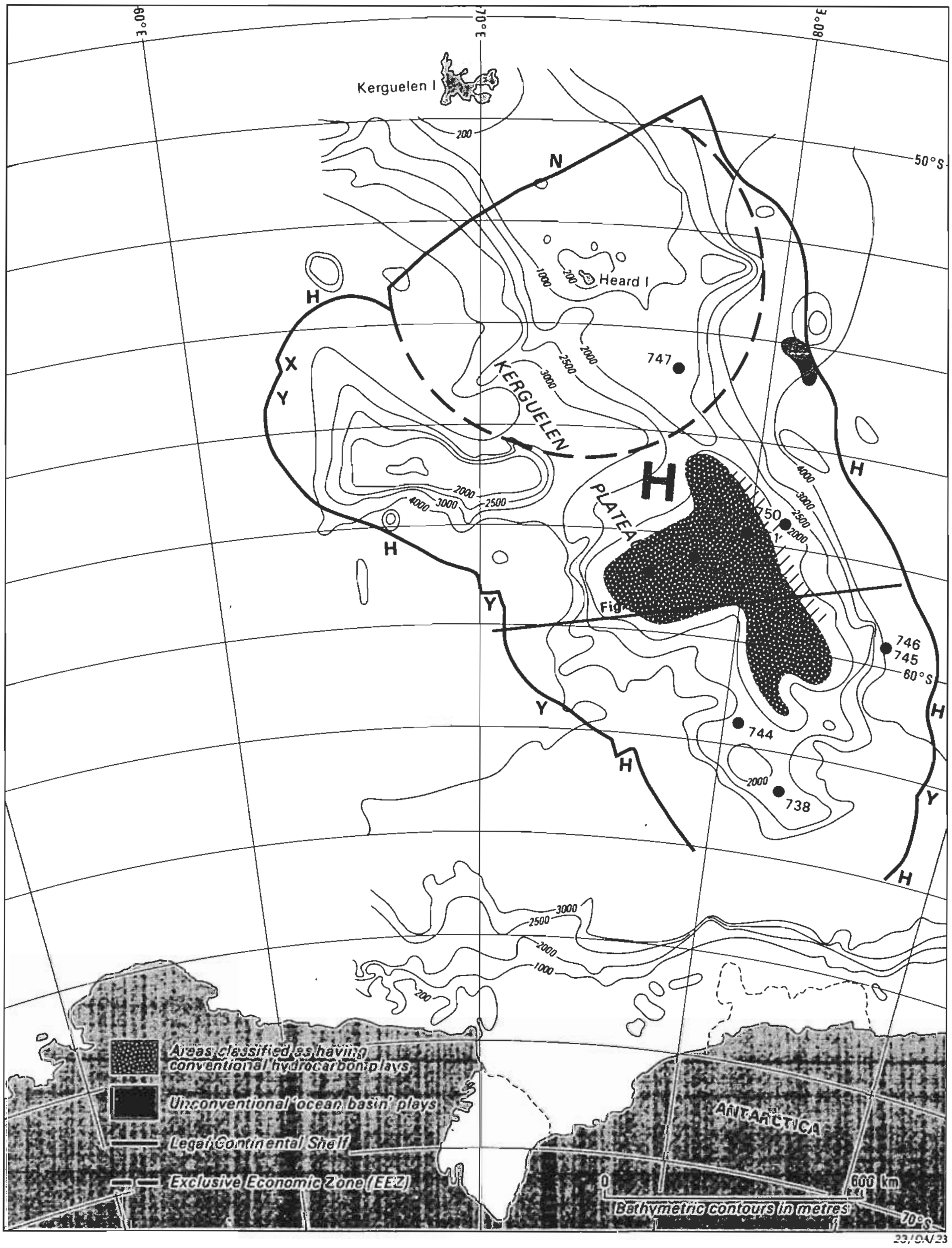

Figure 12. An EEZ and Legal Continental Shelf in the Kerguelen Plateau Region (H).
Criteria used to define a Legal Continental Shelf are: E = EEZ, H = Hedberg line, X = 350 n.m. cutoff, Y = 100 n.m. beyond 2500 m isobath cutoff; N = negotiated boundary with France. Isobaths are in metres. Shading shows areas of 'conventional' and 'unconventional' petroleum plays (see text), with H1 & H2 being the areas referred to in Tables 3, 4 & 5. Hatching shows approximate location of the recently discovered Raggatt Basin (Ramsay & others, 1986b). 738, 744, 745 and 746 are Ocean Drilling Project (ODP) drill sites. Heavy line shows the location of cross-section and seismic profiles in Fig. 13.
Petroleum potential ratings: southern Kerguelen Plateau (H1)- fair/poor (unknown basement type); eastern slope (H2)- poor/unknown.

oceanic or continental origin, and various approaches have been used in attempts to determine this. Houtz & others (1977) suggested that the Plateau (or at least a portion of it) is an uplifted part of a Mesozoic ocean basin; however, their Moho depth of 20–23 km, inferred from gravity modelling, is diagnostic of neither thickened oceanic nor thinned continental crust. Following a revision of the reconstruction of the Australian and Antarctic continents, Mutter & Cande (1983) concluded that they could not demonstrate an oceanic nature for any part of the Kerguelen Plateau. Their study showed that earlier continental reconstructions which resulted in overlap of the Kerguelen Plateau and Broken Ridge, and which were used to support an oceanic or constructional origin for the features, are no longer valid in the light of a recently proposed older breakup age for Australia and Antarctica of at least 90 Ma. On the

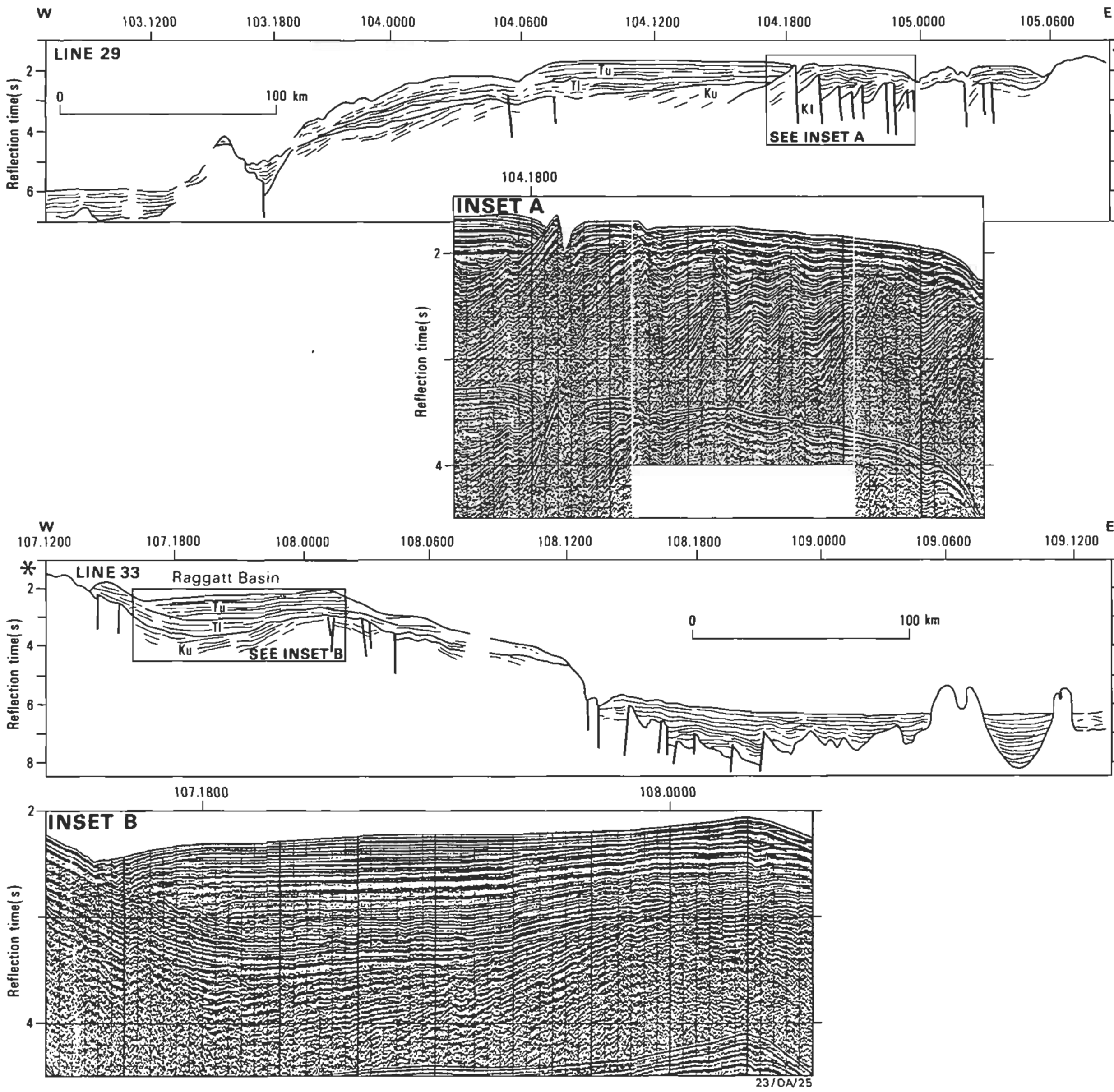

Figure 13. Cross-section of the Kerguelen Plateau (H), based on BMR Lines KP29 & 33 which adjoin at asterisk (Ramsay & others, 1986a). Interpretation by Symonds & Willcox before ODP drilling. Location given in Fig. 12.
Seismic details: (Inset A) Note tilt-blocks indicating extension beneath the central part of the Plateau, and (Inset B) showing relatively thick Tertiary and Cretaceous section in the Raggatt Basin.

basis of the geology of the Kerguelen Islands (Watkins & others, 1974) and isotope studies (Dosso & others, 1979; Dosso & Murthy, 1980), it was concluded that the northern part of the Plateau was oceanic. Although the petrology of basalts obtained from recent ODP drilling on the southern part of the Plateau (ODP Leg 120 Scientific Party, 1988a, 1988b) has also been used to infer oceanic affinity, trace element studies of dredged basalts appear to provide a contrary result by tentatively indicating continental contamination (Davies & others, in press).

Over all, opinion on the origin of the Kerguelen Plateau appears to have swung in favour of oceanic volcanic, possibly related to hotspot activity (Luyendyk & Rennick, 1977; Goslin & Patriat, 1984; Munschy & Schlich, 1987). However, at this stage, we feel that the balance of evidence favours the suggestion of Coffin & others (1986) that the northern and southern parts of the Plateau may have evolved by different processes. In the absence of evidence to the contrary, we have assumed that the southern Kerguelen Plateau was initially continental in origin, although it has undoubtedly experienced episodes of intense basaltic volcanism. Such an origin would be the most favourable for the generation of petroleum in this part of an Australian Legal Continental Shelf.

The present understanding of basin development beneath the southern Kerguelen Plateau comes mainly from limited sampling, and seismic stratigraphic studies (Colwell & others, 1988; Schlich & others, 1988; Coffin & others, 1988, 1989), which revealed the presence of significant sediment accumulations interpreted as Cretaceous–early Tertiary. Recently, nine sites were drilled on the Kerguelen Plateau, six in the south, as part of the Ocean Drilling Program (ODP) (ODP Leg 119 Scientific Party, 1988a,b; ODP Leg 120 Scientific Party, 1988a,b), and these provide the most definitive information on sediment type, palaeogeography and palaeoceanography of the Plateau. The Raggatt Basin is the largest depocentre within this region and lies almost entirely north of the AAT. Ramsay & others (1986a,b) estimated that up to 4000 m of sediment occurs within the Basin; however, from the available seismic data we calculate that in its thickest part there is probably no more than 3000 m of sedimentary section (Fig. 13). ODP drilling penetrated a Late Cretaceous–Tertiary section, which in places was overlying basaltic 'basement' of subaerial origin (ODP Leg 120 Scientific Party, 1988b; Coffin & others, 1988). On the western flank of the Raggatt Basin at ODP Site 748, the Late Cretaceous (Turonian) section contained restricted marine siltstone with a 0.5 per cent organic content, which could have source potential. At the base of this drill hole, undated pre-Turonian terrestrial sediment was recovered, and seismic data indicate that this may lie at least 200 m above acoustic basement. The section thickens substantially basinwards and indicates that the oldest sediment overlying 'basement' is terrigenous. At Site 748 the Campanian and Maastrichtian section consists of about 300 m of 'shelfal' carbonates, overlain by about 400 m of Tertiary foraminiferal ooze. In many places the 'basement complex' beneath the Raggatt Basin contains a thick section of dipping reflectors (Colwell & others, 1988), and drilling shows that the top of this section is subaerially erupted basalt. Whether or not this entire sequence consists of basalt and volcanogenic rocks, or includes rift-related/pre-rift sediments, is unknown at present. This has important implications for the petroleum potential of the region.

Our review of the geology of the Kerguelen Plateau indicates that the most prospective parts of an Australian Legal Continental Shelf in this region are the Raggatt Basin and the smaller basins and half grabens adjacent to the crest of the Plateau (Fig. 12, area H1). We have assumed that these features have a continental rift-related origin and for the purposes of this assessment can be categorised as Klemme Type 3 — Cratonic Rifts. Also included in the assessment is a small deepwater area of relatively thick sedimentary section on the eastern flank of the Plateau (Area H2). This area might overlie oceanic basement.

Petroleum potential

Klemme (1980 p. 187) noted that 'worldwide, more than 600 basins (Huff, 1980) and sub-basins are known to occur – of these, about a quarter by number (Fitzgerald, 1980) and about 50% by area and volume (Klemme, 1980, fig. 23) have production in some portion to almost all of the basin... About 50% of the world's basins by area and volume and three-quarters by number are non-productive'. We thus have every reason to expect that the offshore basins, or at least those which have well-explored analogues both onshore and beneath the shelf, will have similar potential. Krueger (1978) estimated that '65% of the reserves in the offshore will be found out to water depths of 200 m, and 30% from 200 m to 2500 m. In other words, 95% of the offshore hydrocarbon reserves will probably be found in waters shallower than 2500 m. The other 5% is divided 4% for the continental rise segment and 1% for the deep-ocean seabeds.' His estimate is, of course, entirely related to water depth and takes little account of the architecture and tectonic development of individual basins. It also reflects the fact that most thick and potentially productive sedimentary sections are found in shelf, plateau-like, and upper slope situations. Although 'more than half the total volume of marine sediments of the earth lies beneath the surface of deep marginal basins, continental rises, and abyssal plains' (Emery, 1975), such sequences are usually relatively thin and unlikely to contribute significantly to conventional petroleum reserves.

Assessment approach

Estimating resources of crude oil and natural gas in poorly explored regions is fraught with difficulty. There is, however, a need to provide some form of quantitative estimate for the more prospective areas beyond an EEZ, so that their importance relative to each other and to known basins can be assessed. Such calculations will be little more than a rough guide, and should not be used to give an impression of accuracy beyond the meagre knowledge available. As pointed out by Hedberg (1975), 'until at least one well has been drilled and tested in a new area, no one can be entirely certain that the area will produce any petroleum in spite of the rosiest outlook; conversely, in spite of dim advance prospects, no one can be entirely certain that the area will not be a bonanza'.

When evaluating any basinal area, seven multiplying factors need to be considered. These are (1) source beds, (2) migration paths, (3) reservoirs, (4) traps, (5) seals, (6) protection of traps and seals, and (7) timing. Within some remote frontier basins, it might be possible to estimate the presence and/or effectiveness of each of these factors by interpretation of regional seismic data and, in places, geological sampling and deep-sea drilling. However, in many frontier basins these factors are unknown, and only an estimate of sediment volume and structural style can be made.

Numerous basin classifications have been proposed (e.g. Weeks, 1952; Uspenskaya, 1967; Dewey & Bird, 1970; Halbouty & others, 1970a,b; Klemme, 1971a,b, 1975; Perrodon, 1971; McCrossan & Porter, 1973; Bally, 1975; Huff, 1978; Bally & Snelson, 1980; Bois & others, 1982; Kingston & others, 1983), and some of these have attempted to assess the petroleum potential of their various basin categories. Kingston & others (1983) provide a most useful classification in terms of basin-forming tectonics, depositional sequences, and basin-modifying tectonics, but only mention the potential of basins in a qualitative way. Classifications which would be of most use in estimating the quantitative petroleum potential of an area should combine a calculation of total sediment volume with the known petroleum yield of an analogous basin. The only classification of this type known to us is that of Klemme (1975), and we have used this for the basis of our quantitative estimates.

There are different opinions on the effectiveness of methods which use areal and volumetric yields in conjunction with geological analogues to determine the resource potential of poorly explored areas (Bultman, 1986; Miller, 1986; Ulmishek, 1986; Resnick, 1986). For example, Bultman's (1986) study of highly explored North American basins led him to deduce that 'neither the richness or oil field density of a region is correlated to its tectonic setting'. He seriously questioned the use of geological analogy as a resource tool. However, his study did not include any Klemme-type 'cratonic rift' or 'pull-apart' basins of the type which predominate on Australia's continental margin (see Table 4), and which have gross similarities in tectonic and depositional history both within the Australian region and around the world. Despite Bultman's (1986) reservations, the global analogue approach might be appropriate for these basin types. Others (Miller, 1986), have suggested that the geological analogue method can be useful on a broad regional scale or in reconnaissance-type estimates of resource potential, particularly of poorly explored areas; however, the accuracy will depend on the validity of the analogue chosen (Miller, 1986). The more sophisticated assessment approaches, which use quantitative geochemical and geological modelling or projections of historical data (Forman & Hinde, 1986), cannot be applied to unexplored, non-producing areas unless at least some of the parameters are derived from areas with analogous geology (Miller, 1986).

Our assessment of petroleum potential in areas beyond an EEZ relies on:
(1) a *quantitative* evaluation, based on the global statistical analysis of Klemme (1975), with the added refinement of our concept of 'effective sediment volume', which eliminates the inclusion of spuriously large estimates of sediment volume derived from extensive areas of thin section with minimal potential, and
(2) a *qualitative evaluation*, in which the petroleum potential of tectono-stratigraphic units within unexplored basins is compared with analogous units in better known basins around the Australian margin.

The results are expressed numerically as potential petroleum recovery and qualitatively as a basin rating: both are speculative.

Quantitative evaluation

The original Klemme classification was based on those basins with giant fields (over 500 million barrels of oil) which account for a large proportion of present-day oil production; however,

Table 2. 'Yardstick' for evaluation of poorly explored basins (modified from Klemme, 1975)

Basin type	*Recovery/km³ of sediments*[1]		*Chance of*		*Field size*
	Kilolitres (m³)	*Barrels*	*Commercial Production*	*Presence of 'Giant' fields*	*Largest field v total*
1. Cratonic interior	1 400 High 700 Average 100 Low	9 000 4 500 1 000	30%	20%	—
Cratonic basins: 2. Cratonic multicycle (large)	9 900 4 800 1 000	62 500 30 000 6 000	70%	65%	10-50%
(Small)	3 000 1 600 300	19 000 10 000 2 000	50%	30%	30%
3. Cratonic rift	17 900 5 600 800	112 500 35 000 5 000	50%	50%	30%
Intermediate basins: 4. Intermediate extra-continental (4A. Closed)	23 800[2] 6 000 400	150 000[2] 37 500 2 500	50%	50%	14%
(4B. Foredeep)	2 400 1 000 —	15 000 6 000 300	40%	10%	14%
(4C. Open)	11 900 6 300 —	75 000 40 000 800	50%	65%	30%
5. Pull-apart	Average approx. 1 600	10 000	30%	20%	?
6/7. Inter-montane	158 700 7 100 200	1 000 000 45 000 1 300	20%	50%	35%
8. Delta	8 700	55 000	50%	Few giants	6%
Average for all basins	2 000 - 4 000	12 500 - 25 000	50%	50%	25%

[1]These figures represent volumes of oil or equivalent gas. On an approximate basis, 1 kilolitre (or cubic metre) of oil has the energy equivalence of 1000 cubic metres of gas.
1 kilolitre (or cubic metre) is equal to 6.2829 barrels.
1 cubic kilometre of sediment is approximately equal to 0.25 cubic miles, as per Klemme's original table.
[2]These exceptionally high values include Middle East fields.

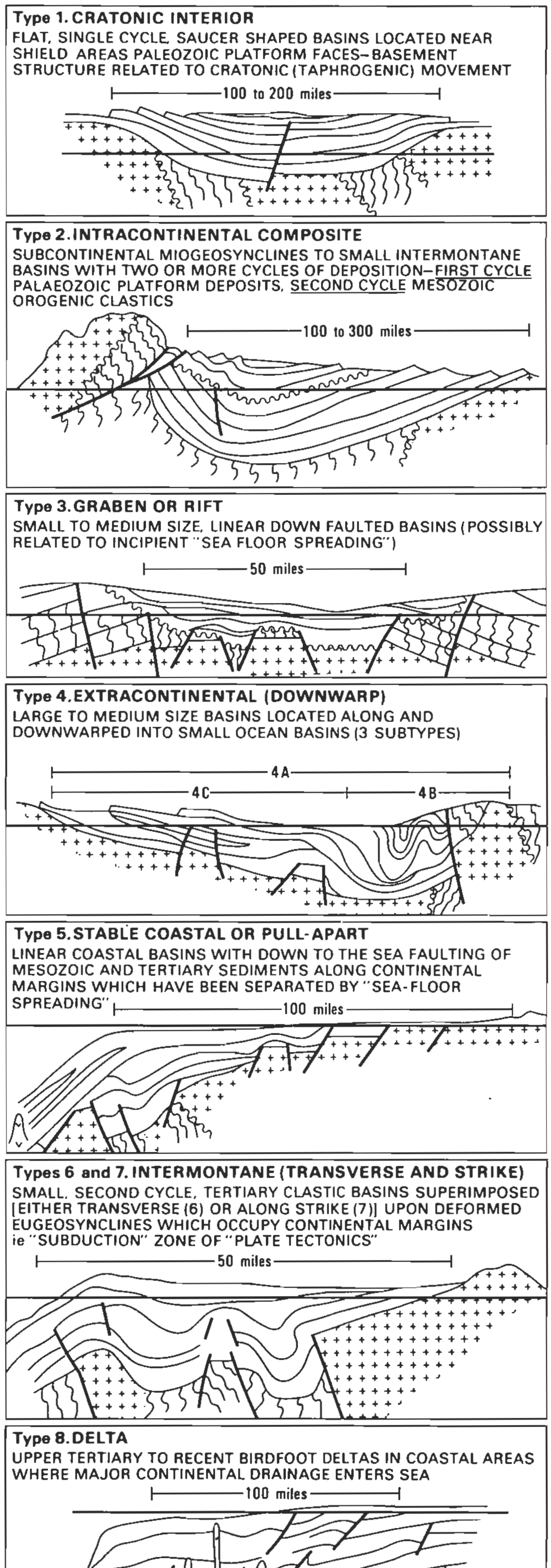

Figure 14. Basin types according to Klemme (1975), based on the classification of Halbouty & others (1970a,b).

it is also applicable to basins without giant fields, including poorly explored basins. Klemme (1975) recognised eight basin types based on the classification system of Halbouty & others (1970 a,b) (Fig. 14) : (1) cratonic interior, (2) intracontinental composite, (3) graben or rift, (4) extracontinental (downwarp), (5) stable coastal or pull-apart, (6) intermontane (transverse), (7) intermontane (strike), and (8) delta; and he assembled statistics on petroleum recovery per cubic mile of sediment, which we have converted to cubic kilometre, and exploration risk (Table 2). For example, we show in Table 2 that Type 5 — pull-apart basins — have a 30 per cent chance of commercial production (i.e. the geological risk is 0.3), that there is a 20 per cent chance of finding giant fields, and that in a producing basin the average oil recovery is about 10 000 barrels per km^3, or about 1600 kL/km^3. In a later version of this classification (Klemme, 1983), the basin categories were refined and related to field-size distribution, but revised petroleum recovery figures were not provided.

Using regional seismic data, we have categorised basins beyond the EEZ in terms of Klemme's Types 1 to 8. The effective sediment volume concept used in our calculations of petroleum recovery takes into account only that part of the section which is at least 2000 m thick — that is, the so-called 'kitchen area' — thus eliminating large areas of thin section which are unlikely to contain mature petroleum source rocks. This is in accord with Krueger (1978) who recognised that although 'the thickness of sediments is not a complete measure of the potential for hydrocarbon occurrences, it is certainly the most important attribute being an integral portion of all seven evaluation parameters' listed above. In regions where a prospective province exists, containing numerous poorly defined sub-basins of similar dimensions and having similar structural and depositional styles, the effective sediment volume of the whole province was calculated as follows (Fig. 15):

- determine total area of basin province (e.g. western flank Lord Howe Rise)
- estimate the proportion occupied by sub-basins with ≥2000 m of sediment, using any available seismic sections or other relevant information
- estimate the average thickness of sediment in the known sub-basins
- compute minimum, best and maximum estimates of area and volume (Table 3) to use in the calculations of potential petroleum recovery.

Using our estimates of effective sediment volume (Table 3) and Klemme's petroleum recovery figures (Table 2), we have calculated the minimum, best, and maximum estimates of potential petroleum recovery for each area (Table 5) as follows:

minimum estimate	=	low recovery x minimum volume estimate
best estimate	=	average recovery x best volume estimate
maximum estimate	=	high recovery x maximum volume estimate.

Qualitative evaluation

The statistical data associated with Klemme's classification have enabled us to provide a quantitative evaluation of the relative potential of basins beyond an EEZ. The method is, however, limited by Klemme's use of 'global'— largely North American and Middle Eastern — production statistics, which might in some cases be less appropriate for basins in the Australian region, even when they are tectonic counterparts of Klemme's basin types. The most significant problems are likely to arise from:

- peculiarities in sedimentation within Gondwanaland and on the Australia-India Plate, related to their particular latitude and climate

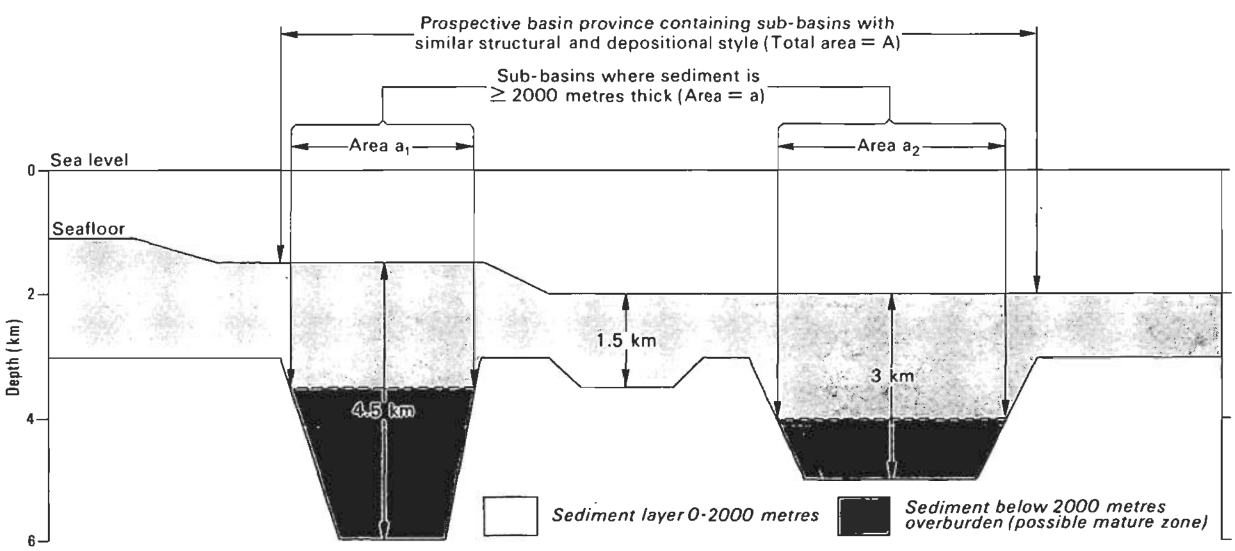

Estimation of effective sediment volume, assuming sub-basins have similar dimensions:

- Total area of basin province = A
- Total area of all sub-basins (≥ 2000 metres sediment) = a
  Area a = $a_1 + a_2$ = 54% A (in this example only)
- Average sediment thickness in sub-basins = 3.750 km
- Approximate sediment volume (≥ 2000 metres) = 3.750a km^3

Note: This volume calculation has only been applied where sub-basins are approximately equidimensional (e.g. Western Lord Howe Rise). The estimate is then within about 20% of the true volume ($4.500a_1 + 3.000a_2$) if all individual sub-basins could have been mapped. In a real situation ratio a/A is estimated from available data.

23/OA/30

Figure 15. Calculation of effective sediment volume. Used in areas with groups of structurally related basins, particularly western Lord Howe Rise. Also illustrates the concept of 'kitchen areas' (ie. the zone of potentially mature sediment), discussed in the text and used in the derivation of Tables 3 & 5.

Table 3: Areas and volumes of thick sediment (≥2000 m) for regions beyond an EEZ

Region	Area name[1]	*Estimated Areas (10^3.km^2)*			*Estimated Volumes (10^3.km^3)*		
		Minimum	*Best*	*Maximum*	*Minimum*	*Best*	*Maximum*
A	Western Lord Howe Rise ($A1_1$ + $A1_2$)	28	40	49	56	100	157
	Eastern Lord Howe Rise (A2)	37	40	43	75	100	128
	Middleton Basin (A3)	25	25	25	42	62	69
	New Caledonia Basin ($A4_1$ +$A4_2$)	43	43	43	108	129	151
	West Norfolk Ridge (A5)	1.6	1.9	2.3	3	5	7
	Taranui Sea Valley (A6)	1.6	1.6	1.6	4	5	5.7
C	South Tasman Rise ($C1_1$ + $C1_2$)	18	19	32	55	57	95
D	Great Australian Bight — mid-slope (D1)	21	21	21	63	73	94
	— lower slope and basin floor (D2)	29	29	29	88	102	131
E	Naturaliste Plateau (E1)	4.9	4.9	4.9	7	10	12
F	Wallaby Plateau (F1)	2	2	2	4	4.9	5.9
	Northwest Exmouth Plateau (F2)	12.8	12.8	12.8	32	38	45
H	Southern Kerguelen Plateau (H1)	52	66	85	104	165	255
	eastern slope (H2)	3.3	3.5	3.7	8.3	9.8	11.8

[1]Refer to Figs 4, 7 and 12 for Areas $A1_1$, $A1_2$, etc.

- tectonic events of local or regional extent, which might, for example, have given rise to features such as silled basins containing anoxic environments favourable to the preservation of kerogen
- the depositional environment of the source beds, the nature of the primary source material (that is, algal, bacterial or higher plant), and its degree of reworking. The oil-prone nature of the terrestrial source material in many Australian basins, for example, is quite different to typical terrestrial source rocks in northern hemisphere basins.

It is also important to distinguish the potential petroleum productivity of the particular tectono-stratigraphic units which make up Australian basins. For example, in the Gippsland Basin, it is the *post-breakup stage* which harbours the large oil and gas fields, owing largely to the occurrence

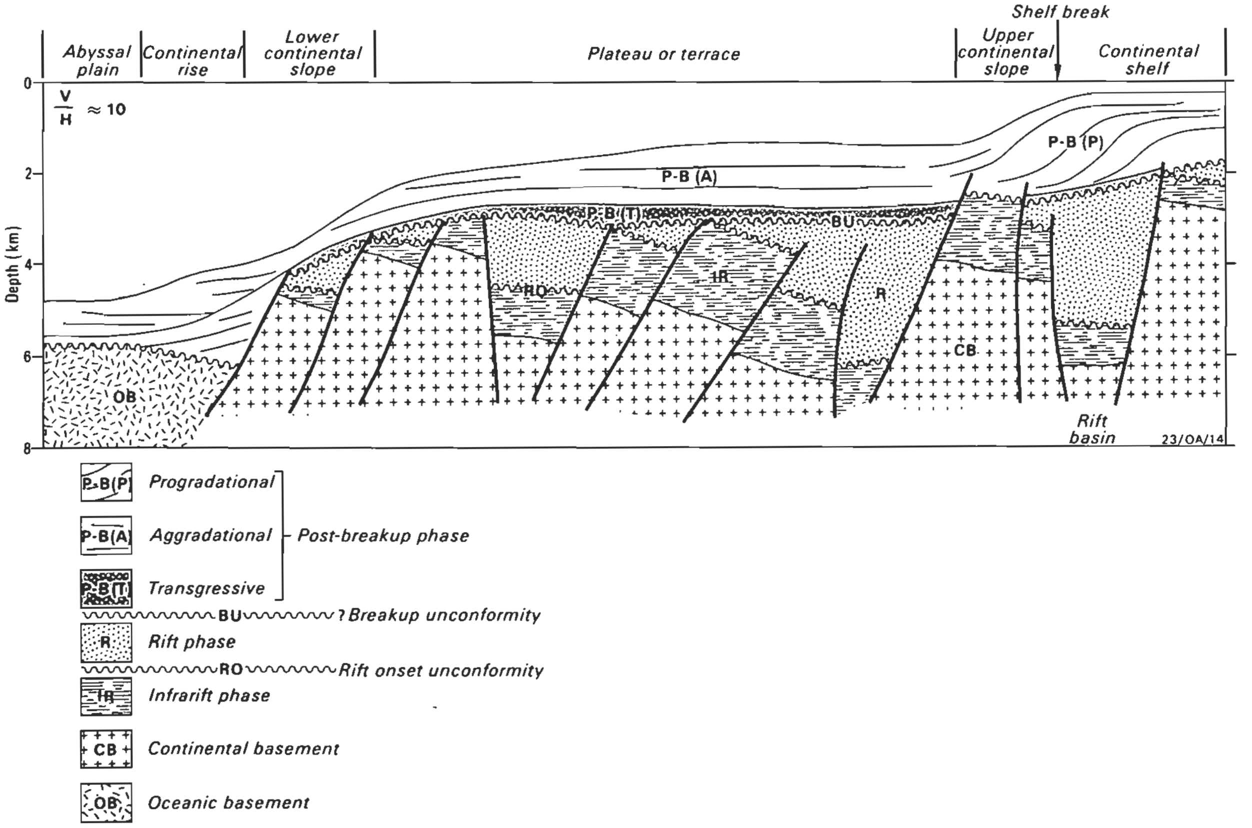

Figure 16. Tectono-stratigraphic units on a typical passive continental margin.

Shows the main phases of structuring and sedimentation — infrarift (prerift), rift and post-breakup — based on the nomenclature of Falvey & Mutter (1981).

Table 4: Geological classification for areas of thick sediment (≥2000 m) for regions beyond an EEZ

Region	*Area name*	*Basin Type Klemme (1975; Fig. 14)*	*Prospective tectono-stratigraphic units with significant plays (Fig. 16)*	*Play-types envisaged*	*Comment*
A	Western Lord Howe Rise ($A1_1$ + $A1_2$) basins	Type 3 — cratonic rift	IR/R	Tilt blocks, composed of infrarift (prerift) sediments in south; structural/stratigraphic traps within rift fill; breakup unconformity traps; possible diapiric structures in north	Gippsland Basin (Strzelecki Group) equivalents could occur within tilt-blocks in some areas
	Eastern Lord Howe Rise (A2)	Type 5 — pull-apart	R/P-B[P]	Mainly stratigraphic traps	Straddle ocean/continent boundary
	Middleton Basin (A3)	Type 4C & 5 — extra-continental (open) or pull-apart	R/P-B[A]	Mainly stratigraphic traps	Straddle ocean/continent boundary
	New Caledonia Basin ($A4_1$ & $A4_2$)	Type 4A? — extra-continental (closed)	P-B[A/oceanic]	'Unconventional' deep-ocean restricted basin	On oceanic crust. Prospectivity of basins of this type is unknown
	West Norfolk Ridge (A5)	Type 5 & 3? — pull-apart & cratonic rift	R		
	Taranui Sea Valley (A6)	Type 6 & 7 — intermontane	Uncertain association	Wrench related anticlines, drapes & unconformity traps	Basin-forming tectonics not understood; restricted basin
C	South Tasman Rise ($C1_1$ + $C1_2$)	Type 3 — cratonic rift	R	Typical half-graben tilt-block plays with reactivation to Oligocene	Some gas anomalies near NE basin boundary. Otway Basin stratigraphy may apply
D	Great Australian Bight — mid-slope (D1)	Type 5 — pull-apart	IR/R/?P-B	Fault-blocks and anti-clines created by rifting and wrenching	Analogous to Otway Basin but fewer Tertiary faults and greater chance of sealed traps
	— lower slope & basin floor (D2)	Type 4C? or 5 — extra continental (open) or pull-apart	R/P-B[A]	Fault-blocks and anti-clines created by rifting and wrenching	Very deep water, highly extended continental crust
E	Naturaliste Plateau (E1)	Type 3 — cratonic rift	?R		Volcanics/volcaniclastics in some places
F	Wallaby Plateau (F1)	Type 3 & 5 — cratonic rift & pull-apart	R		Origin of plateau in doubt — continental or oceanic?
	Northwest Exmouth Plateau (F2)	Type 3 & 5 — cratonic rift & pull-apart	IR/R	Largely fault blocks and associated structures	Analogous with Exmouth Plateau proper &? offshore Canning Basin
H	Southern Kerguelen Plateau (H1)	Type 3 — cratonic rift	?R	Unconf. traps in Raggatt Basin depocentre. ?Cretaceous tilt-block plays; downgraded in places where faults are shallow	Pre-breakup reconstruction against Naturaliste Plateau/Broken Ridge. Origin remains in doubt — dredging/drilling sampled basaltic basement and potential Ku source
	— eastern slope (H2)	Type 4C & 5 — extra-continental (open) & pull-apart	P-B[A/oceanic]	'Unconventional' deep ocean basin	Prospectivity of basins of this type is unknown

P-B = post-breakup; [A] = aggradational; [P] = progradational; [A/oceanic] = aggradation in ocean basin; R = rift; IR = infrarift of suitable source rocks and the presence of reactivation structures which provide the traps. Hence, categorising the Gippsland Basin simply as a *cratonic rift* (that is, a Klemme Type 3 basin) is only part of the story: although its overall rift-setting may be important, it is the peculiarities of the post-breakup sequence which led to the basin's high productivity. Klemme (1975) has recognised this limitation by categorising the Gippsland Basin as a Type 6/7 — Intermontane Basin— thus focussing on the reactivation of its Tertiary section rather than its primary rift phase development. In the case of the western Lord Howe Rise basins, the post-breakup tectono-stratigraphic unit is unlikely to be prospective, even though these basins first developed within the same rift sytem as the Gippsland Basin. This is because these two areas were separated by seafloor spreading from the Late Cretaceous, thus isolating the Lord Howe Rise basins from a high terrigenous sediment supply and the Tertiary reactivation.

We have attempted to overcome the limitation of our quantitative analysis by providing a qualitative, somewhat intuitive, assessment of each area. This involves identification of the tectono-stratigraphic units related to the infra-rift/prerift (IR), rift (R) and post-breakup (P-B) phases of basin development (Fig. 16; Falvey, 1974; Falvey & Mutter, 1981), with a further subdivision of the post-breakup sequence into its transgressive (P-B[T]), aggradational (P-B[A]), and progradative (P-B[P]) components. In the case of deepwater deposition on oceanic basement we also recognise a post-breakup aggradational unit (P-B[A/oceanic]). Comparison of these units with those of other basins in the region enabled us to estimate the most likely play-types present (Table 4) and to provide a speculative rating of petroleum potential (Table 5).

Areas of relatively thick sediment beyond an EEZ can be broadly grouped into two categories. First, there are the areas where sediments have been deposited in structurally controlled basins (rift phase sediments) — mainly grabens and half-grabens — which we categorise as basin Types 3 and 5 (Table 4). By analogy with better explored areas, we envisage the sediment fill in these basins as mostly overlain unconformably by a thin sequence of shallow to deep marine sediments (post-breakup phase). Basins in this category occur on continental lithosphere, and contain the commonly explored petroleum plays. We have designated these as areas of 'conventional' petroleum plays on Figures 4, 7 and 12.

Secondly, there are areas of turbidite and pelagic sediments deposited in or on the flanks of deep ocean basins. Such basins generally occur on oceanic lithosphere and are in an environment beyond current exploration experience. We have categorised them as Type 4 — Intermediate Extracontinental — (Table 4), and have designated them as areas of 'unconventional ocean basin' plays on Figures 4, 7 and 12.

Results and discussion

Our evaluation of the six areas beyond the EEZ with significant sediment accumulation (areas A, C, D, E, F & H), is summarised in Table 5, with a qualitative rating of petroleum potential and a quantitative minimum, best and maximum estimate of speculative petroleum recovery.

The speculative rating given in Table 5 is an estimate of petroleum potential based on our limited knowledge of the areas. On the basis of existing information, there are no areas beyond the EEZ that can be rated as better than 'fair'. The prospectivity of the deep-ocean basin areas is essentially unknown.

Previous quantitative assessments of Australia's undiscovered petroleum resources (BMR, 1989) refer only to conventional oil and gas accumulations in traps that are not presently known to contain petroleum, and that could be produced within the next 20 to 25 years. As such, they have not included the relatively remote and deepwater regions beyond an EEZ considered in this study. Table 5 illustrates the relative importance of the remote areas in terms of their potential to have produced petroleum. Most of these areas are in deep water, and it is unlikely that anything other than 'giant' fields (say 500 million barrels) would be worth exploiting. Even if such giant fields were to exist, the question arises as to whether they could be recognised with an economically feasible exploration program, particularly given the enormous size and remoteness of the areas involved.

Two areas of intermediate water depth, which are within range of current exploration drilling technology, stand out as having relatively large recovery figures (Table 5). These are the western Lord Howe Rise (most likely estimate of 0.56 x 10^9 kL or 3.5 billion barrels) and the southern Kerguelen Plateau (0.95 x 10^9 kL or 5.98 billion barrels). These areas are considered or assumed to be continental in origin, to have stratigraphy and structure related to passive continental margin evolution, and to contain petroleum plays of a kind that have been tested elsewhere in the world. The basins on western Lord Howe Rise and the southern Kerguelen Plateau are considered to be mainly Type 3 — cratonic rift — which on a world-wide basis have a 50 per cent chance of providing commercial production, and also a 50 per cent chance that giant fields are present.

We consider the western Lord Howe Rise basins, although promising in terms of total potential recovery, individually less attractive, because they are mainly small. The accumulation of any large and commercially viable fields could have been limited by relatively small quantities of source rock. For most of the area we might be faced with an 'all or nothing' situation; that is, modest-sized fields could be present in most grabens or, alternatively, these grabens could all be barren. The few larger grabens and basins might be more promising: both the diapiric structures in the basin northeast of Lord Howe Island (Roeser & others, 1985), and possible Mesozoic infrarift (prerift) sequences in fault blocks southeast of Lord Howe Island (Whitworth & Willcox, 1985) warrant further investigation. Taken as a whole, we regard the western Lord Howe Rise basins as having fair (F) potential (Table 5).

The southern Kerguelen Plateau presents a similar problem to Lord Howe Rise, in that there is a vast volume of sediment which could have reached maturity, but we have no knowledge of whether maturation, migration and trapping have actually occurred. The southern Kerguelen Plateau has two problems: the possibility of volcanogenic detritus in potential? Cretaceous reservoirs, which could destroy their permeability; and Tertiary faulting, which is common in some places and could have prevented the sealing of any traps. The greatest disincentive to exploration is, of course, its remote and hostile environment. We rate the petroleum potential of the southern Kerguelen Plateau as fair to poor (F/P), although there is a large unknown component, owing to the Plateau's uncertain origin.

Two other areas which yield significant recovery figures are the South Tasman Rise (most likely estimate of 0.32 x 10^9 kL or 2.0 billion barrels) and the eastern margin of Lord Howe Rise (0.16 x 10^9 kL or 1.0 billion barrels). Although small yields of thermogenically derived hydrocarbons have been recovered from the surface sediments of the South

Table 5: Potential petroleum recovery and their qualitative rating for areas beyond an EEZ

Region	Area name	Estimated recovery[1] Minimum	Best	Maximum	Qualitative rating[3]
A	Western Lord Howe Rise ($A1_1 + A1_2$) basin	0.04(0.28)	0.56(3.50)	2.8(17.70)	F
	Eastern Lord Howe Rise (A2)	0.12(0.75)	0.16(1.00)	0.20(1.28)	F/P
	Middleton Basin (A3)	0.01(0.03)	0.25(1.55)	0.82(5.18)	U
	New Caledonia Basin ($A4_1 - A4_2$)	0.04(0.27)	0.77(4.84)	3.60(22.60)[2]	U
	West Norfolk Ridge (A5)	0.002(0.02)	0.02(0.11)	0.13(0.79)	F/P
	Taranui Sea Valley (A6)	0.001(0.01)	0.04(0.23)	0.91(5.70)	F
C	South Tasman Rise ($C1_1 + C1_2$)	0.04(0.28)	0.32(2.00)	1.70(10.60)	F/P
D	Great Australian Bight — mid-slope (D1)	0.10(0.63)	0.12(0.73)	0.15(0.94)	P
	— lower slope & basin floor (D2)	0.14(0.88)	0.16(1.02)	0.21(1.31)	U
E	Naturaliste Plateau (E1)	0.10(0.04)	0.06(0.35)	0.21(1.35)	P
F	Wallaby Plateau (F1)	0.003(0.02)	0.02(0.11)	0.11(0.66)	P/N
	Northwest Exmouth Plateau (F2)	0.03(0.16)	0.14(0.86)	0.80(5.06)	F/P
H	Southern Kerguelen Plateau (H1)	0.04(0.26)	0.95(5.98)	6.07(38.25)	F/P(U)
	— eastern slope (H2)	0.001(0.01)	0.04(0.25)	0.14(0.89)	P(U)

[1] Recovery in kilolitres x 10^9 and billions of barrels (bracketed)
6.3 barrels are equivalent to a kilolitre (or cubic metre)
Note: Figures are rounded to the second decimal place.

[2] These maximum values are based on Type 4A basins that include recovery statistics from the Middle East (Table 2) : they are therefore unrealistically high.

[3] Qualitative rating : F = fair, P = poor, N = nil, U = unknown

Tasman Rise (Whiticar & others, 1985), indicating active petroleum generation now or in the past, the seismic data show abundant volcanics in the rift basins, which could downgrade reservoir potential. Both the eastern Lord Howe Rise and the South Tasman Rise are considered to have fair to poor (F/P) potential.

Of the deepwater ocean basin areas, the New Caledonia Basin appears to be the most significant. However, it should be noted that the maximum potential recovery figure for the New Caledonia Basin may be unrealistically large, because it has been placed in the Type 4A category, which incorporates the highly productive Middle East fields. The other deepwater areas which yield significant recovery figures are the Middleton Basin and the lower slope and basin floor in the Great Australian Bight. The exploration potential of areas of this type, which lie in such deep water, perhaps partially on oceanic lithosphere, is totally unknown.

As discussed above, any assessment of the kind presented in this paper tends to emphasise regions which generally have large areas and volumes of sediment, and which thus lead to large recovery figures. However, in terms of exploration success, the relatively small, potentially high-yield, areas should not be dismissed. The most notable of these beyond an Australian EEZ is the Taranui Sea Valley on the Norfolk Ridge, which appears to be a Type 6/7 Intermontane Basin. The relatively thick (4000 m) sediment, apparent structural complexity of the Taranui Sea Valley section, and its moderate water depth (about 1600 m), lead us to conclude that this area has fair (F) potential.

In order to dispel uncertainties and cynicism attached to the volumetric/analogue approach of Klemme, we have carried out some 'rule-of-thumb' comparisons of Klemme-type calculations with more sophisticated estimates of resources as determined by Forman & others (BMR, 1989). In doing this we have treated well-explored basins in the Australian continental margin in a very simplistic way commensurate with the meagre knowledge of basinal areas beyond an EEZ. That is, how would the potential petroleum recovery of the explored basins rate if they were known only from a few moderate quality seismic lines, which provide limited information on basin area, sediment thickness and structural style? Consider, for example, our calculations for the Gippsland Basin and Northern & Western Margin Basins given in Table 6 (see footnote).

The volumetric/analogue approach produces potential petroleum recovery estimates of the same order as the resource estimates derived by more sophisticated methods (Table 6). In the case of the Gippsland Basin, the volumetric/analogue estimate is about 0.5 of that derived from the aggregate of the 'demonstrated' (that is, proven by drilling) and 'undiscovered' (statistically predicted) resources. The Gippsland Basin therefore has a recovery factor of approximately 73 000 barrels/km³, somewhat richer than the average of 35 000 presented by Klemme (1975), but well below the maximum of 112 500 for a cratonic rift basin (Table 2). As discussed above, Klemme (1975) categorised the Gippsland Basin as a Type 6/7 — Intermontane Basin — with an average recovery of 45 000 barrels/km³ (Table 2). It is interesting to note that this intermontane value is

Table 6. Comparison of potential petroleum recovery calculations based on a volumetric/analogue approach (Klemme method) with the resource estimates given in BMR (1989)

	Volumetric/analogue (Klemme method)				*Resources[1] BMR, 1989)*		
Basin type (Table 2)	*Average recovery (Bbl/km^3)*	*Dimensions (km)*	*Potential recovery ($Bblx10^9$)*		*Demonstrated ($Bblx10^9$)*	*Average undiscovered ($Bblx10^9$)*	*Total*
Gippsland Basin[3]							
Cratonic rift	35 000	Length ~ 150	2.9	Oil	3.446	0.560	~ 6.2
(Type 3)		Width ~ 80		Condensate	0.254	0.070	
		Thickness ~ 7		Gas[2]	1.635	0.220	
Northern & Western Margin Basins: Bonaparte Basin							
Cratonic rift	35 000	Length ~ 550	~ 6.3				
(Type 3)		Width ~ 65					
		Thickness ~ 5					
Barrow/Dampier Sub-basin				Oil	0.406	1.540	~ 15.0
				Condensate	0.482	1.200	
Cratonic rift	35 000	Length ~ 350		Gas[2]	7.333	4.025	
(Type 3)		Width ~ 60					
		Thickness ~ 6					
Exmouth Sub-basin			~ 6.7				
Cratonic rift	35 000	Length ~ 160					
(Type 3)		Width ~ 100					
		Thickness ~ 4					

[1]Resources for the 'Southern Margin Coastal Basins' (BMR, 1989, table 4) are almost equivalent to those from the Gippsland Basin, which is the major contributor: resources for the 'Northern & Western Margin Basins' (BMR, 1989, table 6) are mainly from the Bonaparte Basin and the Barrow, Dampier and Exmouth Sub-basins (graben).
[2]Salesgas has been converted to energy equivalent oil (see footnote, Table 2).

closer to the calculated recovery of 73 000 barrels/km^3 than the 35 000 barrels/km^3 cratonic rift value used in our calculations. For the 'Northern and Western Margin Basins' the volumetric/analogue estimate is 0.6 times the BMR (1989) figure, implying that the recovery factor might be a little higher than average.

Continued studies of basins in the Australian region should improve both the quality of the analogues and recovery factor estimates, enabling better quantitative assessment of the petroleum potential of unexplored areas.

Conclusions

Under the United Nations Convention on the Law of the Sea, a coastal state has sovereign rights over its Legal Continental Shelf for the purposes of exploring and exploiting the natural resources of its seabed and subsoil. This Shelf is considered to extend throughout the natural prolongation of the land territory to the outer edge of the continental margin, which, where it extends beyond a 200 nautical mile Exclusive Economic Zone, is defined by formulae within Article 76 of the Convention.

The area of a Legal Continental Shelf around Australia and its territories would be approximately 12 million km^2. Eight regions of this Shelf, totalling more than 3 million km^2 in area, would extend beyond an Exclusive Economic Zone. Sediment thicknesses greater than 2000 m — sufficient to have generated petroleum from any potential source rocks — occur in six of these regions: Lord Howe Rise/Norfolk Ridge, South Tasman Rise, Great Australian Bight, Naturaliste Plateau, Exmouth Plateau/Wallaby Plateau and Kerguelen Plateau. These regions are all in relatively deep water (generally over 1000 m), and some are in hostile and remote environments. However, they are not consistently deeper than some better explored areas within an EEZ, such as the Exmouth Plateau, which was drilled during a period of active oil industry exploration that began in the late 1970s.

Our assessment of the petroleum potential of the areas beyond an EEZ is both qualitative and quantitative. We believe that the quantitative approach is a useful tool, which has enabled us to rank and compare the potential petroleum recovery of Australia's remote regions. It is clear that, in terms of the recovery figures, the western flank of Lord Howe Rise and the remote southern Kerguelen Plateau are the most important regions beyond an EEZ. Despite our reservations regarding basin size, the western Lord Howe Rise as a whole is ranked highest, because an equivalent-sized prospective area also lies within the EEZ around Lord Howe Island. The South Tasman Rise and eastern flank of Lord Howe Rise are also of interest, as are small, potentially high-yield features such as the Taranui Sea Valley on the southern limit of an EEZ around Norfolk Island.

Since the early 1960s, the worldwide rate of petroleum discovery has been in apparent decline, although this has been the period of greatest exploration activity (Fitzgerald, 1980). The decline is a result, not of finding fewer fields, but of finding fewer 'super-giants', which account for 50 per cent of all oil yet discovered. Although the petroleum resources of Australia are comparatively small by world standards, the exploration trends and discovery rates have still tended to follow those for the rest of the world. If further giant fields are to be discovered, we should give at least some attention to the deeper water regions. Although exploration of the remote regions beyond an Exclusive Economic Zone is not viable in the present economic environment, these regions may well hold strategic resources that could benefit Australia in the next century.

Acknowledgements

This paper has evolved from numerous studies undertaken over the last 10 years. We acknowledge the helpful comments and criticisms received from our colleagues in BMR's Division of Marine Geosciences and Petroleum Geology and Resource Assessment Division, in particular David Forman, Colin Robertson and Lee Ranford. We thank Victor Prescott (Professor of Geography, University of Melbourne) for reviewing an early version of this paper. Figures were drawn by J. Convine.

References

American Association of Petroleum Geologists, 1978 — Plate Tectonic Map of the Circum-Pacific Region, Southwest Quadrant, Base Map, 1:10,000,000. *American Association of Petroleum Geologists, Tulsa, U.S.A.*

Bally, A.W., 1975 — A geodynamic scenario for hydrocarbon occurrences. *9th World Petroleum Conference Proceedings*, 2, 33-44.

Bally, A.W., & Snelson, S., 1980 — Realms of subsidence. In Miall, A.D.; (editor), Facts and principles of world petroleum occurrence. *Canadian Society of Petroleum Geologists Memoir*, 6, 9-94.

Boeuf, M.G., & Doust, H., 1975 — Structure and development of the southern margin of Australia. *The APEA Journal*, 15, 33-43.

Bois C., Bouche, P., & Pelet, R., 1982 — Global geologic history and distribution of hydrocarbon reserves. *American Association of Petroleum Geologists Bulletin*, 66(9), 1248-1270.

Bultman, M.W., 1986 — An analysis of oil field size distributions in consanguineous basins. *Ph.D thesis, University of Wisconsin-Madison.*

Bureau of Mineral Resources, 1989 — Australia's Petroleum Potential. *In* Petroleum in Australia, the First Century. *Australian Petroleum Exploration Association*, 48-90.

Burke, K., & Dewey, J.F., 1973 — Plume generated triple junctions: key indicators in applying plate tectonics to old rocks. *Journal of Geology*, 81, 406-433.

Burns, R.E., Andrews, J.E., & others, 1973 — Initial reports of the Deep Sea Drilling Project, vol. 21. *U.S. Government Printing Office, Washington.*

Clarke, I., McDougall, I., & Whitford, D.J., 1983 — Volcanic evolution of Heard and MacDonald Islands, southern Indian Ocean. *In* Oliver, R.L., James, P.R., & Jago, J.B., (editors), Antarctic earth science. *Australian Academy of Science, Canberra*, 631-635.

Coffin, M.F., Davies, H.L., & Haxby, W.F., 1986 — Structure of the Kerguelen Plateau province from Seasat Altimetry and seismic reflection data. *Nature*, 324, 134-136.

Coffin, M.F., Kelts, K., Davies, H.L., Colwell, J.B., Royer, J.Y., & Ocean Drilling Program Legs 119 & 120 Shipboard Scientists, 1988 — Late Mesozoic and early Cainozoic history of the Kerguelen Plateau: facies development, palaeogeography, and palaeoceanography. *In* Extended Abstracts — Palaeogeography, Sea Level & Climate, Implications for Resource Exploration, 17th BMR Research Symposium, Canberra, 8-10 November 1988. *Bureau of Mineral Resources, Australia, Record* 1988/42, 48-55.

Coffin, M.F., Munschy, M., Colwell, J.B., Schlich, R., Davies, H.L., & Li, Z.G., 1989 — The Raggatt Basin: a mid-ocean sedimentary basin on the Kerguelen Plateau. *In* Bally, A.W., (editor), Atlas of Seismic Stratigraphy, vol. 3. *American Association of Petroleum Geologists Studies in Geology, 27.*

Colwell, J.B., Coffin, M.F., Pigram, C.J., Davies, H.L., Stagg, H.M.J., & Hill, P.J., 1988 — Seismic stratigraphy and evolution of the Raggatt Basin, southern Kerguelen Plateau. *Marine and Petroleum Geology*, 75-81.

Davies, H.L., Sun, S., Frey, F.A., Gautier, I., McCulloch, M.T., Price, R.C., Bassias, Y., Klootwijk, C.T., & Leclaire, L., in press — Basalt basement from the Kerguelen Plateau and the trail of the DUPAL plume. *Contributions to Mineralogy and Petrology.*

Dewey, J.F., & Bird, J.M., 1970 — Mountain belts and the new global tectonics. *Journal of Geophysical Research*, 75, 2625-2647.

Dooley, J.C., 1963 — Results of southwest Pacific submarine gravity survey 1956. *Bureau of Mineral Resources, Australia, Record* 1963/43.

Dosso, L., & Murthy, R.V., 1980 — A Nd isotope study of the Kerguelen Islands: inferences on enriched oceanic mantle sources. *Earth and Planetary Science Letters*, 48, 268-276.

Dosso, L., Vidal, P., Cantagrel, J.M., Lameyre, J., Marot, A., & Zimine, S., 1979 — Kerguelen, continental fragment or oceanic island? Petrology and isotope geochemistry evidence. *Earth and Planetary Science Letters*, 43, 46-60.

Dow, W.G., 1979 — Petroleum source beds on continental slopes and rises. *In* Watkins, J.S., Montardert, L., & Dickerson, P.W., (editors), Geological and geophysical investigations of continental margins. *American Association of Petroleum Geologists Memoir*, 29, 432-42.

Dubois, J., Ravenne, C., Aubertin, A., Louis, J., Guillaume, R., Launay, J., & Montadert, L., 1974 — Continental margins near New Caledonia. *In* Burk, C.A., & Drake, C.L., (editors), The geology of continental margins. *Springer-Verlag, New York*, 521-535.

Eade, J.V., 1984 — West Norfolk Ridge and the regional unconformity: products of Eocene-Oligocene plate collision? (Abstract). *In* Programme and abstracts, Geological Society of New Zealand Annual Conference. *Miscellaneous Publication of Geological Society of New Zealand*, 3(A), 44.

Emery, K.O., 1975 — Undiscovered petroleum resources of deep ocean floor. *In* Haun, J.D., (editor), Methods of estimating the volume of undiscovered oil and gas resources. *American Association of Petroleum Geologists Studies in Geology*, 1, 162-170.

Etheridge, M.A., Symonds, P.A., & Lister, G.S., in press — Application of detachment model to reconstruction of conjugate passive margins. *In* Tankard, A.J., & Balkwill, H.R., (editors), Extensional tectonics and stratigraphy of the North Atlantic margins. *American Association of Petroleum Geologists Publication.*

Exon, N.F., & Willcox, J.B., 1980 — The Exmouth Plateau: stratigraphy, structure, and petroleum potential. *Bureau of Mineral Resources, Australia, Bulletin*, 199.

Falvey, D.A., 1974 — The development of continental margins in plate tectonic theory. *The APEA Journal*, 14(1), 96-106.

Falvey, D.A., & Mutter, J.C., 1981 — Regional plate tectonics and the evolution of Australia's passive continental margins. *BMR Journal of Australian Geology & Geophysics*, 6, 1-29.

Fitzgerald, T.A., 1980 — Giant field discoveries 1968-1978: an overview. *In* Halbouty, M.T., (editor), Giant Oil and Gas Fields of the Decade. *American Association of Petroleum Geologists Memoir*, 30, 1-5.

Forman, D.J., & Hinde, A.L., 1986 — Examination of the creaming methods of assessment applied to the Gippsland Basin, offshore Australia. *In* Rice, D.D., (editor), Oil and gas assessment — methods and applications. *American Association of Petroleum Geologists Studies in Geology*, 21, 101-110.

Fraser, A.R., & Tilbury, L.A., 1979 — Structure and stratigraphy of the Ceduna Terrace region, Great Australian Bight. *The APEA Journal*, 19(1), 53-65.

Gibbs, A.D., 1984 — Structural evolution of extensional basin margins. *Journal of the Geological Society of London*, 141, 609-620.

Goslin, J., & Patriat, P., 1984 — Absolute and relative plate motions and hypotheses on the origin of five aseismic ridges in the Indian Ocean. *Tectonophysics*, 101, 221-244.

Grim, P.J., 1969 — Heatflow measurements in the Tasman Sea. *Journal of Geophysical Research*, 74, 3933-3934.

Halbouty, M.T., King, R.E., Klemme, H.D., Dott, R.H., & Meyerhoff, A.A., 1970a — World's giant oil and gas fields, geologic factors affecting their formation, and basin classification, part II, factors affecting formation of giant oil and gas fields, and basin classification. *In* Halbouty, M.T., (editor), Geology of giant petroleum fields. *American Association of Petroleum Geologists Memoir*, 14, 528-555.

Halbouty, M.T., Meyerhoff, A.A., King, R.E., Dott, R.H., Klemme, H.D., & Shabad, T., 1970b — World's giant oil and gas fields, geologic factors affecting their formation, and basin classification, part I, giant oil and gas fields. *In* Halbouty, M.T., (editor), Geology of giant petroleum fields. *American Association of Petroleum Geologists Memoir*, 14, 502-528.

Hedberg, H.D., 1975 — The volume of sediment fallacy in estimating petroleum resources. *In* Haun, J.D., (editor), Methods of estimating the volume of undiscovered oil and gas resources. *American Association of Petroleum Geologists Studies in Geology*, 1, 161.

Hedberg, H.D., Moody, J.D., & Hedberg, R.M., 1979 — Petroleum prospects of the deep offshore. *American Association of Petroleum Geologists Bulletin*, 63(1), 286-300.

Hinz, K., & Shipboard Party, 1985 — Geophysical, geological and geochemical studies off West Tasmania and on the South Tasman Rise. *Bundesanstalt fur Geowissenschaften und Rohstoffe Report, Cruise SO36 (2).*

Houtz, R.E., Hayes, D.E., & Markl, R.G., 1977 — Kerguelen Plateau bathymetry, sediment distribution and crustal structure. *Marine Geology*, 25, 95-130.

Huff, K.F., 1978 — Frontiers of world exploration. *Oil and Gas Journal*, 76(40), 214-220.

Huff, K.F., 1980 — Frontiers of world exploration. *In* Miall, A.D., (editor), Facts and principles of world petroleum occurrence. *Canadian Society of Petroleum Geologists Memoir*, 6, 343-362.

Jongsma, D., & Mutter, J.C., 1978 — Non-axial breaching of a rift valley: evidence from the Lord Howe Rise and the southeastern Australia margin. *Earth and Planetary Science Letters*, 39, 226-234.

Jongsma, D., & Petkovic, P., 1977 — The structure of the Naturaliste Plateau. *The APEA Journal*, 17, 3-12.

Kingston, D.R., Dishroon, C.P., & Williams, P.A., 1983 — Global basin classification system. *American Association of Petroleum Geologists Bulletin*, 67, 2175-2193.

Klemme, H.D., 1971a — What giants and their basins have in common. *Oil and Gas Journal*, 69(9), 85-90.

Klemme, H.D., 1971b — To find a giant, find the right basin. *Oil and Gas Journal*, 69(10), 103-110.

Klemme, H.D., 1975 — Giant oil fields related to their geological setting: a possible guide to exploration. *Bulletin of Canadian Petroleum Geology*, 23(1), 30-66.

Klemme, H.D., 1980 — Petroleum basins — classifications and characteristics. *Journal of Petroleum Geology*, 3(2), 187-207.

Klemme, H.D., 1983 — Field size distribution related to basin characteristics. *Oil and Gas Journal*, 81(52), 168-176.

Korsch, R.J., O'Brien, P.E., Sexton, M.J., Wake-Dyster, K.D., & Wells, A.T., 1989 — Development of Mesozoic transtensional basins in easternmost Australia. *Australian Journal of Earth Sciences*, 36, 13-28.

Kreuger, Jr., W.C., 1978 — Sediment thicknesses and percentages. *Oil and Gas Journal*, 76(3), 88-90.

Kroenke, L.W., 1984 — Cenozoic tectonic development of the southwest Pacific. *United Nations Economic and Social Commission for Asia and the Pacific, Committee for Co-ordination of Joint Prospecting for Mineral Resources in the South Pacific Offshore areas, Technical Bulletin* No. 6, 122 pp.

Lister, G.S., Etheridge, M.A., & Symonds, P.A., in press — Detachment models for the formation of passive continental margins. *Tectonics.*

Luyendyk, B.P., & Rennick, W., 1977 — Tectonic history of aseismic ridges in the Eastern Indian Ocean. *Geological Society of America Bulletin* 88, 1347-1356.

McCrossan, R.G., & Porter, J.W., 1973 — The geology and petroleum potential of the Canadian sedimentary basins — a synthesis. *In* McCrossan, R.G., (editor), The future petroleum provinces of Canada. *Canadian Society of Petroleum Geologists Memoir*, 1, 589-720.

Miller, B.M., 1986 — Resource appraisal methods: choice and outcome. *In* Rice, D.D., (editor), Oil and gas assessment — methods and applications. *American Association of Petroleum Geologists Studies in Geology*, 21, 1-23.

Munschy, M., & Schlich, R., 1987 — Structure and evolution of the Kerguelen-Heard Plateau (Indian Ocean) deduced from seismic stratigraphy studies. *Marine Geology*, 76, 131-152.

Mutter, J.C., & Cande, S.C., 1983 — The early opening between Broken Ridge and Kerguelen Plateau. *Earth and Planetary Science Letters*, 65, 369-376.

Nougier, J., 1969 — Contribution a l'etude geologique et geomorphologique des iles Kerguelen (T.T.A.A.F.). *Comite National Francais Recherches Antarctiques*, 27, 440 pp.

Ocean Drilling Program Leg 120 Scientific Party, 1988a — That sinking feeling. *Nature*, 334, 385-386.

Ocean Drilling Program Leg 120 Scientific Party, 1988b — ODP at Kerguelen Plateau — Leg 120 explores origins and history. *Geotimes*, 33(9), 12-16

Officer, C.B., 1955 — Southwest Pacific crustal structures. *Transactions of the American Geophysical Union*, 36, 449-459.

Packham, G.H., & Falvey, D.A., 1971 - A hypothesis for the formation of marginal seas in the western Pacific. *Tectonophysics*, 11, 79-109.

Perrodon, A., 1971 — Essai de classification des bassins sedementaires. *Nancy, France, Sciences de la Terre*, 16, 195-227.

Prescott, J.R.V., 1979 — The Australian continental shelf in its international context. *In* Prescott, J.R.V., (editor), Australia's continental shelf. *Nelson, Melbourne*, 95-120.

Prescott, J.R.V., 1985 — Australia's maritime boundaries — Canberra studies in world affairs no. 16. *Department of International Relations, Australian National University, Canberra*, 189 pp.

Ramsay, D.C., Colwell, J.B., & others, 1986a — 'Rig Seismic' research cruise 2: Kerguelen Plateau — initial report. *Bureau of Mineral Resources, Australia, Report* 270, 41 pp.

Ramsay, D.C., Colwell, J.B., Coffin, M.F., Davies, H.L., Hill, P.J., Pigram, C.J., & Stagg, H.M.J., 1986b — New findings from the Kerguelen Plateau. *Geology*, 14, 589-593.

Resnick, V.S., 1986 — Multiregressional models for ranged estimates of the petroleum potential of sedimentary basins. *Journal of Petroleum Geology*, 10(1), 87-100.

Ringis, J., 1972 — The structure and history of the Tasman Sea and the southeast Australian margin. *Ph.D thesis, University of New South Wales, Sydney.*

Roeser, H., & Shipboard Party, 1985 — Geophysical, geological and geochemical studies on Lord Howe Rise. *Bundesanstalt fur Geowissenschaften und Rohstoffe Report, Cruise SO36 (1).*

Ross, D.A., 1979 — Opportunities and uses of the ocean. *Springer-Verlag, New York*, 320 pp.

Schlich, R., Delteil, J., Moulin, J., Patriat, P., & Guillaume, R., 1971 — Mise en evidence d'une sedimentation de marge continentale sur le plateau Kerguelen-Heard. *Comptes Rendus de l'Academie des Sciences, Paris*, 272, 2060-2063.

Schlich, R., Munschy, M., Boulanger, D., Cantin, B., Coffin, M.F., Durand, J., Humler, E., Li, Z.G., Savary, J., Schaming, M., & Tissot, J.D., 1988 — Resultats preliminaires de la campagne oceanographique de seismique reflexion multitraces MD47 dans le domaine sud du plateau de Kerguelen. *Comptes Rendus de l'Academie des Sciences, Paris*, 306, 635-642.

Shaw, R.D., 1978 — Sea floor spreading in the Tasman Sea: a Lord Howe Rise-eastern Australian reconstruction. *Australian Society of Exploration Geophysicists Bulletin*, 9, 75-81.

Shor, G.G., Kirk, H.K., & Menard, G.L., 1971 — Crustal structure of the Melanesian area. *Journal of Geophysical Research*, 76, 2562-2586.

Stagg, H.M.J., & Willcox, J.B., 1988 — Seismic facies distribution in the central Great Australian Bight. *In* Extended Abstracts — Palaeogeography, Sea Level & Climate, Implications for Resource Exploration, 17th BMR Research Symposium, Canberra, 8-10 November 1988. *Bureau of Mineral Resources, Australia, Record* 1988/42, 29-38.

Symonds, P.A., & Cameron, P.J., 1977 — The structure and stratigraphy of the Carnarvon Terrace and Wallaby Plateau. *The APEA Journal*, 17(1), 30-41.

Symonds, P.A., & Willcox, J.B., 1988 — Definition of the continental margin using U.N. Convention on the Law of the Sea (Article 76), and its application to Australia. *Bureau of Mineral Resources, Australia, Record* 1988/38.

Threlfall, W.F., Brown, B.R., & Griffith, B.R., 1976 — Gippsland Basin, offshore. *In* Leslie, R.E., Evans, H.J., & Knight, C.L., (editors), Economic geology of Australia and Papua New Guinea, 3 — petroleum. *Australasian Institute of Mining and Metallurgy, Monograph Series*, 7, 41-66.

Ulmishek, G., 1986 — Stratigraphic aspects of petroleum resource assessment. *In* Rice, D.D., (editor), Oil and gas assessment — methods and applications. *American Association of Petroleum Geologists Studies in Geology*, 21, 59-68.

United Nations, 1983 — The Law of the Sea: official text of the United Nations Convention on the Law of the Sea, with annexes and index. *United Nations Publication, New York*, 224 pp.

Uspenskaya, N.Y., 1967 — Principles of oil and gas territories, subdivisions, and the classification of oil and gas accumulations. *7th World Petroleum Congress Proceedings*, 2, 961-969. *Elsevier Publishing Company, Amsterdam.*

Veevers, J.J., & Cotterill, D., 1978 — Western margin of Australia — evolution of a rifted arch system. *Geological Society of America Bulletin*, 98, 337-355.

Vogt, P.R., & Conolly, J.R., 1971 — Tasmanid guyots: the age of the Tasman basin and motion between the Australian plate and the mantle. *Geological Society of America Bulletin*, 82, 2577-2584.

Von Herzen, R.P., & Langseth, M.G., 1965 — Present status of heat flow measurements. *In* Ahrens, L.H., Press, F., Runcorn, S.K., & Urey, H.C., (editors), Physics and chemistry of the earth. *Pergamon Press, Oxford*, vol. 6, 365-407.

Von Rad, U., & Exon, N.F., 1983 — Mesozoic-Cenozoic sedimentary and volcanic evolution of the starved passive continental margin off northwest Australia. *In* Watkins, J.S., & Drake, C.L., (editors), Studies in continental margin geology. *American Association of Petroleum Geologists Memoir*, 34, 253-281.

Von Stackelberg, U., Exon, N.F., von Rad, U., Quilty, P., Shafik, S., Beiersdorf, H., Seibertz, E., & Veevers, J.J., 1980 — Geology of the Exmouth and Wallaby Plateaus off northwest Australia: sampling of seismic sequences. *BMR Journal of Australian Geology & Geophysics*, 5, 113-140.

Watkins, N.D., Gunn, B.M., Nougier, J., & Baski, A.K., 1974 — Kerguelen: continental fragment or oceanic island? *Geological Society of America Bulletin*, 85, 201-212.

Weeks, L.G., 1952 — Factors of sedimentary basin development that control oil occurrence. *American Association of Petroleum Geologists Bulletin*, 36, 2071-2124.

Weissel, J.K., & Hayes, D.E., 1977 — Evolution of the Tasman Sea reappraised. *Earth and Planetary Science Letters*, 36, 77-84.

Whiticar, M.J., Berner, U., Poggenburg, J., & Tostmann, H., 1985 — Shipboard report of geochemical surface exploration off western Tasmania and on the South Tasman Rise. In Hinz, K., & Shipboard Party, 1985. Geophysical, geological and geochemical studies off West Tasmania and on the South Tasman Rise. *Bundesanstalt fur Geowissenschaften und Rohstoffe Report, Cruise SO36(2)*, 141-171.

Whitworth, R., Willcox, J.B., & others, 1985 — Rig Seismic research cruise 1: Lord Howe Rise. *Bureau of Mineral Resources, Australia, Report* 266, 27 pp.

Willcox, J.B., 1978 — The Great Australian Bight : a regional interpretation of gravity, magnetic, and seismic data from the Continental Margin Survey. *Bureau of Mineral Resources, Australia, Report* 201.

Willcox, J., 1981 — Petroleum prospectivity of Australian marginal plateaus. *In* Halbouty, M.T., (editor), Energy Resources of the Pacific Region. *American Association of Petroleum Geologists Studies in Geology*, 12, 245-272.

Willcox, J.B., & Stagg, H.M.J., in press — Australia's southern margin: a product of oblique extension. *Tectonophysics.*

Willcox, J.B., Symonds, P.A., Hinz, K., & Bennett, D., 1980 — Lord Howe Rise, Tasman Sea — preliminary geophysical results and petroleum prospects. *BMR Journal of Australian Geology & Geophysics*, 5, 225-236.

Williamson, P.E., Exon, N.F., ul Haq, B., von Rad, U., & Leg 122 Shipboard Scientific Party, 1988 — A northwest shelf Triassic reef play: results from ODP Leg 122. *The APEA Journal*, 29(1), 328-344.

Woodward, D.J., & Hunt, T.M., 1971 — Crustal structures across the Tasman Sea. *New Zealand Journal of Geology and Geophysics*, 14, 39-45.

BMR Journal of Australian Geology & Geophysics, 11, 37-62

Planktonic foraminifera and age of sediments, west Tasmanian margin, South Tasman Rise and Lord Howe Rise.

D.J. Belford[1]

Dredge and core samples of sediments recovered from the west Tasmanian margin, South Tasman Rise and the Lord Howe Rise, on R.V. *Sonne*, are of possible Eocene, late Oligocene, early and late Miocene, early and late Pliocene, and Pleistocene or younger ages. Reworked Paleocene and Eocene specimens occur in some cores and dredge samples of late Oligocene age. Some cores show a major stratigraphical break from late Oligocene to Pleistocene. The coiling direction of *Turborotalia pachyderma* was investigated as a possible method of correlation of younger cores, and also as an indicator of palaeoclimatic changes. No correlation between cores was possible using coiling curves, which indicate rapid and irregular changes in sea-water temperatures over small areas, assuming that the coiling direction of *T. pachyderma* is an indication of sea-water temperature.

Introduction

This paper deals with samples taken during a cruise of the R.V. *Sonne* during April-May 1985 to the west Tasmanian margin, the South Tasman Rise and the Lord Howe Rise. Samples consist of dredge material, piston cores and gravity cores. A list of geological stations is given in Table 1, and a list of registered samples is given in Table 2. Sample localities are shown in Figure 1. All figured specimens are deposited in the Commonwealth Palaeontological Collection, Canberra, Australia, under numbers (prefixed CPC) 27458 to 27594.

Brief shipboard examinations were carried out to provide age determinations, and more detailed work was done later. Only the planktonic fauna has been studied, although several samples contain a considerable benthonic fauna.

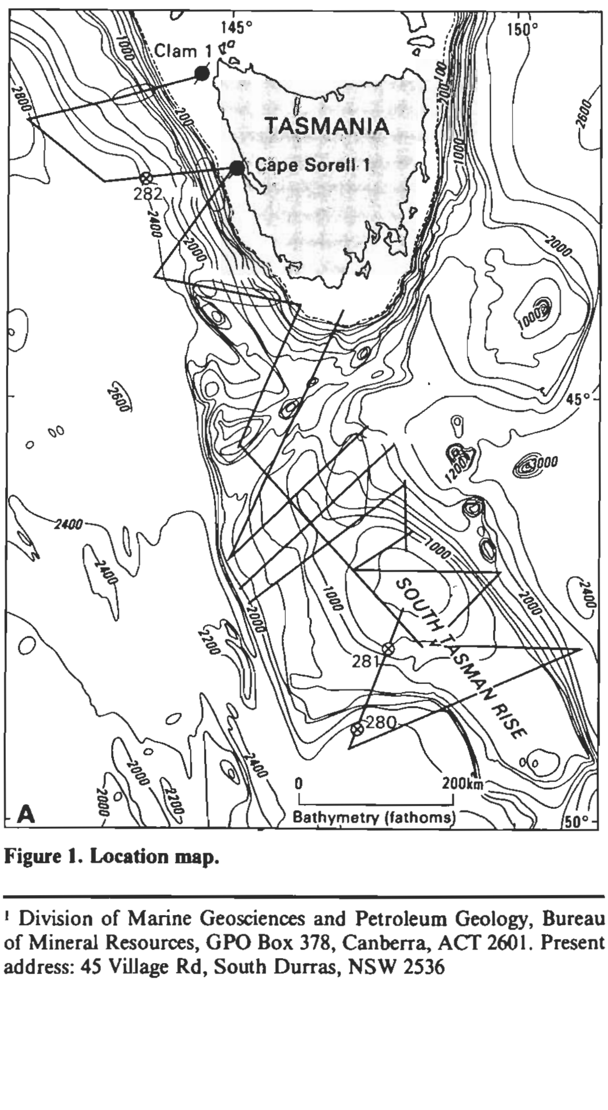

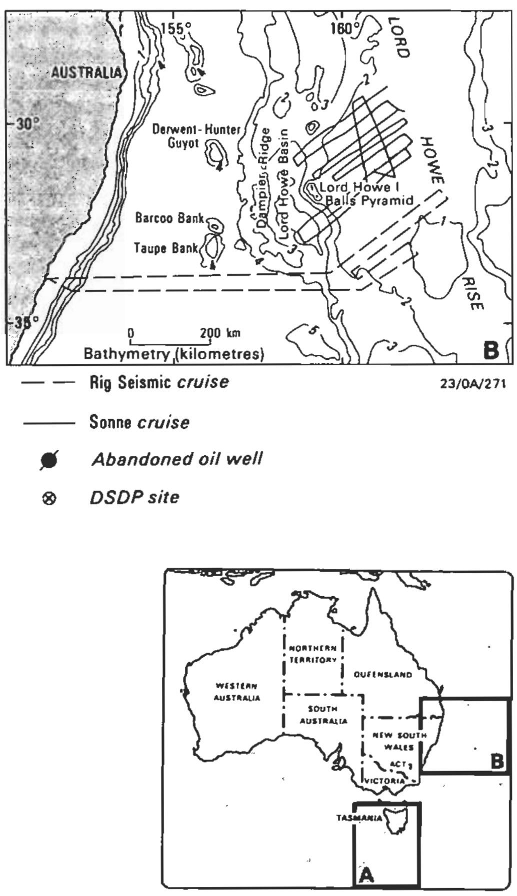

Figure 1. Location map.

Some cores were selected for detailed examination; the fauna of these is given in Tables 3 to 6; Table 7 gives the foraminiferal distribution in other cores examined. The coiling direction of *Turborotalia pachyderma* was also studied in several cores; the results are plotted in Figure 3.

Age and depositional environment of sediments

The faunas of the samples are closely comparable to faunas from the New Zealand succession, and reference is made to New Zealand Stages in the following discussion. The samples are separated into the following groups on the basis of the oldest beds present.

Eocene

The oldest sediments from which foraminifera were obtained, at localities 45KL, 56KL and 32KD, are possibly Eocene.

[1] Division of Marine Geosciences and Petroleum Geology, Bureau of Mineral Resources, GPO Box 378, Canberra, ACT 2601. Present address: 45 Village Rd, South Durras, NSW 2536

Table 1. RV *Sonne* cruise SO-36C. Geological stations.

Station number	*Latitude S*	*Longitude E*	*Depth m*	*Sample type*	*Core recovery m*
Offshore West Tasmania and South Tasman Rise					
SO-36-01	41°03.789′	143°25.120′	2499	KL	1.05
SO-36-02	41°06.246′	143°21.872′	2625	KL	2.80
SO-36-03	41°12.505′	142°53.599′	3795	KL	0.55
SO-36-04	41°20.200′	142°20.055′	4216	KD	
	to	to	to		
	41°20.550′	142°20.135′	4084		
SO-36-05	42°10.798′	144°44.552′	362	SL	2.00
SO-36-06	42°14.449′	144°43.648′	907	SL	2.60
SO-36-07	42°18.520′	144°40.243′	1085	SL	4.30
SO-36-08	42°22.065′	144°37.289′	1409	SL	3.05
SO-36-09	42°25.909′	144°34.004′	1711	SL	3.00
SO-36-10	42°25.319′	144°28.754′	2120	SL	2.60
SO-36-11	42°21.814′	144°31.452′	1855	SL	1.30
SO-36-12	42°17.991′	144°33.945′	1566	SL	2.00
SO-36-13	42°14.320′	144°37.357′	1167	SL	4.60
SO-36-14	42°10.562′	144°40.942′	789	SL	3.80
SO-36-15	42°14.068′	144°47.204′	351	SL	4.50
SO-36-16	42°05.111′	144°41.815′	476	SL	4.70
SO-36-17	42°03.094′	144°35.116′	1042	SL	3.75
SO-36-18	42°08.741′	144°32.272′	1593	SL	3.50
SO-36-19	42°11.156′	144°28.290′	2100	SL	1.20
SO-36-21	43°36.751′	144°22.985′	3574	SL	2.00
SO-36-23	43°38.345′	144°30.699′	3702	SL	1.80
SO-36-24	43°38.761′	144°35.474′	3552	SL	2.40
SO-36-25	43°39.277′	144°34.992′	3597	KL	3.60
SO-36-26	43°37.495′	144°29.336′	3778	KL	1.25
SO-36-27	43°40.137′	144°40.433′	3401	KL	2.90
SO-36-31	43°49.060′	145°56.275′	530	KD	
	to	to	to		
	43°49.050′	145°56.375′	500		
SO-36-32	43°49.100′	145°55.760′	680		
	to	to	to		
	43°49.035′	145°55.870′	650		
SO-36-33	43°48.690′	145°56.505′	510	KD	
	to	to	to		
	43°48.700′	145°56.670′	460		
SO-36-38	45°12.286′	145°22.870′	1886	KL	2.10
SO-36-39	45°48.208′	145°30.142′	2829	KL	2.90
SO-36-40	45°58.556′	145°43.672′	2446	KL	2.65
SO-36-41	46°05.431′	145°51.786′	2449	KL	2.30
SO-36-42	46°22.338′	146°13.308′	1968	KL	1.15
SO-36-43	46°54.253′	145°02.837′	3520	KD	
	to	to	to		
	46°53.861′	145°05.618′	3086		
SO-36-44	47°24.128′	145°10.059′	3968	KD	
	to	to	to		
	47°24.186′	145°10.575′	3670		
SO-36-45	47°04.005′	146°12.867′	2484	KL	0.90
SO-36-46	46°56.488′	145°51.322′	2718	KL	3.60
SO-36-47	46°52.161′	145°59.571′	2497	KL	3.90
SO-36-48	46°45.763′	146°10.161′	2540	KL	3.90
SO-36-49	46°28.766′	146°35.375′	1878	KL	2.30
SO-36-50	46°30.843′	146°32.227′	1812	KL	2.30
SO-36-51	46°17.661′	146°52.059′	2398	KL	3.10
SO-36-53	46°26.355′	147°27.078′	1868	KL	2.35
SO-36-54	46°22.836′	147°33.792′	2215	KL	3.60
SO-36-55	45°36.890′	147°36.514′	3625	KL	7.78
SO-36-56	45°31.904′	147°27.794′	3371	KL	4.98
Dampier and Lord Howe Rise					
SO-36-57	31°51.810′	157°22.690′	2530	KD	
	to	to	to		
	31°56.670′	157°22.780′	2370		
SO-36-58	30°55.300′	160°56.396′	1422	SL	2.68
SO-36-59	30°48.774′	161°05.244′	1435	SL	1.60
SO-36-61	30°33.017′	161°26.294′	1343	SL	3.26
SO-36-62	28°35.815′	163°05.422′	1557	KL	1.05

KL — piston core; SL — gravity core; KD — dredge.

Table 2. RV *Sonne* cruise SO-36C. Registered samples.

Registered number	*Cruise sample*
85640001A	1KL, top
85640001B	1KL, base
85640002A	2KL, top
85640002B	2KL, 2-4cm
85640002C	2KL, 26-28cm
85640002D	2KL, 40-42cm
85640002E	2KL, 45-47cm
85640002F	2KL, 70-72cm
85640002G	2KL, 110-112cm
85640002H	2KL, 140-142cm
85640002I	2KL, 170-172cm
85640002J	2KL, 200-202cm
85640002K	2KL, 230-232cm
85640002L	2KL, 270-272cm
85640002M	2KL, 278-280cm
85640002N	2KL, c.c.
85640003A	3KL, 45cm
85640003B	3KL, c.c.
*85640004	4KD
*85640005A	5SL, top
*85640005B	5SL, 50cm
*85640005C	5SL, 200cm
*85640006	6SL, c.c.
*85640007	7SL, c.c.
*85640008	8SL, c.c.
85640009A	9SL, c.c.
85640009B	9SL, c.c.
85640010A	10SL, grey mud, base
85640010B	10SL, base
85640010C	10SL, c.c.
*85640011	11SL, c.c.
*85640012	12SL, c.c.
85640013A	13SL, 0-2cm
85640013B	13SL, 29-31cm
85640013C	13SL, 58-60cm
85640013D	13SL, 90-92cm
85640013E	13SL, 120-122cm
85640013F	13SL, 150-152cm
85640013G	13SL, 180-182cm
85640013H	13SL, 210-212cm
85640013I	13SL, 240-242cm
856400013J	13SL, 270-272cm
85640013K	13SL, 300-302cm
85640013L	13SL, 330-332cm
85640013M	13SL, 360-362cm
85640013N	13SL, 390-392cm
85640013O	13SL, 420-422cm
85640013P	13SL, 450-452cm
85640013Q	13SL, c.c.
*85640014	14SL, c.c.
*85640015	15SL, c.c.
*85640016A	16SL, 12-15cm
*85640016B	16SL, 394-398cm
*85640017	17SL, 371-375cm
85640018	18SL, c.c
85640019	19SL, c.c.
*85640021A	21SL, 145cm
*85640021B	21SL, 165cm
*85640021C	21SL, c.c.
85640022	22SL, 43-47cm
85640023A	23SL, 0-2cm
85640023B	23SL, 30-32cm
85640023C	23SL, 60-62cm
85640023D	23SL, 90-92cm
85640023E	23SL, 120-122cm
85640023F	23SL, 138-140cm
85640023G	23SL, 140-142cm
85640023H	23SL, 160-162cm
85640023I	23SL, 178-182cm
*85640024A	24SL, 75cm
*85640024B	24SL, 237cm
*85640025A	25KL, surface
*85640025B	25KL, c.c.
85640026A	26KL, 105cm
85640026B	26KL, 125cm
*85640027	27KL, c.c.
**85640031	31KD
**85640032	32KD
**85640033	33KD
85640038	38KL, 200cm
*85640039	29KL, 292-294cm
85640040A	40KL, 31-34cm
*85640040B	40KL, 36-37cm
*85640041	41KL, c.c.
*85640042	42KL, 112-115cm
85640044	44KD
85640045	45KL, 31-32cm
*85640046A	46KL, 300-302cm

Registered number	*Cruise sample*
*85640046B	46KL, c.c.
*85640047	47KL, 388cm
85640048A	48KL, 0-2cm
85640048B	48KL, 30-32cm
85640048C	48KL, 60-62cm
85640048D	48KL, 90-92cm
85640048E	48KL, 120-122cm
85640048F	48KL, 150-152cm
85640048G	48KL, 180-182cm
85640048H	48KL, 210-212cm
85640048I	48KL, 240-242cm
85640048J	48KL, 270-272cm
85640048K	48KL, 300-302cm
85640048L	48KL, 330-332cm
85640048M	48KL, 360-362cm
85640048N	48KL, 388-390cm
*85640049	49KL, c.c.
*85640050	50KL, 360cm
85640051A	51KL, 0-2cm
85640051B	51KL, 30-32cm
85640051C	51KL, 60-62cm
85640051D	51KL, 62-64cm
85640051E	51KL, 90-92cm
85640051F	51KL, 120-122cm
85640051G	51KL, 150-152cm
85640041H	51KL,, 180-182cm
85640051I	51KL, 206-208cm
85640051J	51KL, 210-212cm
85640051K	51KL, 240-242cm
85640051L	51KL, 270-272cm
85640051M	51KL, 298-300cm
85640051N	51KL, c.c.
85640053	53KL, c.c.
*85640054A	54KL, 356-358cm
*85640054B	54KL, c.c.
85640055A	55KL, 0-2cm
85640055B	55KL, 28-32cm
85640055C	55KL, 53-57cm
85640055D	55KL, 78-82cm
85640055E	55KL, 103-107cm
85640055F	55KL, 128-132cm
85640055G	55KL, 153-157cm
85640055H	55KL, 178-182cm
85640055I	55KL, 203-207cm
85640055J	55KL, 228-232cm
85640055K	55KL, 253-257cm
85640055L	55KL, 278-282cm
85640055M	55KL, 303-307cm
85640055N	55KL, 328-332cm
85640055O	55KL, 353-357cm
85640055P	55KL, 378-382cm
85640055Q	55KL, 403-407cm
85640055R	55KL, 428-432cm
85640055S	55KL, 453-457cm
85640055T	55KL, 478-482cm
85640055U	55KL, 503-507cm
85640055V	55KL, 528-532cm
85640055W	55KL, 553-557cm
85640055X	55KL, 578-582cm
85640055Y	55KL, 603-607cm
85640055Z	55KL, 628-632cm
85640055AA	55KL, 653-657cm
85640055BB	55KL, 678-682cm
85640055CC	55KL, 698-702cm
85640055DD	55KL, 723-727cm
85640055EE	55KL, 745-747cm
85640055FF	55KL, 748-752cm
85640055GG	55KL, 763-765cm
85640055HH	55KL, 766-770cm
85640055II	55KL, c.c.
85640056A	56KL, 2-5cm
85640056B	56KL, 50-53cm
85640056C	56KL, 96-98cm
85640056D	56KL, 194-196cm
85640056E	56KL, 210-212cm
85640056F	56KL, 246-248cm
85640056G	56KL, 296-298cm
85640056H	56KL, 397-398cm
85640056I	56KL, 485cm
85640056J	56KL, c.c.
85640057A	57KD, pipe dredge 1
*85640057B	57KD, pipe dredge 2
*85640058	58SL, 257-258cm
*85640059	59SL, 160cm
85640061A	61SL, 0-2cm
85640061B	61SL, 30-32cm
85640061C	61SL, 60-62cm
85640061D	61SL, 90-92cm
85640061E	61SL, 120-122cm
85640061F	61SL, 150-152cm
85640061G	61SL, 180-182cm
85640061H	61SL, 210-212cm
85640061I	61SL, 240-242cm
85640061J	61SL, 270-272cm
85640061K	61SL, 298-300cm
85640061L	61SL, cc.
*85640062	62KL, c.c.

*No detailed work on these samples.
**Composite faunal list given for each of these samples.

Foraminifera were recovered from 31–32 cm and 40–45 cm in core 45KL, and from 296–298 cm in core 56KL. The only forms recovered are poorly preserved specimens of *Haplophragmoides*, usually as casts, most resembling *H.* cf. *incisa* (Stache) of Taylor (1965). Other rare specimens from 40–45 cm in core 45KL have some resemblance to *H. complanata* (Chapman) figured by Taylor, but are broader in relation to the maximum diameter. Taylor (1965) recorded *H. complanata* associated with and present above Paleocene planktonic faunas, but not associated with late Eocene or younger faunas; *H.* cf. *incisa* was said to be associated with late Eocene and younger faunas. The faunas recorded by Taylor are the only ones from the region with which the present specimens can be compared.

A Pleistocene (?early Pleistocene) fauna occurs at 194–196 cm in core 56KL, immediately above a manganese layer. The fauna contains rare *Globorotalia (Truncorotalia) truncatulinoides truncatulinoides, G. (T.) crassaformis crassaformis, G. (Globoconella) triangula, G. (G.) crassula,* and *G. (Obandyella) scitula scitula.* A similar fauna occurs at 210–212 cm, below the manganese layer, but as the sediment is heavily bioturbated the fauna may be present as a contaminant. Pleistocene or younger faunas also occur at higher levels in this core. Apart from the fauna at 296–298 cm, which may be Eocene, there is no indication of age of the sediments below the manganese layer.

One dredge sample from 44KD may also be Eocene, but the evidence is tenuous and inconclusive. The only specimens recovered from the sample are poorly preserved agglutinated forms, *?Bathysiphon* sp., *?Psammosphaera* sp. and one distorted coiled form, probably originally trochoid, referred to *?Trochammina* sp. Agglutinated foraminifera, *Bathysiphon* sp. and *Cyclammina* sp., were recorded from a mid to late Eocene interval at DSDP Site 280 on the South Tasman Rise (Shipboard Scientific Party, 1975a). Paleocene agglutinated foraminifera were recorded from DSDP Site 283 (Shipboard Scientific Party, 1975b; Webb, 1975), but the fauna is more diverse and better preserved than that from dredge sample 44KD.

One small piece of brown limestone in sample 32KD is also probably middle to late Eocene. The limestone contains abundant planktonic foraminifera and bryozoa, and rare algal and molluscan fragments. The planktonic foraminifera consist mainly of small indeterminable globigerinids, together with several specimens considered to be referable to *Globorotalia (Turborotalia).* All specimens appear to be of the *Globorotalia (Turborotalia) cerroazulensis* (Cole) group, as interpreted by Toumarkine & Bolli (1970); rare horizontal sections have been observed, all having four chambers in the final whorl. The range of variation in the specimens is shown in Figure 2. The specimens are referred to *Globorotalia (Turborotalia) cerroazulensis cerroazulensis,* specimens

SPECIES \ SAMPLE	85640002 A	85640002 B	85640002 C	85640002 D	85640002 E	85640002 F	85640002 G	85640002 H	85640002 I	85640002 J	85640002 K	85640002 L	85640002 M	85640002 N
Cruise sample (cm)	2 KL, top	2 KL, 2-4	2 KL, 26-28	2 KL, 40-42	2 KL, 45-47	2 KL, 70-72	2 KL, 110-112	2 KL, 140-142	2 KL, 170-172	2 KL, 200-202	2 KL, 230-232	2 KL, 270-272	2 KL, 278-280	2 KL, c.c.
Catapsydrax dissimilis (Cushman & Bermudez, 1937)					●	●	●	●	●		●	●	●	●
C. unicavus primitiva (Blow & Banner, 1962)												*		*
Dentoglobigerina galavisi (Bermudez, 1961)						●	●							
D. tripartita tripartita (Koch, 1926)						●	●							
Globigerapsis index (Finlay, 1939)									*	cf *		*		*
Globigerina (Beella) digitata digitata (Brady, 1879)			●	●										
G. (Globigerina) bulloides bulloides d'Orbigny, 1826	●	●	●	●										
G. (Globigerina) falconensis Blow, 1959		●	●											
G. (Globigerina) officinalsis Subbotina, 1953							●	●	●					
G. (Globigerina) praebulloides Blow, 1959					●	●	●	●	●	●	●	●	●	●
G. (Globigerina) sp. 1														●
G. (Zeaglobigerina) labiacrassata Jenkins, 1966								●						
Globigerinita glutinata glutinata (Egger, 1893)		●	●	●										
Globigerinoides ruber white form (d'Orbigny, 1839)	●	●	●	●										
Globigerinopsis pseudobesa (Salvatorini, 1967)		●												
Globorotalia (Globoconella) inflata (d'Orbigny, 1839)	●	●		●										
G. (Globoconella) triangula Theyer, 1973	●	●	●											
G. (Obandyella) hirsuta hirsuta (d'Orbigny, 1839)	●	●	●	●										
G. (Truncorotalia) truncatulinoides truncatulinoides (d'Orbigny, 1839)	●	●	●	●										
Globorotaloides suteri Bolli, 1957					●	●	●	●	●					
Hastigerina siphonifera (d'Orbigny, 1839)	●	●	●	●										
Neogloboquadrina dutertrei (d'Orbigny, 1839)	●	●	●	●										
Orbulina universa d'Orbigny, 1839	●	●	●	●										
Paragloborotalia ampliapertura (Bolli, 1957)							●	●						
P. nana (Bolli, 1957)						●				cf	●			
P. opima (Bolli, 1957)						●	●							
P. semivera (Hornibrook, 1961)						●								
Subbotina angiporoides angiporoides (Hornibrook, 1965)					cf.	cf.	●		●					
S. gortanii gortanii (Borsetti, 1959)						●			●					
S. linaperta (Finlay, 1939)									*					
Tenuitella iota (Parker, 1962)			●	●										
T. munda (Jenkins, 1966)						●	●	●						
Turborotalia pachyderma (Ehrenberg, 1861)	●	●	●	●										
T. sp. 1							●							
Turborotalita humilis (Brady, 1884)		●	●	●										
* Reworked species	Pleistocene or younger				Late Oligocene									

Table 3. Distribution of foraminiferal species in core 2KL.
The species below 45 cm are late Oligocene.

20/K55/5

SPECIES \ SAMPLE	85640013 A	85640013 B	85640013 C	85640013 D	85640013 E	85640013 F	85640013 G	85640013 H	85640013 I	85640013 J	85640013 K	85640013 L	85640013 M	85640013 N	85640013 O	85640013 P	85640013 Q
Cruise sample (cm)	13 SL, 0-2	13 SL, 29-31	13 SL, 58-60	13 SL, 90-92	13 SL, 120-122	13 SL, 150-152	13 SL, 180-182	13 SL, 210-212	13 SL, 240-242	13 SL, 270-272	13 SL, 300-302	13 SL, 330-332	13 SL, 360-362	13 SL, 390-392	13 SL, 420-422	13 SL, 450-452	13 SL, c.c.
Globigerina (Globigerina) bulloides bulloides d'Orbigny, 1826	●	●	●	●	●	●	●	●	●	●	●	●	●	●	●	●	●
Globigerinita glutinata glutinata (Egger, 1893)	●	●	●	●	●	●				●	●	●		●	●	●	
Globigerinoides ruber white form (d'Orbigny, 1839)			●							●					●		
Globorotalia (Globoconella) inflata (d'Orbigny, 1839)	●	●	●	●	●	●	●	●	●	●	●	●	●	●	●	●	●
G. (Globoconella) triangula Theyer, 1973	●	●	●	●	●	●	●	●	●	●	●	●	●	●	●	●	●
G. (Obandyella) hirsuta hirsuta (d'Orbigny, 1839)	●	●		●	●	●	●				●	●	●		●	●	●
G. (Truncorotalia) crassaformis crassaformis (Galloway & Wissler, 1927)													●		●		
G. (Truncorotalia) truncatulinoides truncatulinoides (d'Orbigny, 1839)	●	●	●	●	●	●	●	●	●	●	●	●	●	●	●	●	●
Orbulina universa d'Orbigny, 1839	●	●	●	●	●	●	●	●	●	●	●	●	●	●	●	●	●
Tenuitella iota (Parker, 1962)		●	●	●	●	●	●	●	●		●	●		●	●	●	●
Turborotalia pachyderma (Ehrenberg, 1861)	●	●	●	●	●	●	●	●	●	●	●	●	●	●	●	●	●
	Pleistocene or younger																

Table 4. Distribution of foraminiferal species in core 13SL.
All samples are Pleistocene or younger.

20/K55/6

SPECIES \ SAMPLE — BMR registered number	85640051 D	85640051 I	85640051 J	85640051 K	85640051 L	85640051 M	85640051 N
Cruise sample (cm)	51 KL, 62-64	51 KL, 206-208	51 KL, 210-212	51 KL, 240-242	51 KL, 270-272	51 KL, 298-300	51 KL, c.c.
Globigerina (Globigerina) bulloides bulloides d'Orbigny, 1826	●	●	●	●	●	●	
G. (Zeaglobigerina) decoraperta Takayanagi & Saito, 1962							cf
G. (Zeaglobigerina) woodi woodi Jenkins, 1960							●
Globigerinita glutinata glutinata (Egger, 1893)	●						
G. dehiscens dehiscens (Chapman, Parr & Collins, 1934)							●
Globorotalia (Globoconella) conoidea Walters, 1965					●	●	
G. (Globoconella) conomiozea Kennett, 1966					●	●	
G. (Globoconella) inflata (d'Orbigny, 1839)	●		●				
G. (Globoconella) miozea Finlay, 1939							●
G. (Globoconella) puncticulata puncticulata (Deshayes, 1832)				●			
G. (Globoconella) triangula Theyer, 1973	●	●	●				
G. (Obandyella) scitula scitula (Brady, 1882)	●		●	●	●	●	●
G. (Truncorotalia) crassaformis crassaformis (Galloway & Wissler, 1927)	●	●	●	●	●	●	
G. (Truncorotalia) truncatulinoides truncatulinoides (d'Orbigny, 1839)	●	●					
Hastigerina siphonifera (d'Orbigny, 1839)	●						
Neogloboquadrina dutertrei (d'Orbigny, 1839)	●						
Orbulina universa d'Orbigny, 1839	●	●	●	●	●	●	
Sphaeroidinellopsis disjuncta (Finlay, 1940)							●
Turborotalia pachyderma (Ehrenberg, 1861)	●	●	●	●		●	
	Pleistocene or younger		Late Pliocene	Early Pliocene		Late Miocene	Middle Miocene

20/K55/8

Table 5. Distribution of foraminiferal species in core 51KL.
The core catcher sample is middle Miocene.

SPECIES \ SAMPLE — BMR registered number	85640055 A	85640055 B	85640055 C	85640055 D	85640055 E	85640055 F	85640055 G	85640055 H	85640055 I	85640055 J	85640055 K	85640055 L	85640055 M	85640055 N	85640055 O	85640055 P	85640055 Q	85640055 R	85640055 S	85640055 T	85640055 U	85640055 V	85640055 W	85640055 X	85640055 Y	85640055 Z	85640055 AA	85640055 BB	85640055 CC	85640055 DD	85640055 EE	85640055 FF	85640055 GG	85640055 HH	85640055 II
Cruise sample (cm)	55 KL, 0-2	55 KL, 28-32	55 KL, 53-57	55 KL, 78-82	55 KL, 103-107	55 KL, 128-132	55 KL, 153-157	55 KL, 178-182	55 KL, 203-207	55 KL, 228-232	55 KL, 253-257	55 KL, 278-282	55 KL, 303-307	55 KL, 328-332	55 KL, 353-357	55 KL, 378-382	55 KL, 403-407	55 KL, 428-432	55 KL, 453-457	55 KL, 478-482	55 KL, 503-507	55 KL, 528-532	55 KL, 553-557	55 KL, 578-582	55 KL, 603-607	55 KL, 628-632	55 KL, 653-657	55 KL, 678-682	55 KL, 698-702	55 KL, 723-727	55 KL, 745-747	55 KL, 748-752	55 KL, 763-765	55 KL, 766-770	55 KL, c.c.
Globigerina (Beella) digitata dititata (Brady, 1879)	●		●			●						●	●				●										●								
G. (Globigerina) bulloides bulloides d'Orbigny, 1826	●	●	●	●	●	●	●	●	●	●	●	●	●	●	●	●	●	●	●	●	●	●	●		●	●	●	●	●	●	●	●	●	●	●
Globigerinita glutinata glutinata (Egger, 1893)		●	●	●			●	●	●		●				●	●	●	●		●		●	●			●		●		●					●
Globigerinoides cyclostomus (Galloway & Wissler, 1927)	●																																		
G. ruber white form (d'Orbigny, 1839)																	●									●	●								
Globigerinopsis pseudobesa (Salvatorini, 1967)																	cf																		
Globorotalia (Globoconella) inflata (d'Orbigny, 1839)	●	●	●	●	●	●	●	●	●	●	●	●	●	●	●	●	●		●	●	●	●	●	●	●	●	●	●	●	●	●		●	●	
G. (Globoconella) triangula Theyer, 1973	●	●	●	●	●	●	●	●	●	●	●	●	●	●	●	●	●	●	●	●	●	●	●	●	●	●	●	●	●	●	●	●	●	●	●
G. (Obandyella) hirsuta hirsuta (d'Orbigny, 1839)	●	●		●	●	●	●	●	●	●	●	●	●	●	●	●		●		●	●	●	●		●	●	●	●	●	●				●	●
G. (Truncorotalia) crassaformis crassaformis (Galloway & Wissler, 1927)	●												●				●	●	●	●	●	●	●	●	●		●	●	●	●	●	●	●	●	
G. (Truncorotalia) truncatulinoides truncatulinoides (d'Orbigny, 1839)	●	●	●	●	●	●	●	●	●	●	●	●	●	●	●	●	●	●	●	●	●	●	●	●	●	●	●	●	●	●		●	●	●	
Hastigerina siphonifera (d'Orbigny, 1839)	●					●											●									●									
Neogloboquadrina dutertrei (d'Orbigny, 1839)																	●								●										●
Orbulina universa d'Orbigny, 1839	●	●	●	●	●	●		●	●	●	●	●		●	●	●	●	●		●		●	●		●	●	●	●		●	●			●	
Turborotalia pachyderma (Ehrenberg, 1861)	●	●	●	●	●	●	●	●	●	●	●	●	●	●	●	●	●	●	●	●	●	●	●	●	●	●	●	●	●	●	●	●	●	●	●
	Pleistocene or younger																																		Late Pliocene

20/K55/7

Table 6. Distribution of foraminiferal species in core 55KL.
All samples except the core catcher sample, which may be late Pliocene, are Pleistocene or younger.

SPECIES \ SAMPLE (BMR Registered number / Cruise sample)	85640001 A / 1 KL, top	85640001 B / 1 KL, base	85640003 A / 3 KL, 45	85640003 B / 3 KL, c.c.	85640009 A / 9 SL, c.c.	85640009 B / 9 SL, c.c.	85640010 A / 10 SL, grey mud	85640010 B / 10 SL, base	85640010 C / 10 SL, c.c.	85640018 / 18 SL, c.c.	85640019 / 19 SL, c.c.	85640022 / 22 SL, 43-47	85640023 G / 23 SL, 140-142	85640023 H / 23 SL, 160-164	85640023 I / 23 SL, 178-182	85640026 A / 26 KL, 105	85640026 B / 26 KL, 125	85640031 / 31 KD	85640032 / 32 KD	85640033 / 33 KD	85640038 / 38 KL, 200	85640040 A / 40 KL, 31-34	85640053 / 53 KL, c.c.	85640056 A / 56 KL, 50-53	85640056 B / 56 KL, 96-98	85640056 C / 56 KL, 194-196	85640056 D / 56 KL, 210-212	85640057 A / 57 KD, dredge 1
Catapsydrax dissimilis (Cushman & Bermudez, 1937)	●	●	●	●														●	●	●								●
Dentoglobigerina tripartita tripartita (Koch, 1926)																		●	●	●								
D. venezuelana (Hedberg, 1937)																												●
Globigerina (Beella) digitata praedigitata (Parker, 1967)																								●	●			
G. (Beella) digitata digitata (Brady, 1879)																							●					
G. (Globigerina) angustiumbilicata Bolli, 1957																			●									
G. (Globigerina) bulloides bulloides d'Orbigny, 1826					●	●	●	●	●	●	●	●		●		●	●				●	●	●	●	●	●	●	
G. (Globigerina) ciperoensis Bolli, 1957																		●	●									
G. (Globigerina) officinalis Subbotina, 1953	●		cf.																									
G. (Globigerina) praebulloides Blow, 1959		●	●	●							●		●	●	●	*		●	●	●			●					
G. (Globigerina) sp.1			●																									
G. (Globigerina) sp.2																				●								
G. (Globigerina) sp.3											●																	
G. (Zeaglobigerina) decoraperta Takayanagi & Saito, 1962									●							●	●						●					
G. (Zeaglobigerina) labiacrassata Jenkins, 1966	●	●	●	●																								
G. (Zeaglobigerina) sp.1	●	●																										
G. (Zeaglobigerina) woodi woodi Jenkins, 1960	●	●									●			●	●			●		●			●					
Globigerinita glutinata glutinata (Egger, 1893)					●	●	●	●		●				●	●	●					●	●		●	●			
G. uvula (Ehrenberg, 1861)								●																				
Globigerinoides cyclostomus (Galloway & Wissler, 1927)							●																					
G. quadrilobatus quadrilobatus (d'Orbigny, 1846)																												●
G. quadrilobatus sacculifer (Brady, 1877)																												●
G. quadrilobatus triloba (Reuss, 1850)														●	●	●												
G. ruber white form (d'Orbigny, 1839)							●	●								●												
G. sp.1				●																								
G. sp.2														●														
Globigerinopsis pseudobesa (Salvatorini, 1967)						●					●					●					●		●					
Globoquadrina dehiscens dehiscens (Chapman, Parr & Collins, 1934)													●	●	●	*		●	●	●								●
Globorotalia (Globoconella) conoidea Walters, 1965											●					●	●						●					
G. (Globoconella) conomiozea Kennett, 1966											●					cf.							cf.					
G. (Globoconella) crassaconica Hornibrook, 1981																					●							
G. (Globoconella) inflata (d'Orbigny, 1839)					●	●	●	●	●	●		●				●	●				●	●		●	●			
G. (Globoconella) miotumida miotumida Jenkins, 1960											●																	
G. (Globoconella) miotumida explicationis Jenkins, 1971																	cf											
G. (Globoconella) miozea Finlay, 1939													●	●	●													
G. (Globoconella) mons Hornibrook, 1982																●	●											
G. (Globoconella) puncticulata puncticulata (Deshayes, 1832)						●				●																		
G. (Globoconella) puncticulata puncticuloides Hornibrook, 1981					●	●		●	●							●					●						●	
G. (Globoconella) sp.1																					●							
G. (Globoconella) sp.2																					●							
G. (Globoconella) suterae Catalano & Sprovieri, 1971																	●											
G. (Globoconella) triangula Theyer, 1973					●	●	●	●	●	●		●				●						●		●	●	●	●	
G. (Globorotalia) cultrata menardii (Parker, Jones & Brady, 1865)																	●											
G. (Obandyella) hirsuta hirsuta (d'Orbigny, 1839)					●											●	●											
G. (Obandyella) margaritae Bolli & Bermudez, 1965																							cf.					
G. (Obandyella) scitula scitula (Brady, 1882)						●	●	●	●	●		●		●	●	●	●				●	●	●	●	●	●		
G. (Truncorotalia) crassaformis crassaformis (Galloway & Wissler, 1927)					●	●		●	●	●						●	●				●	●	●	●	●	●	●	
G. (Truncorotalia) crassula Cushman & Stewart, 1930						●										●	●				●					●		
G. (Truncorotalia) crozetensis Thompson, 1973																					cf.							
G. (Truncorotalia) truncatulinoides truncatulinoides (d'Orbigny, 1839)					●		●					●										●			●	●	●	
Globorotaloides suteri Bolli, 1957	●	●	●	●															●									
Hastigerina siphonifera (d'Orbigny, 1839)						●	●	●	●	●											●	●			●			
Neogloboquadrina dutertrei (d'Orbigny, 1839)							●	●	●								●				●	●						
Orbulina universa d'Orbigny, 1839					●	●		●	●	●	●		●	●	●	●	●				●		●	●	●	●		
Paragloborotalia ampliapertura (Bolli, 1957)																			●	●								
P. bella (Jenkins, 1967)														●	●													
P. euapertura (Jenkins, 1960)				●														●	●	●								
P. mayeri (Cushman & Ellisor, 1939)																												●
P. nana (Bolli, 1957)	●	●	●	●												*		●	●									
P. opima (Bolli, 1957)	●	●																	●	●								
P. semivera (Hornibrook, 1961)				●										●					●	●								
Sphaeroidinellopsis disjuncta (Finlay, 1940)													●	●	●													
S. seminulina seminulina (Schwager, 1866)																							●					●
Subbotina angiporoides angiporoides (Hornibrook, 1965)			●	●															cf									
S. gortanii gortanii (Borsetti, 1959)																		●		●								
S. linaperta (Finlay, 1939)																cf. *		*		*								
S. triloculinoides (Plummer, 1926)	*	*		*														*	*									
Turborotalia obesa (Bolli, 1957)								●							●		●	●	●	●					●			
T. pachyderma (Ehrenberg, 1861)					●	●	●	●	●	●	●	●				●	●				●	●	●	●	●			
T. Pseudopima (Blow, 1969)								cf.																				
* Reworked species	Late Oligocene	Late Oligocene	Late Oligocene	Late Oligocene	Pleistocene	Late Pliocene	Pleistocene	Pleistocene	Late Pliocene	Late Pliocene	Late Miocene	Pleistocene	Middle Miocene	Middle Miocene	Middle Miocene	Early Pliocene	Early Pliocene	Late Oligocene	Late Oligocene	Late Oligocene	Late Oligocene	Pleistocene	Early Pliocene	Pleistocene	Pleistocene	Pleistocene	Pleistocene	Early Miocene

20/K55/3

Table 7. Distribution of foraminiferal species in core and dredge hauls.

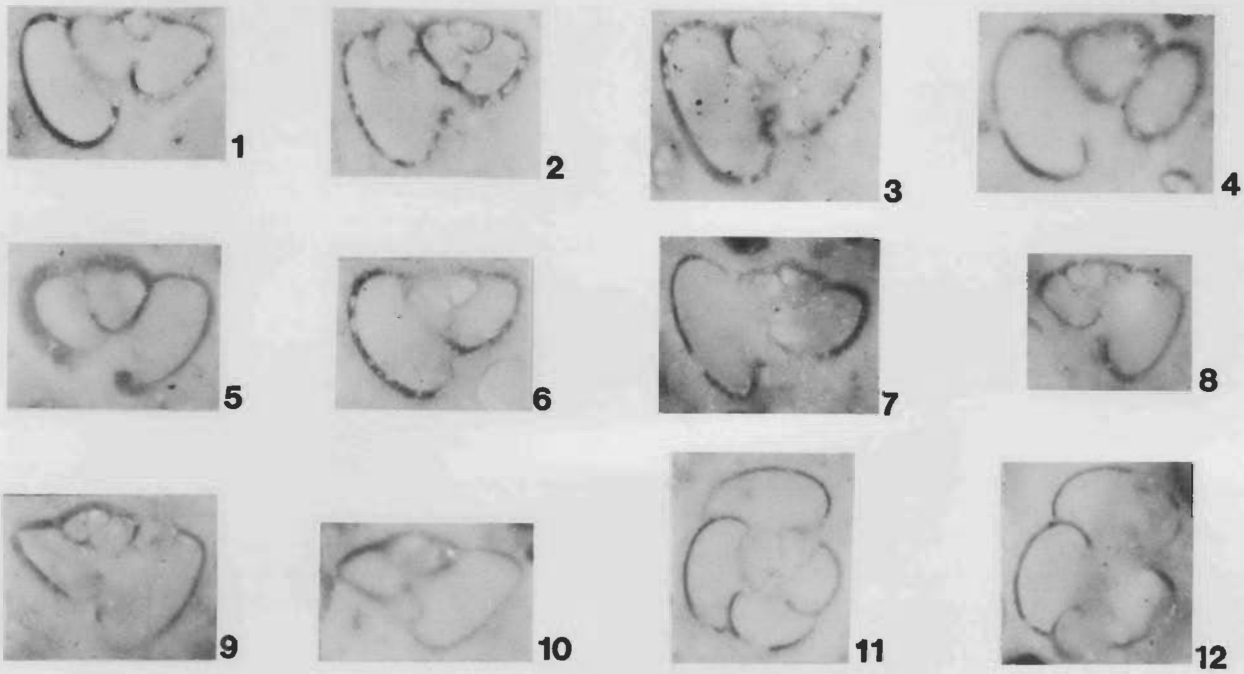

Figure 2. (All figures x80.) Specimens moistened with glycerine and photographed in reflected light. CPC 27458-27461 and CPC 27595-27602, *Globorotalia (Turborotalia) cerroazulensis* (Cole) group, sample 32KD.

1-7: *G.(T.) cerroazulensis cerroazulensis*, 1,CPC 27458; 2, CPC 27459; 3, CPC 27460; 4, CPC 27461; 5, CPC 27595; 6, CPC 27596; 7, CPC 27595. 8-9: Specimens transitional between *G.(T.) cerroazulensis cerroazulensis* and *G.(T.) cerroazulensis cocoaensis* with a narrowly rounded periphery on early chambers of the last whorl, 8, CPC 27598; 9, CPC 27599. 10: *G.(T.) cerroazulensis cocoaensis*, CPC 27600. 11-12: Horizontal sections showing four chambers in the final whorl. Specimens referred to the *G.(T.) cerroazulensis* group, 11, CPC 27601; 12, CPC 27602

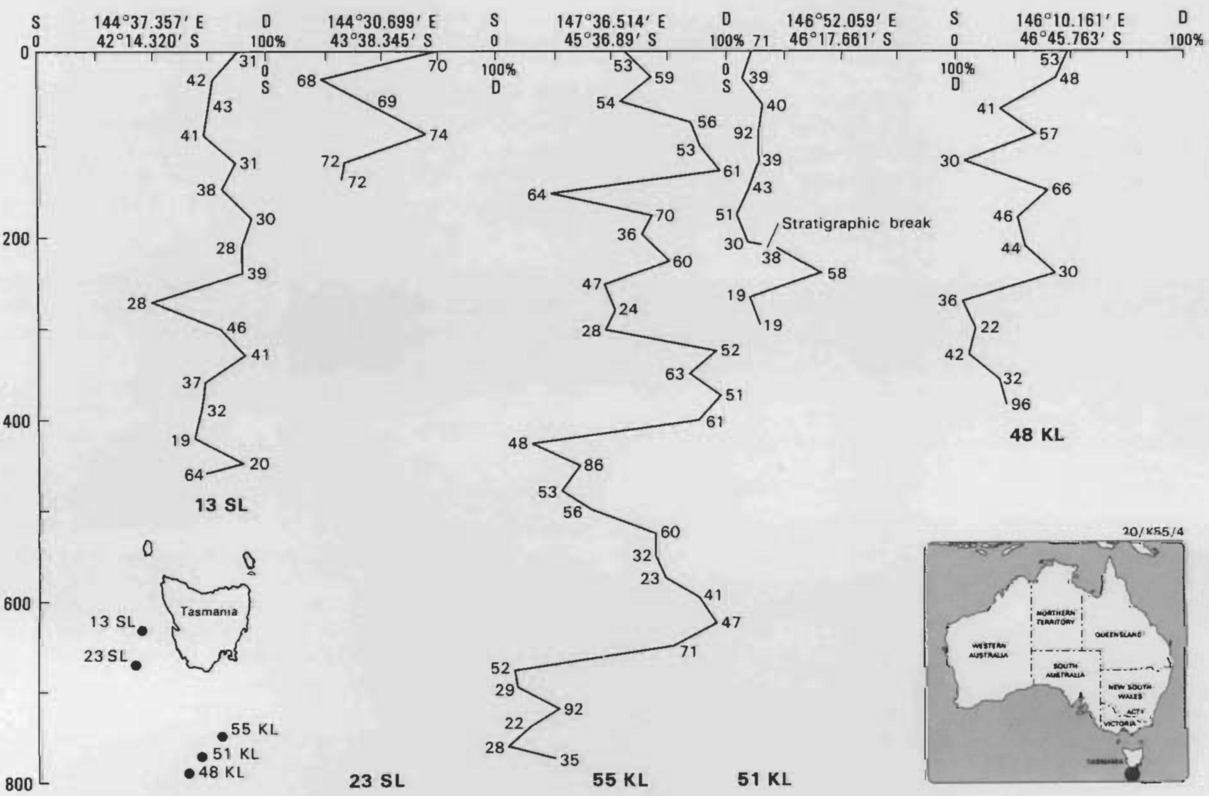

Figure 3. Location of five *Sonne* cores south and west of Tasmania, and variation in their direction of coiling of *Turborotalia pachyderma* with depth in cores.

Numbers of the curves are the number of specimens examined from each sample.

transitional between *G. (T.) cerroazulensis cerroazulensis* and *G. (T.) cerroazulensis cocoaensis*, and *G. (T.) cerroazulensis cocoaensis*. They are closely comparable to the sections of *Globorotalia centralis* Cushman & Bermudez (placed by Toumarkine & Bolli, 1970, in the synonymy of *cerroazulensis cerroazulensis*), and of *G. cerroazulensis*, as figured by Postuma (1971).

Another species to which these specimens have some similarity is *G. (T.) crassaformis* (Galloway & Wissler, 1927). However, this species has a thickened and pustulose test wall, particularly on the early chambers of the last whorl, whereas all the present specimens are thin-walled, and have a smooth test surface. They are considered most probably to be referable to the *cerroazulensis* group, and the sample is therefore given a middle to late Eocene age, Bortonian to Runangan stages of New Zealand.

Late Oligocene

Samples from three cores and three dredge samples are placed in the late Oligocene. The Oligocene/Miocene boundary is placed at the Waitakian/Otaian boundary of the New Zealand sequence, following the suggestion of Jenkins (1970) and the usage of Berggren (1971).

Core 1KL is late Oligocene, Waitakian, throughout, containing species such as *Globigerina (Zeaglobigerina) labiacrassata*, *G. (Z.) woodi woodi*, the *Globigerina (G.) praebulloides* group, *Catapsydrax dissimilis* and *Paragloborotalia opima*. Core 2KL, below 45 cm, also has a late Oligocene fauna, regarded as Whaingaroan, slightly older than that recorded from 1KL. This core is the longest of the three cores that penetrated late Oligocene beds, and it has been examined in more detail; the fauna recorded is given in Table 3. Species recorded include *Catapsydrax dissimilis*, *Dentoglobigerina tripartita tripartita*, *Paragloborotalia opima*, *P. semivera*, *P. ampliapertura*, *Subbotina gortanii gortanii*, *S. angiporoides angiporoides* and *Tenuitella munda*. Towards the bottom of the core the fauna becomes poor, with few specimens. Above 45 cm the core contains a fauna indicating Pleistocene or younger beds, species present including *Globorotalia (Truncorotalia) truncatulinoides truncatulinoides*, *G. (Obandyella) hirsuta hirsuta*, *G. (Globoconella) triangula*, *G. (G.) inflata* and *Turborotalia pachyderma*. At the base of the Pleistocene or younger interval is a coarse band consisting almost wholly of bryozoal fragments, which may be a turbidite deposited at the beginning of this Pleistocene interval. This stratigraphic break, from late Oligocene to Pleistocene, is the same as that recorded by Jenkins (1975, table 1) from DSDP Site 277 on the Campbell Plateau.

Core 3KL is also referred to the late Oligocene, Whaingaroan, and contains a fauna similar to that in core 2KL; this core also has a Pleistocene or younger upper interval, again marked at the base by a coarse bryozoal band.

These three cores also contain rare reworked specimens of Eocene or Paleocene species. 1KL and 3KL contain *Subbotina triloculinoides*; 2KL contains *Catapsydrax unicavus primitiva* and *Globigerapsis index*.

Three dredge samples, 31KD, 32KD and 33KD, also yielded material of late Oligocene age, referred to the Waitakian Stage; the fauna from the dredge samples is similar to that from the cores. *Subbotina triloculinoides* and *S. linaperta* occur as reworked specimens.

The environment of deposition of the sediments in the cores and dredge samples is different. The core material was deposited in deep water; planktonic foraminifera, although often rare, constitute almost the whole of the fauna present. In contrast, the dredge samples, in addition to foraminifera, contain bryozoa, algae, echinoid spines and ostracods. The percentage of planktonic foraminifera in the foraminiferal fauna from these dredge samples ranges from 45% to 66% and reflects the shallower environment of deposition. The dredge samples are considered to be from upper bathyal sediments.

Early Miocene

Early Miocene beds are recorded from only one dredge sample, 57KD, on the Lord Howe Rise. Species recorded are *Globoquadrina dehiscens dehiscens*, *Catapsydrax dissimilis*, *Paragloborotalia mayeri* (including some four-chambered forms resembling *P. nana*), *Globigerinoides quadrilobatus quadrilobatus* and *G. quadrilobatus sacculifer*. These beds are referred to Zone N.6 of Blow (1969). Planktonic foraminifera are dominant in the sample, which is considered to be from deep-water sediments.

Middle Miocene

Cores 23SL and 51KL reached beds of middle Miocene age. 51KL contains *Globorotalia (Globoconella) miozea*, *G. (Obandyella) scitula scitula*, *Globigerina (Zeaglobigerina) woodi woodi*, *Globoquadrina dehiscens dehiscens* and *Sphaeroidinellopsis disjuncta*. The specimens of *G. (Z.) woodi woodi* are very thick-walled, and some develop a thickened apertural lip, and resemble *G. (Z.) labiacrassata*. Some younger species, for example *Turborotalia pachyderma* and *Globorotalia (Truncorotalia) crassaformis crassaformis*, occur in the sample because of contamination during sampling.

Core 23SL contains a similar fauna and in addition *Paragloborotalia bella* and *Orbulina universa* are present. In a sample from 160-170 cm specimens referred to *Paragloborotalia semivera* occur; this species was not recorded above the Clifdenian of New Zealand by Jenkins (1971).

These two cores are regarded as referable to the Lillburnian Stage of the New Zealand succession. They are from deep-water sediments, and planktonic foraminifera are dominant in the fauna.

Late Miocene

One core, 19SL, contains beds of late Miocene, Kapitean, age. Species recorded include *Globorotalia (Globoconella) conoidea*, *G. (G.) conomiozea*, *G. (G.) miotumida miotumida*, *Turborotalia pachyderma* (some specimens integrading with *T. acostaensis*), *Globigerina (Zeaglobigerina) woodi woodi*, *Globigerina (Globigerina) bulloides bulloides* and the *G. (G.) praebulloides* group. Planktonic foraminifera constitute almost all the fauna and the core is considered to be from deep-water sediments.

Early Pliocene

Bottom samples from two cores, 26KL and 53KL, are of early Pliocene, Opotian, age. Species recorded include *Globorotalia (Globoconella) conoidea*, *G. (G.) mons*, *G. (G.)* cf. *conomiozea*, *G. (Truncorotalia) crassaformis crassaformis* and *Sphaeroidinellopsis seminulina seminulina*. One sample from core 26KL, at 105 cm, contains species such as *Globorotalia (Globoconella) triangula* and *G. (Globoconella) inflata* as contamination from younger beds, and also contains as reworked species *Globigerina (G.) praebulloides*, *Globoquadrina dehiscens dehiscens*, *Paragloborotalia nana* and *Subbotina* sp. cf. *linaperta*.

These cores are also regarded as being from deep-water sediments.

Late Pliocene

Several cores penetrated beds of late Pliocene, Mangapanian, age: 9SL, 10SL, 18SL and 38KL. Species recorded include *Globorotalia (Globoconella) triangula*, *G. (G.) puncticulata puncticuloides*, *G. (G.) inflata*, *G. (G.) crassaconica*, *G. (Truncorotalia) crassaformis crassaformis* and *G. (Obandyella) scitula scitula*. Only the sample from the core catcher of 10SL is of late Pliocene age, and it appears that this core extended just below the base of the Pleistocene. Also, only one piece from the core catcher of 9SL contained a fauna referred to the late Pliocene; a second piece contained a Pleistocene or younger fauna.

Core 55KL may have reached beds of latest Pliocene age. The fauna from the core catcher lacks *Globorotalia (Truncorotalia) truncatulinoides truncatulinoides* which appears in beds immediately above.

As planktonic foraminifera are dominant, these cores are regarded as being from deep-water sediments.

Pleistocene or younger

All remaining samples examined contain faunas indicating a Pleistocene, N.22 equivalent, or younger age. No detailed study has been made of these samples. Species recorded include *Globorotalia (Truncorotalia) truncatulinoides truncatulinoides*, *G. (Globoconella) inflata* and *G. (G.) triangula*. Some of the cores previously discussed also contain Pleistocene or younger material.

Samples wholly of Pleistocene or younger age are: 4KD (ooze from small pipe dredge), 5SL, 6SL, 7SL, 8SL, 11SL, 12SL, 13SL, 14SL, 16SL, 17SL, 21SL, 24SL, 25KL, 27KL, 40KL, 41KL, 42KL, 46KL, 47KL, 48KL, 49KL, 50KL, 54KL, 57KD(part), 58SL, 59SL, 61SL and 62KL.

Most samples are from deep-water sediments, with abundant planktonic foraminifera and few benthonic forms. The fauna of 5SL, 6SL, 14SL, 15SL and 16SL contains a considerable proportion of benthonic forms, reflecting the shallower depths in which the sampled sediments were deposited; algae, bryozoa, echinoid spines and mollusca also occur. The percentage of planktonic forms in the foraminiferal fauna from these samples lies within the range of 83% to 98%, a range given for water depths from 320 m to 1600 m by Resig, personal communication, quoted by Chaproniere (1985). Core 25KL, from a water depth of 3597 m, and with abundant plankton, contains worn bryozoal fragments and echinoid spines, possibly transported from shallower depths.

Discussion of selected cores

13SL

Core 13SL, 4.6 m in length, is Pleistocene or younger throughout, the fauna including *Globorotalia (Truncorotalia) truncatulinoides truncatulinoides*, *G. (Globoconella) inflata*, *G. (G.) triangula*, *Globigerina (Globigerina) bulloides bulloides*, *Turborotalia pachyderma* and *Orbulina universa*. The coiling direction of *Turborotalia pachyderma* was examined in detail, and specimens were found to be predominantly dextral.

Distribution of foraminiferal species in this core is shown in Table 4.

23SL

The bottom 40 cm of core 23SL are of middle Miocene, Lillburnian, age, based on the occurrence of species such as *Orbulina universa*, *Globorotalia (Globoconella) miozea*, *Globoquadrina dehiscens dehiscens*, *Sphaeroidinellopsis disjuncta* and *Paragloborotalia bella*. At 140 cm in the core there is a marked lithological change, and the beds above this level are equivalent to N.22, and are Pleistocene, or younger. Species present include *Globorotalia (Truncorotalia) truncatulinoides truncatulinoides*, the *G. (T.) crassaformis* group, *G. (Globoconella) triangula* and *G. (G.) inflata*. The coiling of *Turborotalia pachyderma* in the upper 140 cm of the core has been examined and is discussed in a later section. Distribution of foraminiferal species in the lower part of this core is shown in Table 7.

Jenkins (1975, table 9) recorded a break from middle Miocene to Pleistocene, at DSDP Site 279, and a larger break, from late Oligocene to Pleistocene, at Site 277.

51KL

Core 51KL, 3.10 m in length, also reached beds of middle Miocene age, but has a more complete section than that recovered from 23SL. A sample from the core catcher contains *Globorotalia (Globoconella) miozea*, *Globoquadrina dehiscens dehiscens* and *Sphaeroidinellopsis disjuncta*. *Orbulina* has not been found, but the sample is most probably middle Miocene, because the fauna of the immediately overlying beds in the core, at 298–300 cm, is late Miocene. Species present at this level include *Orbulina universa*, *Globorotalia (Globoconella) conomiozea*, *G. (G.) conoidea* and the *G. (Truncorotalia) crassaformis* group. These beds are late Miocene (Kapitean of the New Zealand succession). Abundant specimens of the *G. (T.) crassaformis* group occur at 270–272 cm, and this sample is placed in the early Pliocene, although very rare *Globorotalia (Globoconella) conomiozea*, regarded by Jenkins (1971) as Kapitean (late Miocene), also occurs. At 210–212 cm a fauna containing *Globorotalia (Globoconella) triangula*, *G. (G.) inflata* and *G. (G.)* cf. *puncticulata puncticulata*, and regarded as late Pliocene, occurs. At 206–208 cm *G. (Truncorotalia) truncatulinoides truncatulinoides* appears, and marks the base of the Pleistocene and younger equivalents in the core. There is a lithological break in the core at 208 cm, and there may be a small stratigraphic break within the late Pliocene-early Pleistocene at this level. Coiling of *Turborotalia pachyderma* is discussed in a later section and Table 5 shows the distribution of foraminiferal species in the core.

55KL

Core 55 KL was the longest core taken, 7.78 m. The sediments are almost entirely Pleistocene or younger. *Globorotalia (Truncorotalia) truncatulinoides truncatulinoides* is absent only from the core-catcher, and the core may have reached beds of latest Pliocene age. Table 6 shows the distribution of foraminiferal species in core 55KL.

Coiling of *Turborotalia pachyderma*

A number of papers have discussed the significance of the coiling direction of *Turborotalia pachyderma* as an indicator of sea water temperature. Ericson (1959) stated that sinistrally coiled populations live in water cooler than 7.2°C in the Arctic, and noted that sinistral coiling is dominant south of latitude 50° south, whereas dextral coiling is dominant farther north. Green (1960) recorded Arctic populations of *T. pachyderma* with 98% sinistral coiling. Bandy (1960) noted that both Arctic and Antarctic Ocean populations are dominantly sinistral coiling and used coiling ratio changes as a criterion for correlation of Pliocene to Recent sediments in the Californian region. Be & Hamlin (1967) recorded the dominance of dextral forms in water temperatures between 11 and 15°C in the North Atlantic, whereas sinistral forms dominated in water between 8.3 and 9.4°C, and they agreed with Ericson's (1959) boundary between dextral and sinistral populations which approximates the 7.2°C isotherm for April. Bandy (1968; 1969) gave a more detailed subdivision of the distribution in which sinistral forms are dominant in waters up to 8°C. He also presented an adaptation of an earlier model of variation in some Neogene planktonic foraminiferal patterns (including *Turborotalia pachyderma*) according to latitude. Cifelli (1971) noted that the nature of the boundary separating dextral and sinistral populations is not clear, and stated that a change in coiling cannot be associated with the 7.2°C April isotherm, and probably not with any single seasonal isotherm. He recorded a wholly dextral assemblage of *'G. pachyderma' (G. incompta*, see also Cifelli & Smith, 1970, for discussion) in waters with a surface temperature of 1.9°C. Cifelli (1971) noted that the sinistral populations recorded by Be & Hamlin (1967) were in waters with July surface temperatures greater than 15°C, and also that specimens collected in this vicinity by Cifelli & Smith (1970) were dextral. Kahn (1981) recorded populations of 100% sinistral *T. pachyderma* at a water temperature as high as 8.5°C in the northeastern Pacific Ocean.

Ericson (1959) found that, in general, the distribution of other species of planktonic foraminifera in cores from the North Atlantic supported the supposition that coiling changes in *T. pachyderma* are influenced by temperature. The significance of planktonic foraminifera as indices of water masses is well established from studies of Recent faunas, and the assumption is made that conclusions resulting from these studies can also be applied to older Quaternary and Tertiary environments and water masses. If this assumption is correct, the coiling ratios of *T. pachyderma* in the present samples show considerable variation in and some rapid changes of water temperature in areas to the west and south of Tasmania (Fig. 3). A more detailed study of a larger number of specimens would probably change the relative proportions of sinistral and dextral forms slightly, but would not affect the general shape of the coiling curves. Most specimens were obtained from the <250 m sediment fraction.

The longest core, 55KL, of 7.78 m, shows three dextral and three sinistral episodes, and intervals of random coiling, including the top 2 cm of the core. Specimens from 51KL are dominantly sinistral through most of the core, with one brief interval tending towards random coiling at 240 cm in the core. The most southerly core examined, 48KL, also contains a majority of sinistral forms, with more fluctuations than found in specimens from core 51KL. The random coiling interval in 48KL at 240 cm matches that of 51KL, and the curves from the lower parts of the two cores also correspond. Core 13SL, the most northerly core examined, has dominantly dextral forms, with one episode of random coiling at 270 cm matching a similar interval in 55KL. Core 23SL, latitudinally midway between 13SL and 55KL, and containing only 140 cm of Pleistocene or younger sediments, shows large and rapid variations between dextral and sinistral coiling.

Bandy (1968) cited occurrences of both dextral and sinistral populations of *T. pachyderma* beyond their usual limits as a result of current action. Cifelli (1971) stated that his data suggest that dextral and sinistral populations are mutually exclusive, but that mixed coiling might be expected where two populations are brought together by mixing of water masses. He did not observe any fixed relationship between coiling direction and temperature. There is no indication in the present material that dextral and sinistral populations are mutually exclusive. The variations observed in coiling ratios could have resulted from fluctuations in the subtropical convergence, or from changes in current patterns. The rapid variations shown by the coiling curves over a small area suggest that changes in small water masses are involved, such as may be caused by current action rather than a large-scale uniform change that would result from a fluctuation in the subtropical convergence. It would be of interest to have oxygen isotope studies carried out on specimens from these cores, for comparison with the coiling curve results.

Jenkins (1967; 1968) investigated the coiling directions of *T. pachyderma* over several New Zealand sections and found ten alternating sinistral and dextral populations which he interpreted as indicating colder and warmer water conditions. Kennett & Watkins (1974) used the changes in frequency of *T. pachyderma*, and the sinistral factor, to determine a palaeoclimatic history of the Blind River section, New Zealand (see also Loutit & Kennett, 1979). They noted a change in the palaeoclimatic record in the latest Miocene, with greater surface-water temperature oscillations during the latest Miocene and Pliocene. Bandy (1968; 1969) delineated world-wide palaeoceanographic cycles in the Neogene; a similar intercontinental pattern of coiling changes occurs in the late Miocene and Pliocene of California and New Zealand (Jenkins, 1967; Bandy, 1968).

The present study is much more detailed than any of these previous investigations, and no correspondence can be found between the resulting coiling curves.

Studies such as those of Kennett (1968), Srinivasan & Kennett (1974), Keller (1978) and Reynolds & Thunell (1986) have established the existence of morphologically distinct forms of *T. pachyderma*, related to palaeoclimatic change and seasonal changes in water temperature. This aspect of *pachyderma* populations has not been studied in detail in the present material. Specimens are generally encrusted and are frequently kummerform; they are referable to form 1 of Keller (1978), or to group A of Reynolds & Thunell (1986). Although group A was considered by Reynolds & Thunell to be similar to form 1 of Keller, group A forms were said to be dominantly sinistral, whereas form 1 was stated by Keller (1978) to be either dextral or sinistral.

Specimens from two levels of core 23SL have been examined; the interval from 0–2 cm has dominantly dextral forms, and the interval from 139–140 cm has dominantly sinistral forms. The degree of encrustation shown by specimens from each level is very similar, and there is no obvious difference in test morphology or thickening between dextral and sinistral forms (see Plate 8). The same result was found by Keller (1978) for her form 1. This suggests that the degree of calcification of the test is independent of water temperature, and possibly is genetically controlled. It may be that the different morphological groups recognised within *T. pachyderma* are genetically different, and do not represent temperature-related ecophenotypic variants.

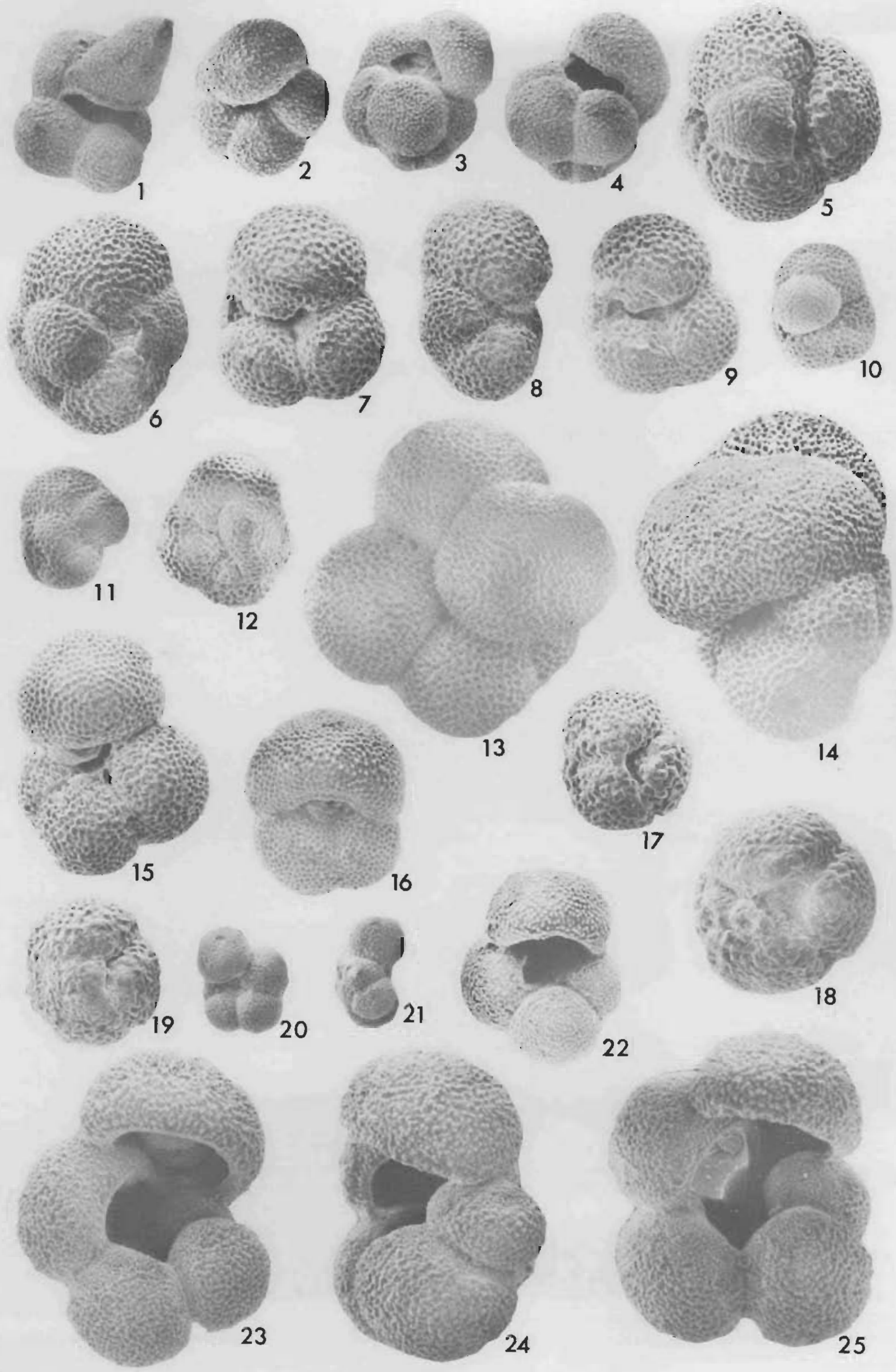

Plate 1.
1: *Beella digitata* (Brady), CPC 27462. 56KL, 50-53 cm, ventral view. **2-4:** *Beella praedigitata* (Parker). 2-3, CPC 27463, 53KL, c.c* 2, ventral view; 3, side view. 4, CPC 27464, same sample, side view. **5-9:** *Catapsydrax dissimilis* (Cushman & Bermudez). 5-6, CPC 27465, 3KL, 45 cm. 5, ventral view; 6, edge view. 7-8 CPC 7466, same sample, specimen with broken bulla. 7, ventral view; 8, edge view. 9, CPC 27467, same sample, specimen with broken bulla, ventral view. **10-12:** *Catapsydrax unicavus primitiva* (Blow & Banner). 10-11, cpc 27468, 2KL, c.c. 10, ventral view; 11, edge view. 12, CPC 27469, same sample, ventral view. **13-15:** *Dentoglobigerina galavisi* (Bermudez). 13-14, CPC 27470, 2KL, 70-72 cm. 13, ventral view; 14, edge view. 15, CPC 27471, 2KL, 110-112 cm, ventral view. **16:** *Dentoglobigerina tripartita tripartita* (Koch). CPC 27472, 32KD, ventral view. **17-19:** *Globigerapsis index* (Finlay). 17, CPC 27473, 2KL, c.c., ventral view. 18, CPC 27474, 2KL, 170-172 cm, ventral view. 19, CPC 27475, 2KL, c.c., ventral view. **20-21:** *Globigerina (Globigerina) angustiumbilicata* Bolli. CPC 27476, 32KD, 20, ventral view; 21, edge view. **22-25:** *Globigerina (Globigerina) bulloides bulloides* d'Orbigny. 22, CPC 27477, 19SL, c.c., ventral view. 23-24, CPC 27478, specimen with wide umbilicus, 51KL, 62-64 cm. 23, ventral view; 24, edge view. 25, CPC 27479, specimen with wide umbilicus, same sample, ventral view.

All figures x80.
* cc = core catcher.

Acknowledgements

I wish to thank Dr Karl Hinz, BGR, Hannover, FRG, for his able leadership of the cruise, and also scientific colleagues of all disciplines for discussions and for assistance with the samples. The master and crew of the R.V. *Sonne* are thanked for their dedication in obtaining samples, often under very difficult conditions. Mr P.W. Davis assisted with sample preparation and photography, and the text-figures and tables were drawn by Brian Pashley. The text has benefited from review by Neville Exon and George Chaproniere of BMR. I also wish to thank Dr D.W. Haig and an anonymous referee for their comments on the manuscript.

Annotated checklist, planktonic foraminifera

Genus ***Beella*** Banner & Blow, 1960
Beella digitata (Brady, 1879). (Pl. 1, fig. 1).

B. digitata has been recorded only rarely. Only one radially elongate chamber is developed on the specimens observed.

Beella praedigitata (Parker, 1967). (Pl. 1, figs 2–4).

Rare specimens of *B. praedigitata* occur in one sample.

Genus ***Catapsydrax*** Bolli, Loeblich & Tappan, 1957
Catapsydrax dissimilis (Cushman & Bermudez, 1937).
(Pl. 1, figs 5–9).

Specimens of *C. dissimilis* are common in several samples; the specimens often lack a bulla. The non-bullate specimens have the same surface texture as bullate forms, and have a distinct apertural lip. They are identical in appearance to bullate forms from which the bulla has been broken.

Catapsydrax unicavus primitiva (Blow & Banner, 1962).
(Pl. 1, figs 10–12).

Rare specimens found in one sample are referred to *C. unicava primitiva.* The test has 4 chambers in the final whorl with an inflated bulla which extends above the umbilicus. The surface of the test is reticulate, and the surface of the bulla is more finely reticulate or punctate. The bulla has only one opening. Blow & Banner (1962) described the bulla of *C. unicavus primitiva* as protruding above the umbilicus, but the relative nature of the bulla of *C. unicavus primitiva* and *C. unicavus unicavus* was reversed by Blow (1969; 1979). The original distinction between these two subspecies is used here, as was done by Fleisher (1974).
Some of the present specimens are almost identical to a specimen figured by Bronnimann & Resig (1971) as *Globigerinita pera* (Todd). The bulla of this species was originally described as covering the umbilicus (Todd, 1957), and Blow & Banner (1962) also noted that the bulla covered the maximum extent of the umbilicus. The bulla of the specimen figured by Bronnimann & Resig is offset to one side of the umbilicus, as in the present specimens, and is triangular in shape, and the wall texture of the specimens is also identical.

The sample from which *C. unicavus primitiva* has been recorded has a limited fauna, but is most probably of Whaingaroan, late Oligocene, age. According to Blow (1969) *C. unicavus primitiva* is a long-ranging taxon, from ?Zone P.13 to within Zone N.1 (=P.20). This upper limit is above the top of the Whaingaroan according to the correlation shown by Berggren (1971, table 52.40). The specimen figured by Bronnimann & Resig (1971), referred to above, was recorded from Zone N.3; the upper limit of *C. unicavus primitiva* possibly is to be extended to this Zone. Because this taxon has a long stratigraphic range, and because the specimens are well-preserved, it is difficult to decide whether the present specimens are autochthonous, or whether they are reworked from older beds.

Genus ***Dentoglobigerina*** Blow, 1979
Dentoglobigerina galavisi (Bermudez, 1961).
(Pl. 1, figs 13–15).

Very rare specimens of *D. galavisi* occur in one sample. The test is large, with a lobate outline, and 4 globular chambers form the last whorl. The aperture is umbilical, and distinct small teeth are visible on the last two chambers. The umbilicus is obscured by a large bulla-like final chamber.

Dentoglobigerina tripartita tripartita (Koch, 1926).
(Pl. 1, fig. 16).

Recorded only rarely in the present samples.

Dentoglobigerina venezuelana (Hedberg, 1937).

D. venezuelana occurs abundantly in only one sample from the Lord Howe Rise.

Genus ***Globigerapsis*** Bolli, Loeblich & Tappan, 1957
Globigerapsis index (Finlay, 1939).
(Pl. 1, figs 17–19).

Rare specimens occur in one core. All specimens have a coarsely pustulose to rugose wall texture, and also may have a small bulla which partly or almost completely covers the umbilicus; in some specimens these are sufficiently large to be regarded as additional chambers. The sutures are deeply incised. The specimens resemble the specimen figured by Blow (1979, pl. 172, fig. 2) and differ from the specimen figured by Jenkins (1971, pl 22, fig. 641) only in having a bulla-like final chamber.

Genus ***Globigerina*** d'Orbigny, 1826
Subgenus ***Globigerina*** d'Orbigny, 1826

Globigerina (Globigerina) angustiumbilicata Bolli, 1957a.
(Pl. 1, figs. 20–21).

Referred here are small specimens with 5 chambers in the last whorl, a small umbilicus and a low aperture with a narrow lip. They have a finely reticulate wall texture.

Globigerina (Globigerina) bulloides bulloides d'Orbigny, 1826.
(Pl. 1, figs. 22–25).

G. bulloides occurs commonly to abundantly in numerous samples. In one sample there are large loosely coiled specimens with 5 chambers in the last whorl, a very wide, open umbilicus and a large arched aperture (see Pl. 1, figs. 23–25); these specimens are regarded as extreme variants of *G. bulloides bulloides.* They have some similarity in umbilical view to the specimen figured by Saito, Thompson & Breger (1981) as *G. megastroma* Earland, but have a wider umbilicus and the test does not have a conical spiral. They are also similar to a specimen figured by Maiya, Saito & Sato (1976) as *Globigerina umbilicata* Orr & Zaitzeff, but are more loosely coiled, with a wider umbilicus.

Globigerina (Globigerina) ciperoensis Bolli, 1954.
(Pl. 2, figs. 1–13).

Specimens referred here are distinguished from *G. (G) angustiumbilicata* by their larger umbilicus and lack of an apertural lip.

Globigerina (Zeaglobigerina) decoraperta Takayanagi & Saito, 1962.

G. (Z.) decoraperta occurs rarely in several samples of Pliocene or younger age.

(Globigerina) falconensis Blow, 1959.
(Pl. 2, figs 4–6).

Rare specimens occur in one core.

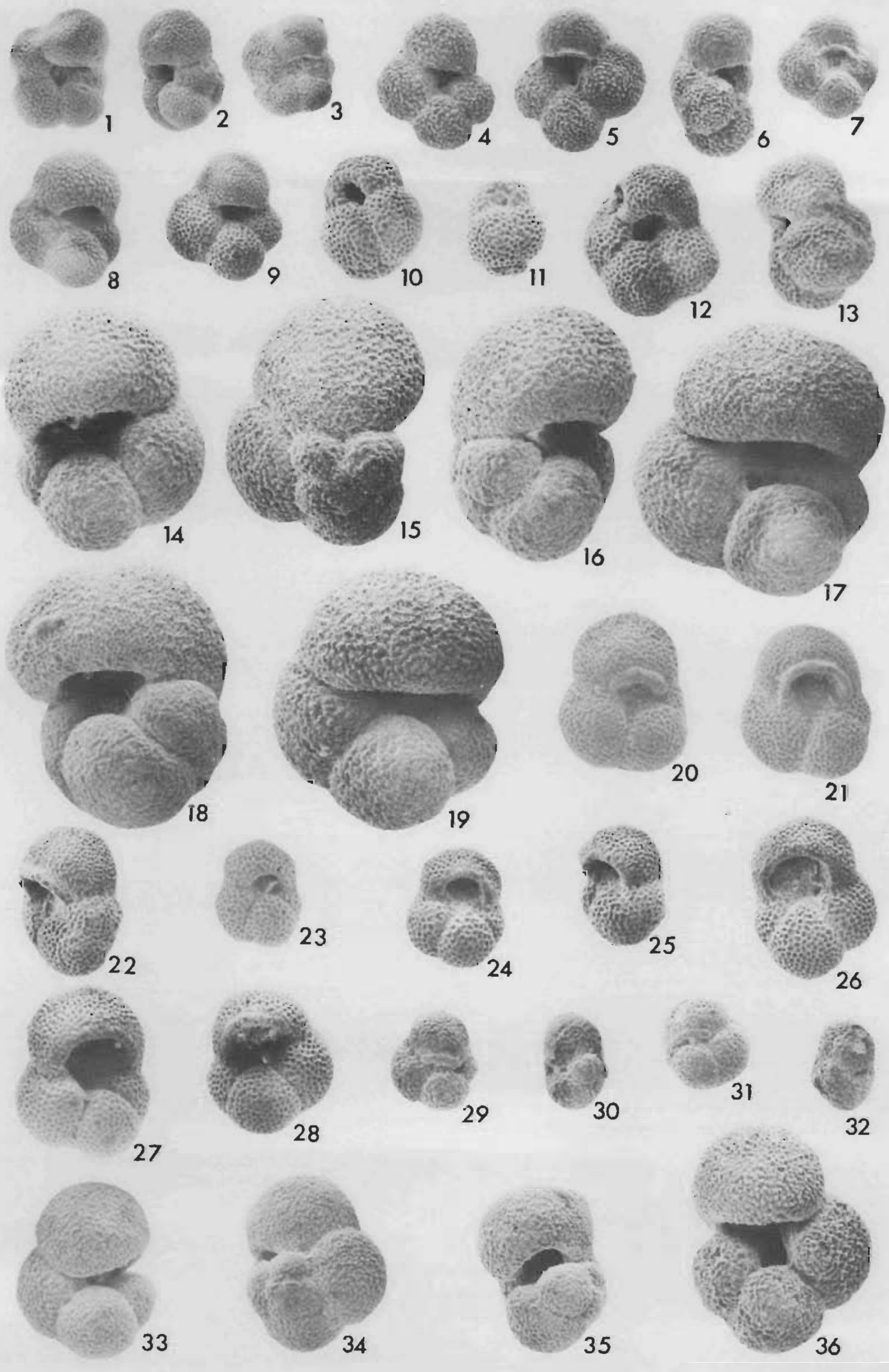

Plate 2.

1-3: *Globigerina (Globigerina) ciperoensis* Bolli. 1-2, CPC 27480, 32KD. 1, ventral view; 2, edge view. 3 CPC 27481, 31KD, ventral view. **4-6:** *Globigerina (Globigerina) falconensis* Blow. 4, CPC 27482, 2KL, 2-4 cm, ventral view. 5-6, CPC 27483, 2KL, 26-28 cm. 5, ventral view; 6, edge view. **7:** *Globigerina (Globigerina) officinalis* Subbotina. CPC 27484, 1KL, top, ventral view. **8-9:** *Globigerina (Globigerina) praebulloides* Blow group. 8, CPC 27485, 3KL, 45 cm, ventral view. 9, CPC 27486, 32KD, ventral view. **10-11:** *Globigerina (Globigerina)* sp. 1. 10, CPC 27487, 2KL, c.c., ventral view. 11, CPC 27488, 3KL, 45 cm, ventral view. **12-13:** *Globigerina (Globigerina)* sp. 2. CPC 27489, 33KD. 12, ventral view; 13, edge view. **14-19:** *Globigerina (Globigerina)* sp. 3. 14-16, CPC 27490, 19SL, c.c. 14, ventral view; 15, dorsal view; 16, edge view. 17-18, CPC 27491, same sample. 17, ventral view; 18, edge view. 19, CPC 27492, same sample, ventral view. **20-22:** *Globigerina (Zeaglobigerina) labiacrassata* Jenkins.20, CPC 27493, 3KL, 45 cm, ventral view. 21-22, CPC 27494, same sample. 21, ventral view; 22, edge view. **23-28:** *Globigerina (Zeaglobigerina) woodi woodi* Jenkins. 23, CPC 27495, 19SL, c.c., ventral view. 24-25, CPC 27496, same sample. 24, ventral view; 25, edge view. 26, CPC 27497, same sample, ventral view. 27, CPC 27498, same sample, ventral view. 28, CPC 27499, same sample, ventral view. **29-32:** *Globigerina (Zeaglobigerina)* sp. 1. 29-30, CPC 27500, 1KL, top. 29, ventral view; 30 edge view. 31-32, CPC 27501, same sample. 31, ventral view; 32, edge view. **33-36:** *Globigerinopsis pseudobesa* (Salvatorini) 33-35, CPC 27502, 19SL, c.c. 33, ventral view; 34, dorsal view; 35, edge view. 36, CPC 27503, 38KL, 200 cm, ventral view.

Globigerina (Globigerina) officinalis Subbotina, 1953.
(Pl. 2, fig 7).

G. (G.) officinalis is rare in the present samples.

Globigerina (Globigerina) praebulloides Blow, 1959 group.
(Pl. 2, figs 8-9).

The *G. (G.) praebulloides* group occurs commonly in the present material. The outline of the test and the apertural characteristics of the specimens vary, and no attempt is made to recognise subspecies within the group. Jenkins (1971) regarded *G. praebulloides* as a junior synonym of *G. bulloides* d'Orbigny.

Globigerina (Globigerina) sp. 1
(pl. 2, figs 10-11).

This is a small species with a high trochoid test, which occurs rarely in samples of late Oligocene age. There are 3 chambers in the final whorl, the test wall is finely reticulate, and the aperture is a small rounded opening without lip or rim.

Globigerina (Globigerina) sp. 2
(Pl. 2, figs 12-13).

Only one specimen of this form has been found, in a sample of late Oligocene age. The test forms a low trochospiral coil with 4 chambers in the final whorl. The test wall is finely reticulate and the aperture is an arched oval opening without lip or rim.

Globigerina (Globigerina) sp. 3
(Pl. 2, figs 14-19).

Several specimens of this large form have been found in a sample of late Miocene age. The test has an oval, lobate outline, with 4 rapidly enlarging inflated chambers forming the final whorl. The test wall is densely and coarsely pustulose; the pustules on some specimens become sparser on the last chamber, and the finely perforate wall is visible. The aperture is a large elongate oval umbilical opening without lip or rim.

In ventral view the specimens resemble *Globigerinoides amplus* Perconig, in particular some specimens figured by Boltovskoy (1974) from DSDP Leg 26 in the Indian Ocean; the present specimens do not have any supplementary aperture.

These specimens may be referable to the *G. obesa/pseudobesa* group, but differ from both of these species in that the chambers enlarge more rapidly, and the final chamber is much broader and more depressed in edge view. No definite identification can be made of these forms.

Subgenus **Zeaglobigerina** Kennett & Srinivasa, 1983
Globigerina (Zeaglobigerina) labiacrassata Jenkins, 1966.
(Pl. 2, figs 20-22).

Specimens referred to *G. (Z.) labiacrassata* show a characteristic moderate to high-arched aperture with a distinct thickened rim.

Globigerina (Zeaglobigerina) woodi woodi Jenkins, 1960.
(Pl. 2, figs 23-28).

Specimens referred to *G. (Z.) woodi woodi* have 4 chambers in the last whorl, a coarsely reticulate test wall, and an arched aperture which in some specimens has a slightly thickened rim, in this respect resembling *G. (Z.) labiacrassata*. The specimens also show a considerable range in size of the aperture; those specimens with a large aperture intergrade with *G. (Z.) apertura* Cushman. Jenkins (1960) noted the variation in development of the aperture, and the similarity to that of *G. (Z.) apertura*; this was also discussed by Kennett & Srinivasan (1983), who noted evidence of a close phylogenetic relationship between *G. (Z.) woodi, G. (Z.) apertura* and *G. (Z.) decoraperta Takayanagi & Saito*.

Jenkins (1971) recorded *G. (Z.) woodi* from the Waitakian to the Lillburnian/Waiauan Stages of New Zealand (late Oligocene-middle Miocene), but Kennett & Srinivasan (1983) recorded it from the late Pliocene. It occurs in the present material in samples regarded as late Miocene (Kapitean).

Globigerina (Zeaglobigerina) sp. 1.
(Pl. 2, figs 29-32).

Rare small specimens occur in one sample. They are tightly coiled, with 4 chambers in the final whorl, a finely pitted wall texture, and a low elongate umbilical aperture with a distinct thickened lip. They may be referable to the *G. (Z.) druryi/decoraperta* group, but have a finer wall texture than these species and the aperture is low and elongate.

Genus **Globigerinita** Bronnimann, 1951
Globigerinita glutinata glutinata (Egger, 1893).

Occurs frequently to abundantly in Pleistocene and younger samples.

Globigerinita uvula (Ehrenberg, 1861).

Only one specimen referred to *G. uvula* has been found. It has a high trochoid test, with a smooth test wall and a small interiomarginal aperture.

Genus **Globigerinopsis** Bolli, 1962
Globigerinopsis pseudobesa (Salvatorini, 1967).
(Pl. 2, figs 33-36).

This species is recorded rarely in several samples.

G. pseudobesa was originally referred to the genus *Turborotalia*, and was placed by Kennett & Srinivasan (1983) in *Globigerinella*. It is here placed in *Globigerinopsis* because of the extension of the aperture to the spiral side, but not to the extent shown by the type species, *G. aguasayensis* Bolli, or by other described species. It resembles *G. grilli* Schmid in ventral view, but this species has a small supplementary aperture in addition to the well-developed spiroumbilical aperture.

Boltovskoy (1974) recorded as *Globigerinopsis aguasayensis* specimens from DSDP site 254 in the Indian Ocean which are very similar to *G. pseudobesa* and are possibly referable to this species. They do not have the extensive spiral apertural development of *G. aguasayensis*.

Kennett & Srinivasan (1983) gave the range of *G. pseudobesa* as middle Miocene (N.13) to early Pliocene (N.19), but it occurs in samples here referred to the late Pliocene. Rare specimens from Pleistocene sediments are also similar to *G. pseudobesa*, but do not have a high arched aperture.

Genus **Globigerinoides** Cushman, 1927
Globigerinoides cyclostomus Galloway & Wissler, 1927).
(Pl. 3, figs 1-2).

G. cyclostomus occurs very rarely.

Globigerinoides quadrilobatus quadrilobatus (d'Orbigny, 1846).

Recorded from only one sample on the Lord Howe Rise.

Globigerinoides quadrilobatus sacculifer (Brady, 1877).

Also recorded from only one sample on the Lord Howe Rise.

Globigerinoides quadrilobatus triloba (Reuss, 1850).

Very rare specimens occur in one core; they are characterised by having a large final chamber which forms more than one-half of the test.

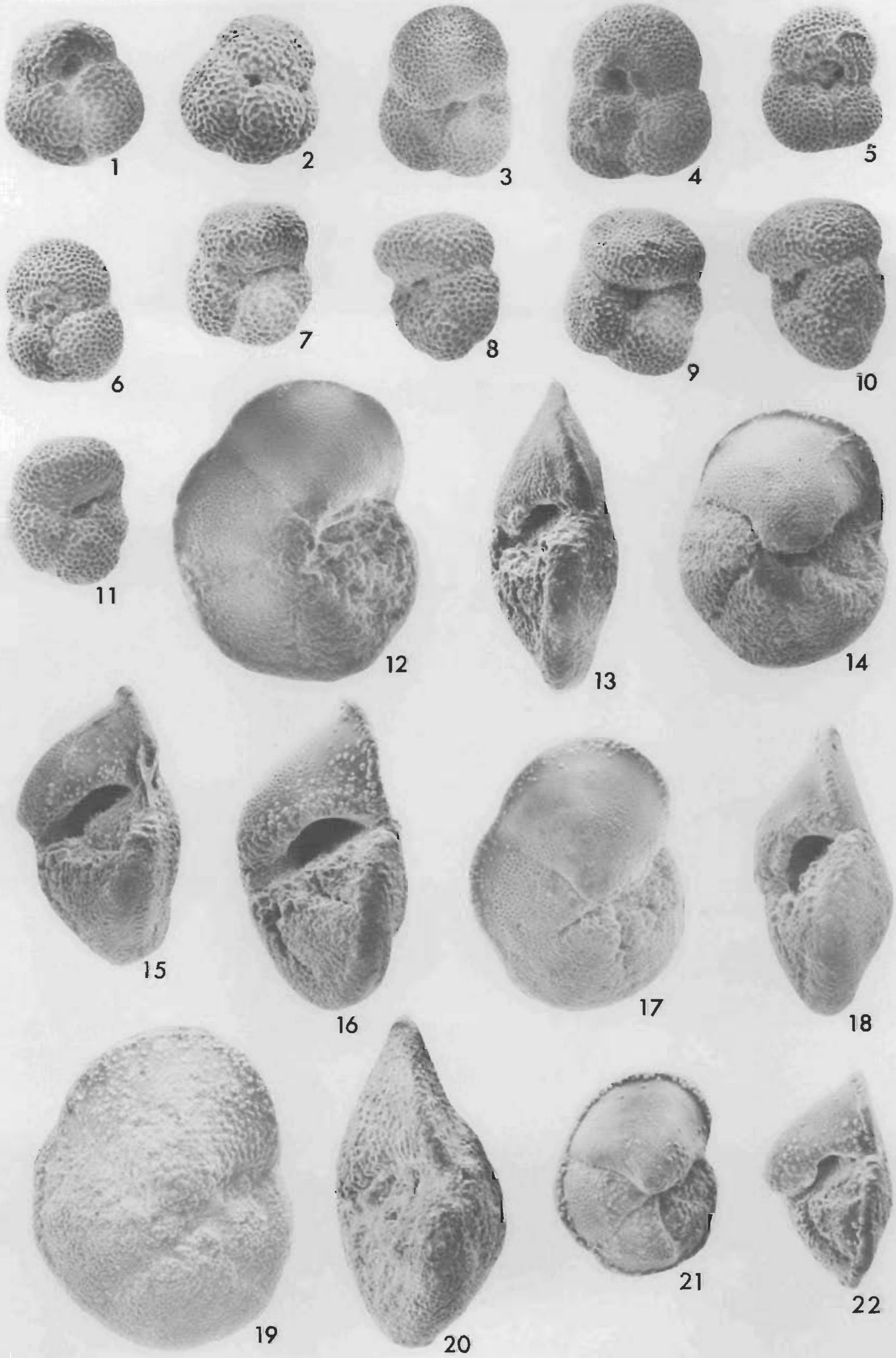

Plate 3.

1-2: *Globigerinoides cyclostomus* (Galloway & Wissler). CPC 27504, 10SL, grey mud at base. 1, ventral view; 2, dorsal view. **3-4:** *Globigerinoides* sp. 1. CPC 27505, 3KL, c.c. 3, ventral view; 4, dorsal view. **5-6:** *Globigerinoides* sp. 2. CPC 275066, 23SL, 160-164 cm. 5, ventral view; 6, dorsal view. **7-11:** *Globoquadrina dehiscens dehiscens* (Chapman, Parr & Collins). 7-8, CPC 27507, 33KD. 7, ventral view; 8, edge view. 9-10, CPC 27508, same sample. 9, ventral view; 10, edge view. 11, CPC 27509, 23SL, 160-164 cm, ventral view. **12-13:** *Globorotalia (G.) cultrata menardii* (Parker, Jones & Brady). CPC 27510, 26KL, 125cm. 12, ventral view; 13, edge view. **14-20:** *Globorotalia (Globoconella) conoidea* Walters. 14-15, CPC 27511, 19SL, c.c. 14, ventral view; 15, edge view. 16, CPC 27512, same sample, edge view. 17-18, CPC 27513, same sample. 17, ventral view; 18, edge view. 19-20, CPC 27514, 51KL, 298-300 cm. 19, ventral view; 20, edge view. **21-22:** *Globorotalia (Globoconella) conomiozea* Kennett. CPC 27515, 19SL, c.c. 21, ventral view; 22, edge view.

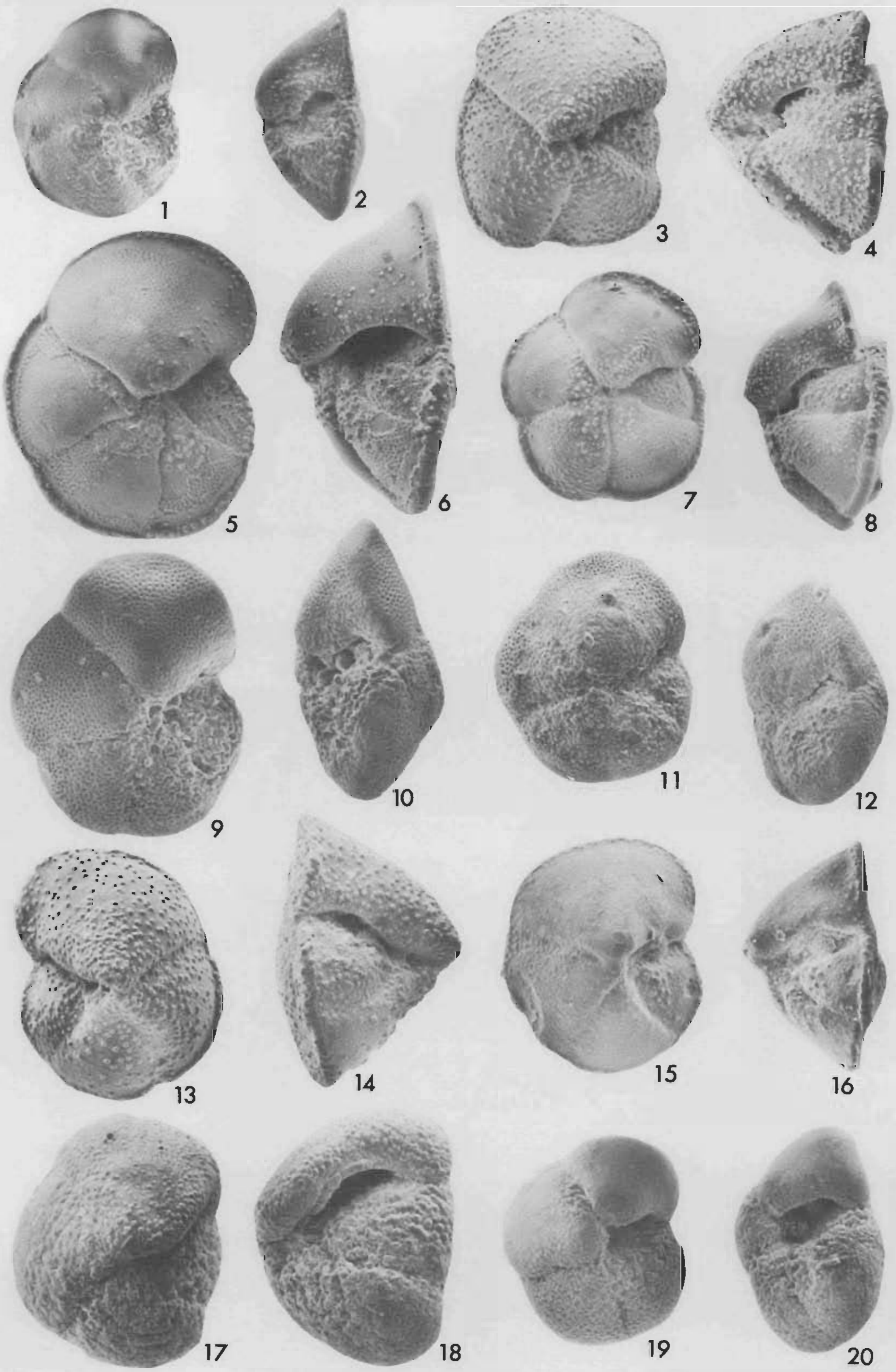

Plate 4.

1-2: *Globorotalia (Globoconella)* sp. cf. *G. conomiozea* Kennett. CPC 27516, 26KL, 105 cm. 1, ventral view; 2, edge view. **3-4:** *Globorotalia (Globoconella) crassaconica* Hornibrook. CPC 27517, 38KL, 200 cm. 3, ventral view; 4, edge view. **5-6:** *Globorotalia (Globoconella) miotumida miotumida* Jenkins. CPC 27518, 19SL, c.c. 5, ventral view; 6, edge view. **7-8:** *Globorotalia (Globoconella)* sp. cf. *G. miotumida explicationis* Jenkins. CPC 27519, 26KL, 125 cm. 7, ventral view; 8, edge view. **9-12:** *Globorotalia (Globoconella) miozea* Finlay. 9-10, CPC 27520, 23SL, 160-162 cm. 9, ventral view; 10, edge view. 11-12, CPC 27521, same sample. 11, ventral view; 12, edge view. **13-16:** *Globorotalia (Globoconella) mons* Hornibrook. 13-14, CPC 27522, 26KL, 125cm. 13, ventral view; 14, edge view. 15-16, CPC 27523, same sample. 15, ventral view; 16, edge view. **17-18:** *Globorotalia (Globoconella) puncticulate puncticulata* (Deshayes). CPC 27524, 9SL, c.c. 17, ventral view; 18, edge view. **19-20:** *Globorotalia (Globoconella) puncticulata puncticuloides* (Hornibrook). CPC 27525, 10SL, base. 19, ventral view; 20, edge view.

Globigerinoides ruber (d'Orbigny, 1839).

Occurs rarely in several samples of late Pliocene or younger age.

Globigerinoides sp. 1.
(Pl. 3, figs 3–4).

Only one specimen of this form has been found. The test has 4 chambers in the last whorl, and a coarsely reticulate test surface. The primary aperture is umbilical, low and elongate; only one dorsal supplementary aperture is present, which is circular, with a distinct lip.

Globigerinoides sp. 2.
(Pl. 3, figs 5–6).

Only one specimen has been found. Three chambers form the last whorl, and the test surface is coarsely reticulate. The primary aperture is umbilical, small and circular, with a thickened lip; only one small, low dorsal aperture, with a thickened lip has been observed.

Genus ***Globoquadrina*** Finlay, 1947
Globoquadrina dehiscens dehiscens (Chapman, Parr & Collins, 1934).
(Pl. 3, figs 7–11).

Specimens of *G. dehiscens dehiscens* in the present material are very similar to the holotype, except that in most cases they have a rounded rather than an angular umbilical shoulder on the apertural face. The test surface is finely reticulate and the test wall is not secondarily thickened; the apertural lip is thin and elongate in contrast to the heavy, triangular tooth often shown by specimens from tropical areas.

Genus ***Globorotalia*** Cushman, 1927
Subgenus ***Globorotalia*** Cushman, 1927
Globorotalia (Globorotalia) cultrata menardii (Parker, Jones & Brady, 1865).
(Pl. 3, figs 12–13).

Very rare specimens are referred to this species. They closely resemble the specimen figured by Jenkins (1971).

Subgenus ***Globoconella*** Bandy, 1975
Globorotalia (Globoconella) conoidea Walters, 1965.
(Pl. 3, figs 14–20).

This is one of the more abundant species of the *Globoconella* group in the present samples. Most specimens have a bluntly rounded axial periphery on the early chambers of the last whorl, and a thickened test wall masking the peripheral keel; later chambers are sharply keeled. There is considerable variation in the relative convexity of the dorsal and ventral sides and in the height of the test.

Globorotalia (Globoconella) conomiozea Kennett, 1966.
(Pl. 3, figs 21–22).

Specimens referred to *G. (G) conomiozea* occur rarely in the present material. They show the characteristic features of the species, a planoconvex test with a strong keel, 4 to 4.5 chambers in the last whorl and a finely perforate test wall with pustules on the early chambers on the ventral side. Loutit & Kennett (1979) suggested that the most reliable criterion for identification of *G. (G.) conomiozea* is the number of chambers in the final whorl, rather than development of the keel or conical nature of the test.

Globorotalia (Globoconella) sp. cf. ***conomiozea Kennett***, 1966.
(Pl. 4, figs 1–2).

Only one specimen has been found; it has the features of *G. (G.) conomiozea*, with a flat dorsal surface and a narrow peripheral keel, but has 6 chambers in the final whorl.

Globorotalia (Globoconella) crassaconica Hornibrook, 1981.
(Pl. 4, figs 3–4).

Very rare specimens of *G. (G.) crassaconica* occur in one sample.

Globorotalia (Globoconella) inflata (d'Orbigny, 1839).

This species is common in late Pliocene and younger beds.

Globorotalia (Globoconella) miotumida miotumida Jenkins, 1960.
(Pl. 4, figs 5–6).

Rare specimens referred to *G. (G.) miotumida miotumida* occur in one sample.

Globorotalia (Globoconella) sp. cf. ***miotumida explicationis*** Jenkins, 1971.
(Pl. 4, figs 7–8).

Only one specimen of this form has been found. It shows the features of G. *(G.) miotumida explicationis*, a narrow strongly keeled periphery and later chambers moving towards the umbilical side of the test. It is planoconvex, rather than biconvex, and the ventral side is higher than in the type specimens, and for these reasons it is not referred definitely to this subspecies.

Globorotalia (Globoconella) miozea Finlay, 1939.
(Pl. 4, figs 9–12).

This species occurs abundantly in some samples. The specimens have 4.5–5 chambers in the final whorl with a rounded axial periphery. The test is thickened on the early chambers of the final whorl, and the test wall has coarse pustules; on later chambers the test wall is thinner and finely perforate. None of the specimens has later chambers as sharply angulate as those of the specimen figured by Kennett & Srinivasan (1983).

Globorotalia (Globoconella) mons Hornibrook, 1982.
(Pl. 4, figs 13–16).

Rare specimens found in one core are referred to *G.(G.) mons*. The test surface is mainly finely hispid, but one specimen has an almost smooth test.

Globorotalia (Globoconella) puncticulata puncticulata (Deshayes, 1832).
(Pl. 4, figs 17–18).

This species is recorded only rarely. The specimens are very similar to that figured by Kennett & Srinivasan (1983).

Globorotalia (Globoconella) puncticulata puncticuloides Hornibrook, 1981.
(Pl. 4, figs 19–20; Pl. 5, figs 1–4).

Specimens referred to *G. (G.) puncticulata puncticuloides* are similar in ventral view to the holotype, and similar in profile to the paratypes figured by Hornibrook (1981, fig 7, f–g). No specimens have a strongly inflated final chamber. They occur in two samples of late Pliocene age, and as Recent contamination in a third sample of early Miocene age.

Globorotalia (Globoconella) suterae Catalano & Sprovieri, 1971.
(Pl. 5, figs 5–7).

Only one specimen of this species has been found. It is planoconvex, with an oval lobate outline and a rounded axial periphery.

The specimen is more compressed than the type specimens, but is very similar to a specimen of *G. suterae* figured by Poore (1979).

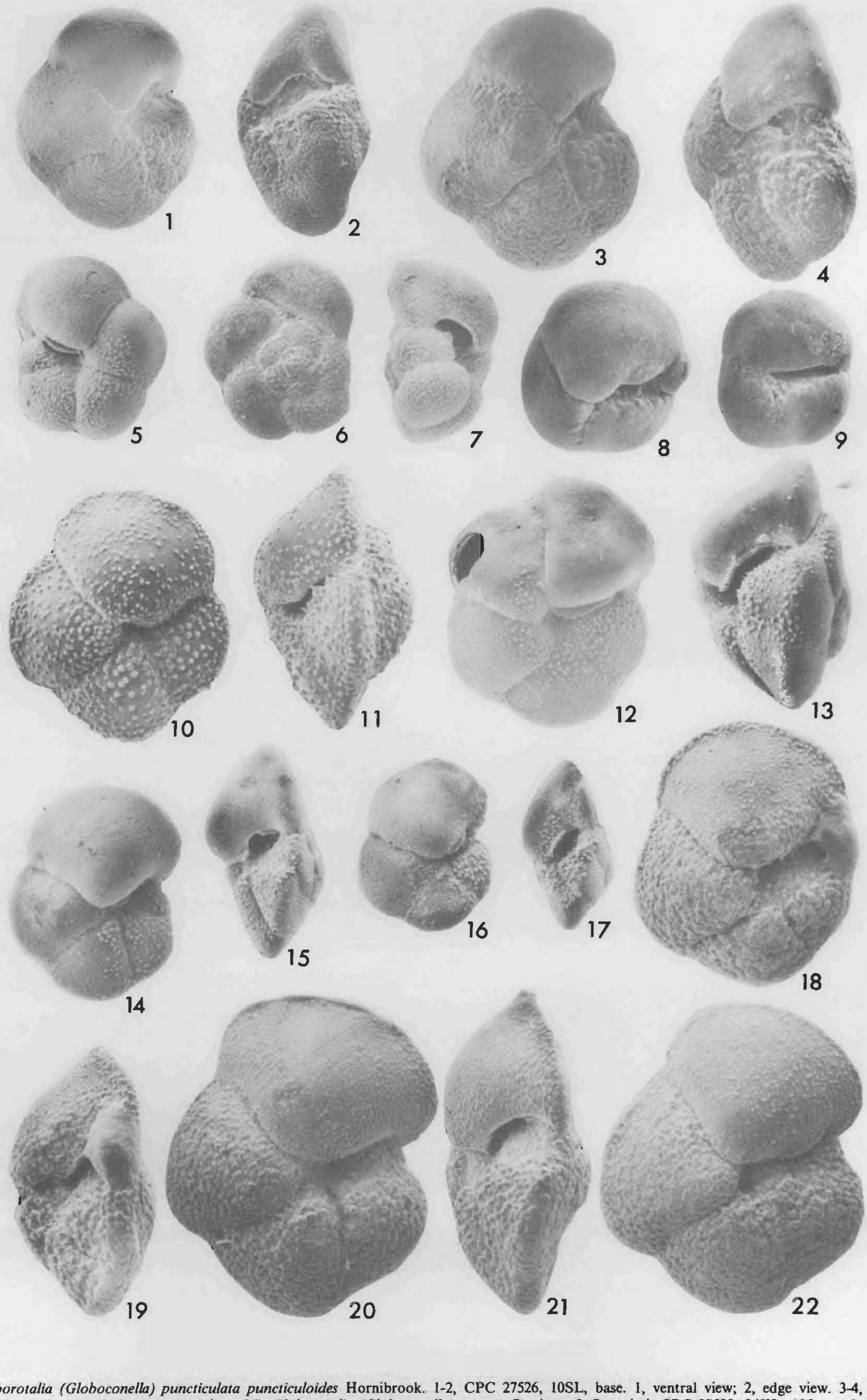

Plate 5.
1-4: *Globorotalia (Globoconella) puncticulata puncticuloides* Hornibrook. 1-2, CPC 27526, 10SL, base. 1, ventral view; 2, edge view. 3-4, CPC 27527, 26KL, 125 cm. 3, ventral view; 4, edge view. **5-7:** *Globorotalia (Globoconella) suterae* Catalano & Sprovieri. CPC 27528, 26KL, 125 cm. 5, ventral view; 6, dorsal view; 7, edge view. **8-9:** *Globorotalia (Globoconella) triangula* Theyer. 8, CPC 27529, 55KL, 763-765 cm, ventral view. 9, CPC 27530, same sample, ventral view. **10-11:** *Globorotalia (Globoconella)* sp. 1. CPC 27531, 38KL, 200 cm. 10, ventral view; 11, edge view. **12-13:** *Globorotalia (Globoconella)* sp. 2. CPC 27532, 38KL, 200 cm. 12, ventral view; 13, edge view. **14-17:** *Globorotalia (Obandyella)* sp. cf. *G. margaritae* Bolli & Bermudeez. 14-15, CPC 27533, 53KL, c.c. 14, ventral view; 15, edge view. 16-17, CPC 27534, same sample. 16, ventral view; 17, edge view. **18-22:** *Globorotalia (Truncorotalia) crassula* Cushman & Stewart. 18-19, CPC 27535, 9SL, c.c. 18, ventral view; 19, edge view. 20-21, CPC 27536, same sample. 20, ventral view; 21, edge view. 22, CPC 27537, same sample, ventral view.

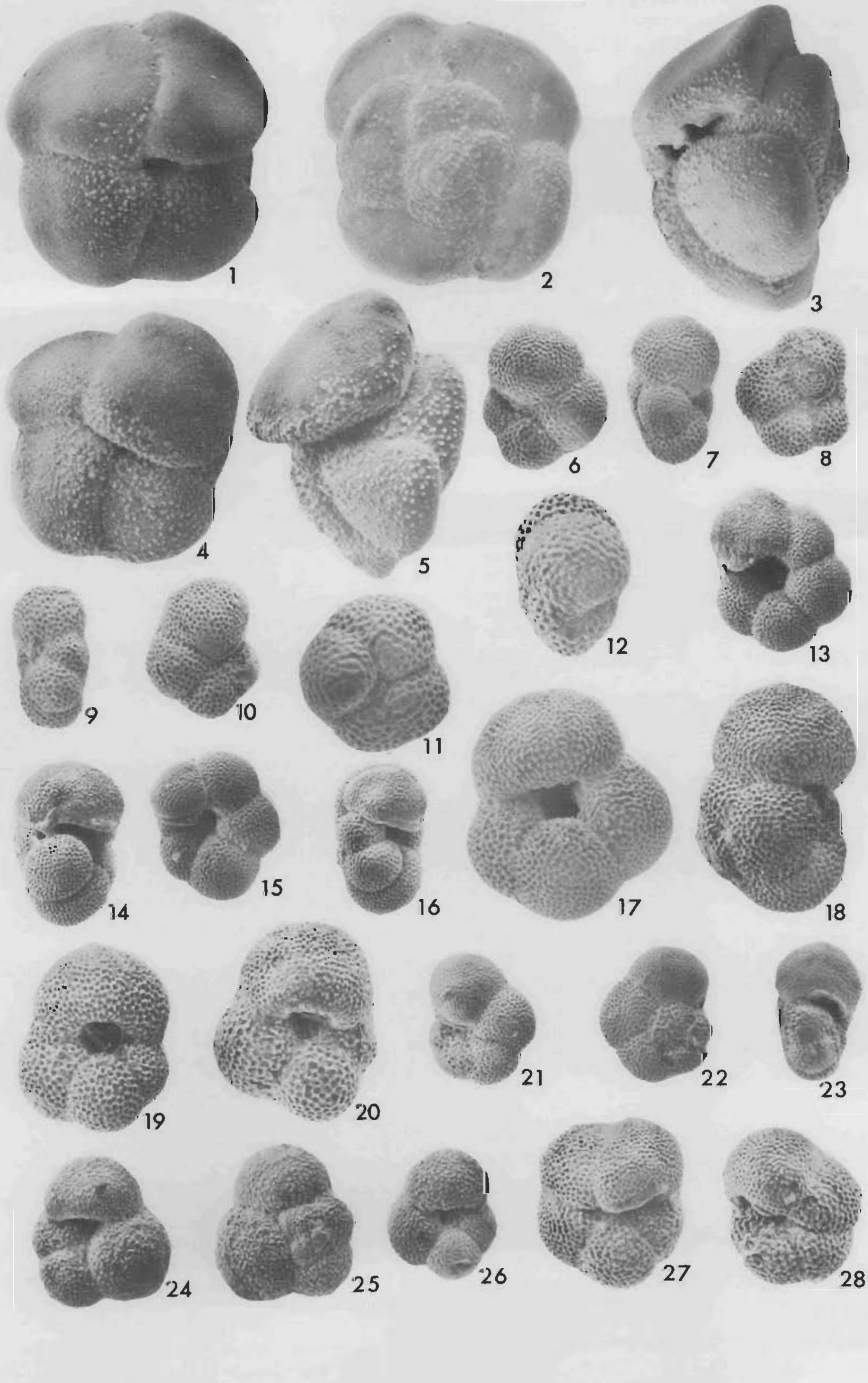

Plate 6.

Figures 1-5: *Globorotalia (Truncorotalia)* sp. cf. *G. crozetensis* Thompson. 1-3, CPC 27538, 38KL, 200 cm. 1, ventral view; 2, dorsal view; 3, edge view. 4-5, CPC 27539, same sample. 4, ventral view; 5, edge view. **6-12:** *Globorotaloides suteri* Bolli. 6-7, CPC 27540, 1KL, top. 6, ventral view; 7, edge view. 8-9, CPC 27541, same sample. 8, ventral view; 9, edge view. 10, CPC 27542, 1KL, base, ventral view. 11-12, CPC 27543, 2KL, 70-72 cm, specimen with bullate last chamber. 11, ventral view; 12, edge view. **13-16:** *Neogloboquadrina dutertrei* (d'Orbigny). 13-14, CPC 27544, 2KL, 26-28 cm. 13, ventral view; 14, edge view. 15-16, CPC 27545, same sample. 15, ventral view; 16, edge view. **17-20:** *Paragloborotalia ampliapertura* (Bolli) group. 17-18, CPC 27546, 2KL, 110-112 cm. 17, ventral view; 18, edge view. 19, CPC 27547, 33KD, ventral view. 20, CPC 27548, same sample, ventral view. **21-23:** *Paragloborotalia bella* (Jenkins). CPC 27549, 23SL, 160-164 cm. 21, ventral view; 22, dorsal view; 23, edge view. **24-26:** *Paragloborotalia euapertura* (Jenkins). 24-25, CPC 27550, 33KD. 24, ventral view; 25, dorsal view. 26, CPC 27551, 32KD, ventral view. **27-28:** *Paragloborotalia mayeri* (Cushman & Ellisor). 27, CPC 27552, 57KD, ventral view. 28, CPC 27553, same sample, ventral view.

Globorotalia (Globoconella) triangula Theyer, 1973.
(Pl. 5, figs 8–9).

G. (G.) triangula is abundant in Pleistocene or younger material in the present samples. In one core, 26KL, *G. (G.) triangula* occurs in a fauna of early Pliocene age, probably as a result of contamination from younger beds.

Globorotalia (Globoconella) sp. 1.
(Pl. 5, figs 10–11).

Only one specimen of this form has been found. It is biconvex, with 4 chambers in the last whorl, a circular lobate outline and a narrowly rounded periphery. The ventral surface is pustulose, and the pustules become finer on later chambers. On the dorsal surface the central area is obscured by pustules and secondary thickening, and the later chambers are finely pustulose. The aperture is a low elongate interiomarginal umbilical-extraumbilical opening.

Globorotalia (Globoconella) sp. 2.
(Pl. 5, figs 12–13)

Only one specimen of this form has been found. The test is biconvex, and the ventral surface is the more strongly convex; five chambers form the last whorl, and the later chambers are displaced towards the ventral side of the test. The periphery of the test is narrowly rounded but not carinate, and the aperture is a low elongate umbilical-extraumbilical opening with a narrow lip.

Subgenus ***Obandyella*** Haman, Huddleston & Donahue, 1980
Globorotalia (Obandyella) hirsuta hirsuta (d'Orbigny, 1839)

Recorded from a number of samples, but is rare.

Globorotalia (Obandyella) sp. cf. ***margaritae*** Bolli & Bermudez, 1965.
(Pl. 5, figs 14–17).

Numerous specimens closely resembling *G. (O.) margaritae* occur in one sample. They have only slightly more than 4 chambers in the final whorl, rather than 5, with a convex dorsal surface and a narrowly rounded periphery.

Globorotalia (Obandyella) scitula scitula (Brady, 1882).

Occurs rarely to commonly in several samples.

Subgenus ***Truncorotalia*** Cushman & Bermudez, 1949
Globorotalia (Truncorotalia) crassaformis crassaformis (Galloway & Wissler, 1927) group.

Included here are four-chambered quadrate planoconvex specimens. The assemblages are very variable; most specimens can be referred to *G. (T.) crassaformis crassaformis*, but no attempt has been made to recognise subspecific categories.

Globorotalia (Truncorotalia) crassula Cushman & R.E. Stewart, 1930.
(Pl. 5, figs 18–22).

Published figures of *G. (T.) crassula* show considerable variation in test outline, profile, wall thickness, test ornament and in the development of a peripheral keel. The present specimens are quadrate in outline, ranging in profile from planoconvex to biconvex, with usually a thickened peripheral margin rather than a keel. The specimens are mainly thin-walled and distinctly pustulose on the early chambers of the last whorl, becoming sparsely pustulose on later chambers; some thick-walled forms are present.

Globorotalia (Truncorotalia) sp. cf. ***crozetensis*** Thompson, 1973.
(Pl. 6, figs 1–5).

Rare specimens from one sample are placed here. They have 5 chambers in the last whorl and a biconvex test, and the later chambers are displaced to the ventral side of the test. The periphery of the test is not angular or keeled as in the type specimens of *G.(T.) crozetensis;* the aperture of most specimens also lacks the distinct narrow lip of the types.

This species was originally described from the late Pleistocene of the southwest Indian Ocean; the present specimens are from late Pliocene beds.

Globorotalia (Truncorotalia) truncatulinoides truncatulinoides (d'Orbigny, 1839).

Occurs abundantly in Pleistocene and younger samples.

Genus ***Globorotaloides*** Bolli, 1957
Globorotaloides suteri Bolli, 1957a.
(Pl. 6, figs 6–12).

This species occurs rarely in samples of late Oligocene age. Most specimens show the turborotaliid stage of development of the species, having an elongate interiomarginal umbilical-extraumbilical aperture with a narrow lip. Only rare bullate specimens have been found.

Specimens of *G. suteri* are similar to those referred to *Catapsydrax unicavus primitiva.* Blow (1979) noted the similarity of these two taxa, and expressed little doubt that they derive from a common ancestor. Some of the criteria given by Blow for distinguishing these forms are applicable to the present specimens. Specimens of *G. suteri* have a flatter dorsal surface and less inflated chambers; rate of chamber enlargement is difficult to apply. Specimens of *G. suteri* in the present material are more coarsely reticulate than those of *C. unicavus primitiva.*

Genus ***Hastigerina*** Thompson, 1876
Hastigerina siphonifera (d'Orbigny, 1839).

Occurs as a minor element of the fauna in most samples from younger beds.

Genus ***Neogloboquadrina*** Bandy, Frerichs & Vincent, 1967
Neogloboquadrina dutertrei (d'Orbigny, 1839).

(Pl. 6, figs 13–16).

Rare specimens referred to *N. dutertrei* occur in numerous samples. The specimens resemble *N. dutertrei dutertrei* Group A of Srinivasan & Kennett (1976), which they regarded as a tropical form. This occurrence may reflect expansions of tropical conditions into high latitudes referred to by Bandy & others (1967).

Genus ***Orbulina*** d'Orbigny, 1839
Orbulina universa d'Orbigny, 1839.

O. universa occurs abundantly in surface sediments, but is often absent from deeper samples in Holocene-Pleistocene cores.

Genus ***Paragloborotalia*** Cifelli, 1982

Phylogenetic considerations as outlined in such papers as Jenkins (1960), Blow & Banner (1962), Fleischer (1974), Chaproniere (1981) and Cifelli (1982) lead me to refer species such as *opima* Bolli, *ampliapertura* Bolli, *euapertura* Jenkins, and *semivera* Jenkins to the genus *Paragloborotalia*, which is considered to be a senior synonym of *Jenkinsella* Kennett & Srinivasan, 1983.

Paragloborotalia ampliapertura (Bolli, 1957a) group.
(Pl. 6, figs 17-20).

Included here are specimens ranging from forms with an inflated last chamber and an arched laterally restricted aperture, to specimens with a depressed final chamber and a low elongate aperture. All have a coarsely reticulate wall texture and are from samples of late Oligocene age.

Paragloborotalia bella (Jenkins, 1967).
(Pl. 6, figs 21-23).

Specimens identified as *P. bella* are identical in all respects with the original description and figures except for the nature of the test wall. This was described by Jenkins (1967) as slightly roughened and glassy, but in the present specimens is finely reticulate. In this feature it resembles *G. mayeri nympha* Jenkins, but lacks the small final chamber of this species.

Paragloborotalia euapertura (Jenkins, 1960).
(Pl. 6, figs 24-26).

Rare tightly coiled specimens with a low elongate aperture are referred to *P. euapertura*.

Paragloborotalia mayeri (Cushman & Ellisor, 1939).
Pl. 6, figs 27-28).

Specimens of *P. mayeri* occur commonly in one sample from the Lord Howe Rise.

Paragloborotalia nana (Bolli, 1957a).

Occurs rarely in late Oligocene samples.

Paragloborotalia opima (Bolli, 1957a).
(Pl. 7, figs 1-3).

Recorded rarely in samples of late Oligocene age.

Paragloborotalia semivera (Hornibrook, 1961).
(Pl. 7, figs 4-8).

Small five-chambered coarsely reticulate specimens with an arched aperture with a distinct lip are referred to *P. semivera*.

Genus ***Sphaeroidinellopsis*** Banner & Blow, 1959
Sphaeroidinellopsis disjuncta (Finlay, 1940).
(Pl. 7, figs 9-10).

Occurs rarely in three samples.

Sphaeroidinellopsis seminulina seminulina (Schwager, 1866).

Rare specimens occur in one sample.

Genus ***Subbotina*** Brotzen & Pozaryska, 1961
Subbotina angiporoides (Hornibrook, 1965).
(Pl. 7, figs 11-14).

Specimens referred to *S. angiporoides* show the typical form of the species, a tightly coiled three or four-chambered test, a coarsely reticulate wall and a low elongate aperture with a narrow lip. The species is rare in those samples in which it occurs.

Subbotina sp. cf. ***S. angiporoides*** (Hornibrook, 1965).
(Pl. 7, figs 15-16).

Placed here are specimens which resemble *S. angiporoides* in gross test morphology, but have a finely reticulate or pustulose test surface, and which also in some cases lack an apertural lip. These specimens occur in samples referred to the Waitakian Stage of the New Zealand succession, which is above the recorded upper level of *S. angiporoides* in this area.

Subbotina gortanii gortanii (Borsetti, 1959).
(Pl. 7, fig 17).

Very rare specimens of *S. gortanii gortanii* occur in one sample.

Subbotina linaperta (Finlay, 1939).
(Pl. 7, figs 18-20).

Rare specimens referred to *S. linaperta* occur in samples regarded as late Oligocene, and are therefore thought to be reworked. Some specimens have a compressed final chamber, but not to the extent shown by the holotype; other specimens have a more rounded equidimensional final chamber. The specimens have the other features of *S. linaperta*, such as the coarsely reticulate test wall and low elongate aperture with a distinct lip. They closely resemble the specimen figured by Bolli (1957b) as *Globigerina linaperta*, but are not as lobate as that figured by Carter (1958). Jenkins (1971) stated that the specimens figured by Bolli and by Carter appear to be closely related to *linaperta*. The present specimens are also very similar to specimens of *S. linaperta* figured by Blow (1979).

Boltovskoy (1974) recorded well-preserved specimens referred to *Globigerina linaperta* from an early Miocene sample in the Indian Ocean, and was uncertain if the specimens were reworked or if the stratigraphic range of *G. linaperta* should be changed. The present specimens are well-preserved and are regarded as most probably reworked.

Subbotina triloculinoides (Plummer, 1926).
(Pl. 7, figs 21-26).

Numerous specimens from sediments of late Oligocene age are placed here. The reticulation of the test surface varies from coarse to fine, and the apertural characteristics also vary, but all have 3 chambers visible ventrally and appear to fall within the range of variation of *S. triloculinoides* (Plummer). The range of variation observed is illustrated. These specimens are also most probably reworked.

Genus ***Tenuitella*** Fleisher, 1974
Tenuitella iota (Parker, 1962).
(Pl. 7, fig 27).

Rare specimens occur in a number of samples from two cores.

Tenuitella munda (Jenkins, 1966).
(Pl. 7, figs 28-31).

Rare specimens occur in one sample. The small test has usually 4 chambers in the final whorl, with a rounded, lobate periphery; the test wall has minute pustules. The aperture is interiomarginal, umbilical-extraumbilical, with a thin lip.

Included here is one five-chambered form which has the same wall texture as the more usual four-chambered specimens, and is very similar to a paratype figured by Jenkins (1966, fig. 14, no. 133).

Genus ***Turborotalia*** Cushman & Bermudez, 1949
Turborotalia obesa (Bolli, 1957).

Rare specimens with 4 chambers in the last whorl, a small umbilicus and narrow, elongate, interiomarginal umbilical-extraumbilical aperture are referred to *T. obesa*.

Turborotalia pachyderma (Ehrenberg, 1861).
(Pl. 7, figs 32-34).

T.pachyderma is recorded from most samples of late Miocene or younger age. The final chamber is usually inflated and has a distinct lip; kummerform final chambers are rare. Specimens transitional to *T. acostaensis* Blow occur in one late Miocene sample. Kennett & Srinivasan (1983) referred to the intergradation of *T. pachyderma* and *T. acostaensis* in temperate to polar areas.

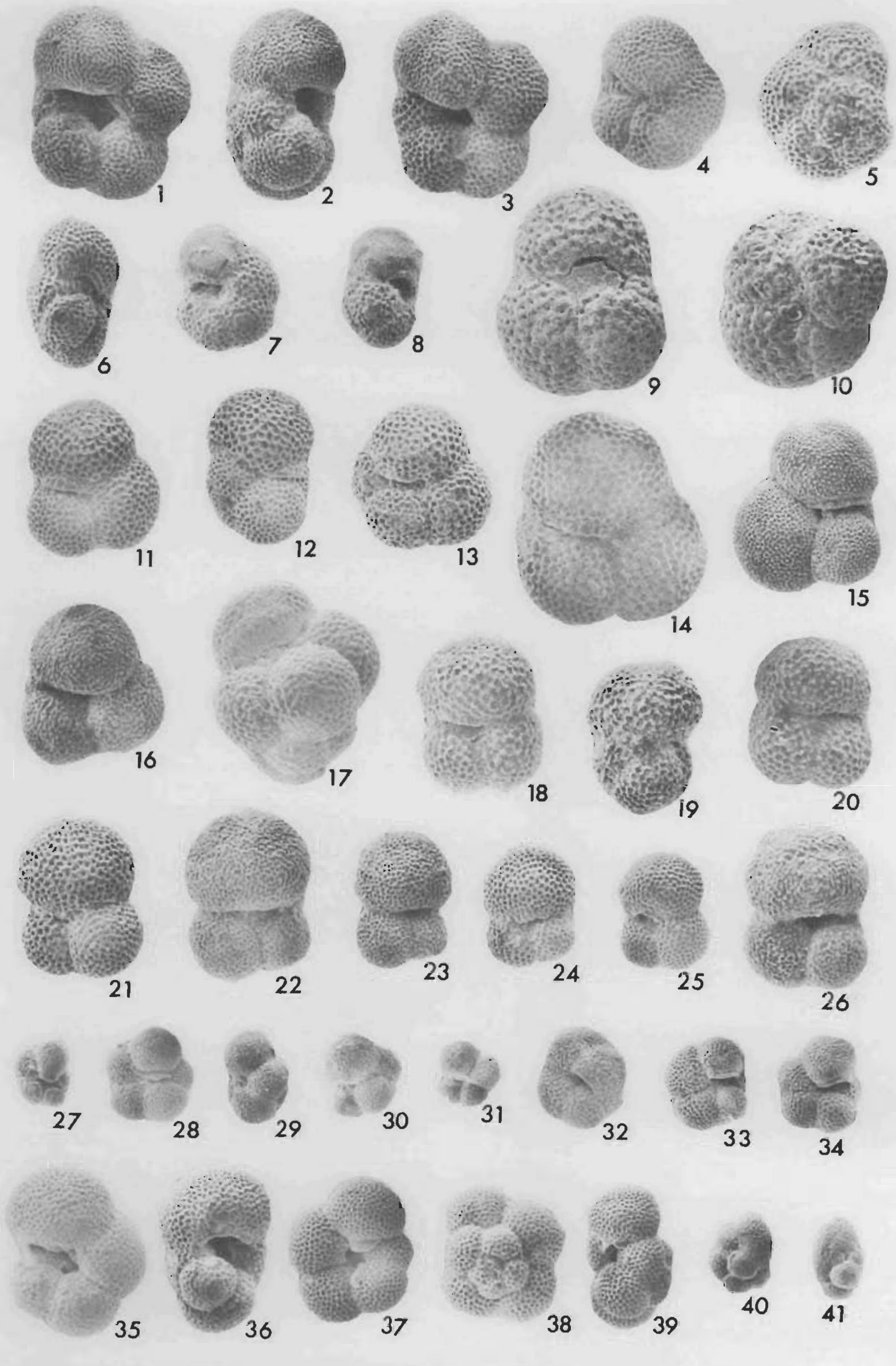

Plate 7.

1-3: *Paragloborotalia opima* (Bolli). 1-2, CPC 27554, 32KD. 1, ventral view; 2, edge view. 3, CPC 27555, same sample, ventral view. **4-8:** *Paragloborotalia semivera* (Hornibrook). 4-6, CPC 27556, 2KL, 70-72 cm. 4, ventral view; 5, dorsal view; 6, edge view. 7-8, CPC 27557, 3KL, c.c. 7, ventral view; 8, edge view. **9-10:** *Sphaeroidinellopsis disjuncta* (Finlay). 9, CPC 27558, 23SL, 160-170 cm, ventral view. 10, CPC 27559, same sample, ventral view. **11-14:** *Subbotina angiporoides* (Hornibrook). 11-12, CPC 27560, 3KL, c.c. 11, ventral view; 12, edge view. 13, CPC 27561, same sample, ventral view. 14, CPC 27562, 2KL, 170-172 cm, ventral view. **15-16:** *Subbotina* sp. cf. *S. angiporoides* (Hornibrook). 15, CPC 27563, 32KD, ventral view. 32KD, ventral view. 16, CPC 27564, 33KD, ventral view. **17:** *Subbotina gortanii gortanii* (Borsetti). CPC 27565, 2KL, 70-72 cm, side view. **18-20:** *Subbotina linaperta* (Finlay). 18-19, CPC 27566, 31KD. 18, ventral view; 19, edge view. 20, CPC 27567, 33KD, ventral view. **21-26:** *Subbotina triloculinoides* (Plummer). 21, CPC 27568, 3KL, c.c., ventral view. 22, CPC 25769, 32KD, ventral view. 23, CPC 27570, same sample, ventral view. 24, CPC 27571, 3KL, 45 cm, ventral view. 25, CPC 27572, same sample, ventral view. 26, CPC 27573, 32KD, ventral view. **27:** *Tenuitella iota* (Parker). CPC 27574, 2KL, 26-28 cm, ventral view. **28-31:** *Tenuitella munda* (Jenkins). 28-29, CPC 27575, 2KL, 70-72 cm. 28, Ventral view; 29, edge view. 30, CPC 27576, 2KL, 110-112 cm, ventral view. 31, CPC 27577, same sample, ventral view. **32-34:** *Turborotalia pachyderma* (Ehrenberg). 32, CPC 27578, 55KL, 763-765 cm, ventral view. 33, CPC 27579, 19SL, c.c., ventral view. 34, CPC 27580, specimen transitional to *T. acostaensis*, same sample, ventral view. **35-36:** *Turborotalia* sp. cf. ***T. pseudopima*** (Blow). CPC 27581, 10SL, base. 35, ventral view; 36, edge view. **37-39:** *Turborotalia* sp. 1. CPC 27582, 2KL, 110-112 cm. 37, ventral view; 38, dorsal view; 39, edge view. **40-41:** *Turborotalita humilis* (Brady). CPC 27583, 2KL, 2-4 cm. 40, ventral view; 41, edge view.

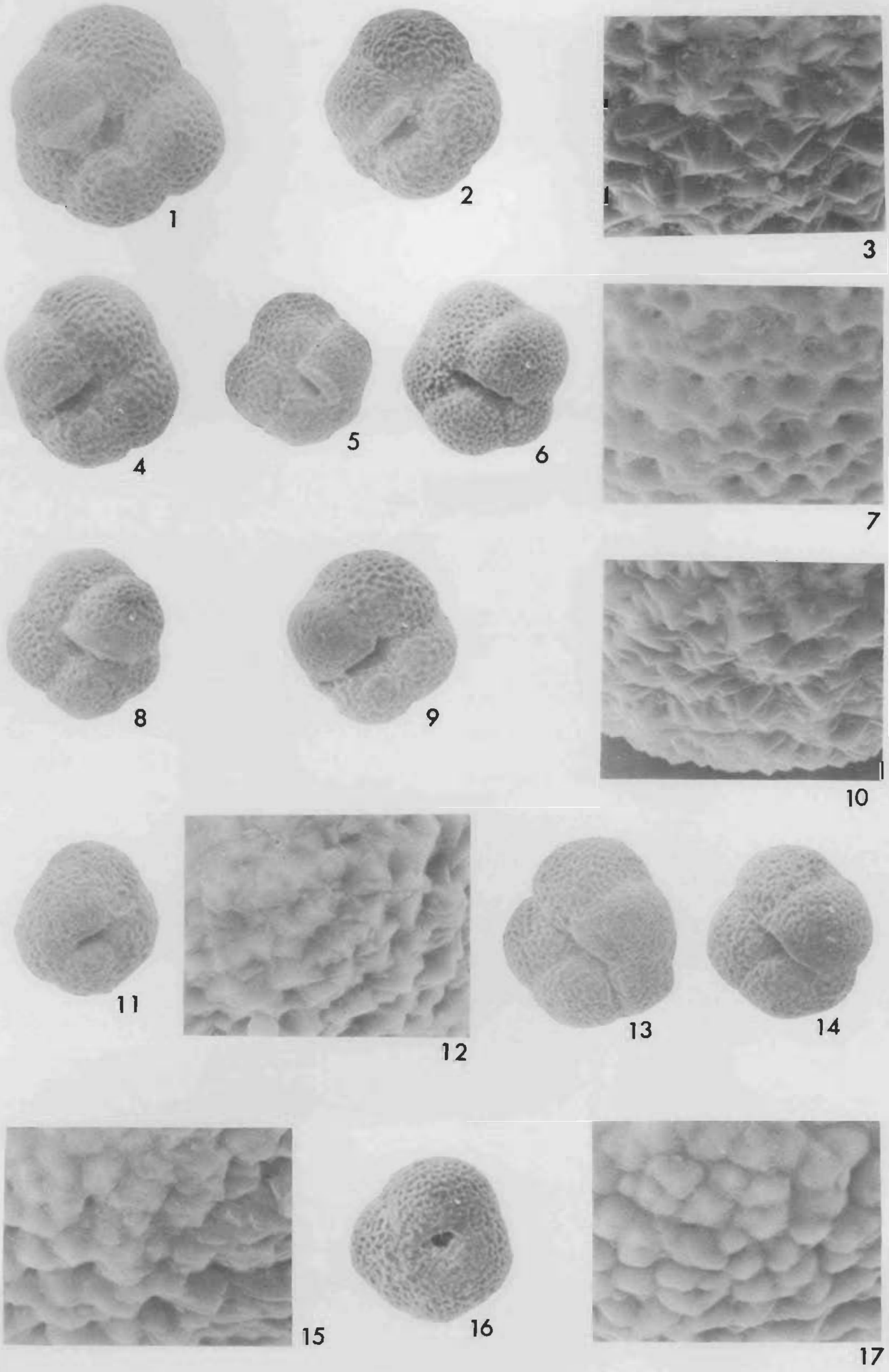

Plate 8. Variation in test morphology and surface texture of *Turborotalia pachyderma* (Ehrenberg).

Figures 1, 2, 4, 5, 6, 8 (CPC 27584 to 27589) from core 23SL, 0-2 cm. Figure 3, surface detail of specimen in figure 2; figure 7, surface detail of specimen in figure 6. Figures 9, 11, 13, 14, 16 (CPC 27590 to 27594) from core 23SL, 138-140 cm. Figure 10, surface detail of specimen in figure 9; figure 12, surface detail of specimen in figure 11; figure 15, surface detail of specimen in figure 14; figure 17, surface detail of specimen in figure 16. Illustrations of specimens, x150. Detail of surface texture, taken on antepenultimate chamber, x about 1,200.

Turborotalia sp. cf. ***pseudopima*** (Blow, 1969).
(Pl. 7, figs 35–36).

Specimens closely resembling *T. pseudopima* occur rarely in one sample of late Pliocene age. They have four chambers in the last whorl, and radial depressed ventral sutures. The umbilicus is open and the aperture has a distinct extraumbilical extension rather than being in a more peripheral position. They are also more compressed in edge view than illustrated specimens of *T. pseudopima.*

Turborotalia sp. 1.
(Pl. 7, figs 37–39).

Very rare specimens occur in one sample. They have a flat trochospiral test, 5 chambers in the final whorl, and a distinctly reticulate test surface. The aperture is interiomarginal, umbilical-extraumbilical, with a thin wide lip.

Genus ***Turborotalita*** Blow & Banner, 1962
Turborotalita humilis (Brady, 1884).
(Pl. 7, figs 40–41).

Rare specimens occur in Recent sediments at one locality.

References

Bandy, O.L., 1960 — The geologic significance of coiling ratios in the foraminifer *Globigerina pachyderma* (Ehrenberg). *Journal of Paleontology*, 34(4), 671–681.

Bandy, O.L., 1968 — Cycles in Neogene paleoceanography and eustatic changes. *Palaeogeography, Palaeoclimatology, Palaeoecology*, 5(1), 63–75.

Bandy, O.L., 1969 — Relationships of Neogene planktonic foraminifera to paleoceanography and correlation. *Proceedings of the First International Conference on Planktonic Microfossils, Geneva*, 1967 1, 46–57. *E.J. Brill, Leiden.*

Bandy, O.L., 1975 — Messinian evaporite deposition and the Miocene/Pliocene boundary, Pasquasia-Capodarso sections, Italy. *In* Saito, T., & Burckle, L.H. (editors), Late Neogene Epoch Boundaries, 49–63. *Micropaleontology Press, New York.*

Bandy, O.L., Frerichs, W., & Vincent, E., 1967 — Origin, development and geologic significance of *Neogloboquadrina* Bandy, Frerichs and Vincent, gen. nov. *Contributions from the Cushman Foundation for Foraminiferal Research*, 18(4), 152-152.

Banner, F.T., & Blow, W.H., 1959 — The classification and stratigraphical distribution of the Globigerinaceae. *Palaeontology*, 2(1), 1–27.

Banner, F.T., & Blow, W.H., 1960 — The taxonomy, morphology and affinities of the genera included in the subfamily *Hastigerininae. Micropaleontology*, 6(1), 19–31.

Be, A.W.H., & Hamlin, W.H., 1967 — Ecology of Recent planktonic foraminifera. Part 3 - Distribution in the North Atlantic during the summer of 1962. *Micropaleontology*, 13(1), 87–106.

Berggren, W.A., 1971 — Tertiary boundaries and correlations. *In* Funnel, B.M., & Riedel, W.R. (editors), Micropaleontology of the Oceans, 693–809, *Cambridge University Press, London.*

Bermudez, P.J., 1961 — Contribución al estudio de las Globigerinidae de la región Caribe-Antillana (Paleoceno-Reciente). Memoria del III Congreso Geológico Venezolano, vol 3. *Boletín de Geología Publicación Especial* 3, 1119–1393.

Blow, W.H., 1959 — Age, correlation and biostratigraphy of the upper Tocuyo (San Lorenzo) and Pozon Formations, eastern Falcon, Venezuela. *Bulletins of American Paleontology*, 39(178), 67–251.

Blow, W.H., 1969 — Late middle Eocene to Recent planktonic foraminiferal biostratigraphy. *Proceedings of First International Conference on Planktonic Microfossils, Geneva*, 1967, 199–422. *E.J. Brill, Leiden.*

Blow, W.H., 1979 — The Cainozoic Globigerinida, vol I-III, *E.J. Brill, Leiden.*

Blow, W.H., & Banner, F.T., 1962 — The Mid-Tertiary (Upper Eocene to Aquitanian) Globigerinaceae. *In* Eames, F.E., Banner, F.T., Blow, W.H., & Clarke, W., Fundamentals of mid-Tertiary stratigraphical correlation, 61-147. *Cambridge University Press, London.*

Bolli, H.M., 1954 — Note on *Globigerina concinna* Reuss, 1850. *Contributions from the Cushman Formation for Foraminiferal Research*, 5(1), 1-3.

Bolli, H.M., 1957a — Planktonic Foraminifera from the Oligocene-Miocene Cipero and Lengua formations of Trinidad, B.W.I. *United States National Museum Bulletin*, 215, 97–123.

Bolli, H.M., 1957b — Planktonic foraminifera from the Eocene Navet and San Fernando Formations of Trinidad, B.W.I. *United States National Museum Bulletin*, 215, 155-172.

Bolli, H.M., 1962 — *Globigerinopsis*, a new genus of the foraminiferal family *Globigerinidae. Eclogae geologicae Helvetiae*, 55(1), 281-284.

Bolli, H.M., & Bermudez, P.J., 1965 — Zonation based on planktonic foraminifera of middle Miocene to Pliocene warm-water sediments. *Boletin Informativo Asociacion Venezolana de Geologia, Minera y Petroleo*, 8(5), 121-149.

Bolli, H.M., Loeblich, A.R., Jr., & Tappan, Helen, 1957 — Planktonic families *Hantkeninidae, Orbulinidae, Globorotaliidae* and *Globotruncanidae. United States National Museum Bulletin*, 215, 3–50.

Boltovskoy, E., 1974 — Neogene planktonic foraminifera of the Indian Ocean (DSDP, Leg 26). *In* Davies, T.A., Luyendyk, B.P., & others, Initial reports of the Deep Sea Drilling Project, volume 26, 675–741. *U.S. Government Printing Office, Washington.*

Borsetti, A. M., 1959 — Tre nuovi foraminiferi planctonici dell' Oligocene Piacentino. *Giornale di Geologia*, ser. 2a, 27, 205-212.

Brady, H.B., 1877 — Supplementary note on the foraminifera of the Chalk (?) of the New Britain Group. *Geological Magazine*, n.s., decade 2,4, 534–536.

Brady, H.B., 1879 — Notes on some of the reticularian Rhizopoda of the 'Challenger' Expedition; II — Additions to the knowledge of porcellaneous and hyaline types. *Quarterly Journal of the Microscopical Society of London*, n.s., 19, 261–299.

Brady, H.B., 1882 — Report on the foraminifera. *In* Tizard, Staff-Commander, & Murray, J., — Exploration of the Faroe Channel during the summer of 1880, in Her Majesty's hired ship 'Knight Errant'. *Proceedings of the Royal Society of Edinburgh*, 11(111), 708–717.

Brady, H.B., 1884 — Report on the foraminifera dredged by HMS Challenger during the years 1873-76. Report of the Challenger Expedition, 1873-1876, *Zoology*, vol. 9, 1-814.

Bronnimann, P., 1951 — *Globigerinita naparimaensis*, n. gen., n.sp., from the Miocene of Trinidad, B.W.I. *Contributions from the Cushman Foundation for Foraminiferal Research*, 2(1), 16–18.

Bronnimann, P., & Resig, J., 1971— A Neogene globigerinacean biochronologic time-scale of the southwestern Pacific. *In* Winterer, E.L., & others, Initial reports of the Deep Sea Drilling Project, volume 7, 1235-1469. *U.S.Government Printing Office, Washington.*

Brotzen, F., & Pozaryska, K., 1961 — Foraminiferes du Paleocene et de l'Eocene inferieur en Pologne Septentrionale remarques paleogeographiques. *Revue de Micropaleontologie*, 4(3), 155-166.

Carter, A.N., 1958 — Tertiary foraminifera from the Aire District, Victoria. *Geological Survey of Victoria Bulletin*, 55, 1-76.

Catalono, R. & Sprovieri, R., 1971 — Biostratigrafia di alcune serie saheliane (Messiniano inferiore) in Sicilia. *Proceedings of the Second Planktonic Conference, Rome*, 1970, 211-249. *Edizioni Tecnoscienza, Rome.*

Chapman, F., Parr, W.J., & Collins, A.C., 1934 — Tertiary foraminifera of Victoria, Australia — the Balcombian deposits of Port Phillip; part III. *Journal of the Linnean Society of London, Zoology*, 38(262), 553-577.

Chaproniere, G.C.H., 1981 — Late Oligocene to early Miocene planktic Foraminiferida from Ashmore Reef No. 1 Well, northwest Australia. *Alcheringa*, 5, 103-131.

Chaproniere, G.C.H., 1985 — Late Neogene and Quaternary planktonic foraminiferal biostratigraphy and palaeobathymetry of dredge samples from the southern Tonga Platform (Cruise L5-82-SP). *In* Scholl, D.W., & Vallier, T.L., (editors), Geology and Offshore Resources of Pacific Island arcs - Tonga region. *Circum-Pacific Council for Energy and Mineral Resources. Earth Science Series*, vol. 2, 131-139.

Cifelli, R., 1971 — On the temperature relationships of planktonic foraminifera. *Journal of Foraminiferal Research*, 1(4), 170-177.

Cifelli, R., 1982 — Early occurrences and some phylogenetic implications of spiny, honeycomb-textured planktonic foraminifera. *Journal of Foraminiferal Research*, 12(2), 105-115.

Cifelli, R., & Smith, R.K., 1970 — Distribution of planktonic foraminifera in the vicinity of the North Atlantic Current. *Smithsonian Contributions to Paleobiology*, 4, 1-52.

Cushman, J.A., 1927 — An outline of a re-classification of the foraminifera. *Contributions from the Cushman Laboratory for Foraminiferal Research*, 3(1), 1-105.

Cushman, J.A., & Bermudez, P.J., 1937 — Further new species of Foraminifera from the Eocene of Cuba. *Contributions from the Cushman Laboratory for Foraminiferal Research*, 13(1).

Cushman, J.A., & Bermudez, P.J., 1949 — Some Cuban species of *Globorotalia*. *Contributions from the Cushman Laboratory for Foraminiferal Research*, 25(2), 26-45.

Cushman, J.A., & Ellisor, A.C., 1939 — New species of foraminifera from the Oligocene and Miocene. *Contributions from the Cushman Laboratory for Foraminiferal Research*, 15(1), 1-14.

Cushman, J.A., Stewart, R.E., & Stewart, K.C., 1930 — Tertiary Foraminifera from Humboldt County, California. *Transactions of the San Diego Society of Natural History*, 6(2), 41-94.

Deshayes, G.P., 1832 — Encyclopedie Methodique; Histoire Naturelle des Vers, Paris, *Mme. v. Agasse*, vol. 2(2), 1-594; vol. 3, 595-1152.

Egger, J.G., 1893 — Foraminiferen aus Meeresgrundproben gelotet von 1874 bis 1876 von S.M. Sch. *Gazelle. Bayerische Akademie der Widdenschaften, Mathematisch-physikalische Classe, Abhandlungen*, 18(2), 193-458.

Ehrenberg, C.G., 1861 — Elemente des tiefen Meeresgrundes im Mexikanischen Golfstrome bei Florida. Uber die Tiefgrund-Verh altnisse des Oceans am Eingange der Davisstrasse und bei Island. *Konigliche Preussische Akademie der Wissenschaften Berlin, Monatsberichte*, 220-240, 275-315.

Ericson, D.B., 1959 — Coiling direction of *Globorotalia pachyderma* as a climatic index. *Science*, 130(3369), 219-220.

Finlay, H.J., 1939 — New Zealand Foraminifera: key species in stratigraphy — No. 2. *Transactions of the Royal Society of New Zealand*, 69(1), 89-128.

Finlay, H.J., 1940 — New Zealand Foraminifera: key species in stratigraphy — No. 4. *Transactions of the Royal Society of New Zealand*, 69(4), 448-472.

Finlay, H.J., 1947 — New Zealand Foraminifera: key species in stratigraphy - No. 5. *New Zealand Journal of Science and Technology*, 28(5), 259-292.

Fleisher, R.L., 1974 — Cenozoic planktonic foraminifera and biostratigraphy, Arabian Sea Deep Sea Drilling Project, Leg 23A. *In* Whitmarsh, R.B., Weser, O.E., & others, Initial Reports of the Deep Sea Drilling Project, volume 23, 1001-1072. *U.S. Government Printing Office, Washington.*

Galloway, J.J., & Wissler, S.G., 1927 — Pleistocene Foraminifera from the Lomita Quarry, Palos Verdes Hills, California. *Journal of Paleontology*, 1, 35-87.

Green, K.E., 1960 — Ecology of some Arctic foraminifera. *Micropaleontology*, 6(1), 57-78.

Haman, D., Huddleston, R.W., & Donahue, J.P., 1980 — *Obandyella*, a new name for *Hirsutella* Bandy, 1972 (Foraminiferida), non Cooper and Wood, 1951 (Brachiopoda). *Proceedings of the Biological Society of Washington*, 93, 1264-1265.

Hedberg, H.D., 1937 — Foraminifera of the middle Tertiary Carapita Formation of northeastern Venezuela. *Journal of Paleontology*, 11(8), 661-697.

Hornibrook, N. de B., 1961 — Tertiary Foraminifera from Oamaru District (N.Z.) Part 1 — Systematics and Distribution. *New Zealand Geological Survey, Palaeontological Bulletin*, 34(1), 1-192.

Hornibrook, N. de B., 1965 — *Globigerina angiporoides* n.sp. from the upper Eocene and lower Oligocene of New Zealand and the status of *Globigerina angipora* Stache, 1865. *New Zealand Journal of Geology and Geophysics*, 8(5), 834-838.

Hornibrook, N. de B., 1981 — *Globorotalia* (planktic foraminiferida) in the Late Pliocene and Early Pleistocene of New Zealand. *New Zealand Journal of Geology and Geophysics*, 24, 263-292.

Hornibrook, N. de B., 1982 — Late Miocene to Pleistocene *Globorotalia* (Foraminiferida) from DSDP Leg 29, site 284, southwest Pacific. *New Zealand Journal of Geology and Geophysics*, 25, 83-99.

Jenkins, D.G., 1960 — Planktonic foraminifera from the Lakes Entrance oil shaft, Victoria, Australia. *Micropaleontology*, 6(4), 345-371.

Jenkins, D.G., 1966 — Planktonic foraminiferal zones and new taxa from the Danian to lower Miocene of New Zealand. *New Zealand Journal of Geology and Geophysics*, 8(6), 1088-1126.

Jenkins, D.G., 1967 — Recent distribution, origin and coiling ratio changes in *Globorotalia pachyderma* (Ehrenberg). *Micropaleontology*, 13(2), 195-203.

Jenkins, D.G., 1968 — Planktonic Foraminiferida as indicators of New Zealand Tertiary paleotemperatures. *Tuatara*, 16(1), 32-37.

Jenkins, D.G., 1970 — Foraminiferida and New Zealand Tertiary biostratigraphy. *Revista Espanola de Micropaleontologia*, 2(1), 13-26.

Jenkins, D.G., 1971 — New Zealand Cenozoic planktonic foraminifera. *New Zealand Geological Survey Palaeontological Bulletin*, 42, 1-278.

Jenkins, D.G., 1975 — Cenozoic planktonic foraminiferal biostratigraphy of the southwestern Pacific and Tasman Sea — DSDP Leg 29. *In* Kennett, J.P., Houtz, R.E., & others, Initial Reports of the Deep Sea Drilling Project, volume 29, 449-467. *U.S. Government Printing Office, Washington.*

Kahn, M.I., 1981 — Ecological and palaeoecological implications of the phenotypic variation in three species of living planktonic foraminifera from the northeastern Pacific Ocean (50 N, 145 W). *Journal of Foraminiferal Research*, 11(3), 203-211.

Keller, G., 1978 — Morphologic variation of *Neogloboquadrina pachyderma* (Ehrenberg) in sediments of the marginal and central Northeast Pacific Ocean and paleoclimatic interpretation. *Journal of Foraminiferal Research*, 8(3), 208-224.

Kennett, J.P., 1966 — The *Globorotalia crassaformis* bioseries in north Westland and Marlborough, New Zealand. *Micropaleontology*, 12(2), 235-245.

Kennett, J.P., 1968 — Latitudinal variation in *Globigerina pachyderma* (Ehrenberg) in surface sediments of the southwest Pacific ocean. *Micropaleontology*, 14(3), 305-318.

Kennett, J.P., & Srinivasan, M.S., 1983 — Neogene Planktonic Foraminifera. A Phylogenetic Atlas. *Hutchison Ross Publishing Company, Pennsylvania.*

Kennett, J.P., & Watkins, N.D., 1974 — Late Miocene-Early Pliocene paleomagnetic stratigraphy, paleoclimatology and biostratigraphy in New Zealand. *Geological Society of America Bulletin*, 85, 1385-1398.

Koch, R., 1926 — Mitteltertiare Foraminiferen aus Bulongan, Ost-Borneo. *Eclogae Geologicae Helvetiae*, 19(3), 722-751.

Loutit, T.S., & Kennett, J.P., 1979 — Applications of carbon isotope stratigraphy to Late Miocene shallow marine sediments, New Zealand. *Science*, 204, 1196-1199.

Maiya, S., Saito, T., & Sato, T., 1976 — Late Cenozoic planktonic foraminiferal biostratigraphy of northwest Pacific sedimentary sequences. *In* Takayanagi, Y., and Saito, T., (editors), Progress in Micropaleontology, 395-422. *Micropaleontology Press, New York.*

Orbigny, A.D., d', 1826 — Tableau Methodique de la classe des Céphalopodes. *Annales Sciences Naturales, Paris*, series 1, 7, 96-314.

Orbigny, A.D., d', 1839 — Foraminiferes. *In* Sagra, R. de la. Histoire Physique, Politique et Naturelle de 'Ile de Cuba. *A. Bertrand, Paris.*

Orbigny, A.D., d', 1846 - Foraminiferes fossiles du Bassin Tertiare de Vienne (Autriche). *Gide et Compe, Paris, France*, I-XXXVII, 1-312.

Parker, F.L., 1962 — Planktonic foraminiferal species in Pacific sediments. *Micropaleontology*, 8(2), 219-254.

Parker, F.L., 1967 — Late Tertiary biostratigraphy (planktonic foraminifera) of tropical Indo-Pacific Deep-Sea Cores. *Bulletins of American Paleontology*, 52(235), 115-208.

Parker, W.K., Jones, T.R., & Brady, H.B., 1865 — On the Nomenclature of the Foraminifera. Pt. 12. The species enumerated by d'Orbigny in the 'Annales des Sciences Naturelles', vol. 7, 1826. *Annals and Magazine of Natural History*, Ser. 3, 16, 15-41.

Plummer, H.J., 1926 — Foraminifera of the Midway Formation in Texas. *Bulletin of the University of Texas*, 2644, 1-206.

Poore, R.Z., 1979 — Oligocene through Quaternary planktonic foraminiferal biostratigraphy of the North Atlantic: DSDP Leg 49. *In* Luyendyk, B.P., Cann, J.R. & others, Initial Reports of the Deep Sea Drilling Project, volume 49, 447-517. *U.S. Government Printing Office, Washington.*

Postuma, J.A., 1971 — Manual of Planktonic Foraminifera. *Elsevier Publishing Company, Amsterdam.*

Reuss, A.E., 1850 — Neues Foraminiferen aus den Schichten des Osterreichischen Tertiar Beckens. *Akademie des Wissenschaften Wien, Denkschrifte Mathematisch-Naturwissenschaftliche Klasse*, 1, 365-390.

Reynolds, L.A., & Thunell, R.C., 1986 — Seasonal production and morphologic variation of *Neogloboquadrina pachyderma* (Ehrenberg) in the northeast Pacific. *Micropaleontology*, 32(1), 1-18.

Saito, T., Thompson, P.R., & Breger, D., 1981 — Systematic Index of Recent and Pleistocene Planktonic Foraminifera. *University of Tokyo Press, Tokyo.*

Salvatorini, G., 1967 — Alcune nuove specie di foraminiferi del Miocene superiore della Toscano Marittima. *Atti della Società Toscana Toscand di Naturali, ser. A, Memorie*, 73, 1-13.

Schwager, C., 1866 — Fossile Foraminiferen von Kap Nikobar. *Novara* Expedition, 1857-1859. *Geologischen Teil, Wien, Osterreich*, 2(2), 187-268.

Shipboard Scientific Party, 1975a — Site 270. *In* Kennett, J.P., Houtz, R.E., & others, Initial Reports of the Deep Sea Drilling Project, volume 29, 225-270. *U.S. Government Printing Office, Washington.*

Shipboard Scientific Party, 1975b — Site 283. *In* Kennett, J.P., Houtz, R.E., & others, Initial Reports of the Deep Sea Drilling Project, volume 29, 365-402. *U.S. Government Printing Office, Washington.*

Srinivasan, M.S., & Kennett, J.P., 1974 — Secondary calcification of the planktonic foraminifer *Neogloboquadrina pachyderma* as a climatic index. Science, 186, 630-632.

Srinivasan, M.S., & Kennett, J.P., 1976 — Evolution and phenotypic variation in the Late Cenozoic *Neogloboquadrina dutertrei* plexus. *In* Takayanagi, Y., & Saito, T., (editors), Progress in Micropaleontology, 329-355. *Micropaleontology Press, New York.*

Subbotina, N.N., 1953 — Fossil Foraminifera of the USSR: *Globigerinidae, Hantkeninidae, Globorotaliidae. Trudy UNIGRI*, 76, 1-296 (in Russian) [English Translation, 1971: London and Wellingborough : *Collet's (Publishers) Ltd.*]

Takayanagi, Y., & Saito, T., 1962 — Planktonic foraminifera from the Nobori Formation, Shikoku, Japan. *Science Reports, Tohoku University, series 2 (Geology)*, 5, 67-106.

Taylor, D.J., 1965 — Preservation, composition and significance of Victorian Lower Tertiary '*Cyclammina* faunas'. *Proceedings of the Royal Society of Victoria*, 78(2), 143-160.

Theyer, F., 1973 — *Globorotalia inflata triangula*, a new planktonic foraminiferal subspecies. *Journal of Foraminiferal Research*, 3(4), 199-201.

Thompson, P.R., 1973 — Two new late Pleistocene planktonic foraminifera from a core in the southwest Indian Ocean. *Micropaleontology*, 19, 469-474.

Thomson, W., 1876 — *In* Murray, J., Preliminary reports to Professor Wyville Thomson, F.R.S., director of the Civilian Scientific Staff, on work done on board the 'Challenger'. *Proceedings of Royal Society of London*, 24, 471-544.

Todd, R., 1957 — Smaller Foraminifera. *Professional Paper United States Geological Survey*, 280H, 265-320.

Toumarkine, M., & Bolli, H.M., 1970 — Evolution de *Globorotalia cerroazulensis* (Cole) dans l'Eocene moyen et superieur de Possagno (Italie). *Revue de Micropaleontologie*, 13(3), 131-145.

Walters, R., 1965 — The *Globorotalia zealandica* and *G. miozea* lineages. *New Zealand Journal of Geology and Geophysics*, 8, 109-127.

Webb, P.N., 1975 — Paleocene foraminifera from DSDP Site 283, South Tasman Basin. *In* Kennett, J.P., Houtz, R.E. & others, Initial Reports of the Deep Sea Drilling Project, volume 29, 833-843. *U.S. Government Printing Office, Washington.*

BMR Journal of Australian Geology & Geophysics, 11, 63-79

Youngest Permian marine macrofossil fauna from the Bowen and Sydney Basins, eastern Australia

J.M. Dickins[1]

The marine invertebrate macrofauna from the upper part of the Blenheim Subgroup of the Bowen Basin and the Kulnura Marine Tongue of the Sydney Basin is described. The fauna is assigned to 12 genera, one of which — *Pseudonucula* — is newly recognised, and to 13 species, of which one is new. On the basis of these descriptions and existing published information, three zones are recognised in the Blenheim subgroup, in ascending order, the *Martiniopsis magna*, the *Martiniopsis pelicanensis* and the *Martiniopsis havilensis* zones. An explanation is given of the conclusions of Waterhouse & Jell (1983) about the lower part of the subgroup. From the fauna, particularly the occurrence of *Martiniopsis havilensis*, it is concluded that a hiatus occurs in the Blenheim Subgroup between the Black Alley Shale and the Peawaddy Formation in the southwestern part of the Bowen Basin, and that the Black Alley Shale is equivalent to the MacMillan Formation in the central part of the basin and the Exmoor Formation in the northeastern part. The upper part of the Blenheim Subgroup (zone of *Martiniopsis havilensis*) seems to be younger than the Mulbring Shale of the Sydney Basin, and the Kulnura·Tongue is not likely to be significantly younger than the Blenheim Subgroup. The faunas described appear to be younger than Kungurian, but are not likely to be younger than the Kazanian. They are rather low in diversity relative to older Permian faunas in the two basins, and this probably reflects the rather restricted marine conditions at the end of the open sea in the two basins.

Introduction

Use of the term, and the extent and relationships of the Blenheim Subgroup, remain controversial. The problems have been discussed by Dickins (1983). This paper supports the conclusions in Dickins (1983) with description of the fauna from the upper part of Blenheim Subgroup, and further discussion on the group.

Fauna from the upper part of the Blenheim Subgroup and the Kulnura Tongue.

MacMillan Formation (UDC1 and UDC2) — Pelecypods: *Pseudonucula bradshawensis* nom. nov.; *Paleyoldia* sp.; *Glyptoleda flexuosa* Waterhouse, 1965; *Atomodesma* sp.; *Vacunella curvata* (Morris), 1845. Gastropods: *Mourlonia (Mourlonia) strzeleckiana* (Morris), 1845; *Discotomaria?* sp. Brachiopods: *Martiniopsis havilensis* (Campbell), 1960. Conulariid indet.

Black Alley Shale — Gastropods: *Peruvispira* cf. *modesta* Waterhouse, 1963. Brachiopods: *Martiniopsis havilensis* (Campbell), 1960.

Upper part of the Blenheim Subgroup (Cherwell Range immediately below MacMillan Formation; Tay Glen Crossing): *Martiniopsis havilensis* (Campbell), 1960.

Upper Part Blenheim Subgroup (Blenheim area, MC 803) — Pelecypods: *Pseudonucula bradshawensis* nom. nov.; *Glyptoleda flexuosa* Waterhouse, 1965. Gastropods: *Warthia perspecta* Fletcher 1959; *Mourlonia (Mourlonia) strzeleckiana* (Morris), 1845; *Peruvispira* cf. *modesta* Waterhouse, 1963. Brachiopods: *Terrakea solida* (Etheridge & Dun), 1909; *Echinalosia* cf. *minima* Dear, 1971; *Martiniopsis havilensis* (Campbell), 1960.

Upper part of Blenheim Subgroup — Brachiopods: (Parrot Creek, CB1572) *Martiniopsis havilensis* (Campbell), 1960. Exmoor Formation (MC292) *Martiniopsis havilensis* (Campbell), 1960. Exmoor Formation (MC292) — Brachiopods: *Martiniopsis havilensis* (Campbell), 1960.

Kulnura Marine Tongue — Brachiopods: *Echinalosia* cf. *minima* Dear, 1971; *Echinalosia* cf. *ovalis* (Maxwell), 1954.

Faunal subdivision of the Blenheim Subgroup

During the joint mapping project of the Bowen Basin by the Geological Survey of Queensland and the Bureau of Mineral Resources, the top part of the Middle Bowen beds (= Back Creek Group) was found to contain a distinctive geological sequence, the Blenheim Subgroup, with a distinctive fauna, Fauna IV (Malone & others 1966, 1969; Mollan & others, 1969; Dickins & Malone, 1968, 1973; Dickins, 1983). At that time, because of the considerable range of many species within the subgroup, a subdivision of Fauna IV was not attempted (see Dickins, 1966, p. 71). The following discussion indicates that such a division still remains difficult.

Dear (1972) described four faunal assemblages within Fauna IV in the northern part of the Basin. The oldest fauna, which he called the Exmoor fauna, contained the diagnostic species *Wyndhamia blakei* Dear, *Ingelarella magna* Campbell, *Ingelarella isbelli* Campbell, *Terrakea elongata exmoorensis* Dear, *Notospirifer duodecimcostatus* (McCoy), and *Notospirifer minutus* Campbell (the taxonomic nomenclature is that of Dear).

The next youngest, called the Scottville fauna, was marked by the abundance of *Wyndhamia clarkei* (Etheridge Snr) and *Terrakea elongata* (Etheridge & Dun), but the ingelarellid species diagnostic of the Exmoor fauna were lacking. The next fauna, the Pelican Creek fauna, contained several species not found in the lower faunas, including *Streptorhynchus pelicanensis* Fletcher, *Ingelarella pelicanensis* Campbell, *Maorielasma globosum* Campbell, a new species of *Gilledia*, and *Gilledia pelicanensis* Campbell. The youngest Havilah fauna was distinguished by the presence of *Ingelarella havilensis* Campbell.

Runnegar & McClung (1975) proposed recognising two zones within the Blenheim Subgroup, the *isbelli* zone in the lower part and the *ovalis* zone in the upper part. The relation of these zones to Dear's scheme has yet to be investigated — the upward range of *I. isbelli* is not clear, nor is the incoming of *E. ovalis*, although I believe that *E. ovalis* can be identified from the base of the Blenheim Subgroup upwards in the sense used by Dickins & Malone (1973) and Dickins (1983).

Waterhouse & Jell (1983) have proposed a faunal subdivision of the Blenheim Subgroup (or Formation). I conclude that the *Notospirifer (Glendonia) duodecimcostatus-Merismopteria macroptera-Etheripecten plicata* Faunal Assemblage is found in the Blenheim Subgroup and represents Fauna IV. This supports my previous conclusions and is not contrary, as claimed by Waterhouse & Jell. The assemblage contains *Martiniopsis magna*, *Megadesmus grandis*, *Myonia carinata*,

[1]Division of Continental Geology, Bureau of Mineral Resources, GPO Box 378, Canberra, ACT 2601

Vacunella curvata, and other species, whose incoming is used to determine Fauna IV. As indicated by Waterhouse & Jell, the lithology is that of the Blenheim Subgroup. At Exmoor and Gebbie Creek, the lower boundary of the Blenheim Subgroup may be shown somewhat too far to the west by Malone & others (1966), and the boundary shown in measured sections may need some revision, which is not surprising, given the map scale and the preliminary state of work at that time. Clarification was given in later publications (Dickins & Malone, 1968, 1973). There is no basis for considering that this assemblage represents Fauna IIIC. Near Homevale, the base of beds with Fauna IV ('*Notospirifer (Glendonia) duodecimcostatus-Merismopteria macroptera-Etheripecten plicata* Faunal Assemblage') overlies beds of IIIC with *'Ingelarella' undulosa* (see Jensen & others, 1966; Malone & others, 1966).

I do not understand the statement by Waterhouse & Jell (1983, p. 236), 'The Exmoor area was considered to provide the best example of Fauna III of Dickins (1964) and three subdivisions were recognised by Dickins (in Malone & others 1966; Dickins & Malone, 1973)'. The Exmoor section was not one we considered in detail, and Fauna III and its subdivisions were worked out mainly in the Gebbie Creek and Homevale sections (Dickins & others, 1964; Malone & others, 1966).

No justification is given by Waterhouse & Jell (1983) for the use of Moonlight Sandstone at some considerable distance from the type area at Homevale. Apparently the Moonlight Sandstone as used by them (containing the '*Notospirifer (Glendonia) duodecimcostatus-Merismopteria macroptera-Etheripecten plicata* Faunal Assemblage') represents the top part of the Moonlight Sandstone at Homevale and, therefore, the basal part of the Blenheim Subgroup(see Dickins, 1983).

Waterhouse recognised three overlying faunas, the *Wyndhamia ingelarensis* Faunal Assemblage, the *Echinalosia ovalis* Faunal Assemblage and the *Wyndhamia clarkei* Faunal Assemblage. *Wyndhamia ingelarensis* Dear had not previously been recognised in the Blenheim Subgroup, and the figures given by Waterhouse (in Waterhouse & Jell, 1983, pl. 1, figs 7,8; pl. 6, fig. 1) are rather inadequate. I have not observed this species in the many hundreds of specimens I have examined, nor apparently has Dear (1971, 1972). The *Wyndhamia ingelarensis* Faunal Assemblage and the following *Echinalosia ovalis* Faunal Assemblage must be treated cautiously, because of the long range indicated by other workers. The *Wyndhamia clarkei* Faunal Assemblage corresponds in part to the Scottville fauna of Dear (1972), but apparently, Waterhouse & Jell (1983, p. 238) consider it extends into younger beds.

I agree with Waterhouse & Jell's conclusion that the Crocker Formation and the Catherine Sandstone cannot be correlated, nor can the Ingelara Shale and Maria Formation (Dickins, 1983).

Waterhouse & Jell (1983) add valuable detail for elaborating the palaeontological and stratigraphical sequence, and give further evidence on the distinctiveness of the Glendoo Fauna (Fauna IIIB) and its distinctiveness from Fauna IV. They substantiate the character of Fauna IV, although, unfortunately, they seem to confuse it with Fauna IIIC.

The base of Fauna IV is marked by the incoming of a considerable number of new forms. Amongst the significant brachiopods are the *Terrakea brachythaerus-elongata-solida* group[1], the *Echinalosia ovalis* group[1], *Martiniopsis* (= *Ingelarella*) *isbelli*, *Martiniopsis* (= *Ingelarella*) *magna*, *Notospirifer minutus* and several spiriferid species whose names are not yet clear. Amongst the pelecypods, *Astartila cythera* group, *Megadesmus grandis*, *Myonia carinata*, *Vacunella curvata*, and a new species of *Schizodus* are particularly conspicuous. A more exhaustive list was given by Dickins & Malone (1973, table 13).

Martiniopsis magna appears to be confined to the basal part of the Blenheim Subgroup, the Exmoor fauna of Dear (1972), and the *Etheripecten plicata* and *Wyndhamia ingelarensis* Faunal Assemblages of Waterhouse & Jell (1983); *magna* seems more satisfactory as the nominate species for this zone than *isbelli*, which appears to range higher in the sequence. Unfortunately, neither is known from the southwest or southeast of the basin, but *magna* is known from the western part (Clermont area) as well as the eastern part. In the Clermont area it occurs at the unconformity of the Blenheim Subgroup on pre-Permian beds.

Martiniopsis pelicanensis is known from the middle part of the sequence, and in particular from the Pelican Creek fauna of Dear (1972). It is recorded from its type locality in the northern part of the basin (Campbell, 1960; Dear, 1972), apparently from the southeastern part of the basin in the upper part of the Barfield Formation and the lower part of the Flat Top Formation (Dear, 1972; Dickins, 1972), and from the central part of the basin from the Crocker Formation (Dickins, 1969a). The species therefore seems particularly useful for recognising the middle part of the Blenheim Subgroup and for correlating this part of the sequence. Elsewhere (Dickins, 1969b; 1972), I have considered evidence that the upper part of the Mantuan *Productus* bed, the pelecypod bed of the Clermont area, the lower part of the Crocker Formation, the *Streptorhynchus pelicanensis* bed containing *Martiniopsis pelicanensis* in the northern part of the basin, and the uppermost part of the Barfield Formation and the lower part of the Flat Top Formation are to be correlated.

Martiniopsis havilensis is widespread in the upper part of the Blenheim Subgroup, and its distribution is discussed in this paper and in Dickins (1983). The best faunas are found at localities UDC1 and UDC2 from the MacMillan Formation and from MC 803 in the Blenheim area. Most of the species seem to range through the Blenheim Subgroup, with the exception of *Martiniopsis havilensis*. The occurrence at this level of a *Peruvispira* related to *P. modesta* Waterhouse, 1963 is of interest, since the Stephens Formation, which contains the species, is apparently younger than the Blenheim Subgroup (see Dickins, 1983).

Age and correlation of the Blenheim Subgroup

The correlation and nature of the Blenheim Subgroup were considered by Dickins (1983) and are further considered here. Evidence is given in Dickins (1983) that the Blenheim Subgroup (or any part of it) does not overlap in time the underlying Gebbie Subgroup, and that the upper boundary is more or less coeval in the various parts of the Bowen Basin, which differs from the interpretation of Koppe (1978) and Staines & Koppe (1979). This discussion was apparently unknown to Martini & Johnson (1987). Although their conclusions agree with those in Dickins (1983), their Figure

[1]The lack of standardisation in the names for these groups is unfortunate and confusing (Dear, 1971; Waterhouse, 1983; McClung, 1983). The differences between some of the species names used seems rather arbitrary and, in my opinion, a broader grouping would be more practical and useful.

10 shows the Gebbie Subgroup (or Formation) as coeval with part of the Blenheim Subgroup (and apparently all of the Tiverton Subgroup). This is not supported by any field or drilling evidence given by them (for other information see Malone & others, 1966).

Presumably, Martini & Johnson (1987, p. 368) use McClung (1981) in support of their idea, for they state 'McClung...considered the faunas to be facies related, so the time connation may be invalid'. Dickins & Malone (1973) considered carefully the environmental effects on the ranges and distribution of the fossils, and McClung does not really dispute their data. He claims (1981, p. 28) that few collections 'have been accurately located within measured sections', but clearly this contradicts the published reports on the Bowen Basin (see Dickins & Malone, 1973). In earlier publications, e.g. David & Browne (1950), the entire Back Creek Group (Middle Bowen beds), including its upper part, the Blenheim Subgroup, was considered Lower Permian[2].

Campbell (1959) suggested that the upper beds of the Middle Bowen (later referred to as Back Creek Group) might be Upper Permian (Kazanian), and Dickins (1961, 1970) concluded that a Kazanian age seemed likely on the basis of the occurrence of *Atomodesma bisulcatum* Dickins, 1961 and species of '*Licharewia*'. Dickins also concluded that the fauna of the Blenheim Subgroup seemed to be intermediate between the faunas of the lower and upper marine parts of the Liveringa Group of the Canning Basin, Western Australia, i.e., between the faunas of the Lightjack and Hardman Formations. The intervening sequence is represented by non-marine beds or a hiatus. This evidence also suggested a Kazanian age.

Waterhouse (1976, p. 137) considered the Exmoor fauna of Dear (1972) to be Ufimian (lowermost Upper Permian), the next two faunas of Dear to be Kazanian, and the Havilah fauna possibly post-Kazanian. Use of Ufimian as the lowest stage of the Upper Permian has presented difficulties because of its poorly developed marine fauna. It has often been ignored or included with the underlying Kungurian or overlying Kazanian. In a recent review of mid-Permian correlation, Dickins, Archbold, Thomas & Campbell (in press) have concluded that a fauna younger than Kungurian and older than Kazanian can be recognised . They consider this fauna Ufimian. On this basis, the basal part of the Blenheim Subgroup is probably Ufimian, as suggested by Waterhouse (1976). Dickins (1983) recorded *Aulosteges* in the Wairaki Breccia of Southland, New Zealand, suggesting a correlation with the Hardman fauna and tending to confirm the intermediate character of Fauna IV (the fauna of the Blenheim Subgroup) between that of the Lightjack and Hardman Formations. Although the evidence for the age of the Blenheim Subgroup is indirect, it seems substantial.

The evidence from the present descriptions does not add a great deal, but the relations with New Zealand help to confirm existing conclusions. *Glyptoleda flexuosa* Waterhouse, 1965a, has been described previously from the Mangarewa Formation, and *Peruvispira modesta* Waterhouse, 1963, from the Stephens Formation. The Stephens Formation has a similar fauna to that of the Wairaki Breccia, and on this basis the fauna of the top of the Blenheim Subgroup could be only slightly younger than the Kazanian, if at all.

The Hardman Formation has been regarded (Dickins, 1963; Dickins, Archbold & Thomas, in press) as equivalent to the Kalabagh Member of the Wargal Formation (Middle Productus) and the Chhidru Formation (Upper Productus) of the Salt Range, Pakistan. The correlation of the Kalabagh Member and the Chhidru Formation is not altogether clear. Grant (1970) argued strongly that not only are these units pre-Dzhulfian, but that they are Wordian, the lower part of the Guadalupian. If this is correct they can hardly be younger than Kazanian, and it would follow that the upper part of the Blenheim Subgroup is not likely to be younger than Kazanian.

Age and correlation of the Mulbring Formation and the Kulnura Marine Tongue.

Dickins (1970) correlated the Mulbring Formation in a general way with the Blenheim Subgroup (i.e. 'the upper part of the Middle Bowen Beds'), as both contained Fauna IV.

On the basis of the description of the fauna from the upper part of the Blenheim Subgroup (*havilensis* zone), the Mulbring Formation is probably older than the upper part of the Blenheim Subgroup. Most of the species in the *havilensis* zone range through the Blenheim Subgroup and are also found in the Mulbring Formation. *Martiniopsis havilensis*, however, has not been found in the Mulbring Formation, nor has *Peruvispira modesta*, which in New Zealand is apparently found in beds higher in the sequence.

The Kulnura Marine Tongue contains *Echinalosia* cf. *minima* and *Echinalosia* cf. *ovalis*, which are characteristic of Fauna IV and, therefore, the Kulnura Marine Tongue seems unlikely to be significantly younger than the Blenheim Subgroup.

On the basis of palynological examination, McMinn (1985) regarded the top of the Blenheim Subgroup (Black Alley Shale) as younger than the Mulbring Formation. However, he also regarded the top of the Aldebaran Sandstone and the rest of the overlying Gebbie and Blenheim Subgroups as younger than the Mulbring Formation in contradiction to the marine fauna (Dickins, 1970). The correlation of the marine fauna is based on a large number of species and has taken into account differences in ranges apparently caused by water temperature differences (Dickins, 1981). In these circumstances *Dulhuntyispora parvithola*, on which McMinn bases his correlation, apparently appears earlier in the Bowen than the Sydney Basin. This could be an accident of preservation or sampling but a more likely cause is climatic difference. This apparently also affects McMinn's usage of Middle Permian, which, accordingly, would differ in the two basins. He does not, however, define his usage of Middle Permian, and since there are already so many different usages of Middle Permian in different parts of the world, this appears to introduce, accidentally, another one. Use of Middle Permian seems best avoided, at least until its definition has been considered formally by the Subcommission of Permian Stratigraphy of the International Union of Geological Sciences.

Palaeoecology

The lithology of the samples varies from sandstone to siltstone and at UDC1 and MC803 the fossils occur in nodules. In

[2]A twofold subdivision of the Permian is used here, corresponding to the usage in the classical area of the Russian Platform-Ural Mountains area. Although some authors use a threefold subdivision, there is no international agreement on the scope of a threefold subdivision, and the different usages at present limit the value of the term.

the sandstone, *Martiniopsis havilensis* occurs in considerable numbers, whereas other fossils are rare. In the nodules a number of species are represented, but even here, the fauna is of low diversity compared with the fauna found at a lower level in the *pelicanensis* and *magna* zones.

The fauna from the nodules is apparently from relatively shallow water below wave base, as the productids would have rested in the substratum anchored only by their spines. *Martiniopsis havilensis* could also have lain in a shallow sublittoral position (Campbell, 1961).

The normal shallow sublittoral fauna, characterised by such forms as *Megadesmus*, *Astartila*, *Stutchburia*, and *Schizodus* (Dickins, 1963), appears to be absent. The low diversity suggests conditions of limited access to the open sea, and may reflect fluctuations in the composition of the water.

Systematic palaeontology

Pelecypods
Superfamily **Nuculacea** Gray 1824
Family **Praenuclulidae** McAlister 1969
Genus ***Pseudonucula*** nov. nom.[3]

Type species. *Pseudonucula bradshawensis* nov. nom. herein.

Diagnosis. Similar in shape to *Nuculopsis*, but apparently lacking a resilifer.

Discussion. The specimen taken as the holotype is the external of a left valve and the dentition is beautifully preserved. Not even a reduced resilifer seems to be present. The teeth seem to be slightly larger on the more compressed side of the shell and, according to the criteria of Bradshaw & Bradshaw (1971), the shell has the normal nuculid orientation, i.e., long side towards the front.

Figure 1. *Pseudonucula bradshawensis* gen. et. sp. nom. nov. External view of holotype, a left valve to show dentition, x5.5 approx.

[3]Nov. nom. is preferred here to gen. nov. and sp. nov. to indicate that, although a taxon is newly recognised, the possibility of its previous existence is not being denied.

Pseudonucula bradshawensis nov. nom.
Pl. 1, figs 1–7

Description. The holotype is an external impression, taken to be a right valve. The dentition and musculature are well shown. The anterior adductor is oval in a dorso-ventral direction. The mark of the posterior adductor is more rounded. The teeth are continuous around the dorsal margin of the shell. The ligament is apparently external, but was not found. Similar characters are shown in the other illustrated specimens. Poorly differentiated pedal scars are associated with the anterior and posterior adductor scars. Externally, the shell is smooth with concentric growth ornament.

Dimensions (mm).

	Length	*Height*	*Width*
Holotype (right valve)	12	10	5
Paratype A (bivalved specimen)	13	10.5	10
Paratype B (bivalved specimen)	17	12	11
Paratype C (bivalved specimen)	14	12	10

Occurrence. Holotype, CPC25255, and Paratypes A & B CPC25256, 25257, MC803, Paratype C, CPC25258, UDC1.

Superfamily **Nuculanacea** Adams & Adams 1858
Family **Nuculanidae** Adams & Adams 1858
Genus ***Paleyoldia*** Lintz, 1958 (p. 108)

Type Species (by original designation). *Yoldia glabra* Beede & Rogers (1899, p. 133, pl. 34, figs 4a–b).

Discussion. Although represented by a single incomplete specimen, the evenly rounded anterior part of the shell and the shape behind the umbo indicate the shell is not *Phestia* or a closely related genus, but is related to *Yoldia*. The nature of the distinctive ornament of the anterior part of the shell is not known.

Paleyoldia sp.
Pl. 1., figs 16–18

Description. The details of the external ornament are shown in Plate 1, fig. 16. The gross ornament is concentric. Superimposed on this is a fine irregular ornament, which is approximately concentric. At the front, a number of radiating lines are formed by elongated pustules.

Dimensions (mm).

Length	*Height*	*Thickness*
—	19	4

Occurrence. CPC25259, UDC1.

Genus ***Glyptoleda*** Fletcher 1945

Type species. *Glyptoleda reidi* Fletcher 1945, p. 299; pl. 19, figs 1–5, by original designation of Fletcher 1945, p. 208.

Discussion. This nuculanid is strikingly distinguished by its V-shaped external ornament. In this respect it can be separated from *Nucundata* Waterhouse (1965a, p. 641), which departs relatively slightly from the concentric ribbing pattern of *Nuculana*. According to Puri (1969, p. N239), the nuculanid *Veteranella* Patte (1926, p. 158) from the Permian–Triassic of Indo-China has a V-shaped ornament, but is oval in outline. Patte's paper is not available to me but, from

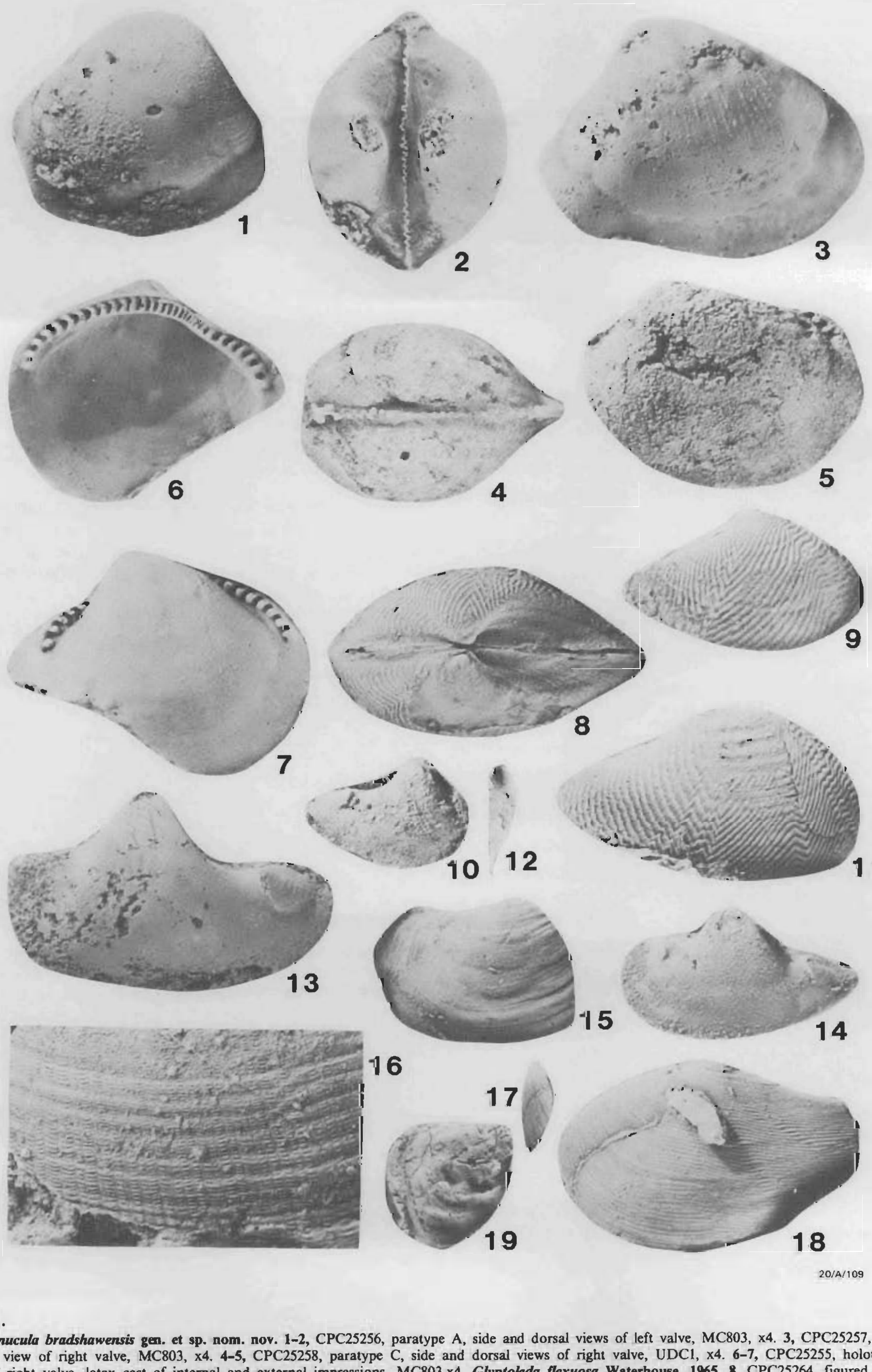

Plate 1.
***Pseudonucula bradshawensis* gen. et sp. nom. nov. 1–2,** CPC25256, paratype A, side and dorsal views of left valve, MC803, x4. **3,** CPC25257, paratype B, side view of right valve, MC803, x4. **4–5,** CPC25258, paratype C, side and dorsal views of right valve, UDC1, x4. **6–7,** CPC25255, holotype, side view of right valve, latex cast of internal and external impressions, MC803,x4. ***Glyptoleda flexuosa* Waterhouse, 1965. 8,** CPC25264, figured specimen E, latex dorsal view, UDC1, x2. **9,** CPC25263, figured specimen D, latex side view, UDC1, x2. **10,** CPC25261, figured specimen B, side view, MC803, x1. **11,** CPC25260, figured specimen A, side view, MC803, x2. **12–13,** CPC25262, figured specimen C, front view x1, side view MC803. **14,** CPC25265, figured specimen F, side view, UDC1, x2. ***Vacunella curvata* (Morris), 1845. 15,** CPC25268, side view, UDC1, x2. ***Paleyoldia* sp. 16–18,** CPC25259, anterior ornament x16, front view x1 and side view x2, UDC1. ***Atomodesma* sp. 19,** CPC25267, side view, UDC1, x1.

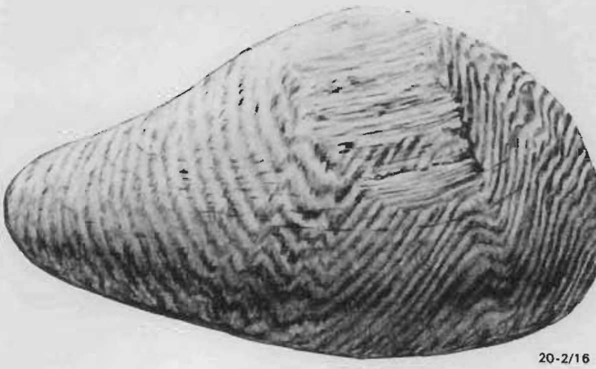

Figure 2. *Glyptoleda flexuosa* Waterhouse, 1965, CPC25260, to show external ornament of a right valve, x5.5 approx.

Puri's description, *Veteranella* seems to differ in shape from *Glyptoleda*.

In 1945 *Glyptoleda* was recorded from the Permian of eastern and western Australia, and in 1965 from the Permian of New Zealand. Now it has been recorded from the Permian of Nova Zemlya (Muromtseva, 1981; 1984). This distribution pattern in beds of broadly similar age within the Permian is thought provoking.

Glyptoleda flexuosa Waterhouse

(1965a, p. 658, pl. 98, figs 6–12)
Pl. 1 figs 8–14

Type specimens. From the Mangarewa Formation, Productus Creek area, Otago, South Island, New Zealand.

Diagnosis (of Queensland specimens). Distinctly tumid in front of the umbo, relatively short at the rear. Shell thickened in the umbonal region, so that the anterior and posterior muscle impressions are distinct; v-shaped ornament complicated.

Description. Figured specimens A, D, and F show the shape and the ornament. There are V-shaped indentations not only in the middle part of the shell as in other species, but also in the anterior and posterior parts of the shell.

Figured specimen E shows the lunule and escutcheon. An inner and outer escutcheon ridge and a posterior umbonal ridge are visible as recognised by Waterhouse (1965a, text-fig. 2).

The internal features are shown by Figured specimens B, C and F. Anterior and posterior pedal scars are visible. The anterior is joined by a ridge to the anterior adductor and the posterior appears to be attached to the top front of the adductor. A large umbonal muscle is associated with an internal ridge running down from the umbo. At least one small umbonal muscle is found at the back tip of the external impression of the umbo.

Dimensions (mm).

	Length	*Height*	*Width*
Figured specimen A	30	19 (approx.)	5
Figured specimen B	33 (approx.)	21	6
Figured specimen C	35 (approx.)	24 (approx.)	8
Figured specimen D	23	14	8 (approx.)
Figured specimen E	38	—	16
Figured specimen F	24	14	9 (bivalve)
CPC 25266	28	18 (approx.)	4 (approx.)

Occurrence. Figured specimens A–C, CPC25260–25262, MC803; figured specimens D–F, CPC25263–25265, UDC1, measured specimens, CPC25266, UDC1.

Discussion. The species from the Bowen Basin bears some resemblance to the three species *G. intricata*, *G. flexuosa* and *G. simplicata*, described by Waterhouse (1965a) from the Mangarewa Formation of New Zealand. In the shape and nature of the ornament the Queensland specimens seem closest to *G. flexuosa*. The Queensland and New Zealand specimens are close in age (discussed elsewhere) and younger than other described species of *Glyptoleda* from Western Australia and Queensland, which have less complicated ornament.

Superfamily ?
Family **Inoceramidae?** Giebel 1852
Subfamily **Atomodesminae** Waterhouse 1976
Genus ***Atomodesma*** Beyrich 1864 (p. 68)

Type species. *Atomodesma exarata* Beyrich 1864, p. 71, pl. 3, figs 4a-b by subsequent designation of Wanner 1922, p. 63.

Discussion. *Atomodesma* and related genera, including their type species, were discussed by Dickins (1963, p. 66). Recently, considerable interest has been caused in the family relationship of *Atomodesma* by the discovery of multiple ligament grooves in what otherwise appear to be ordinary *Atomodesma* (Browne & Newell, 1966). *Atomodesma* can be fairly readily incorporated in the Myalinidae of the superfamily Ambonychiacea, although it seems to be the direct ancestor of the Inoceramidae, and can as readily be included in this family.

Contrary to the then current usage, Waterhouse (1979) proposed restricting the *Atomodesma* to species with one or more radial plicae or grooves[4], and excluding species that otherwise do not seem to differ significantly. The latter species would then be assigned to a number of genera on doubtful grounds. This proposal is likely to cause only confusion.

Waterhouse (1979), also proposed two new generic names for New Zealand shells, *Mytilidesmatella* (p. 13) and *Trabeculala* (p. 15). On the basis of the information and figures provided, there seems little basis for separating the type species of these genera from *Atomodesma trechmanni* Marwick 1935, the type Marwick 1935, the type species of *Maitaia* Marwick 1935. I figure here (Fig. 3) a specimen of *A. woodi* Waterhouse 1963, the type species of *Mytilidesmatella*, which is *A. trechmanni* in my opinion. The alleged differences, e.g. in the development of the septum, are not apparent in the figured material.

Atomodesma sp.
Pl. 1, fig. 19

Discussion. The single right valve might be placed either in *Atomodesma* or *Aphanaia* if the latter is regarded as generically separable.

[4]Waterhouse (1979, p. 2) proposed a new name for a specimen which I would refer to *A. exarata* Beyrich 1864 (Dickins, 1963, fig. 5). The specimen was said by Waterhouse and Kauffman & Runnegar (1975) to be from the Noonkanbah Formation. The identification of the formation is apparently a mistake, because this species is known from many localities in the Lightjack Formation of the Liveringa Group, but is unknown from the Noonkanbah Formation, as indicated by Dickins (1956, p. 25; 1963, fig. 5).

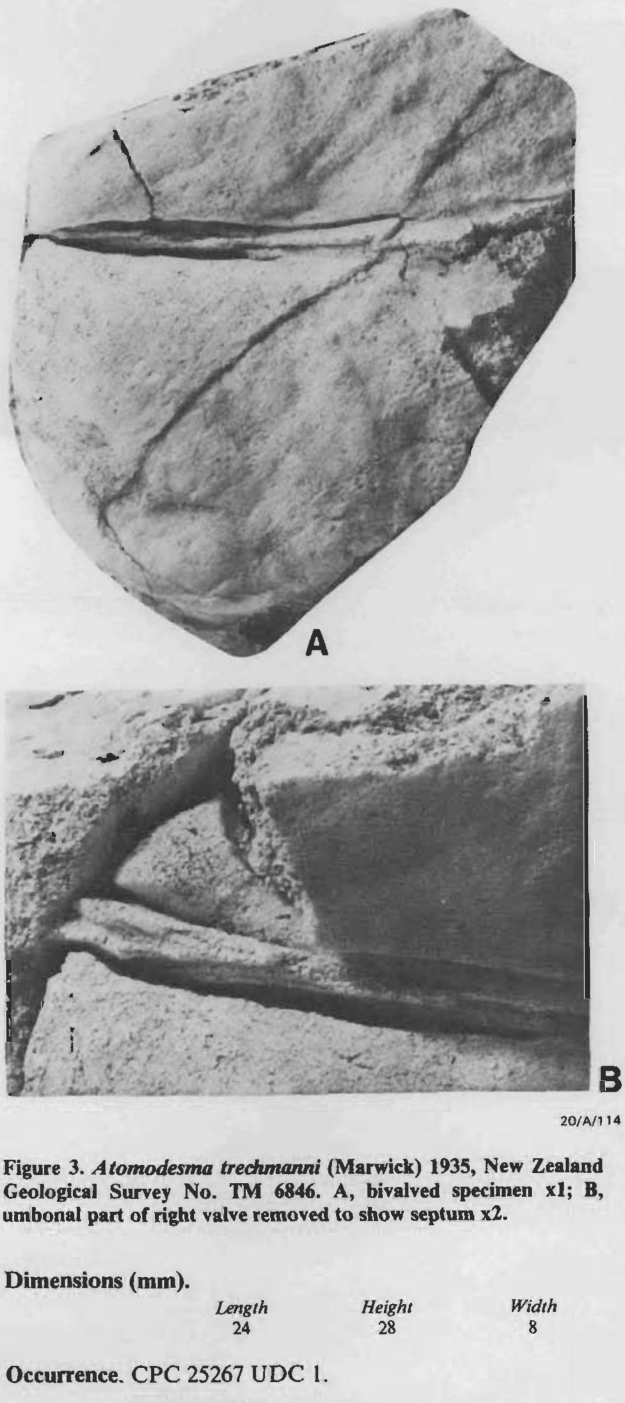

Figure 3. ***Atomodesma trechmanni*** **(Marwick) 1935, New Zealand Geological Survey No. TM 6846. A, bivalved specimen x1; B, umbonal part of right valve removed to show septum x2.**

Dimensions (mm).

Length	*Height*	*Width*
24	28	8

Occurrence. CPC 25267 UDC 1.

Superfamily **Pholadomyacea** King 1844
Family **Megadesmidae** Vokes 1967
Subfamily **Vacunellinae** Astafieva-Urbaitis 1973
Genus **Vacunella** Waterhouse 1965

Vacunella curvata (Morris) 1845
Pl. 1, fig. 15

Type species. *Allorisma curvatum* Morris 1845, p. 270, pl. 10, fig. 1, by original designation of Waterhouse 1965b, p. 377.

Description. A single small right valve shows the characteristic shape of this species — the posterior dorsal margin is upturned towards the back; and the umbo, towards the front. From above, the shell is wider towards the front and evenly curved towards the back; it lacks a distinct umbonal sinus.

Dimensions (mm).

Height	*Width*
12	3

Occurrence. CPC25268, UDC1.

Discussion. This distinctive species occurs in Queensland, New South Wales, and Tasmania, where it is characteristic of Fauna IV as defined in the Bowen Basin, Queensland.

Gastropods

Superfamily **Pleurotomariacea** Swainson 1940
Family **Pleurotomariidae** Swainson 1940
Genus ***Mourlonia*** de Koninck 1883 (p. 10)

Type species (by original designation). *Helix carinatus* J. Sowerby (1812,.P. 34).

Synonym. *Mourlonopsis* Fletcher 1958.

Discussion. Fletcher (1958, p. 129) proposed the name *Mourlonopsis* (type *Pleurotomaria strzeleckiana* Morris 1845) for *Mourlonia*-like shells with 'a more erect spire'. The height of the spire seems, however, to be a rather variable feature and the higher spire does not seem sufficient for the use of a separate generic name. The relationship between *Neoplatyteichum* Maxwell 1964 (p. 20) proposed for Upper Carboniferous shells from Queensland and *Mourlonia* is not clear. *Neoplatyteichum* does not appear to differ much from *Mourlonia*.

Mourlonia (Mourlonia) strzeleckiana (Morris 1845, p. 287, pl. XVIII, fig. 5)
Pl. 2., figs 12–19

For synonymy see Fletcher (1958)

Description. The material includes numerous impressions that show the external ornament beautifully. The conical spire is of moderate height. The sutures are moderately well marked, although the whorls are more or less rounded and not particularly step-shaped. The ornament is made up of numerous fine spiral lirae and growth lines forming pustules where they cross. The selenizone is well marked by a carina on either side, and ornamented only by numerous lunulae. No umbilicus is present. Poor development of the spiral lunae on the smaller whorls of some specimens may be due to abrasion or exfoliation.

Dimensions (mm). UDC1

Height	*Width*	*Apical angle*
18	22	69°
16 (approx)	20	71°
22	22	68°
24	22	76°
22	24	74°
25	35	75°
28 (approx.)	32	62°

Occurrence. Figured specimens A–E, CPC25269–25273, UDC1, MC803.

Discussion. The rounded nature of the whorl cross-section above and below the selenizone indicates this form is not a *Platyteichum*. The specimens described by Fletcher (1958)

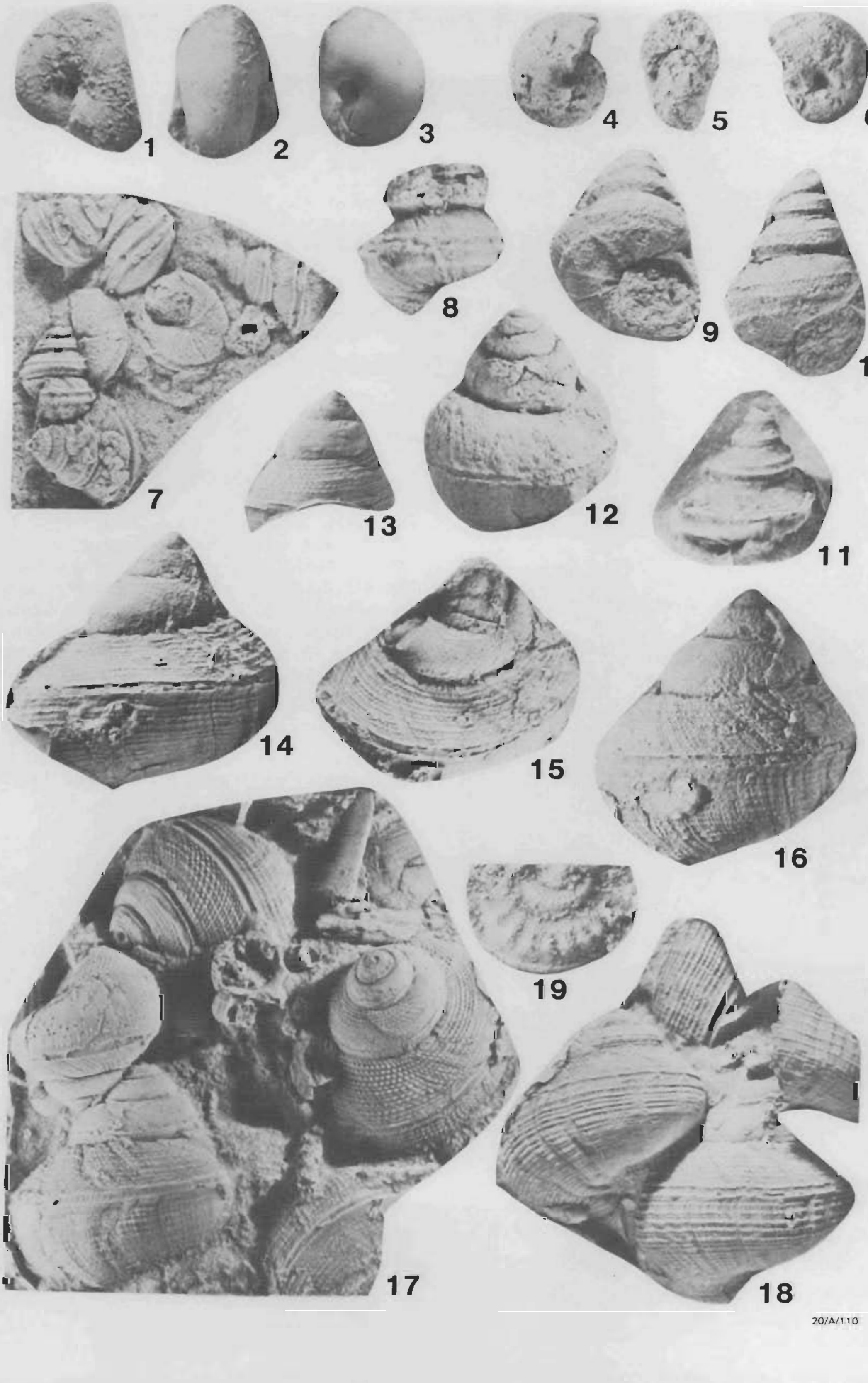

20/A/110

Plate 2.

***Warthia perspecta* Fletcher, 1958. 1-3**, CPC25277, figured specimen A, side and vertical views, MC803, x1. **4-6**, CPC25278, figured specimen B, side and vertical views, MC803, x1. ***Peruvispira* cf. *modesta* Waterhouse, 1963. 7**, CPC25287, Black Alley Shale, x4. **8**, CPC25274, MC803, x2. **9-10**, CPC25275, MC803, tilted and normal apertural view, x3. ***Peruvispira imbricata* Waterhouse, 1963. 11**, Latex of New Zealand Geological Survey No. GS 12641 from Tramway Sandstone, x4. ***Mourlonia (Mourlonia) strzeleckiana* (Morris), 1845. 12**, New Zealand Geological Survey TM3877, macrofossil locality GS9477, in loose boulder along road to French Pass, 0.5 miles southwest of roadman's hut and 4.5 miles north of saddle at trig. LXIXA above Croisilles Harbour, latex, x2. **13**, CPC25269, figured specimen A, latex, UDC1, x1. **14-15**, CPC25270, figured specimen B, latex side and tilted top view, UDC1, x2. **16**, CPC25271, figured specimen C, latex side view, UDC1, x2. **17**, CPC25272, figured specimen D, latex, UDC1, x2. **18**, CPC25273, figured specimen E, latex, UDC1, x2. ***Discotomaria?* sp. 19**, CPC25279, latex, UDC1, x4.

are internal impressions as, apparently, was the original specimen described by Morris (1845). The internal of the Bowen species, however, seems similar in shape, and Fletcher indicated that the small portions of shell preserved had spiral ribbing above and below the selenizone. The apical angles of Fletcher's shells are similar, but perhaps the spire was slightly higher in the New South Wales specimens, as the Queensland shells seem slightly wider than high, although they vary considerably. The specimens differ considerably from *?Neoplatyteichum numerosum* (Waterhouse, in Waterhouse & Jell, 1983, p. 253, pl. 6, figs 19–21), apparently from the lower part of the Blenheim Group (see earlier discussion on this). *?N. numerosum* apparently has different dimensions and spiral lirae on the selenizone. In Waterhouse's plate caption, the species is said to be from the Glendoo Sandstone, but, from the locality given in the text and Table 7, and by implication from Table 6, this is apparently incorrect. Fletcher recorded *M. (M.) strzeleckiana* from Gerringong, Rylstone, and Glendon, where it is associated with Fauna IV.

Note on *?Mourlonia impressa* Waterhouse 1966

The identification and relation of the species from the Croisilles Volcanics, Eastern Nelson, South Island, New Zealand, are of particular interest because they afford evidence on the age of these volcanics. Waterhouse compared *?M. impressa* to a species from the Callytharra Formation of the Carnarvon Basin, Western Australia, and concluded the Croisilles Volcanics were Lower Permian. He also compared it to much younger specimens from the Clermont area of the Bowen Basin.

A latex cast of Waterhouse's holotype (1966, p. 178, pl. 1, figs 1–3), is figured here (Pl. 2, fig. 11). *?Mourlonia impressa* appears to resemble *M. (M.) strzeleckiana*, with which it may be conspecific, more closely than *M. (M.)* sp. nov. Dickins (1963, pl. 23, figs 18–21). In *M. (M.)* sp. nov., the width of the whorls is considerably less and the selenizone is relatively wider. The whorls also expand in size at a faster rate. The ornament of *?M. impressa* is poorly preserved, but it appears to be similar to that of *M. (M.) strzeleckiana*. I have little doubt of the close relationship of *?M. impressa* with the specimens of *M. (M.) strzeleckiana* described here, and possibly also with the specimen mentioned by Waterhouse from Clermont. On this basis, the Croisilles Volcanics appear to be no older than Late Permian (see also Dickins & others, 1986).

Genus ***Peruvispira*** Chronic 1949 (p. 146)

Type species (by original designation). *Peruvispira delicata* Chronic (1949, p. 147) *in* Newell & others (1953, p. 139, pl. 28, figs 9–12).

Synonym. *Pleurocinctosa* Fletcher 1958 (p. 137)

Discussion. The reasons given by Waterhouse (in Waterhouse & Jell, 1983) for the resurrection of the generic name *Pleurocinctosa* are puzzling. *Pleurotomaria trifilata* Dana (1847), the type species of *Pleurocinctosa*, is said to differ from *Peruvispira delicata*, the type species of *Peruvispira*, by having a convex upper whorl cross-section, but Chronic's photographs of *P. delicata* show a convex whorl cross-section. Even if the whorl cross-section did differ as stated, this would not necessarily be a basis for generic differentiation. Waterhouse stated that *P. trifilata* also differs in having (apparently) a carina on the upper whorl. Such a carina is not described by Fletcher, and I have not seen it in specimens I have examined. This carina is not apparent in Waterhouse's figured specimen (in Waterhouse & Jell, 1983, Pl. 6, fig. 18), which is barely recognisable. On the basis of the evidence considered, there seems no justification for the use of the name *Pleurocinctosa*.

Peruvispira cf. ***modesta*** Waterhouse 1963
(p. 608, figs 26, 28–30, and table 6)
Pl. 2, figs 7–10

Description. The upper whorl cross-section is slightly convex, and there is a moderate angle at the periphery where the selenizone (or slit-band) is situated. The angle in the cross-section is thus more acute than some described species and more rounded than others. Some variation occurs in the upper whorl cross-section, paralleling the specimens figured by Waterhouse from New Zealand. The selenizone is well marked by a carina on either side and, underneath, has a distinct concave area bounded below by a third carina. The parallel growth ornament varies from faint to distinct.

Dimensions (mm).

	Height	*Width*	*Pleural angle*
MC 803	12	10	54°
Black Alley Shale	4	3	50°
Black Alley Shale	5	6	48°

Occurrence. CPC25274–25275, MC803, CPC25276, Black Alley Shale.

Discussion. Except perhaps for the pleural angle, the specimens from the Bowen Basin are close to *P. modesta* from the Stephens Formation, near Nelson, north South Island, New Zealand. The difference in pleural angle is small. Waterhouse (1963) records two specimens with an angle of 53° and another with 45°. The variation in parallel ornament may be due to preservation.

Peruvispira imbricata Waterhouse 1963
(p. 513, figs 1, 16–23, 39, and table 3)
Pl. 2, fig. 11

Description. Whorl cross-section very angular with the upper whorl surface concave. The selenizone is well marked and at an angle to the columella. The growth ornament is distinct.

Dimensions (mm).

Height	*Width*	*Pleural angle*
11 (approx)	9	40°

Occurrence. Latex cast made from GS 12641; loose slab at first ford across United Creek on track to smelter from Roding River; Tramway Sandstone.

Discussion. The specimen can be referred with little doubt to *P. imbricata*, which so far has been described from the Letham and Mangarewa Formations. The occurrence of the species in the Tramway Sandstone is, therefore, of considerable interest in correlation between the northern and southern parts of South Island, New Zealand. Specimens belonging to, or closely related to, *P. imbricata* also occur in the Peawaddy Formation of the Bowen Basin. Thus, in both New Zealand and the Bowen Basin there is a parallel occurrence of specimens related to *P.imbricata*, lower in the sequence (in the Letham, Mangarewa and Tramway Formations) and in the lower part of the Blenheim Subgroup, i.e. the lower part of the sequence with Fauna IV and the occurrence of *P. modesta* forms higher in the Blenheim Subgroup and higher in the sequence in New Zealand (Stephens Formation).

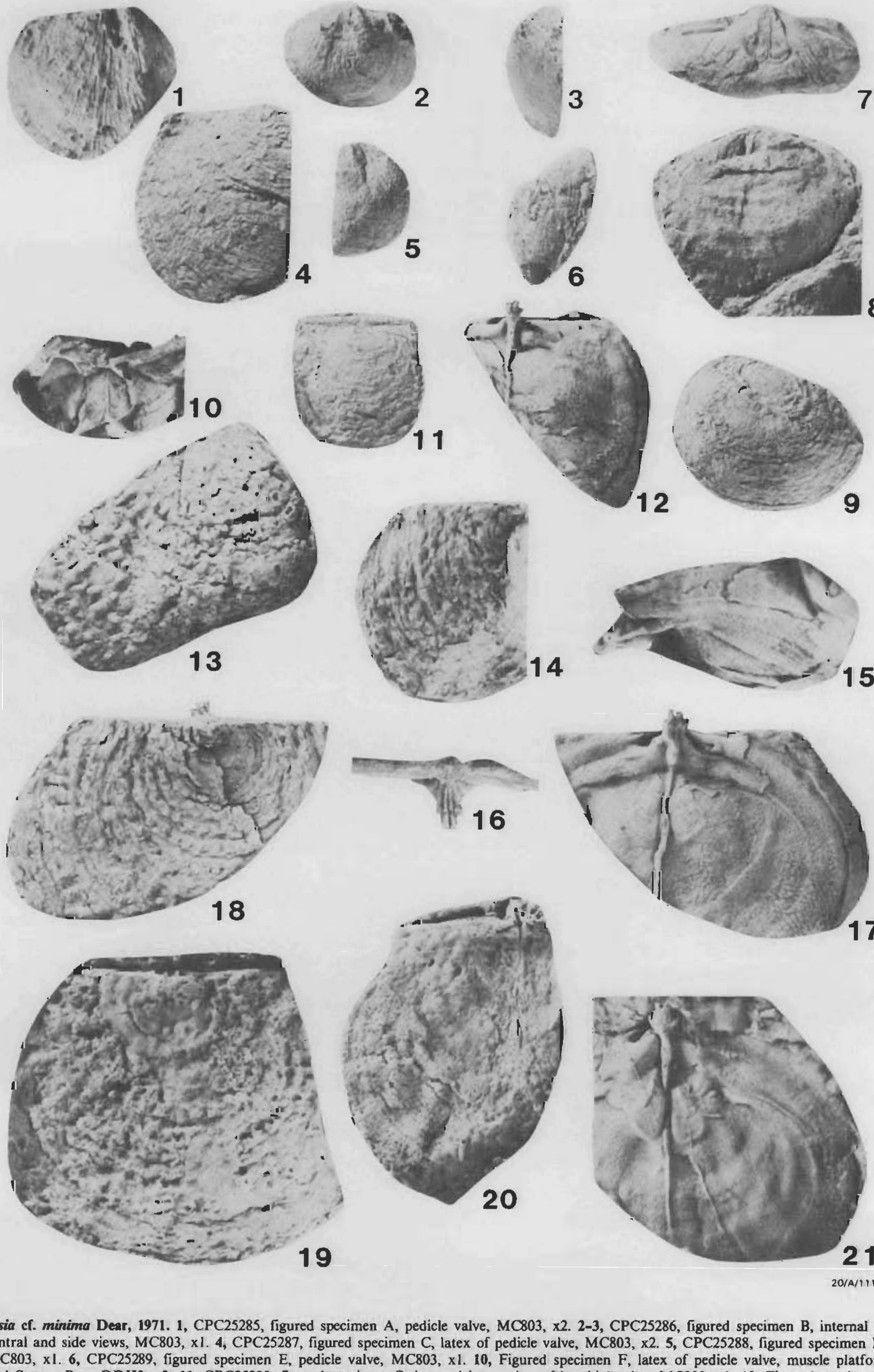

Plate 3.

***Echinalosia* cf. *minima* Dear, 1971. 1,** CPC25285, figured specimen A, pedicle valve, MC803, x2. **2-3,** CPC25286, figured specimen B, internal of pedicle valve, ventral and side views, MC803, x1. **4,** CPC25287, figured specimen C, latex of pedicle valve, MC803, x2. **5,** CPC25288, figured specimen D, pedicle valve, MC803, x1. **6,** CPC25289, figured specimen E, pedicle valve, MC803, x1. **10,** Figured specimen F, latex of pedicle valve, muscle platform, NSW Geological Survey Bore DDH3, x2. **11,** CPC25290, figured specimen G, internal impression of brachial valve, MC803, x1. **12,** Figured specimen H, latex of inside of brachial valve, NSW Geological Survey Bore DDH3, x2. **13,** Figured specimen I, latex of pedicle valve, NSW Geological Survey Bore DDH3, x2. **14,** Figured specimen J, latex of outside of brachial valve, NSW Geological Survey Bore DDH3, x2. **15-18,** Figured specimen K, latex of brachial valve, side, posterior, inside and outside views, NSW Geological Survey Bore DDH3, x2. **19,** Figured specimen L, latex of outside of brachial valve, NSW Bore DDH3, x2. **20,** Figured specimen M, latex of outside of brachial valve, NSW Geological Survey Bore DDH3, x2. **21,** Figured specimen N, latex of inside of brachial valve, NSW Geological Survey Bore DDH3, x2. ***Echinalosia* cf. *ovalis* (Maxwell), 1954. 7,** Figured specimen B, internal of pedicle valve, NSW Geological Survey F15009, Bore DM Camden 75, x1. **8,** Figured specimen C, internal of pedicle valve, NSW Geological Survey F15010, Bore DM Camden 75, x1. **9,** Figured specimen A, internal of brachial valve, NSW Geological Survey F15006, Bore DM Camden 75, x1.

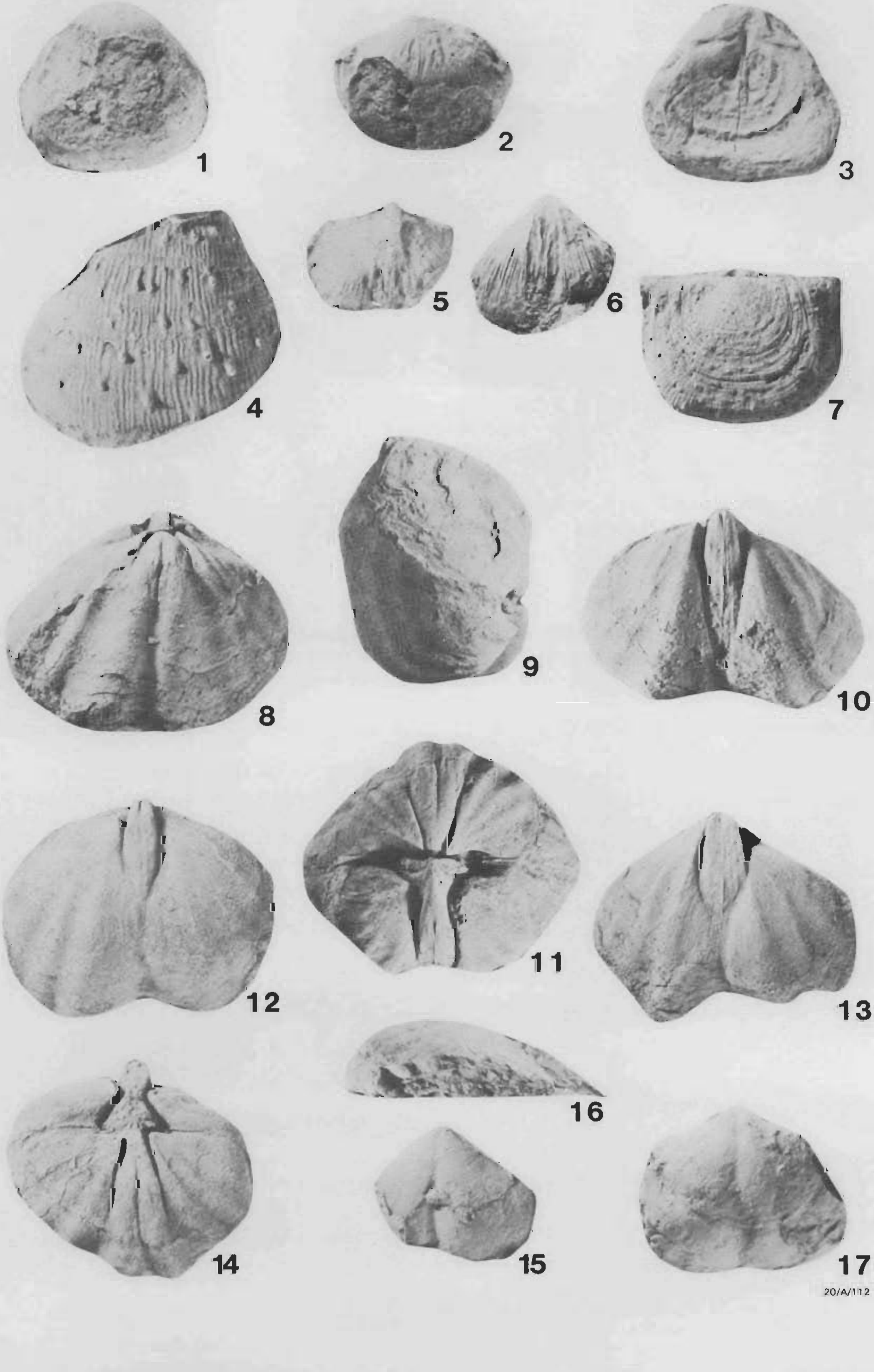

Plate 4.

***Terrakea solida* (Etheridge Jnr & Dun), 1909. 1-3,** CPC25280, figured specimen A, pedicle valve, pedicle valve tilted and brachial valve, MC803, x1. **4,** CPC25281, figured specimen B, ornament of pedicle valve, MC803, x2. **5,** CPC25282, figured specimen C, internal of pedicle valve, MC803, x1. **6,** CPC25284, figured specimen E, internal of pedicle valve, MC803, x1. 7, CPC25283, figured specimen D, internal impression of brachial valve, MC803, x1. ***Martiniopsis havilensis* (Campbell), 1968. 8-11,** CPC25291, figured specimen A, dorsal side, ventral and posterior views, Tay Glen Crossing, x1. **12,** CPC25292, figured specimen C, pedicle valve, Tay Glen Crossing, x1. **13,** CPC25293, figured specimen C, pedicle valve, Tay Glen Crossing, x1. **14,** CPC25294, figured specimen D, brachial valve, Tay Glen Crossing x1. **15,** CPC25295, figured specimen E, Black Alley Shale type section, pedicle valve, x1. **16-17,** CPC25296, figured specimen F, pedicle valve, side and tilted ventral view of pedicle valve, UDC2, x1.

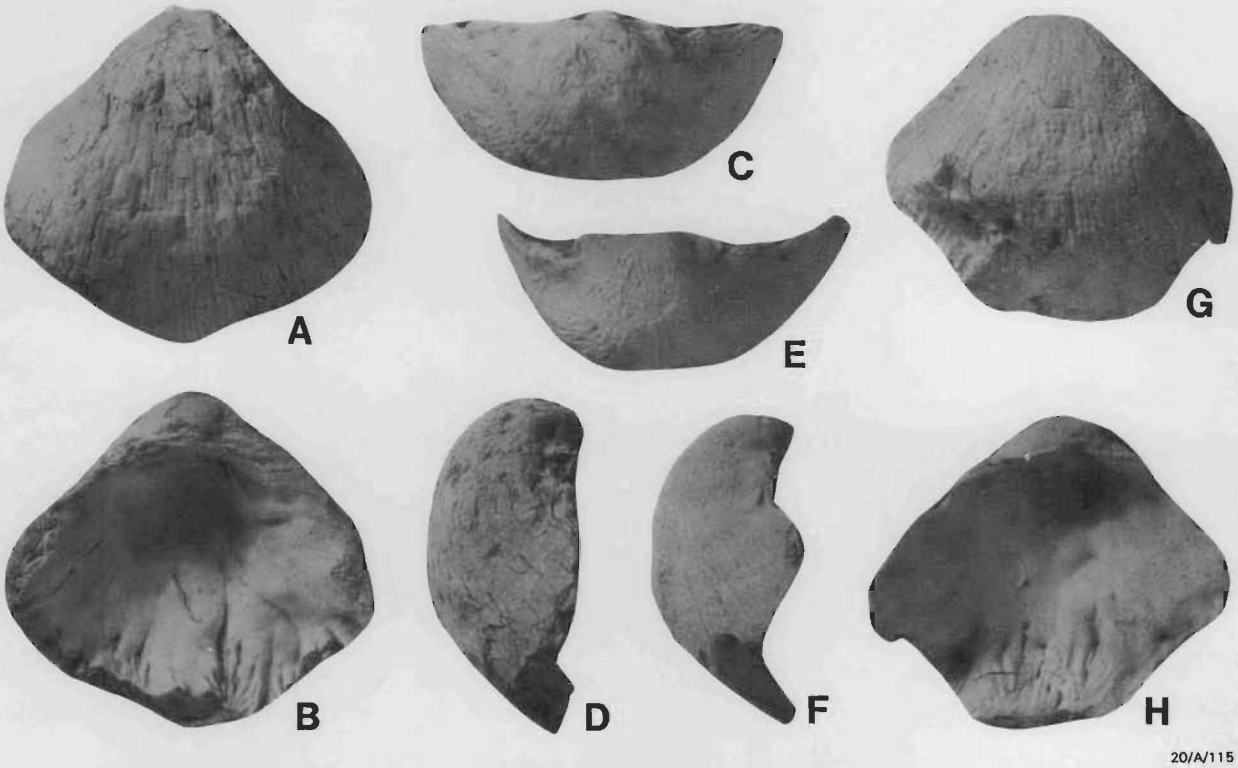

Figure 4. ***Terrakea solida*** **(Etheridge Jnr & Dun) 1909. A–D,Lectotype, Australian Museum No. F.35782, dorsal, ventral, posterior and side views x2; E–H, Australian Museum No. F.35478, posterior, side, dorsal and ventral views x2. Both specimens from Darr (?Don) River.**

Superfamily **Bellerophontacea** McCoy 1851

Discussion. The present material throws no light on whether the bellerophontids (in the broad sense) are gastropods or monoplacophorans (see Yochelson, 1967). However, their structure leads me to include them in this paper in the gastropods.

Family **Sinuitidae** Dall 1913
Genus ***Warthia*** Waagen 1880 (p. 13)

Type species (by subsequent designation of de Koninck, 1882, p. 81): *Warthia brevisinuata* Waagen (1880, p. 161, pl. 15, figs 6a–g).

Warthia perspecta Fletcher 1958
p. 149, pl. 15, figs 3–10)
Pl. 2, figs 1–6

Type. Specimen figured by Dana (1849, pl. X, figs 6, 6a); plaster replica figured by Fletcher (1958, pl. 15, figs 9, 10) from Gerringong Volcanics of the Illawarra District, South Coast, Sydney Basin, New South Wales.

Description. The material is made up mainly of internal impressions, in which the umbilicus is rather narrow. The outer whorl surface is evenly rounded. The shell is moderately wide, and increase in size is gradual.

Dimensions (mm).

	Lengthwise diameter	*Cross diameter*	*Width of aperture*	*Height of aperture*	*Axial width*
Figured specimen A	28	26	22	—	19
Figured specimen B	23	20	15	8	16

Occurrence. CPC25277 and CPC25278, MC803

Discussion. Species differentiation of *Warthia* is mainly based on the dimensions, a characteristic rather limited in scope. There seems no basis for separating our specimens from *W. perspecta*, which occurs in rocks of similar age in New South Wales.

Family **Phymatopleuridae** Batten 1956
Genus ***Discotomaria*** Batten 1956

Type species (by original designation). *Discotomaria basisulcata* Batten (1956, p. 43).

Discotomaria? sp.
Pl. 2, fig. 19

Description. A single rather incomplete specimen shows a low spine with a distinct keel. The upper whorl surface has a distinct carina which has prominent nodes associated with it. Faint spiral ornament can be seen.

Discussion. Unfortunately, this interesting shell is too incomplete to be sure of its affinities. Probably a selenizone is associated with the peripheral keel.

Brachiopods
Superfamily **Productacea** Gray 1840
Family **Linoproductidae** Stehli 1954
Genus ***Terrakea*** Booker 1930 (p. 66)

Type species (by original designation). *Productus brachythaerus* Morris 1845 (p. 284, pl. 14, fig. 40).

Terrakea solida (Etheridge Jnr & Dun) 1909 (pp. 303–304, pl. 43, figs 1–4). Pl. 4, figs 1–7

Lectotype F35478 Australian Museum, Sydney, the specimen figured by Etheridge Jnr & Dunn (1909, pl. 43, figs 1 & 2) designated by Dear (1971, p. 20). The lectotype designated by Dear is figured here (Australian Museum No. F.35782) with an accompanying specimen from the same locality, Darr River, (Australian Museum No. F35478). I have no reason to disagree with Dear's conclusion that the specimens came from the Mantuan *Productus* bed, although they could equally well have come from the east side of the basin, for example from the Oxtrack Formation. I am also not sure that the lectotype can be readily distinguished from other species from the Bowen Basin, such as *Terrakea elongata* Booker of Dear (1971, p. 16).

Description. Shell of moderate size and only moderately geniculate, not particularly elongate. Spines fairly sparse and of moderate size, smaller in younger parts of shell. Ornament consists of spines, radial capillae and growth lines. The interior of the pedicle valve had heavily thickened posterior walls.

Dimensions (mm).

	Width	*Length*	*Height*
Figured specimen A:		28	20 (approx.)
brachial valve	36		
pedicle valve	36	38	20 (approx.)
Figured specimen C:			11
pedicle valve	29		
Figured specimen D:		29	13
brachial valve	40		

Occurrence. Figured specimens A–E, CPC25280–25284, MC803.

Discussion. In shape, ornament and nature of spines, these specimens seem to conform to *Terrakea solida*.

Superfamily **Strophalosiacea** Schuchert 1913
Family **Strophalosiidae** Schuchert 1913
Genus ***Echinalosia*** Waterhouse 1967 (p. 167).

The type species and generic relationships are discussed in Dickins (1981, p. 30).

Echinalosia cf. ***minima*** Dear 1971 (p. 17, pl. 3, figs 11–16) Pl. 3, figs 1–6, 10–21

Description. A number of incomplete specimens. Pedicle valve rather convex and not particularly wide. Apparently originally with numerous spines, the brachial valve is concave and has a number of spines apparently arranged rather irregularly. Adductor muscles lacking a distinct platform.

Dimensions (mm).

	Width	*Length*
Brachial valve (DDH3)	36	29
Figured specimen L Brachial valve (DDH3)	36	28

Occurrence. Figured specimens A–G, CPC25285–25290, MC803 and DDN3.

Discussion. Separating species of strophalosiids in the Blenheim Subgroup presents considerable difficulties (Dickins, 1969b, p. 89). In examining large numbers of specimens, I commented on the difficulty of separating the species *clarkei*, *clarkei* var. *minima* (later separated by Dear, 1971, as a species of *Echinalosia*), *ovalis*, and *brittoni* var. *gattoni* (later transferred by Dear, 1971, to *Wyndhamia clarkei gattoni* subsp. nov.). Waterhouse (in Waterhouse & Jell, 1983) complicated the picture by assigning *Wyndhamia blakei* to the synonymy of *W. ingelarenis* Dear 1971 and claiming that *Echinalosia ovalis* Maxwell 1954 is confined to a single limited horizon in the Blenheim Subgroup. The holotype of *W. blakei* is narrow, especially at the umbonal (posterior) end, which is characteristic of many specimens from the basal part of the Blenheim Subgroup. The specimens of this type have been referred by Dear (1971) to *Wyndhamia blakei* and *Echinalosia minima gattoni* subsp. nov. The type of *W. ingelarensis* is quite different, having a relatively wider, less convex pedicle valve. The consistency of these differences is confirmed by the specimens I have examined. I consider *E. ovalis* is quite long ranging, from the base of the Blenheim Subgroup and possibly through Fauna IV, as concluded by Maxwell (1954), Dear (1971) and McClung (1978).

The specimens assigned to *E.* cf. *minima* are those from MC 803 and from bore DDH3 Stockton 3 (413.80) in the Sydney Basin. The specimens from MC 803 are similar in shape to *E. ovalis*, but lack the muscle platform. Those from the Sydney Basin are somewhat broader, but also lack the distinct muscle platform of *E. ovalis*.

Echinalosia cf. ***ovalis*** (Maxwell) 1954 (p. 548, pl. 57, figs 4-14) Pl. 3, figs 7–9

Description. 3 specimens in which the valves are moderately wide, with numerous spines on the pedicle valve and scattered spines on the brachial valve. The adductor muscles are lodged on a distinct platform and differ considerably in length in the two pedicle valves.

Dimensions (mm).

	Width	*Length*	*Height*
Figured specimen A: brachial valve (F15006)	38	30	8
Figured specimen B: pedicle valve (F15009)	40	40	—
Figured specimen C: pedicle valve (F15010)	34	38	—

Occurrence. Bore DM Camden 75, 2880–2890 ft.

Discussion. The specimens are compared with *E. ovalis* because of the dimensions, the nature of the ornament, and the distinct adductor muscle platform.

Superfamily **Reticularinacea** Waagen 1883
Family **Martiniidae** Waagen 1883
Genus ***Martiniopsis*** Waagen 1883

Type species (by subsequent designation of Hall & Clarke, 1894 — fide Brown, 1953, p. 103). *Martiniopsis inflata* Waagen (1883, p. 525, pl. 41, figs 7, 8), from the Upper Productus Limestone (Chhidru Formation) of Chhidru, Salt Range, Pakistan.

Discussion. The difficulties of generic names for this group of forms have been outlined in Dickins (1981, p. 30). N.W. Archbold (personal communication) favours the retention of *Ingelarella* for forms with low C-shaped protuberances at the posterior end of elongate, narrow, shallow grooves

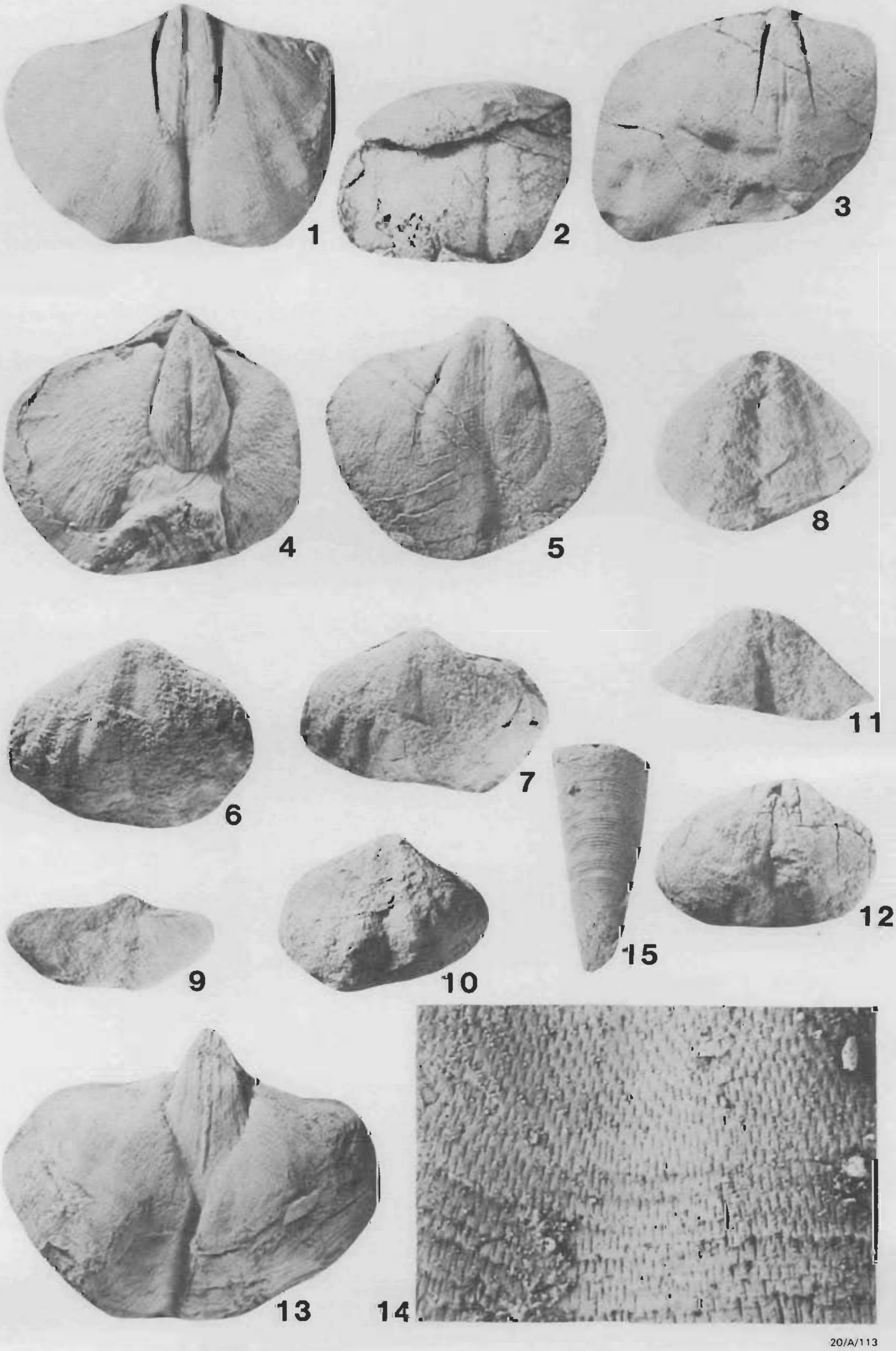

Plate 5.

***Martiniopsis havilensis* (Campbell), 1960. 1,** CPC25298, figured specimen I, pedicle valve, MC803, x1. **2,** CPC25300, figured specimen K, latex of pedicle valve, MC803, x1.5. **3,** CPC25297, figured specimen H, internal of brachial valve, UDC2, x1. **4,** CPC25296, figured specimen G, internal of pedicle valve, UDC2, x1. **5,** CPC25299, figured specimen J, internal of pedicle valve, MC803, x1. **6–7,** CPC25302, figured specimen M, pedicle valve and tilted pedicle valve, MC292, x1. **8–10,** CPC25303, figured specimen N, pedicle valve, posterior view and tilted pedicle valve, MC292, x1. **11,** CPC25301, figured specimen L, pedicle valve, MC292, x1. **12,** CPC25305, figured specimen P, pedicle valve, B1572, x2. **13,** CPC25304, figured specimen O, internal of pedicle valve, B1572, x2. **14,** CPC25306, figured specimen Q, latex showing external ornament of brachial valve, MC803, x12. ***Conulariid* indet. 15,** CPC25307, latex, x4.

arranged in quincunx. The micro-ornament of *M. inflata* is still not known in detail. In many specimens the micro-ornament is not preserved, and a classification based on it may present more difficulty than a broader scheme. The specimens described below are placed in *Martiniopsis* because they lack a well-developed fold and sulcus. Shallow grooves arranged in quincunx are present, but no C-shaped protuberances.

Martiniopsis havilensis (Campbell), 1960
(p. 1120, pl. 139, figs 3-6)
Pl. 4, figs 8-7; Pl. 5, figs 1-14

Description. The shells assigned to this species are distinguished by a relatively wide shallow sulcus containing a narrow groove, although this is variably developed in specimens from the same locality. The fold is also relatively broad and has a corresponding groove in the fold. Young shells are wider than long, but older shells vary from being almost smooth to having distinctly marked plicae. The original specimens were described as smooth, but the specimens figured here from the type locality (Pl. 5, figs 12, 13) show low but distinct plicae. Older specimens are thickened at the umbo, and the adminicula vary considerably in length and shape. In the brachial valve they are rounded, divergent, and reasonably long. The micro-ornament comprises elongated shallow grooves arranged in quincunx, slightly wider towards the umbonal end. No C-shaped protuberances are visible (Pl. 5, fig. 14).

Dimensions (mm).

		Length	*Height*	*Width*
Figured specimen A	Brachial valve	40	52	28
(Tay Glen Crossing)	Pedicle valve	49	53	24
Figured specimen B (Tay Glen Crossing)	Pedicle valve	40	52	17
Figured specimen C (Tay Glen Crossing)	Pedicle valve	35	50	20
Figured specimen D (Tay Glen Crossing)	Brachial valve	33	47	22
Figured specimen F (UDC2)	Pedicle valve	40	45 (approx.)	19
Figured specimen G (UDC2)	Pedicle valve	50 (approx.)	60 (approx.)	20
Figured specimen I (MC 803)	Pedicle valve	50	63	20
Figured specimen J (MC 803)	Pedicle valve	48	51	12
Figured specimen M (MC 292)	Pedicle valve	41	50	12
Figured specimen N (MC 292)	Pedicle valve	34	41	12
Figured specimen O	Brachial valve	50	68	19
(B 1572)	Pedicle valve	55	68	22
Figured specimen P (B 1572)	Pedicle valve	35	42	16

Occurrence. Figured specimens A–P (as above), CPC25291–25305, Figured specimen Q, CPC25306, MC803, Tay Glen, UDC 2, MC 803, MC292, B1572 and base of Black Alley Shale.

Discussion. *Martiniopsis havilensis* is widespread in the upper part of the Blenheim Subgroup. Its occurrence in the Black Alley Shale (type section) and at MC 292 is particularly significant. The occurrence in the Black Alley Shale indicates an important hiatus between the Peawaddy Formation and the Black Alley Shale. The evidence of *M. havilensis* is corroborated by the occurrence of *Peruvispira* cf. *modesta* at the same locality. The occurrence at MC 292 is important because this locality is in the Exmoor Formation and, therefore, suggests correlation with the MacMillan Formation and the Black Alley Shale.

At some localities the species is represented by numerous specimens, as at Tay Glen Crossing (CL 21/5) and MC 292 where other faunal elements are poorly represented.

Some ventral valves with a relatively poorly developed sulcus resemble *Martiniopsis woodi* Waterhouse (1964, p. 148, pl. 30, figs 3-5, 8, pl. 37, figs 2, 3 and figs 71, 72, A,B) from the Arthurton Group of the Southland syncline, New Zealand.

Conulariid Indet.
Pl. 5, fig. 15

Description. Two faces and the furrow between are shown by a single specimen. The transverse ribs are evenly arcuate and lack a mid-longitudinal bar. The transverse grooves are closely spaced. The relations of the ribs in the furrow are obscure.

Discussion. The characters of the specimen appear to be somewhat unusual. At first it was considered likely to be *Calloconularia* Sinclair (1952, p. 140), but it is possible that the specimen is not referrable to any described genus.

Occurrence. CPC25307, UDC 1.

Localities from the Bowen Basin

B 1572 — Bowen 1:250 000 Sheet area; 20°47′15″S, 147°44′45″E; upper part of Blenheim Subgroup.
CL 21/5 — Clermont 1:250 000 Sheet area (BMR Report No. 66); crossing of Phillips Creek immediately north of Tay Glen Homestead. Also specimens without number referred to as Tay Glen Crossing; upper part of Blenheim Subgroup.
MC 292 — Mount Coolon 1:250 000 Sheet area; Collinsville Road crossing of Blenheim Creek; Exmoor Formation.
MC 803 — Mount Coolon 1:250 000 Sheet area; 4 km north-northwest of Blenheim Homestead; upper part of Blenheim Subgroup.
UDC (Utah Development Co.) 1 — Duaringa 1:250 000 Sheet area (BMR Report No. 121); on fence about 4 km northeast of Lyra Park Homestead; MacMillan Formation.
UDC 2 — Duaringa 1:250 000 Sheet area (BMR Report No. 121); Cattle Creek, 8 km northwest of Mount Stuart Homestead; MacMillan Formation.
Black Alley Shale — Springsure 1:250 000 Sheet area; about 2 m above base of type section, in the main west branch of Dry Creek, about 3 km southeast of Black Alley Peak.

Localities of New South Wales Bore Holes
DDH3 Stockton 3
Newscastle 1:250 000, ISG Metric

	371614.7 E
	136476.3 N
Newcastle 50 000	9232 II
DM Camden 75	
Wollongong 1:250 000	ISG Metric
	298629.2 E
	1226333.1 N
Wollongong 50 000	9029 I

Acknowledgements

Important specimens were supplied by Utah Development and by the Geological Survey of New South Wales. I thank the Director of the Survey for access to the latter specimens and I am particularly grateful to Viera Scheibnerova who organised the loan and supplied information. Many colleagues in BMR and the Geological Survey of Queensland were involved in the collection of specimens and stratigraphic work, and their participation is acknowledged. D.J. Belford helped put together the report. Photography was by R.W. Brown and H.M. Doyle, and the drawings of fossils, by J. Mifsud. Typing and secretarial work were done by Beryl Marshall and Pushpa Nambiar.

References

Batten, R.L., 1956 — Some new pleurotomarian gastropods from the Permian of west Texas. *Journal of the Washington Academy of Sciences*, 46(2), 42–44.

Beede, J.W., & Rogers, A.E., 1899 — New and little known pelecypods from the coal measures. *Kansas University Quarterly*, 8, 31–134.

Beyrich, E., 1864 — Uber eine Kohlenkalk fauna von Timor. *Abhandlungen Akademie Wissenschaften Berlin*, 61–98.

Booker, F.W., 1930 — A review of some of the Permo-Carboniferous Productidae of New South Wales with a tentative reclassification. *Journal and Proceedings of the Royal Society of New South Wales*, 64, 65–77.

Bradshaw, J.D., & Bradshaw, M.A., 1971 — Functional morphology of some fossil palaeotaxodont bivale hinges as a guide to orientation. *Palaeontology*, 14(2), 242–249.

Brown, I.A., 1953 — *Martiniopsis* Waagen from the Salt Range, India. *Journal and Proceedings of the Royal Society of New South Wales*, 86, 100–107.

Browne, I.A., & Newell, N.D., 1966 — The genus *Aphanaia* Koninck, 1877, a Permian representative of the Inoceramidae. *American Museum Novitates*, 2252.

Campbell, K.S.W., 1959 — The *Martiniopsis*-like Spiriferids of the Queensland Permian. *Palaeontology*, 1(4), 333–350.

Campbell, K.S.W., 1960 — The brachiopod genera *Ingelarella* and *Notospirifer* in the Permian of Queensland. *Journal of Paleontology*, 34(6), 1106–1123.

Campbell, K.S.W., 1961 — New species of the Permian spiriferoids *Ingelarella* and *Notospirifer* from Queensland and their stratigraphic implications. *Palaeontographica*, Band 117, Abt A, 159–192.

Chronic, J., 1949 — *In* Newell, N.D., Chronic, J., & Roberts, T.G., — Upper Palaeozoic of Peru. Columbia University, New York, (reprinted 1953 as Memoir of the Geological Society of America, 58).

Dana, J.D., 1849 — Fossils of New South Wales. *In* United States exploring expedition during the years 1838-42 under the command of Charles Wilkes, U.S.N., Vol. 10, Geology, 681–713.

David, T.W.E., & Browne, W.R., 1950 — The geology of the Commonwealth of Australia, 1. *Edward Arnold & Co., London.*

Dear, J.F., 1971 — Strophomenid brachiopods from the higher Permian faunas of the Back Creek Group in the Bowen Basin. *Geological Survey of Queensland, Publication* 347, *Palaeontological Papers*, 21.

Dear, J.F., 1972 — Preliminary biostratigraphic subdivision of the Permian fauna in the northern Bowen Basin and their distribution throughout the basin. *Geological Survey of Queensland, Report* 49.

de Koninck, L.G., 1882 — Notice sur la famille des Bellerophontidae suivie de la déscription d'un nouveau genre de cette famille. Annales *Societe géologique de Belgique*, 9, 72–90.

de Koninck, L.G., 1883 — Faune du calcaire carbonifere de la Belgique, 4e partie, Gastéropodes (suite et fin). *Annales du Musee royal d'histoire naturelle de Belgique, sér. paléont*, 8.

Dickins, J.M., 1956 — Permian pelecypods from the Carnarvon Basin, Western Australia. *Bureau of Mineral Resources, Australia, Bulletin* 29.

Dickins, J.M., 1961 — Permian pelecypods newly recorded from eastern Australia. *Palaeontology*, 4(1), 119–130.

Dickins, J.M., 1963 — Permian pelecypods and gastropods from Western Australia. *Bureau of Mineral Resources, Australia, Bulletin* 63.

Dickins, J.M., 1966 — Permian marine macrofossils from the Bowen and Mackay 1:250 000 Sheet areas. *In* Malone, E.J., Jensen, A.R., & Gregory, C.M., Geology of the southern half of the Bowen 1:250 000 Sheet area, Queensland. *Bureau of Mineral Resources, Australia, Report* 100, 68–87.

Dickins, J.M., 1969a — Permian marine macrofossils from the Duaringa and Saint Lawrence Sheet areas, Queensland. *In* Malone, E.J., Olgers, F., & Kirkegaard, A.G., The Geology of the Duaringa and Saint Lawrence 1:250 000 Sheet areas, Queensland. *Bureau of Mineral Resources, Report* 121, 96–117.

Dickins, J.M., 1969b — Permian marine macrofossils from the Springsure sheet area. *In* Mollan, R.G., Dickins, J.M., Exon, N.F., & Kirkegaard, A.G., The Geology of the Springsure 1:250 000 Sheet area, Queensland. *Bureau of Mineral Resources, Australia, Report* 121, 96–117.

Dickins, J.M., 1970 — Correlation and subdivision of the Permian of eastern and western Australia. *Bureau of Mineral Resources, Australia, Bulletin* 116, 17–27 (also *Report of Twenty-second International Geological Congress, New Delhi, 1964*, part 8, 39–49).

Dickins, J.M., 1972 — Permian marine macrofossils from the Munduberra and Monto Sheet areas. *In* Mollan, R.G., Forbes, V.R., Jensen, A.R., Exon, N.F., & Gregory, C.M., Geology of the Eddystone, Taroom, and western part of the Munduberra Sheet areas, Queensland. *Bureau of Mineral Resources, Australia, Report* 142, 106–120.

Dickins, J.M., 1981 — A Permian invertebrate fauna from the Warwick area. *In* Palaeontological Papers, 1981. *Bureau of Mineral Resources, Australia, Bulletin*, 209, 23–43.

Dickins, J.M., 1983 — The Permian Blenheim Subgroup of the Bowen Basin and its time relationships. *Proceedings of the symposium on the Permian Geology of Queensland*, 269–274. *Geological Society of Australia, Queensland Division, Brisbane.*

Dickins, J.M.; Archbold, N.W., & Thomas, G.A., in press — Correlation and age of the Western Australian marine faunas. *Geological Survey of Western Australia.*

Dickins, J.M., Archbold, N.W., Thomas, G.A., & Campbell, H.J., in press — Mid-Permian correlation. *Compte Rendu, 11th Carboniferous Congress, Beijing.*

Dickins, J.M., Johnston, M.R., Kimbrough, D.L., & Landis, C.A., 1986 — The stratigraphic and structural position and age of the Croisilles Melange, east Nelson, New Zealand. *New Zealand Journal of Geology and Geophysics*, 29, 291–301.

Dickins, J.M., & Malone, E.J., 1968 — Regional subdivision of the Back Creek Group (Middle Bowen Beds), Bowen Basin, Queensland. *Queensland Government Mining Journal*, 64(801), 292–301.

Dickins, J.M., & Malone, E.J., 1973 — Geology of the Bowen Basin, Queensland. *Bureau of Mineral Resources, Australia, Bulletin* 130.

Dickins, J.M., Malone, E.J., & Jensen, A.R., 1964 — Subdivision and correlation of the Permian Middle Bowen Beds, Queensland. *Bureau of Mineral Resources, Australia, Report*, 70.

Etheridge, R., Jnr., & Dun, W.S., 1909 — Notes on the Permo-Carboniferous Producti of eastern Australia, with synonymy. *Records of the Geological Survey of New South Wales*, 8, 293–304.

Fletcher, H.O., 1945 — A new genus *Glyptoleda* and a revision of the genus from the Permian of Australia. *Records of the Australian Museum*, 21(6), 293–312.

Fletcher, H.O., 1958 — The Permian gastropods of New South Wales. *Records of the Australian Museum*, 24(10), 115–164.

Grant, R.E., 1970 — Brachiopods from Permian-Triassic boundary beds and age of Chhidru Formation, West Pakistan. *In* Kummel, B., & Teichert, C., (editors), Stratigraphic boundary problems: Permian and Triassic of West Pakistan *University of Kansas, Department of Geology, Special Publication* 4, 117–151.

Jensen, A.R., Gregory, C.M., & Forbes, V.R., 1966 — Geology of the Mackay 1:250 000 Sheet area, Queensland. *Bureau of Mineral Resources, Australia, Report* 104.

Kauffman, E.G., & Runnegar, B., 1975 — *Atomodesma* (Bivalvia) and Permian species of the United States. *Journal of Paleontology*, 49(1), 23–51.

Koppe, W.H., 1978 — Review of the stratigraphy of the upper part of the Permian succession in the northern Bowen Basin. *Queensland Government Mining Journal*, 79, 35–45.

Lintz, J., Jnr, 1958 — The fauna of the Ames and Brush Creek Shales of the Conemaugh Formation of Western Maryland. *Journal of Palaeontology*, 32(1), 97–112.

McClung, G.R., 1978 — Morphology, palaeoecology and biostratigraphy of *Ingelarella* (Brachiopoda: Spiriferacea) in the Bowen and Sydney Basins of eastern Australia. *Geological Survey of Queensland Publication* 365, *Palaeontological Paper*, 40.

McClung, G.R., 1981 — Review of the stratigraphy of the Permian Back Creek Group in the Bowen Basin, Queensland. *Geological Survey of Queensland Publication* 371, *Palaeontological Paper*, 44.

McClung, G.R., 1983 — Faunal sequence and palaeoecology of the marine Permian in GSQ Eddystone 1, Denison Trough, Queensland. *Geological Survey of Queensland, Publication* 384, 43-80.

McMinn, A., 1985 — Palynostratigraphy of the Middle Permian coal sequences of the Sydney Basin. *Australian Journal of Earth Sciences*, 32(3), 301-309.

Malone, E.J., Jensen, A.R., Gregory, C.M., & Forbes, V.R., 1966 — Geology of the southern half of the Bowen 1:250 000 Sheet area, Queensland. *Bureau of Mineral Resources, Australia, Report* 100.

Malone, E.J., Olgers, F., & Kirkegaard, A.G., 1969 — The geology of the Duaringa and Saint Lawrence 1:250 000 sheet areas, Queensland. *Bureau of Mineral Resources, Australia, Report* 121.

Martini, I.P., & Johnson, D.P., 1987 — Cold-climate, fluvial to paralic coal-forming environments in the Permian Collinsville Coal Measures, Bowen Basin, Australia. *International Journal of Coal Geology*, 7(4), 365-388.

Maxwell, W.G.H., 1954 — *Strophalosia* in the Permian of Queensland. *Journal of Paleontology*, 28(5), 553-559.

Maxwell, W.G.H., 1964 — The geology of the Yarrol region, part 1. Biostratigraphy. *University of Queensland Papers, Department of Geology*, 5(9).

Mollan, R.G., Dickins, J.M., Exon, N.F., & Kirkegaard, A.G., 1969 — Geology of the Springsure 1:250 000 Sheet area, Queensland. *Bureau of Mineral Resources, Australia, Report* 123.

Morris, J., 1845 — Description of fossils. *In* Strzelecki, P. E. de, Physical description of New South Wales and Van Diemen's Land. *London*, 270-291.

Muromtseva, V.A., 1981 — Bivalved Mollusca. *In* Permian Deposits of Nova Zemla. *Academy of Sciences of the USSR, Komi Filial, Institute of Geology, Science, Leningrad*, 26-51.

Muromtseva, V.A., 1984. Permian marine deposits and bivalved molluscs of the Soviet Arctic. *Allunion Oil Scientific Investigation Geological Research Institute, Trudy.*

Newell, N.D., Chronic, B.J., & Roberts, T.G., 1949 — Upper Paleozoic of Peru. *Columbia University, New York*, (reprinted 1953 as *Memoir of the Geological Society of America*, 58).

Patte, E., 1926 — Études paléontologiques relatives à la géologie de l'est du Tonkin (Paléozoique et Trias). *Service géologique du Indo-Chine, Bulletin*, 15(1).

Puri, H.S., 1969 — Family Nuculanidae. *In* Treatise on Invertebrate Paleontology, Part N, 1, Mollusca 6, N235-N241.

Runnegar, B., & McClung, G.R., 1975 — A Permian time-scale for Gondwanaland. *In* Campbell, K.S.W., (editor), Gondwana geology. Papers presented at the Third Gondwana Symposium, Canberra, Australia, 1973. *Australian National University Press, Canberra*, 425-441.

Sinclair, G.W., 1952 — A classification of the Conularida. *Fieldiana Geology*, 10(13),135-145.

Sowerby, J., 1812 — The mineral conchology of Great Britain, 1. *London.*

Staines, H.R.E., & Koppe, W.H., 1979 — The geology of the North Bowen Basin. *Queensland Government Mining Journal*, 80 (930), 172-195.

Waagen, W., 1880 — Salt Range fossils, Part 2, Gastropods. *Palaeontologia Indica*, Series 13, 1, 86-183.

Waagen, W. 1883 — Salt Range fossils, Part 4(2), Brachiopods. *Palaeontologia Indica*, Series 13, 1, 391-546.

Wanner, C., 1922 — Die Gastropoden und Lamellibranchiaten der Dyas von Timor. *Palaontologie von Timor*, 11(18).

Waterhouse, J.B., 1963 — Permian Gastropods of New Zealand, Part 3 — Pleurotomariacea (concluded). *New Zealand Journal of Geology and Geophysics*, 6(4), 588-622.

Waterhouse, J.B., 1964 — Permian brachiopods of New Zealand. *New Zealand Geological Survey, Palaeontological Bulletin*, 35.

Waterhouse, J.B., 1965a — Palaeotaxodont bivalves from the Permian of New Zealand. *Palaeontology*, 7(4), 630-655.

Waterhouse, J.B., 1965b — Generic diagnoses for some burrowing bivalves of the Australian Permian. *Malacologia*, 3(3), 367-380.

Waterhouse, J.B., 1966 — The age of the Croisilles Volcanics, eastern Nelson. *Transactions of the Royal Society of New Zealand, Geology*, 3(13), 175-181.

Waterhouse, J.B., 1967 — Proposal of series and stages for the Permian in New Zealand. *Transactions of the Royal Society of New Zealand, Geology*, 5(6), 161-180.

Waterhouse, J.B., 1976 — World correlations for Permian marine faunas. *University of Queensland Papers, Department of Geology*, 7(2)

Waterhouse, J.B., 1979 — New members of the Atomodesminae (Bivalvia) from the Permian of Australia and New Zealand. *University of Queensland Papers, Department of Geology*, 9(1).

Waterhouse, J.B., & Jell, J.S., 1983 — The sequence of Permian rocks and faunas near Exmoor Homestead south of Collinsville, north Bowen Basin. *Proceedings of the symposium on the Permian geology of Queensland*, 231-267. *Geological Society of Australia, Queensland Division.*

Watson, R.A., 1983 — A critique of chronostratigraphy, *American Journal of Science*, 283(2), 173-177.

Yochelson, E.L., 1967 — Quo Vadis, *Bellerophon? In* Teichert, C., & Yochelson, E.L., (editors), Essays in paleontology and stratigraphy, R.C. Moore Commemorative Volume. *Department of Geology, University of Kansas, Special Publication*, 2, 141-161.

BMR Journal of Australian Geology & Geophysics, 11, 81-87

Probabilistic earthquake risk maps of Tasmania

Marion O. Michael-Leiba[1] & Brian A. Gaull[1]

New earthquake risk maps of Tasmania have been prepared depicting risk by contours of peak ground velocity, acceleration and intensity with a 10 per cent probability of being exceeded in a 50 year period. The Cornell-McGuire method was used. The maps are based on seismicity up to the end of 1984, including the events of the 1883-1892 earthquake swarm east of Flinders Island and other historical data. The earthquake process was assumed to be Poissonian, so foreshocks and aftershocks were eliminated from the analysis. For this earthquake risk assessment, average eastern Australian background seismicity and attenuation for average site conditions were used.
The earthquake source zones most affecting the risk in the Tasmanian region are the West Tasman Sea Zone and the Western Tasmanian Zone. The West Tasman Sea Zone, east of Flinders and Cape Barren Islands, appears to have been the site of the 1883-1892 swarm, with at least three intensity-deduced Richter magnitude 6.0-7.0 events. Consequently, the highest risk land areas are Flinders and Cape Barren Islands, which lie predominantly between the 60 $mm.s^{-1}/0.6$ $m.s^{-2}$ and 120 $mm.s^{-1}/1.2$ $m.s^{-2}$ contours, with the risk increasing to the east. In the Western Tasmanian Zone, the largest event recorded was in 1880. It had an intensity-deduced Richter magnitude of 5.5. The northern part of western Tasmania (enclosed by the 59 $mm.s^{-1}/0.55$ $m.s^{-2}$ contour) is the second highest risk region. At Hobart and Launceston, outside the source zones, the values are 23 $mm.s^{-1}/0.21$ $m.s^{-2}$ and 30 $mm.s^{-1}/0.29$ $m.s^{-2}$ respectively, corresponding to a 10 per cent chance of an intensity MMIV-V being exceeded in a 50-year period. However, it appears that site amplification of strong ground motion takes place in some parts of Launceston, and this should be considered when zoning for the Building Code. The chief contributions to uncertainty in the estimates of earthquake risk are uncertainties in early earthquake locations and magnitudes, and in strong ground motion attenuation.

Introduction

The first seismic risk map of Tasmania (Underwood, 1973) gave contours of intensity at a 10-year return period, based on 10.5 years of data. McCue (1978) contoured the return periods of peak ground velocities of 50 $mm.s^{-1}$ and 100 $mm.s^{-1}$ for the Tasmanian region. In the present zoning map for Australia (Standards Association of Australia, AS2121-1979 based on the studies of McEwin & others, 1976, and Denham, 1979) the Tasmanian mainland is rated Zone 0 and Flinders Island is Zone A. As the available Tasmanian earthquake data have increased considerably since this map was drawn, we considered it an appropriate time to prepare new maps, as part of the re-zoning of Australia.

In this study, we have produced probabilistic seismic risk maps of Tasmania for the area 39-44°S, 142-150°E, using the Cornell-McGuire methodology (Cornell, 1968; McGuire, 1976) as described by Basham & others (1985), and earthquake data from the BMR earthquake data file up to the end of 1984, Ripper (1963) and Michael-Leiba (1989, this issue).

The magnitudes of historic events from Michael-Leiba (1989, this issue) are designated MI. MI is an approximation to the Richter Magnitude, ML. It is determined (Michael-Leiba, 1989, this issue) by comparing the more reliable isoseismal radii, measured from an isoseismal map of the earthquake, with the average eastern Australian attenuation curves for various magnitudes (Gaull & others, in press).

Method

Seismic risk estimation using the Cornell-McGuire methodology requires the definition of:

1. earthquake source zones, each having its own magnitude-frequency recurrence relationship, mean focal depth, and maximum magnitude (which was chosen to be the maximum observed magnitude + 0.5, then rounded to the nearest 0.5 magnitude unit following Basham & others, 1985)
2. background seismicity, and
3. attenuation of strong ground motion.

Australian seismicity is assumed to be concentrated largely in a number of source zones, each having a uniform level of seismic activity within its boundaries. Seismicity outside source zones is taken into account as background seismicity, averaged over a large area. If the geographic location of each source zone and the characteristics of its seismicity are specified, then the earthquake risk at any point in Australia can be calculated, if the manner in which strong ground motion attenuates with distance from an earthquake is also known.

The McGuire (1976) computer program, as modified by Basham & others (1985), uses the attenuation and recurrence relations to integrate numerically contributions from the source zones to evaluate probabilities of exceeding different levels of ground motion at a site.

The earthquake process was assumed to be Poissonian, so foreshocks and aftershocks were not used in determining the magnitude-frequency recurrence relationship.

Earthquake source zones

Earthquake source zones (Fig. 1) were chosen primarily on the basis of the spatial distribution of magnitude ML>4.0 earthquakes. Only events for which epicentres have been reliably determined are shown in this figure. Although microearthquakes occur throughout the region with clusters of events sometimes being related to regional geology (Shirley, 1980), the larger earthquakes occur in two distinct areas: the Western Tasmanian Zone, and the West Tasman Sea Zone extending from east of Flinders and Cape Barren Islands into the Tasman Sea (Fig. 1). These, with the Southern Victorian Zone, the Lachlan Fold Belt Zone, and the 40°S Zone (East), were used as earthquake source zones for the earthquake risk analysis.

Western Tasmanian Zone (Table 1)

As instrumental magnitudes for this zone are available only from 1958, after the first station of the University of Tasmania seismic net became operational (Carey, 1960), felt reports (Michael-Leiba, 1989, this issue) were used to obtain data for earthquakes of magnitude MI≥5.0 since 1853.

[1]Australian Seismological Centre, Bureau of Mineral Resources, GPO Box 378, Canberra, ACT 2601

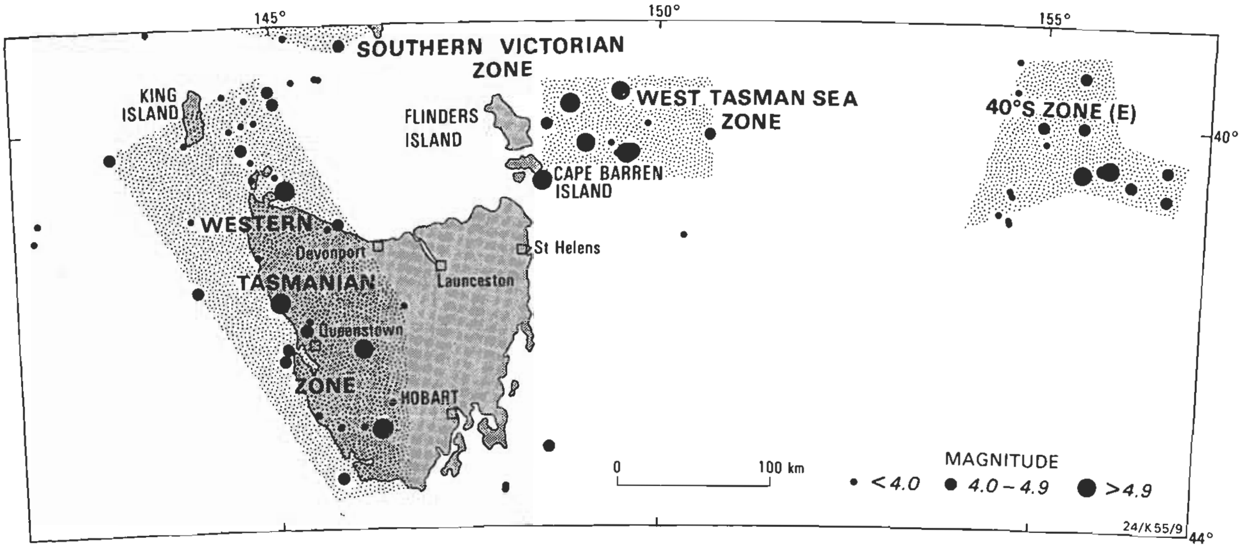

Figure 1. Earthquake source zones and epicentres in the Tasmanian region.

Table 1. Main shocks in the Western Tasmanian Zone (1853–1984). Foreshocks and aftershocks are not included.

Date *y*	*m*	*d*	*Latitude* *°S*	*Longitude* *°E*	*Depth* *km*	*Magnitude*	*Comments*
1859	11	21	40.7	145.2	—	5.4 MI	Isoseismal map drawn (Michael-Leiba, 1989, this issue)
1880	02	03	43.0	145.3	—	5.5 MI	Isoseismal map drawn (Michael-Leiba, 1989, this issue)
1908	05	04	42.0	145.4	—	4.8 MI	Isoseismal map drawn (Michael-Leiba, 1989, this issue)
1911	11	04	42.2	145.2	—	4.8 MI	Isoseismal map drawn (Michael-Leiba, 1989, this issue)
1924	03	01	41.7	145.0	—	5.2 MI	Isoseismal map drawn (Michael-Leiba, 1989, this issue)
1958	01	01	42.2	146.1	10G	5.3 ML(RIV)	BMR EDF
1962	06	01	42.85	145.51	10G	3.2 ML(TAU)	BMR EDF
1963	11	03	43.49	145.80	10G	4.4 ML(BMR)	BMR EDF
1964	11	14	40.22	144.60	10G	4.5 ML(TAU)	BMR EDF
1964	12	09	41.80	146.62	10G	3.4 ML(TAU)	BMR EDF
1966	07	05	39.65	144.96	10G	4.1 ML(CAN)	BMR EDF
1967	11	30	42.76	146.45	10G	3.5 ML(TAU)	BMR EDF
1969	03	13	41.32	144.75	10G	3.5 ML(TAU)	BMR EDF
1971	05	26	40.48	145.01	10G	3.0 ML(TAU)	BMR EDF
1971	06	15	40.98	145.83	10G	4.0 ML(TAU)	BMR EDF
1971	10	22	40.90	143.93	10G	3.2 ML(TAU)	BMR EDF
1972	03	04	41.93	145.41	10G	3.0 ML(TAU)	BMR EDF
1973	06	03	42.32	145.08	10G	4.0 ML(BMR)	BMR EDF
1975	05	03	41.62	143.98	—	4.5 ML(TAU)	BMR EDF
1975	08	31	39.95	144.77	—	3.5 ML(TAU)	BMR EDF
1977	12	21	42.98	146.08	—	3.0 ML(TAU)	BMR EDF
1978	05	04	41.02	145.68	12	3.0 ML(BMR)	BMR EDF
1978	08	25	42.98	145.78	20	3.0 ML(TAU)	BMR EDF
1979	07	11	39.97	144.61	11	3.9 MD(PIT)	BMR EDF
1979	07	28	40.52	144.72	—	3.0 ML(TAU)	BMR EDF
1979	09	10	39.72	144.65	15	3.6 (MD(PIT)	BMR EDF
1981	12	08	39.67	144.38	—	3.0 ML(TAU)	BMR EDF
1982	04	01	40.26	142.93	—	4.0 ML(TAU)	BMR EDF
1982	08	19	40.61	145.19	0	3.6 ML(BMR)	BMR EDF
1982	12	10	40.15	143.87	—	3.0 ML(TAU)	BMR EDF
1983	10	15	39.78	145.03	10	4.4 ML(PIT)	BMR EDF

ML — Instrumentally determined Richter magnitude
MI — Magnitude (Richter equivalent) determined from isoseismal radii on an isoseismal map.
G — Depth estimated
BMR — Bureau of Mineral Resources
CAN — Australian National University
PIT — Phillip Institute of Technology
RIV — Riverview Observatory
TAU — University of Tasmania
BMR EDF — BMR Earthquake Data File

Records of magnitude MI≥5.5 events are probably complete for the entire period for the whole Western Tasmanian Zone. However, 5.5≥MI≥5.0 events may be complete only for 95 per cent of the source zone before 1958 because, if they occurred in the northwestern corner of the zone, they probably would not have been felt strongly enough in mainland Tasmania for this magnitude to be identified. This incompleteness of the data has been considered by taking the mean number per year, for the period 1853-1984, as 0.0317 instead of 0.0305. This makes a negligible difference in Figure 2 compared with the 'plus or minus one standard deviation' error bars, calculated according to the method of Weichert (1980). Figure 2 gives an average recurrence interval of about 30 years for a magnitude ML≥5.0 event, 90 years for a magnitude ML≥5.5 event, and 290 years for a magnitude ML≥6.0 earthquake. Because of uncertainties in the data plotted in Figure 2, the line was fitted by eye. Its equation is

$$\log N = 3.54 - 1.00\ ML$$

where N is the mean yearly number of earthquakes with Richter magnitudes ≥ML. It gives most weight to the magnitude ML≥4.0 and ML≥4.5 data, as these are based on instrumental data collected over more than 20 years. The data for the smaller events appear to be incomplete (but this is unlikely because, from 1977 on, there was good coverage from Phillip Institute of Technology seismographs in Victoria, as well as from the Tasmanian seismographs) or unrepresentative, as they are for a period of only 8 years. The data for the larger events are based mainly on felt reports and are less reliable.

The completeness periods used for plotting the points in Figure 2 were: for ML≥3.0 and 3.5, 1977-1984; for ML≥4.0, 1962-1984; for ML≥4.5, 1958-1984; and for ML≥5.0, 1853-1984.

We chose a maximum magnitude of ML6.0 for this source zone. The largest earthquake (Fig. 1) occurred on 3 February 1880 and had a magnitude MI5.5 (Michael-Leiba, 1989, this issue).

McCue (1978) mentioned the existence of two possible Holocene fault scarps. One of these, the Lake Edgar Fault, although probably an old fracture, appears to have been recently active and is the site of large earthquakes, according to the field observations of Carey (1960). Microearthquake activity occurs near its northern end (Shirley, 1980). The 3 February 1880 event, although poorly located, could have occurred on this fault (Michael-Leiba, 1989, this issue). The boundary of the Western Tasmanian Zone was therefore extended to include the Lake Edgar fault.

Because focal depth determinations for this zone are poor, a depth of 10 km was chosen to conform with that considered an eastern Australian average (Gaull & others, in press).

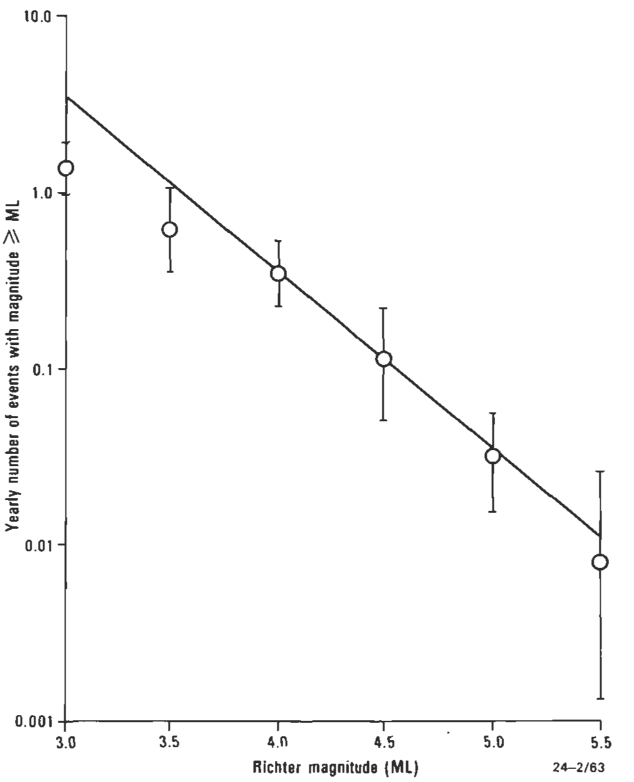

Figure 2. Magnitude-frequency recurrence relation showing ±1 standard deviation error bars for the Western Tasmanian Zone.

Table 2. Main shocks in the West Tasman Sea Zone (1853-1984). Foreshocks and aftershocks and swarm events within 1 month of one another are not included.

Date *y*	*m*	*d*	*Latitude* *°S*	*Longitude* *°E*	*Depth* *km*	*Magnitude*	*Comments*[1]
1885	05	28	39.8	148.8	—	6.8 MI	Michael-Leiba 1989 (this issue)
1888	05	28	—	—	—	?5.0-5.5MI	Felt E. Tas
1889	12	07	—	—	—	?4.0-4.5MI	Felt III Goulds Country
1890	04	29	—	—	—	?4.0-4.5MI	Felt III Goulds Country
1890	08	11	—	—	—	?4.0-4.5MI	Felt III Goulds Country
1891	05	30	—	—	—	?4.5-5.0MI	Felt IV St. Marys
1891	07	02	—	—	—	?4.0-4.5MI	Felt III St. Helens
1892	01	26	40.3	149.5	—	6.9MI	Michael-Leiba (1989, this issue)
1894	01	26	—	—	—	?4.0-4.5MI	Felt III Goulds Country
1894	11	22	—	—	—	?5.0-5.5MI	Felt Eastern Tasmania
1895	12	02	—	—	—	?4.0-4.5MI	Felt III Goulds Country
1897	05	25	—	—	—	?4.0-4.5MI	Felt IV Eddystone
1897	08	11	—	—	—	?4.5-5.0MI	Felt NE. Tas.
1903	12	31	—	—	—	?4.5-5.0MI	Felt IV St. Helens
1907	01	31	—	—	—	?5.0-5.5MI	Felt E. Tas.
1928	01	18	—	—	—	?4.0-4.5MI	Felt III Scottsdale
1929	12	28	39.69	149.45	10G	5.4 ML(RIV)	BMR EDF
1946	09	14	40.20	149.00	33G	5.7 ML(RIV)	BMR EDF
1948	08	10	—	—	—	?4.0-4.5MI	Felt IV Flinders Is.
1954	12	11	—	—	—	?4.0-4.5MI	Felt IV Flinders Is.
1961	02	03	40.0	148.5	0G	4.0 ML(CAN)	BMR EDF
1965	03	18	40.29	149.59	33G	5.0 ML(CAN)	BMR EDF
1972	05	14	40.10	150.33	0G	4.3 ML(CAN)	D. Denham-prs. comm

[1]Felt reports from Ripper, 1963

?MI Rough estimate of Richter magnitude from scant intensity data — no isoseismal map drawn.

Other symbols and abbreviations are the same as in Table 1.

West Tasman Sea Zone (Table 2)

Carey (1960) catalogued 2540 events felt in northeastern Tasmania during the period 1883–1886. The activity continued intermittently until 1892. The maximum intensity reported in northeastern Tasmania in 1883 was MMV (Carey, 1960), MMVI–VIII in 1884–5, and MMVI–VII in 1892, (Michael-Leiba, 1989, this issue). This swarm of earthquakes appears to have originated in the West Tasman Sea Zone (Shirley, 1980) but, unfortunately, there were no felt reports from Flinders Island. The recent study by Michael-Leiba (1989, this issue) suggests, however, that the three largest events (13 July 1884, 12 May 1885 and 26 January 1892) had magnitudes MI6.4, 6.8 and 6.9 respectively, and that their epicentres were situated in the West Tasman Sea Zone.

The events of 1884 and 1885 occurred during a period of almost continuous swarm activity and consequently are not necessarily independent. There were several periods with no felt reports in the years 1888–1891, so we considered the earthquake of 26 January 1892 to be an independent event. Hence, there are at least two independent magnitude MI≥6.5 events in the 131 years since 1853.

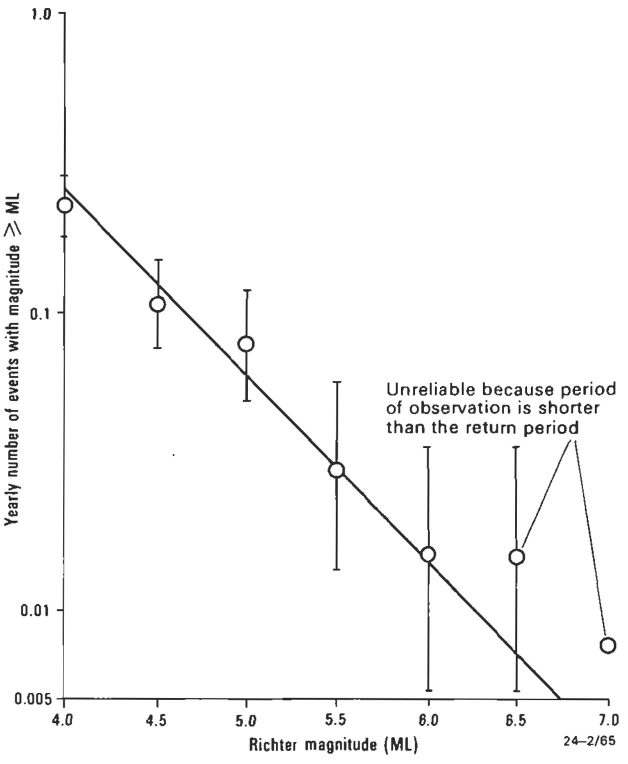

Figure 3. Magnitude-frequency recurrence relation showing ±1 standard deviation error bars for the West Tasman Sea Zone.

An examination of the felt reports tabulated in Ripper (1963) and of events catalogued in the BMR earthquake data file, suggests that approximately 23 independent events with ML≥4.0 occurred in the West Tasman Sea Zone during the period 1883–1984 (Table 2). Events were considered dependent, as in Michael-Leiba (1987), if they occurred within 30 km and one month of each other. In that paper, it was found that if these dependent events were excluded, the data appeared to follow a Poisson distribution, but that when all events were included, they did not fit a Poisson distribution. Two earthquakes in Table 2 had magnitude MI≥6.5, as discussed above. We assigned approximate magnitudes, ?MI, to those earthquakes whose magnitudes had not been determined instrumentally or from isoseismal maps. This was done on the basis of maximum reported intensity (Ripper, 1963) at an estimated distance from the epicentres, and of area over which the event was felt (Ripper, 1963), by using the eastern Australian attenuation curves. We plotted these magnitude–frequency recurrence data (Fig. 3) using 1883–1984 as the completeness period for ML4.0–5.9, and 1853–1954 as the completeness period for events with ML≥6.0. The relation determined by eye is

$$\log N = 1.93 - 0.63\ ML$$

The b-value of 0.6 is low, but low values have also been obtained for some source zones in Canada (Basham & others, 1985) and Queensland (Rynn, 1987). Pre-instrumental data were included to increase the period of observation. If instrumental data only were considered for ML<6.0 events, and felt reports for ML≥6.0 events (as these would almost certainly be reported felt on land), then the b-value would tend to be even lower. If the events in Table 2 are considered independent only when they are at least six months apart, the number of ML<5.0 earthquakes would decrease. This would also tend to decrease the b-value.

The maximum magnitude for the West Tasman Sea Zone was taken to be 7.5 because of the magnitude MI6.5–7.0 events in the swarm (Table 2). There are no reliable focal depths for the zone; a depth of 10 km was used for the earthquake risk calculations.

The average recurrence interval is about 70 years for a magnitude ML≥6.0 event, 140 years for a magnitude ML≥6.5 earthquake, and 290 years for a magnitude ML≥7.0 event (Fig. 3).

Other zones

Because of their proximity to Tasmania (Fig. 1), the Southern Victorian and Lachlan Fold Belt Zones and the 40° S Zone (East) contribute to earthquake risk there and have been included in the analysis. The parameters of the earthquake source zones are given in Table 3. ML(MIN) is the minimum magnitude for which data are assumed to be complete for a source zone. Events with magnitudes less than ML(MIN)

Table 3. Earthquake source zone parameters.

Source zone	*ML(Min)*	*ML(Max)*	*b*	*A(Min)*	*Area (km²)*	*A*	*N(0)*
Western Tasmania	3.0	6.0	1.00	3.50	75250	3.54	461
West Tasman Sea	4.0	7.5	0.63	0.30	16800	1.93	51
40° S (East)	4.0	7.0	0.88	0.59	22600	3.29	83
Southern Victoria	3.0	6.0	0.77	2.26	43900	2.66	104
Lachlan Fold Belt	3.0	6.1	1.16	14.69	284200	4.65	1572
Background	2.0	5.5	0.83	0.14	10000	0.81	6

ML(Min) — Minimum Richter magnitude for which data are assumed complete.
ML(Max) — Adopted Maximum Richter magnitude for earthquake risk estimates.
A(Min) — Number of earthquakes per annum with magnitudes > ML(Min).
A — log number of earthquakes per annum with ML>0
b — b-value (slope) of magnitude-frequency relationship.
N(0) — Number of earthquakes per annum per 10 000km² with ML>0.

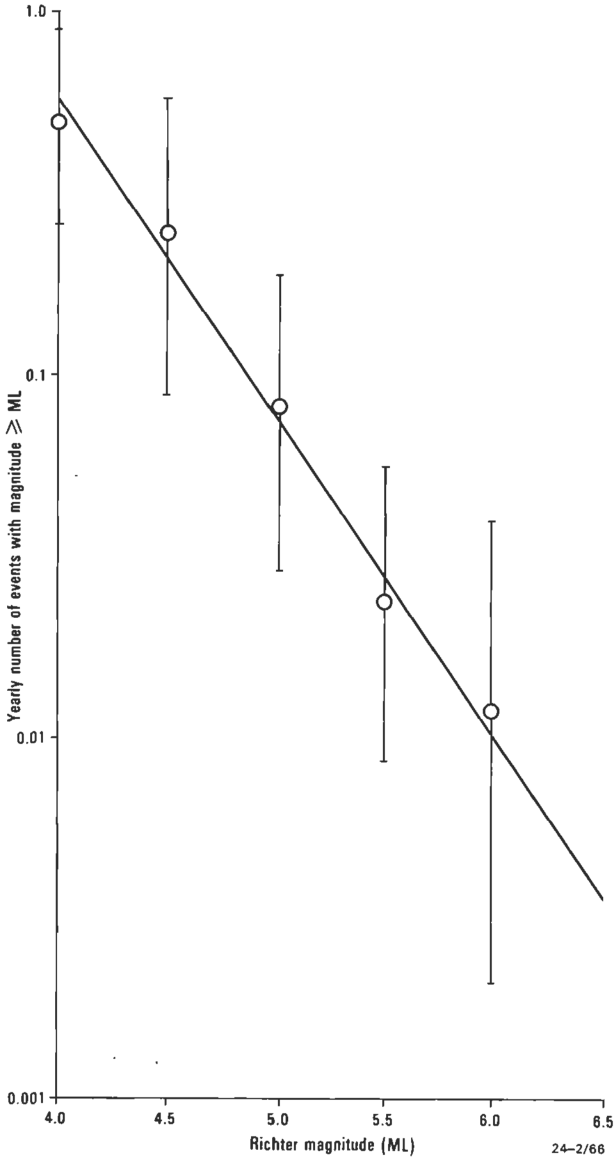

Figure 4. Magnitude-frequency recurrence relation showing ±1 standard deviation error bars for the 40° S Zone (East).

are not included in the risk calculations. The parameters for the Southern Victorian and Lachlan Fold Belt Zones were obtained from Gaull & others (in press).

The magnitude-frequency recurrence relation

$$\log N = 3.29 - 0.88ML$$

fitted by eye for the 40° S Zone (East), is based on instrumental data from 1903–1984 and shown in Figure 4. The completeness periods used were 1977–1984 for ML4.0–4.9, 1961–1984 for ML5.0–5.4, and 1903–1984 for ML≥5.5.

Background seismicity

The epicentres not included in the source zones are considered to be background seismicity. For the Tasmanian earthquake risk calculations, the mean eastern Australian background seismicity (Gaull & others, in press) was used. The parameters are shown in Table 3, where the seismicity rate has been normalised to refer to an area of 10 000 km^2.

Strong ground-motion attenuation

As isoseismal maps have been published for only four Tasmanian earthquakes where instrumental magnitudes are available (Everingham & others, 1982), we used the average southeastern Australian attenuation of Gaull & others (in press) for the earthquake risk assessment. These attenuation constants are given in Table 4.

Table 4. Attenuation constants adopted for Tasmanian earthquake risk map.

Using the Kanai (1961) form
$Y = ae^{bML}R^{-c}$, where Y is the peak ground motion
ML is Richter magnitude and
R is hypocentral distance in kilometres

Peak ground motion (Y)	*a*	*b*	*c*
Intensity (MM) = ln Y	50	1.50	1.7
Velocity (mm.s^{-1})	12.20	1.04	1.18
Acceleration (m.s^{-2})	0.088	1.10	1.20

Three of the isoseismal maps had irregular isoseismals and no individual felt intensities marked on the maps, and the fourth (Queenstown, 1 January 1958) was based on felt reports from only 11 places, so it is difficult to assess how the Tasmanian attenuation compares with that used in this study, except to say that it is not grossly inconsistent.

Results

Earthquake risk for the Tasmanian region was computed and plotted on a 0.25° grid near the source zones and a 0.5° grid elsewhere. The contours of peak ground velocity, peak ground acceleration, and Modified Mercalli intensity with a 10 per cent probability of being exceeded in a 50 year period are shown in Figures 5, 6 and 7. Because the effect of water on strong motion on the sea floor is unknown, the offshore contours are dotted.

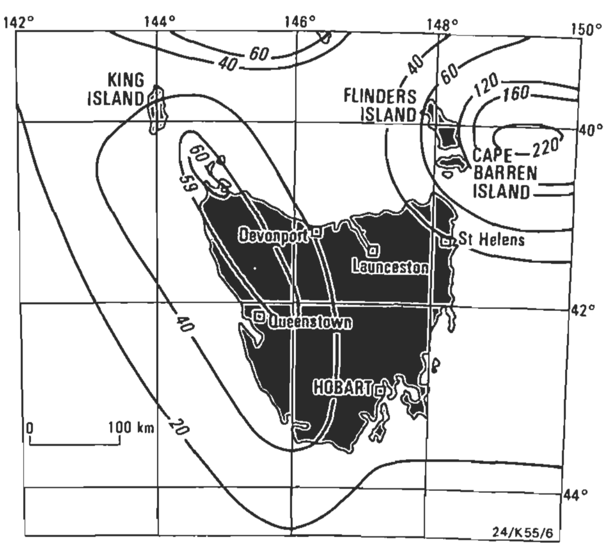

Figure 5. Peak ground velocity (mm.s^{-1}) with a 10 per cent probability of being exceeded in a 50 year period. Note the variable contour interval.

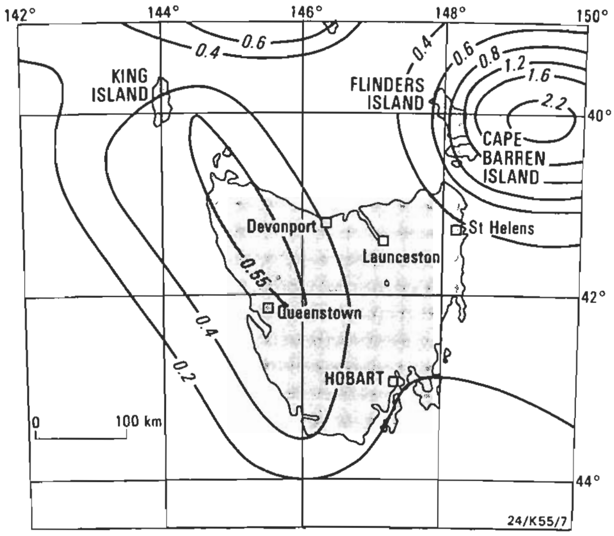

Figure 6. Peak ground acceleration (m.s^{-2}) with a 10 per cent probability of being exceeded in a 50 year period. Note the variable contour interval.

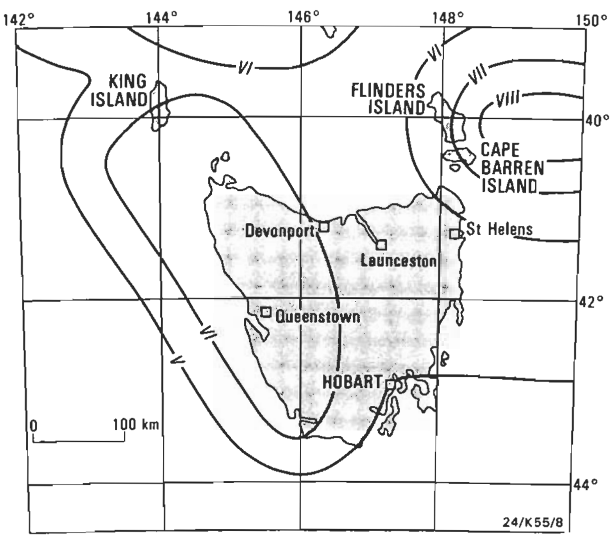

Figure 7. Peak ground intensity (Modified Mercalli scale) with a 10 per cent probability of being exceeded in a 50 year period.

The land areas subject to the highest risk are Flinders and Cape Barren Islands, which lie adjacent to the West Tasman Sea Zone and are predominantly between the 60 mm.s^{-1}/0.6 m.s^{-2} and 120 mm.s^{-1}/1.2 m.s^{-2} contours in Figures 5 and 6. The second highest risk land area is that part of western and northwestern Tasmania within the 59 mm.s^{-1}/ 0.55 m.s^{-2} contour. It is estimated that at Queenstown there is a 10 per cent chance that the ground motion will exceed 58 mm.s^{-1} or 0.54 m.s^{-2} during a 50 year period. According to our scaling rule this corresponds to an intensity of MMVI–VII, which is the threshold at which damage can occur.

At Devonport, just outside the Western Tasmanian source zone, there is a 10 per cent probability that ground motion will exceed 33 mm.s^{-1} or 0.31 m.s^{-2} (intensity MMV–VI) during a 50 year period. At Hobart, the corresponding figures are 23 mm.s^{-1} or 0.21 m.s^{-2} (intensity MMIV–V), and at Launceston 30 mm.s^{-1} or 0.29 m.s^{-2} (intensity MMIV–V), well below the damage threshold.

Discussion

The earthquake risk calculations indicate that the 100 year intensities at Queenstown and Flinders Island should be MMV–VI, while at Devonport, Launceston, and Hobart they should be MMIV–V. These results are reasonably consistent with the macroseismic data available for the period 1885–1984. Queenstown recorded intensity MMIV–VIII in 1908 (Michael-Leiba, 1989, this issue), MMIV-VI in 1911 (Michael-Leiba, 1989, this issue), and intensity MMV in 1958 (Everingham & others, 1982). MMIV was experienced at Devonport in 1909 (Ripper, 1963), and MMII-VI in 1924 (Michael-Leiba, 1989, this issue). Hobart recorded intensities of MMIV-VI in 1885 and 1892 (Michael-Leiba, 1989, this issue), and MMIV in 1922 (Ripper, 1963). Intensity MMIV has been observed at Flinders Island in 1948 and 1954 (Ripper, 1963), but the felt reports from Flinders Island are obviously incomplete.

Launceston experienced intensity MMIV in 1900 and 1948, and twice in 1887 (Ripper, 1963), MMV in 1946 (Ripper, 1963), MMIV–VII in 1885 and MMV–VII in 1892 (Michael-Leiba, 1989, this issue). For seven out of eight earthquakes for which isoseismal maps were drawn, and which were felt in Launceston during the period 1859–1964 (Everingham & others, 1982; Michael-Leiba, 1989, this issue), the maximum intensity experienced there was one or two intensity units greater than that expected for an average site. For six out of eight events, even the mean intensity at Launceston was about one intensity unit greater than that for an average site. Consequently, the ground motion in some parts of Launceston appears to be underestimated by the risk maps.

This is because the risk calculations assume average site conditions and there appears to be a local site effect in parts of Launceston, particularly the area (including the central business district) immediately south and southeast of the junction of the Tamar and North Esk Rivers. Minor damage occurred in this area during the 1883–1892 earthquake swarm (Michael-Leiba, 1989, this issue), and a magnitude ML 5.7 event on 14 September 1946, 200 km away, was felt in Launceston with intensity MMV (Ripper, 1963). This is because Launceston is built on a complex north-northwest-trending Tertiary graben (in Jurassic dolerite), in which Tertiary lake sediments have been deposited. The area in which the maximum intensities were experienced during the swarm overlies up to 200 m of Tertiary clays. Because of the complex nature of the graben, their thickness varies from an estimated 200 m to zero where dolerite crops out in City Park at the eastern extremity of the area (P. Stephenson, Tasmanian Mines Department, personal communication). The estimated effect of this amplification by the lake sediments of the city is to increase the risk estimates in peak ground velocity from about 30 mm.s^{-1} to about 60 mm.s^{-1} (corresponding accelerations from 0.29 m.s.$^{-2}$ to 0.60 m.s^{-2}). This should be considered in seismic zoning in those parts of Launceston underlain by the Tertiary lake sediments.

The earthquake risk map produced by Underwood (1973) bears a broad resemblance to our maps. Differences arise because it was based on only 10.5 years of data and used a site-assessment methodology. However, the earthquake risk assessed by us for the Tasmanian region is very similar to that of McCue (1978), although his western Tasmanian seismic region extends 50–100 km further east, and our northeastern Tasmanian risk area extends about 50 km south of his.

An uncertain parameter in the Western Tasmanian Zone is the maximum magnitude. The largest event in this region in historic times was a magnitude Ml5.5 earthquake, and we used magnitude ML6.0 for our risk assessment. McCue (1978) deduced an upper bound of magnitude ML6.5 for the Type III extreme value distribution for southeastern Australia. If this is taken as the maximum magnitude for western Tasmania, then the risk at Queenstown, Devonport and Hobart would be increased by up to 10 per cent.

Another uncertainty is the attenuation of strong ground motion. We have used an average southeastern Australian attenuation (Gaull & others, in press). Strong motion data are needed for the Tasmanian region to define the attenuation in this area. In southwestern Western Australia, the standard deviation of the residuals about the mean isoseismal radii was 0.24 intensity units for the Meeberrie, Meckering and Cadoux earthquakes (Gaull & Michael-Leiba, 1987). Taking this into account could cause the risk to vary by about 20 per cent, so the uncertainty in attenuation in the Tasmanian region would probably have at least this effect on the risk figures.

A third uncertainty in the estimation of Tasmanian earthquake risk results from lack of instrumental information on the locations and magnitudes of earthquakes which occurred before the establishment of the Tasmanian seismic net in 1957 (Carey, 1960). Some errors and omissions in existing catalogues have been corrected for this study (Tables 1 and 2; Michael-Leiba, 1989, this issue), but more research is required into the magnitudes and epicentres of early earthquakes, particularly those related to footnote 1 in Table 2.

Conclusions

The earthquake risk maps presented in this paper depict contours of peak ground velocity, acceleration and intensity with a 10 per cent probability of being exceeded in a 50 year period. Because of the unknown effect of water on strong motion on the ocean floor, the offshore contours have been dotted.

The highest risk land areas are Flinders and Cape Barren Islands (which lie predominantly between the 60 $mm.s^{-1}/0.6$ $m.s^{-2}$ and 120 $mm.s^{-1}/1.2$ $m.s^{-2}$ contours), followed by the northern part of western Tasmania (59 $mm.s^{-1}/0.55$ $m.s^{-2}$).

The chief contributors to uncertainty in estimating earthquake risk are uncertainties in early earthquake locations and magnitudes, and in strong ground motion attenuation.

We recommend that special attention be given to the microzoning of Launceston because of site effects.

Acknowledgements

We would like to thank P.W. Basham, D.H. Weichert, F.M. Anglin and M.J. Berry of the Earth Physics Branch, Energy, Mines and Resources, Canada for supplying the software used for the earthquake risk calculations. We also thank K. McCue for bringing the Weichert (1980) method of estimating errors in the recurrence relations to our attention and for helpful discussions, and D. Denham, K. McCue, J. Rynn and R. Underwood for critically reading the manuscript. The figures were drafted by John Convine and Larry Hollands.

References

Basham, P.W., Weichert, D.H., Anglin, F.M., & Berry, M.J., 1985 — New probabilistic strong ground motion maps of Canada. *Bulletin of the Seismological Society of America*, 75(2), 563–595.

Carey, S.W., 1960 — Tasmania University Seismic Net. *Geology Department, University of Tasmania Publication* 84.

Cornell, C.A., 1968 — Engineering seismic risk analysis. *Bulletin of the Seismological Society of America*, 58(5), 1583–1606.

Denham, D., 1979 — Earthquake hazard in Australia. *In* Heathcote, R.L., & Thom, B.G., (editors), Natural hazards in Australia. *Australian Academy of Science, Institute of Australian Geographers & Academy of the Social Sciences in Australia, Canberra*, 94–118.

Everingham, I.B., McEwin, A.J., & Denham, D., 1982 — Atlas of isoseismal maps of Australian earthquakes. *Bureau of Mineral Resources, Australia, Bulletin* 214.

Gaull, B.A., & Michael-Leiba, M.O., 1987 — Probabilistic earthquake risk maps of southwest Western Australia. *BMR Journal of Australian Geology and Geophysics*, 10, 145–151.

Gaull, B.A., Michael-Leiba, M.O., & Rynn, J.M.W., in press — Probabilistic earthquake risk maps of Australia. *Australian Journal of Earth Sciences.*

Kanai, K., 1961 — An empirical formula for the spectrum of strong earthquake motions. *Bulletin of the Earthquake Research Institute, University of Tokyo*, 39(1), 85–96.

McCue, K.F., 1978 — Seismic risk in Eastern Australia. *University of Adelaide, Physics Department, Publication* ADP 153.

McEwin, A., Underwood, R., & Denham, D., 1976 — Earthquake risk in Australia. *BMR Journal of Australian Geology & Geophysics*, 1, 15–21.

McGuire, R.K., 1976 — Fortran computer program for seismic risk analysis. *United States Geological Survey Open File Report* 76–67.

Michael-Leiba, M.O., 1987 — Temporal variation in the seismicity of the Southwest Seismic Zone, Western Australia: implications for earthquake risk assessment. *BMR Journal of Australian Geology & Geophysics*, 10, 133–137.

Michael-Leiba, M.O., 1989 — Macroseismic effects, locations and magnitudes of some early Tasmanian earthquakes. *BMR Journal of Australian Geology & Geophysics*, 11, (this issue).

Ripper, I.D., 1963 — Local and regional events recorded by the Tasmania seismic net. *Honours thesis, University of Tasmania.*

Rynn, J.M.W., 1987 — Queensland seismic risk study. Final report to the State Government of Queensland, 30 June 1987. *University of Queensland Department of Geology and Mineralogy Report*, 191 pp.

Shirley, J.E., 1980 — Tasmanian seismicity — natural and reservoir induced. *Bulletin of the Seismological Society of America*, 70(6), 2203-2220.

Underwood, R., 1973 — Progress report on seismic zoning in Australia. *In* Denham, D., (editor), Seismicity and earthquake risk in eastern Australia. *Bureau of Mineral Resources, Australia, Bulletin* 164, 61–66.

Weichert, D.H., 1980 — Estimation of the earthquake recurrence parameters for unequal observation periods for different magnitudes. *Bulletin of the Seismological Society of America*, 70(4), 1337-1346.

BMR Journal of Australian Geology & Geophysics, 11, 89-99

Macroseismic effects, locations and magnitudes of some early Tasmanian earthquakes

Marion O. Michael-Leiba[1]

The Richter magnitude, ML, for historical earthquakes can be obtained from the Modified Mercalli intensity, I, and hypocentral distance, R (km) using the formula ML = 1.13 ln R + 0.667I - 2.60. A magnitude is calculated from each intensity contour with a mean radius greater than 35 km, and the arithmetic mean of these magnitudes is designated MI. It approximates ML, usually to half a magnitude unit or better. For Tasmanian and Victorian events where the MMIII contour is not included in the magnitude determination, a correction of -0.2 should be applied to MI. For New South Wales earthquakes, the correction is -0.1.

Isoseismal maps prepared from felt reports in contemporary newspapers were used to determine the epicentres and magnitudes of what are probably the five largest western Tasmanian earthquakes from 1853 to 1957: Circular Head, 21 November 1859, MI 5.4; South West Tasmania, 3 February 1880, MI 5.5; Queenstown, 4 May 1908, MI 4.8; West Coast, 4 November 1911, MI 4.8; and West Coast, 1 March 1924, MI 5.2. All were felt with a maximum intensity of at least MMVI. The South West Tasmania event, the largest historic western Tasmanian earthquake, may have occurred on the Lake Edgar fault, but its epicentre is not well-constrained.

The Tasmanian earthquake swarm of 1883-1892 consisted of around 2000 events felt in the northeastern Tasmanian region. The activity occurred at the rate of at least one event per month from April 1883 to May 1887, and there were at least two events each year up to and including 1892, when the series ended. Isoseismal maps were drawn from contemporary newspaper reports and publications, and epicentres and magnitudes determined for the three largest events: 26 January 1892, MI 6.9; 12 May 1885, MI 6.8; and 13 July 1884, MI 6.4. All three earthquakes were felt from southeastern New South Wales in the north to Hobart in the south, and each caused minor damage in Launceston. Their epicentres were located in the Tasman Sea off the northeastern tip of Tasmania. The MI 6.9 (±0.4) event of 1892 is the largest historic earthquake recorded in eastern Australia.

In 1883, Alfred Barrett Biggs of Launceston, Tasmania, built and operated the first seismoscopes used in Australia. From his measurements and the epicentres determined above, the instrumental Richter magnitudes of the 1884 and 1885 events have been calculated as ML 6.2 and 6.5, respectively, in good agreement with their intensity-deduced magnitudes, MI 6.4 and 6.8.

Introduction

I undertook this work primarily to improve the earthquake data base used for a recent earthquake risk assessment of Tasmania (Michael-Leiba & Gaull, 1989, this issue). During the risk study, we found that earthquakes in the Tasmanian region tend to occur in two zones: the Western Tasmanian Zone (western and northwestern Tasmania and King Island), and the West Tasman Sea Zone, extending into the Tasman Sea from east of Flinders and Cape Barren Islands. However, in the Western Tasmanian Zone, there were no instrumental magnitudes before 1958. Moreover, in the BMR earthquake data file, the primary data base for the earthquake risk study, most events tabulated in Ripper (1963) had been omitted because their epicentral coordinates were not given.

Ripper (1963) compiled a catalogue of all pre-instrumental tremors recorded in Tasmania, from which I identified, for further study in this paper, five events which probably occurred in the Western Tasmanian Zone and had Richter magnitudes of around 5.0. Ripper also catalogued about 2000 events felt in northeastern Tasmania or on the islands off the coast from 1883 to 1892. Events occurred at the rate of at least one per month from April 1883 to May 1887, and there were at least two events each year up to and including 1892, when the series ended. Carey (1960) noted that, while the number of shocks decreased with time, the individual intensity appeared to become greater, peaking in January 1892. Underwood (1972) prepared a catalogue of Victorian felt earthquakes and intensities. It included a number of events in the Tasmanian swarm, which were reported felt at Gabo Island, less commonly in other parts of coastal Victoria, and occasionally in Melbourne.

A.B. Biggs of Launceston, in his paper read to the Royal Society of Tasmania in June 1885 (Biggs, 1886), stated that the earthquake of 13 July 1884 was the greatest of the series. Denham (1985), on the other hand, thought that the event of 12 May 1885 seemed the largest of the earthquakes occurring between 1883 and 1886. Gibson (1982) also stated that this 1885 event was the largest of the 1883-1886 swarm, and drew the isoseismal map showing two Modified Mercalli intensity zones MMII-IV and MMV+. He put the epicentre slightly east of Flinders Island, and considered it likely that all the shocks originated there. The 13 July 1884 and 12 May 1885 earthquakes thus appeared to be the biggest during the swarm activity of April 1883 to May 1887, and were felt throughout Tasmania and in parts of Victoria and New South Wales (Ripper, 1963). I decided to study them further.

The two earthquakes are also of particular interest because, in 1883, A.B. Biggs of Launceston built and operated the first seismoscopes used in Australia. The vertical seismoscope had a magnification of 5 and wrote on smoked glass (Biggs, 1886). Biggs gave no information on the period and damping of his instrument, but gave its static magnification as 5. He measured the maximum trace amplitudes of the July 1884 and May 1885 events (Biggs, 1886). From these I estimated the first instrumental Richter magnitudes, ML, for Australian earthquakes, by assuming that the magnification of 5 was applicable to his measured amplitudes.

The earthquake of 26 January 1892 was also felt at least as widely as the 1884 and 1885 events (Ripper, 1963), and was also selected for further investigation. Unfortunately, Biggs' vertical seismoscope was then no longer operating. Hogben (1898) estimated that the epicentre was at about 41°S, 154°E. He got a similar location for the event of 12 May 1885, and an epicentre about 80 km north-northwest for the earthquake of 13 July 1884. He stated that Biggs' epicentre for the 1892 event was 730 miles due east of Hobart. Shortt (1885) mentioned his previously published opinion that the earthquakes in 1883 and 1884 originated under the sea, east of Cape Barren Island. His epicentre was 'confirmed by a consideration of subsequent observations... as well as by reports from ships at sea in that neighbourhood'.

I have assessed the intensities for all the isoseismal maps with reference to the Modified Mercalli Scale, 1956 version (Richter, 1958), and the eight earthquakes are described below, in chronological order. Tasmanian places mentioned in the text are shown in Figure 1.

[1]Australian Seismological Centre, Bureau of Mineral Resources, GPO Box 378, Canberra, ACT 2601

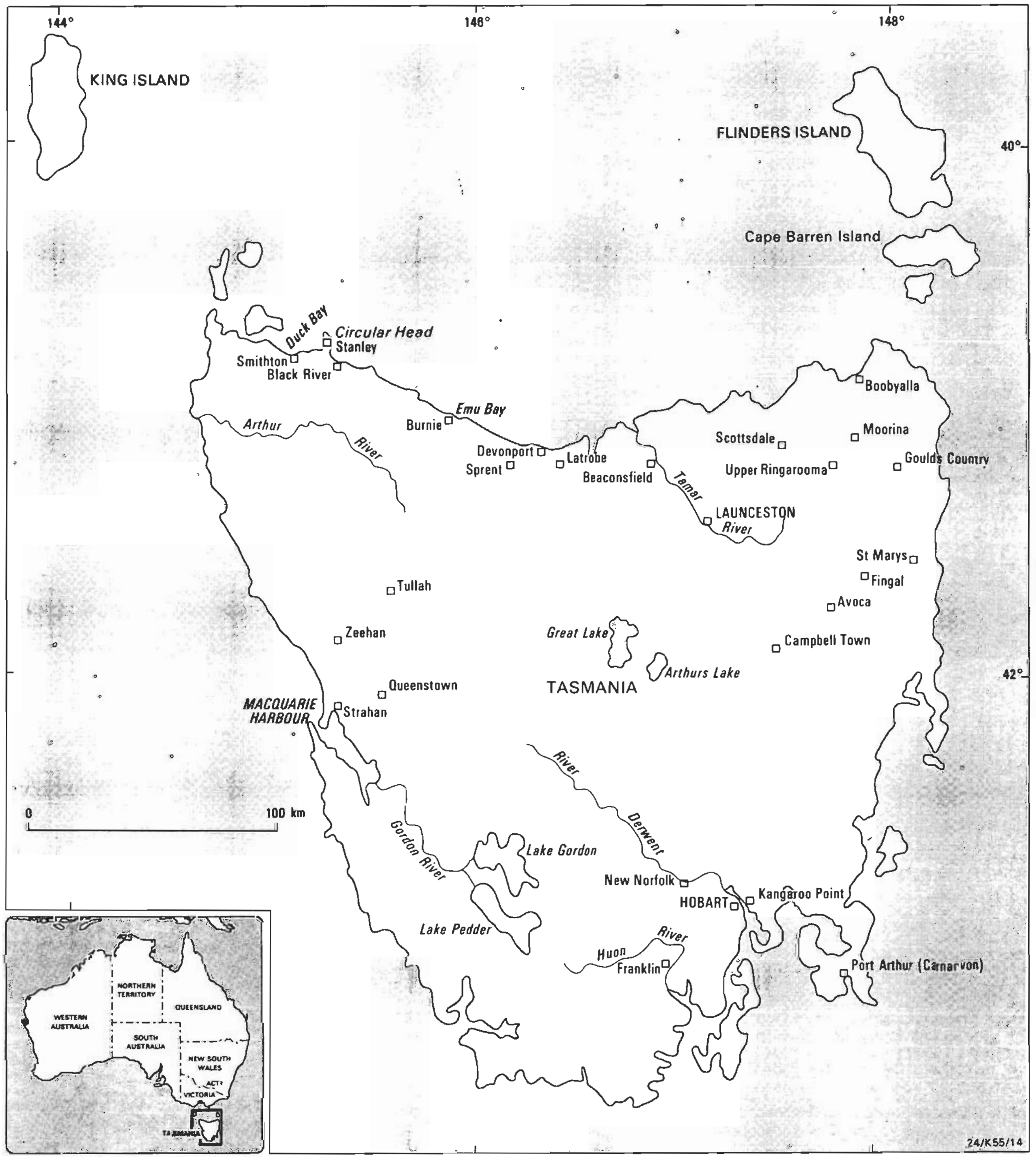

Figure 1. Locality map.

Method of magnitude estimation from mean isoseismal radii

McCue (1980) derived an empirical relation, $M = 1.01 \ln R_p + 0.13$, between magnitude and the radius of perceptibility, R_p, which he defined as 'the radius of the circular area equal to that enclosed by the III isoseismal line on either the Modified Mercalli or Rossi-Forel scales'. The magnitude, M, estimates local magnitude (ML) if below 6.0, and surface wave magnitude (MS) if greater than or equal to 6.0. Here, following popular usage by the Australian seismological community, his magnitude derived from this relation has been designed ML(I). This is a good way to estimate pre-instrumental Richter magnitudes *provided that R_p can be determined accurately.* In this paper, MS has been converted to ML by the method of McGregor & Ripper (1976), plate 7.

The surrounding sea, and the sparse population of at least one third of the island, make it hard to determine accurately R_p of many Tasmanian earthquakes. In addition, if the event occurs at night, when most people are asleep, the minimum Modified Mercalli intensity likely to be recorded is MMIV–V.

Method

To overcome these problems, magnitudes have been determined from the average southeastern Australian attenuation function derived from lines fitted by eye (Gaull & others, in press),

$I = 3.9 + 1.5\ ML - 1.7 \ln R$ .... (1)

where I is Modified Mercalli intensity, ML is Richter magnitude, and R is hypocentral distance in kilometres. This can be rearranged (Morris & others, 1987) to give

$ML = 1.13 \ln R + 0.667I - 2.60$ .... (2)

The more reliable mean isoseismal radii, R(I), of the earthquakes were measured from their isoseismal maps. Where the entire isoseismal contour was equally well-constrained but not circular, the geometric mean of the greatest and smallest radii of the contour were taken to be R(I).

Where only part of the contour was well-constrained, R(I), the mean distance from the epicentre to the contour, was determined more subjectively, the quality of the data being considered. R was calculated (for use in formula 2) from R(I) by means of the formula

$R = [R(I)^2 + h^2]^{1/2}$ .... (3)

where R(I) is the isoseismal radius in kilometres and h is the focal depth in kilometres. Very poorly determined contours, or those with mean radii less than 35 km, were not used. This was to reduce errors of uncertainty in depth and epicentre, although the effect of depth is not great for shallow earthquakes. For example, the difference in magnitude determined from a single contour, at an epicentral distance of 35 km, is only 0.1 if the assumed depth is 0 km instead of 15 km.

R and the corresponding Modified Mercalli intensity, I, were substituted in equation 2 to give a magnitude. The arithmetic mean of these magnitudes is designated MI, to avoid confusion with ML(I) (McCue, 1980). MI is an approximation to ML. The variation in MI caused by variations in determining the mean isoseismal radii from maps with well-located epicentres and isoseismals (the ideal situation) is estimated to be usually less than 0.2 of a magnitude unit. However, for reasonable estimation of errors in R(I), uncertainties in ML(I) are probably less than ±0.5 (Morris & others, 1987). As many reliable contours as possible (with mean isoseismal radius greater than 35 km) were used for determining MI, to minimise the effect of attenuation differing from that implied in the formula.

Examples

The mean isoseismal radii for MMV, IV, III and II for the ML 4.4 Port Davey (Tasmania) earthquake of 3 November 1963 are approximately 45 km, 88 km, 117 km and 145 km (Everingham & others, 1982), giving magnitudes of 5.0, 5.1, 4.8 and 4.4 respectively. The mean of these is 4.8, with a standard deviation of 0.3, giving this earthquake an intensity-based magnitude MI 4.8 (±0.3). To check the accuracy of the method, MI was determined from isoseismal maps for six New South Wales events (Michael-Leiba & Denham, 1987; McCue & others, 1989, this issue; Everingham & others, 1982; Rynn & others, 1987); three Victorian earthquakes (Everingham & others, 1982; Rynn & others, 1987) for which reliable instrumental magnitudes have been measured recently and where ML≥4.0; and the only three Tasmanian earthquakes with ML≥4.0 for which instrumental magnitudes and isoseismal maps (Everingham & others, 1982) are available. The accuracy of the Tasmanian magnitudes, however, is not known. Two of these events, the Port Davey earthquake (discussed above) and the Bass Strait earthquake of 14 November 1964, have very irregular contours and no individual felt intensities marked on them, and the third (at Queenstown, 1958) is based on felt reports from only 11 places, so the reliability of all three maps for MI determination is rather questionable. I also calculated ML(I) from the radius of perceptibility.

Table 1. Comparison of MI with ML and ML(I) for twelve southeastern Australian earthquakes.

Earthquake	*ML*	*ML(I)*	*MI*	*MI-ML*	*ML(I)-ML*	*MI-ML(I)*
Queenstown (Tas) 1/1/58	5.3	4.9	5.0	-0.3	-0.4	+0.1
Port Davey (Tas) 3/11/63	4.4	4.9	4.8	+0.4	+0.5	-0.1
Bass Strait (Tas) 14/11/64	4.5	4.9	4.9	+0.4	+0.4	0.0
Balliang (Vic) 2/12/77	5.0	5.2	5.0	0.0	+0.2	-0.2
Bass Strait (Vic) 16/11/81	4.9	5.3	5.1	+0.2	+0.4	-0.2
Wonnangatta (Vic) 21/11/82	5.4	5.4	5.5	+0.1	0.0	+0.1
Oolong (NSW) 18/11/34	5.6	5.7	5.5	-0.1	+0.1	-0.2
Appin (NSW) 15/11/81	4.6	5.4	5.65	+1.05	+0.8	+0.25
West Wyalong (NSW) 26/11/82	4.6	3.7	3.4	-1.2	-0.9	-0.3
Milparinka (NSW) 8/4/83	4.5	5.0	4.9	+0.4	+0.5	-0.1
Oolong (NSW) 9/8/84	4.3	4.3	4.2	-0.1	0.0	-0.1
Lithgow (NSW) 13/2/85	4.3	4.4	4.4	+0.1	+0.1	0.0

Table 1 shows ML, ML(I) and MI for these 12 earthquakes. For 10 of the 12 events, the difference between MI and ML is no more than 0.4, and between ML(I) and ML, no more than 0.5, so either method will usually estimate ML with an accuracy of half a magnitude unit or better. The mean absolute value of the error is 0.36 for both methods for the 12 earthquakes. The two events for which both methods give poor estimates of ML are the 1981 Appin (NSW) earthquake (felt over a much larger area than would have been expected) and the 1982 West Wyalong (NSW) earthquake (the felt area of which was considerably less than expected, and the MMIII isoseismal radius only 34 km). For all 12 earthquakes, MI and ML(I) differ by no more than 0.3 of a magnitude unit.

Corrections to MI estimates for earthquakes where a reliable MMIII contour cannot be drawn

Tasmania's geography can make it difficult to draw a reliable MMIII contour on the isoseismal map of a Tasmanian earthquake. In such a case, MI must be determined from isoseismal radii relating to intensities greater than MMIII. This might also be necessary for earthquakes occurring when most people are asleep. Consequently, it is necessary to see whether any correction to MI is required when the MMIII contour cannot be used.

This has been done by comparing MI calculated from isoseismal contours for intensities *greater* than MMIII with MI calculated from *all* isoseismal contours, *including* MMIII, for earthquakes where a reliable MMIII contour *can* be drawn (Table 2).

For the seven Tasmanian earthquakes with reasonably reliable MMIII contours, MI calculated from intensity contours greater than MMIII is an average of 0.2 magnitude units higher than that determined from all reliable contours. To prevent over-estimation of the magnitude, 0.2 has been subtracted from MI estimates for the four early Tasmanian earthquakes for which a reliable MMIII contour could not be drawn.

Results for the three Victorian earthquakes in Table 2 suggest that the same correction might be appropriate for MI when a reliable MMIII contour cannot be drawn.

Table 2. Difference between MI derived from contours of intensities greater than MMIII and MI calculated from all reliable contours, including MMIII.

Earthquake	*Difference in MI*
Circular Head (Tas) 1859	+0.1
Queenstown (Tas) 1908	0.0
West Coast (Tas) 1911	+0.1
West Coast (Tas) 1924	+0.1
Queenstown (Tas) 1958	+0.6
Port Davey (Tas) 1963	+0.25
Bass Strait (Tas) 1964	+0.3
Balliang (Vic) 1977	+0.25
Bass Strait (Vic) 1981	+0.2
Wonnangatta (Vic) 1982	+0.1
Oolong (NSW) 1934	0.0
Appin (NSW) 1981	+0.3
West Wyalong (NSW) 1982	—
Milparinka (NSW) 1983	0.0
Oolong (NSW) 1984	+0.2
Lithgow (NSW) 1985	+0.2

For the six New South Wales earthquakes in Table 2, the mean difference between MI calculated from contours greater than MMIII and that calculated from all reliable contours is 0.1, so a correction of -0.1 should be applied to MI for New South Wales earthquakes where a reliable MMIII contour cannot be drawn.

MI for larger events

There are no ML≥6.0 earthquakes in southeastern Australia with which to check the accuracy of MI for larger events. Therefore, MI was determined, using equation 2, for the 1941 Meeberrie (W.A.) earthquake (ML 7.2), 1968 Meckering (W.A.) earthquake (ML 6.9), and 1979 Cadoux (W.A.) earthquake (ML 6.2) (Everingham & others, 1982). Only for the Meckering earthquake could a reliable MMIII contour be drawn. For this event, MI was calculated from the MMVI, V, IV and III mean isoseismal radii as 6.7, with a standard deviation of 0.3. After conversion from MS to ML, ML(I) was also 6.7. These magnitudes both agree well with the Richter magnitude, ML 6.9. MI calculated without the MMIII contour is unchanged. Because of this, no correction is deemed necessary to MI determined for the Meeberrie and Cadoux earthquakes using only the MMVI, V and IV contours. For the Meeberrie earthquake MI = 7.5 with a standard deviation of 0.1, compared with ML 7.2, and for the Cadoux earthquake MI = 6.2 with a standard deviation of 0.7, compared with ML 6.2. Thus, for all three events, MI provides a good estimate of ML. The large standard deviations (0.3 and 0.7) in the individual contour estimates of ML for Meckering and Cadoux are at least partially due to the fact that the attenuation curves for the Meckering and Cadoux earthquakes differ from the average southeastern Australian attenuation.

The formula of Greenhalgh & others (1987), $ML = 0.31 (\log R(IV))^2 + 0.65 (\log R(IV)) + 2.25$, was used where R(IV) is the MMIV mean isoseismal radius, to calculate magnitudes for these three earthquakes. The resulting ML values were 6.6, 6.1 and 6.0 (compared with 7.2, 6.9 and 6.2 for the Meeberrie, Meckering and Cadoux earthquakes respectively), an average of 0.5 magnitude units too low. Consequently, I did not use this method of estimating ML for the large events in this paper.

Uncertainty estimates for adopted magnitudes, MI, for historical earthquakes

Variations in the epicentre will lead to different values of R(I) and hence to variations in MI. In this paper, I have estimated uncertainties in the epicentral locations derived from the isoseismal maps, and, hence, uncertainty in MI.

Description of historical Tasmanian earthquakes

The Circular Head earthquake, 1850 UT, 21 November 1859

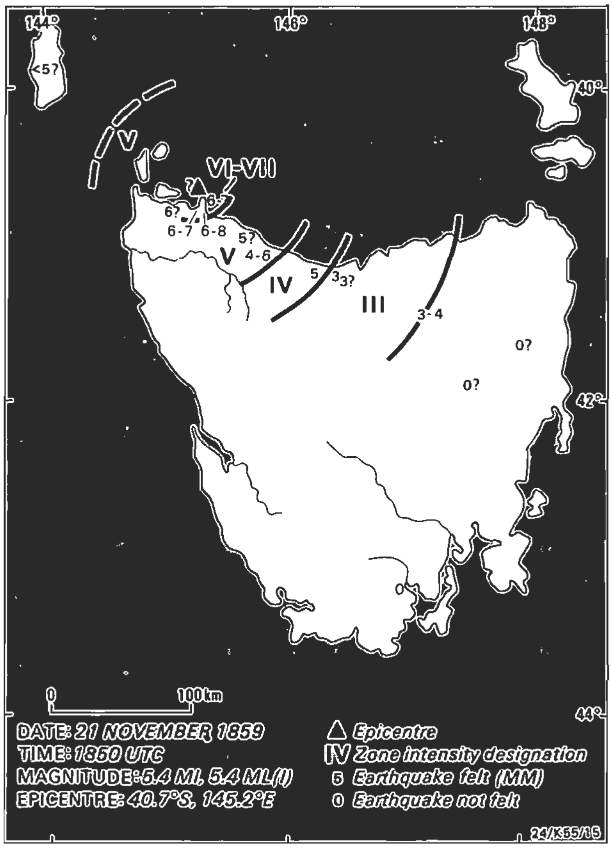

Figure 2. Isoseismal map of the Circular Head earthquake of 21 November 1859.

This earthquake struck at 4.50 am local time on 22 November 1859, and its isoseismal map is shown in Figure 2. The map and description of the effects of the earthquake have been compiled from reports in the 1859 editions of the *Hobart Town Daily Mercury*, the *Cornwall Chronicle* (Launceston), the *Examiner* (Launceston), the *Argus* (Melbourne), the *Age* (Melbourne), and the *Geelong Advertiser*. The tremor was felt along the north coast of Tasmania, from Duck Bay (west of Circular Head) to Launceston. The occurrence so etched itself in the memories of those who experienced it, that it was recalled by readers of the *Mercury* and the *Examiner* 20 years later, following the South West Tasmania earthquake in February 1880. One of the *Examiner*'s correspondents in 1880 said that a permanent effect of the shock was the increased flow of water from a spring at Boyndie (near Circular Head).

The earthquake was felt most strongly in the Circular Head–Black River area, where it destroyed a brick oven and part of a stone chimney (which broke the roof of a stable), cracked another chimney, caused slight cracks in several stone and brick walls, and upset bottles and crockery. People in the area were frightened out of their beds and houses. A schooner at anchor in Duck Bay was moved several feet. S.B.E., a correspondent to the *Examiner* of December 1, 1859, made the apt comment that 'the people...upon the whole feel satisfied that after all a wooden house is far superior to stone'.

Residents of Circular Head also felt three tremors in July and two in October 1859. Foreshocks occurred at around 3 pm on 20 November, one on the night of 21 November, one in the early morning of 22 November, and another at 3.30 am. The main shock at 4.50 am was not reported as felt in Hobart, Melbourne, Geelong, Campbell Town or Fingal.

The following isoseismal radii were measured from Figure 2: MMV, 76 km; MMIV, 109 km; MMIII, 185 km, giving a magnitude of MI 5.4 with a standard deviation of 0.2. Taking 185 km as R_p, ML(I) would also be 5.4.

The epicentre is at 40.7° S, 145.2° E, with an uncertainty of about 30 km, giving an uncertainty in MI of ± 0.3.

The Southwest Tasmania earthquake, 0630 UT, 3 February 1880

This event was felt throughout Tasmania at about 4.30 pm local time on 3 February 1880 and, from reports in the *Mercury*, appears to have been the largest Tasmanian earthquake since the Circular Head one in 1859. Its isoseismal map (Fig. 3) and the description of its effects have been compiled from reports in the *Mercury* (Hobart), the *Launceston Examiner*, the *Devon Herald* (Latrobe), the *Tasmanian Mail* (Hobart), and the *Cornwall Chronicle* (Launceston). There was no report in the *Age* (Melbourne) or the *Argus* (Melbourne) of its being felt in Victoria.

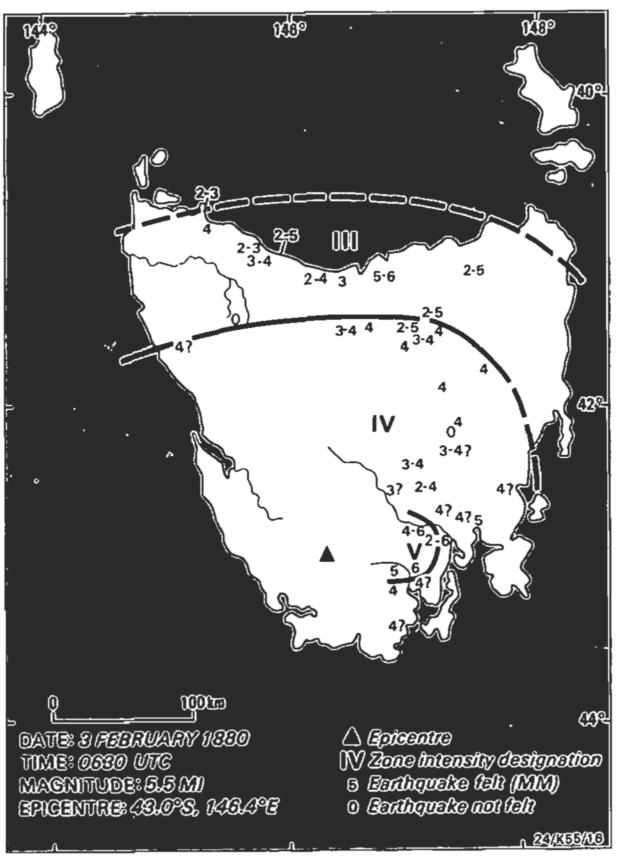

Figure 3. Isoseismal map of the Southwest Tasmania earthquake of 3 February 1880.

The earthquake was felt most strongly in the Huon and Derwent valleys. In New Norfolk, it shook goods off shop shelves and glass from windows. A pane of glass was broken in the public school. In Franklin, plaster was shaken from the ceilings of two or three buildings, and a chimney at the Kent Hotel was cracked. There was one instance of bells being set ringing, and one or two cases of crockery being displaced and furniture 'stirred', causing the residents to run outside. The earthquake was felt on board a steamer travelling between Hobart Town and Kangaroo Point, and also on board a hulk, presumably anchored at Hobart Town.

An earthquake was reported as being felt very strongly at Beaconsfield (on the Tamar River, northern Tasmania) at about 2 pm. Some boys on the cricket ground almost fell down, and a woman indoors grasped a door handle to steady herself. I have assumed that this is the same earthquake, but the time discrepancy is very large.

However, at Emu Bay, on the North West Coast, the event at 4.30 pm displaced crockery, rocked tables, and stopped clocks, so the Beaconsfield time may have been wrong. The effects appeared very site-dependent at Emu Bay, because people whose houses were close to the igneous rocks on the northwest shores of the bay were not troubled by the earthquake, whereas those on sedimentary rocks to the southwest were terrified.

From the isoseismal map, I have deduced that the epicentre was at 43.0° S, 146.4° E, on or near the Lake Edgar Fault (Carey, 1960). However, as there are no near-epicentral felt reports in this virtually unpopulated part of Tasmania, the error in the epicentre could be at least 50 km. The isoseismal radii for the MMV and IV contours are 61 km and 178 km respectively, giving a mean magnitude of 5.7 with a standard deviation of 0.4. Applying the correction of –0.2, because the MMIII isoseismal radius cannot be determined reliably, gives a magnitude of MI 5.5. The estimated uncertainty in MI due to the uncertainty in the epicentre is about ± 0.6.

The Cape Barren Island earthquake, 0355 UT, 13 July 1884

This event was part of the 1883–1892 earthquake swarm, and occurred during the period of highest seismic activity. In 1884, about 900 tremors were felt in northeastern Tasmania.

The 13 July 1884 event occurred at about 1.55 pm local time. A foreshock one day earlier (at 1.45 pm on 12 July 1884) was felt severely in northeastern Tasmania (MMV–VI in Goulds Country). The 13 July earthquake appears to have been the largest event until then, and the third largest in recorded history in Tasmania. It was felt throughout Tasmania, and in parts of eastern Victoria and southeastern New South Wales as far north as Bega.

The isoseismal map (Fig. 4) and description of the effects of the earthquake have been compiled from reports in Biggs (1886), Shortt (1885), the Committee on Seismological Phenomena in Australasia (1892), the *Mercury* (Hobart), the *Launceston Examiner*, the *Devon Herald* (Latrobe), the *Argus* (Melbourne), and the *Sydney Morning Herald*. The head lighthouse keeper at Kents Group (Bass Strait) reported in his log that a 'very heavy shock of Earthquake occurred'. I have assigned this an intensity of MMIV–V.

The earthquake was felt most strongly in northeastern Tasmania and at Launceston. The walls of a house cracked

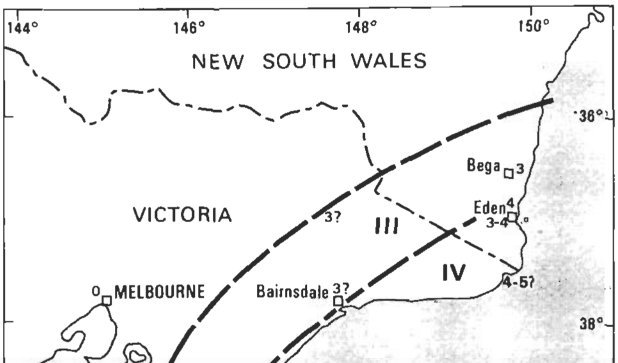

Figure 4. Isoseismal map of the Cape Barren Island earthquake of 13 July 1884.

at Avoca, and some things fell off shelves in Scottsdale. In Moorina, the *Launceston Examiner* reported, 'People rushed out of their houses in great alarm, little children screamed with fright, and even dogs showed great alarm at the violent shaking. Great anxiety is felt throughout the village, everyone being much upset'.

In Upper Ringarooma, according to the *Examiner* 'The shock was so severe as to cause people to rush out of their houses. Large trees were distinctly seen to tremble and shake, causing birds to fly out in alarm. Cattle were observed to leave off grazing, and look about in wonder'.

The following is an extract from the *Examiner's* report, dated 14 July 1884, on the earthquake at Launceston.

> 'During the last few days the earth tremors have been so regular and unusually strong that a good deal of uneasiness has been created. For three days running we have experienced shocks within a few minutes of the same hour each day, and each successive one has been more violent, culminating in a really startling shock yesterday, which appears to have been felt all over the island...
>
> 'At 1.40 pm on Friday an ordinary tremor was experienced; at 1.45 pm on Saturday a much stronger one, lasting a considerable time, and accompanied by a distinct rumbling sound, and at 1.55 pm yesterday came what really appears to have been the most serious shock yet experienced, producing effects that certainly were sufficient to create uneasiness. The shock was accompanied by a loud roaring or rumbling sound and its duration is variously estimated at from 34 to 60 seconds. The tremor yesterday commenced with the usual undulatory movement, which seemed to subside, and then commenced with renewed violence, and not with the usual swaying motion, but with a sharp jerky movement. Plaster fell from the ceilings in several houses, bells rung, pictures moved, and crockery jingled. The greatest alarm prevailed, and a large number of people ran into the streets, expecting to see the houses fall about them...
>
> 'The top of one of the pinnacles which surround the roof of St Andrew's Presbyterian Church was broken off and thrown down, causing an indentation of about six inches in the ground. Children were waiting to go into Sunday school, but fortunately they escaped without any injury. One, if not more, of the other pinnacles has been put out of the perpendicular...
>
> 'At the evening service at St John's Church, thanksgiving was offered up for escape from what might have been a terrible calamity.'

Other damage at Launceston, mainly in and near the central business district, included fallen plaster, cracked ceilings, two cases of cracked walls, and three of damaged chimneys.

Biggs' (1886) vertical seismoscope, with a magnification of 5, recorded a maximum deflection of 0.15 inches peak to peak. This is equivalent to a zero-to-peak vertical ground displacement of 0.38 mm. From the isoseismal map, I derived epicentral coordinates of 40.5° S, 148.5° E (with an estimated uncertainty of about 50 km). Assuming a period of 0.3 to 0.5 s at Launceston, Biggs' (1886) reading would give an instrumental Richter magnitude of ML 6.2.

The amplitude in Biggs (1886) differed from that (0.056 inches) published in the *Launceston Examiner* of 14 July 1884, the day after the earthquake. This latter amplitude would give a Richter magnitude of ML 5.8, but I consider it as probably less reliable, because it might well have been read in haste for a timely report to the Press.

From the isoseismal map, I measured the following isoseismal radii: MMVI, 106 km; MMV, 183 km; and MMIV, 267 km. The MMIII contour is not well-constrained. These isoseismal radii give a mean magnitude of 6.6, with a standard deviation of 0.2. Applying the correction of –0.2 for not using the MMIII contour, MI = 6.4, with an estimated uncertainty of ±0.4 from the uncertainty in the epicentre. This agrees well with the magnitude ML 6.2 derived above.

The Tasman Sea earthquake, 2337 UT, 12 May 1885

This earthquake also occurred during the 1883 to 1892 swarm. In 1885 the activity had diminished somewhat, and about 200 tremors were felt that year.

The earthquake struck at 9.37 am local time on 13 May 1885, and was felt strongly in Tasmania, southeastern Victoria, and the southeastern corner of New South Wales. The isoseismal map (Fig. 5) and description of the effects of the earthquake have been compiled from reports in Biggs (1886), the Committee on Seismological Phenomena in Australasia (1892), Burke-Gaffney (1952), the *Mercury* (Hobart), the *Launceston Examiner*, the *Devon Herald* (Latrobe), the *Tasmanian Mail* (Hobart), the *Age* (Mel-

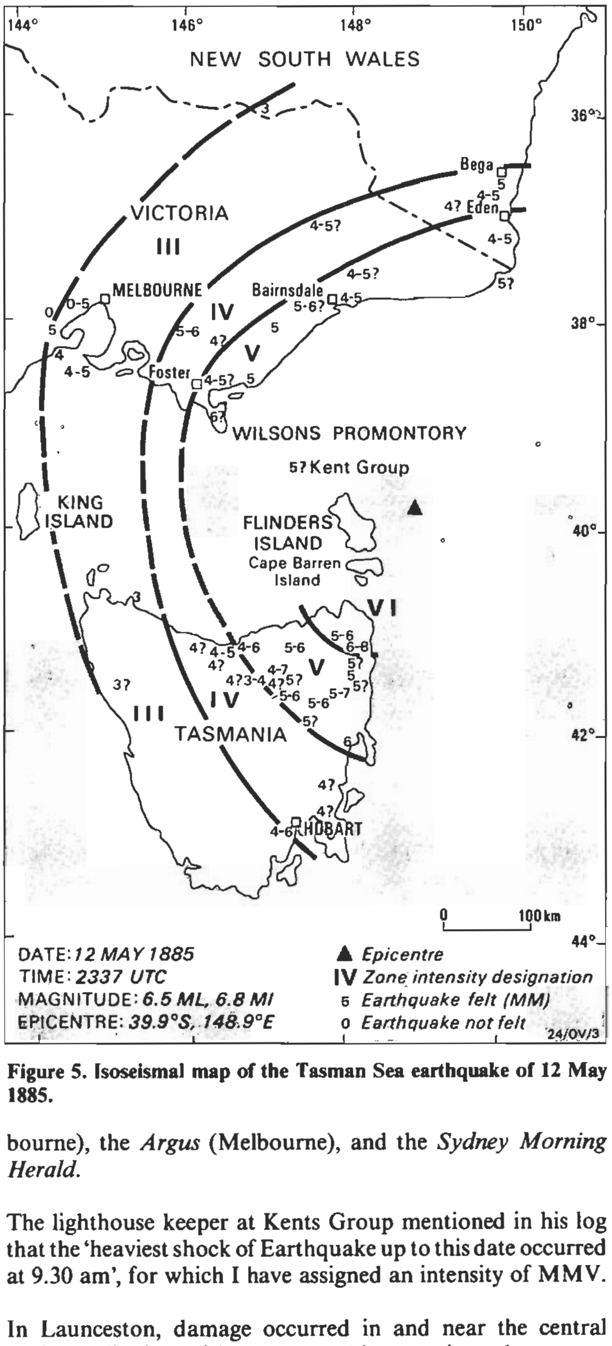

Figure 5. Isoseismal map of the Tasman Sea earthquake of 12 May 1885.

bourne), the *Argus* (Melbourne), and the *Sydney Morning Herald*.

The lighthouse keeper at Kents Group mentioned in his log that the 'heaviest shock of Earthquake up to this date occurred at 9.30 am', for which I have assigned an intensity of MMV.

In Launceston, damage occurred in and near the central business district, with people rushing out into the streets, chimneys being damaged, windows cracked, a wall cracked, a couple of cases of falling plaster, and several instances of objects being thrown down and damaged. At St Andrew's Church, the finial of one of the pinnacles fell to the ground.

In Hobart, a large clock over a shop stopped, bells in some of the offices were set ringing, and the St David's Cathedral bell is said to have tolled twice.

The *Mercury* stated that, at Fingal, the earth tremor was 'considered the severest felt, and was very violent... The water in the South Esk quivered, and ripples were formed from each bank. The sheep and cattle grazing in the paddocks ran together in mobs'. At Scottsdale, 'buildings and trees swayed quite perceptibly'. At Moorina, 'articles were shaken off the mantlepiece in many houses' and it was the most severe ever felt. At Avoca, 'houses were shaken from roof to foundation, but without damage; trees in the garden were swaying, as if under a heavy blast of wind; sick feeling and headache affected individuals'. At Goulds Country, the earthquake 'shook limbs off trees and frightened everybody out of their houses'.

The *Mercury* also reported that Biggs' vertical seismoscope had a maximum deflection of 0.116 inches, whereas the *Launceston Examiner* gave the deflection as 0.112 inch. The first value indicates a ground motion (zero-to-peak) of 0.295 mm, the second 0.284 mm. Taking the epicentre as 39.9° S, 148.9° E (with an uncertainty of about 75 km), and a period of around 0.4 s, either figure gives a Richter magnitude of ML 6.5.

The isoseismal radii are: MMVI, 171 km; MMV, 268 km; and MMIV, 334 km. The MMIII contour is not reliable. The mean magnitude from these measurements is 7.0, with a standard deviation of 0.3. Subtracting 0.2 for not using the MMIII contour gives MI 6.8. The two magnitudes MI and ML from Biggs (1886) seismoscope are in reasonable agreement. The estimated uncertainty in MI from the uncertainty in the epicentre is ±0.4.

The Tasman Sea earthquake, 1648 UT, 26 January 1892

This earthquake, at 2.48 am local time on 27 January 1892, occurred at the end of the 1883 to 1892 swarm, when the activity had dwindled to about four events per year. It was, however, the largest earthquake of the series.

The isoseismal map (Fig. 6) and the description of the effects of the earthquake have been compiled from reports in the *Mercury* (Hobart), the *Launceston Examiner*, the *Wellington Times* (Burnie), the *North-West Post* (Devonport), the *Zeehan and Dundas Herald*, the *Age* (Melbourne), the *Sydney Morning Herald*, and Hogben (1898).

It appears that there were at least two very large events, 5 to 10 minutes apart, the first probably being larger. The earthquake effects were felt all over Tasmania, in southeastern Victoria, and in New South Wales as far north as Kiama, where they woke people, made house timbers creak, and caused things to rattle.

There are discrepancies in reports of the time. The times reported in Tasmania were from 2.41 am to 3.05 am, whereas those in Victoria were from 2.30 am to 3.45 am, and in New South Wales from 3.05 am to 3.30 am. I assume that this is because of the early hour of the morning, as it would be coincidental if there were two or three earthquakes with very different epicentres, so close in time. The time reported from Kiama is 3.08 am, which is in reasonable agreement with those from Tasmania.

In Launceston, the tremor woke most people, and a number jumped out of bed in alarm, some running out into the street. The shocks were felt more strongly by people living on the hills. House bells rang at two houses on Windmill Hill, and a step in front of a house on Cataract Hill split. There were several instances of falling chimneys, ornaments, and plaster from walls. However, the greatest damage was at the General Hospital (near the southern end of Charles Street) where a chimney fell. The bricks landed in Dr Jermyn's room and crashed on to the verandah, greatly alarming the patients, 'some of whom fainted and others went into fits', according to the *North-West Post* of January 28, 1892. There were cracks in several walls. Thus it appears that site amplification of ground motion took place in some parts of Launceston. This is discussed further in Michael-Leiba & Gaull (1989, this issue).

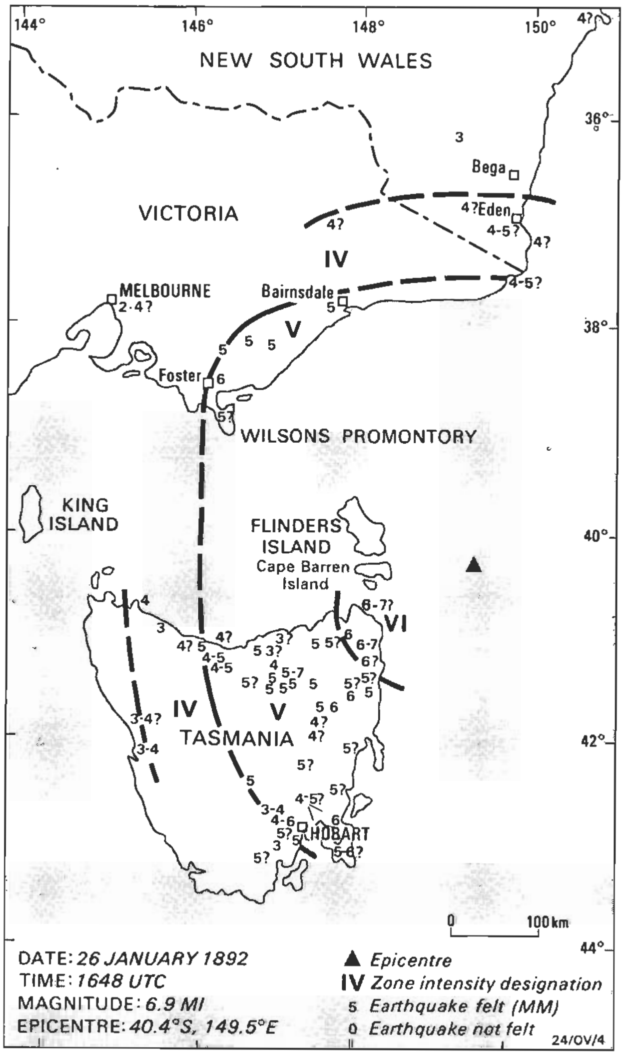

Figure 6. Isoseismal map of the Tasman Sea earthquake of 26 January 1892.

The earthquake was felt very strongly in northeastern Tasmania, as the following reports from the *Mercury* show. At Boobyalla, near the northeastern tip of the island, it was 'accompanied with sound of rushing water. Heavy surf broke on bar when tremor passed'. At Goulds Country, it was 'the severest ever felt'. At Avoca, a 'brick was knocked off a chimney by the vibration', and at Moorina

> 'cattle and horses were much alarmed, as also were most of the inhabitants who, in a great many instances, sought safety by rushing out of their houses'.

A telegram from St Mary's stated that

> 'the most severe shock of earthquake ever felt at St. Mary's took place at 2.50 am. Some seconds before the shock came a rumbling noise was heard like thunder in the distance. The houses seemed to rock to and fro, and the inhabitants were terror-stricken. A second shock of shorter duration took place a few minutes afterwards, and still we are living'.

At Scottsdale, several clocks stopped. The tremor was

> 'sufficiently strong to create some alarm among the townsfolk, some of whom rose hastily and struck a light. In some instances, articles of furniture were thrown from shelves to the floor, the doors and windows rattled and shook unpleasantly, and in bed the oscillations and jerking were anything but agreeable'.

The *Launceston Examiner* stated that, in Fingal, the earthquake was the severest experienced in the district. Everyone was greatly alarmed, and many people rushed into the streets. Clocks stopped, and some which had been stopped for months started, bells rang, and plaster was shaken from walls.

According to the *Tasmanian Mail*, at Carnarvon, now known as Port Arthur, a large brick wall was badly damaged, and stone columns were thrown out of the perpendicular. In Hobart, Hogben (1898) reported that the earthquake stopped clocks, overturned flower pots, threw down bowls, rang bells, rocked beds, rattled windows, and dislodged rocks.

The maximum intensity in Victoria was reported from Foster, just north of Wilsons Promontory, where the *Age* stated that

> 'the chimney lamps at the Royal Hotel, as well as the crockery and glassware at Ridgway's store, were shaken down, and the residents were in a state of fear. It appeared as if the town was going to be levelled'.

Because the earthquake happened when most people were asleep, only the MMVI, V and IV contours in Figure 6 are considered reliable. Their isoseismal radii are 160 km, 330 km and 400 km respectively. Taking the epicentre as 40.4° S, 149° E (with a possible error of about 75 km), the mean magnitude becomes 7.1 with a standard deviation of 0.2, with an estimated uncertainty of ±0.4 from the uncertainty in the epicentre. Applying the –0.2 correction, as the MMIII isoseismal radius is not included, gives MI 6.9. This makes it the largest earthquake recorded in eastern Australia.

The Queenstown Earthquake, 0950 UT, 4 May 1908

This earthquake occurred at 7.50 pm local time on 4 May 1908, and its isoseismal map is shown in Figure 7. The map

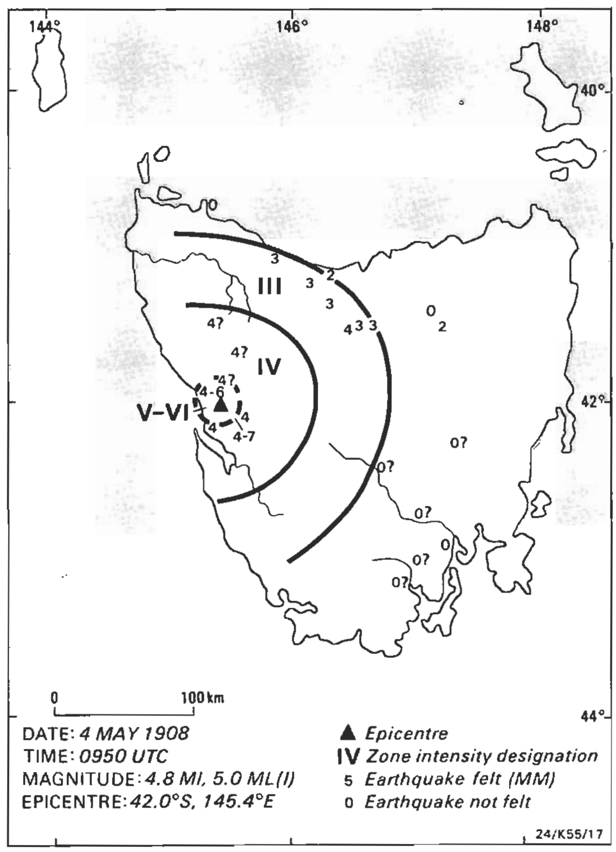

Figure 7. Isoseismal map of the Queenstown earthquake of 4 May 1908.

and description of its effects have been compiled from reports in the *Zeehan and Dundas Herald*, the *Advocate and Times* (Devonport and Burnie), the *North West Post* (Devonport), the *Circular Head Chronicle*, the *Mercury* (Hobart) and the *Launceston Examiner*.

The earthquake was felt most strongly in Queenstown, where people rushed out of their houses and, in some places, crockery was thrown from shelves and plaster fell from walls and ceilings. One or two buildings had slight cracks, two water tanks burst, and the top of one chimney was shaken off.

In Zeehan, windows, furniture, crockery and utensils rattled violently, and wooden floors vibrated like a drum. According to the *Zeehan and Dundas Herald*, 'in the two storied structures of wood the vibration was intense, causing inmates to seek the open'. I have assumed that the writer was referring to Zeehan, but it is not certain from the report, and no other newspaper mentions it. If he was not referring to Zeehan, then the Modified Mercalli intensity there would have been IV–V instead of IV–VI, and the epicentre may have been a little closer to Queenstown.

The epicentral coordinates from Figure 7 are 42.0° S, 145.4° E, with an uncertainty of about 20 km. Because of the sparse population of western Tasmania, the isoseismals are not very well-constrained. The MMIV isoseismal radius is 67 km, and MMIII, 119 km, giving a magnitude of MI 4.8 with a standard deviation of 0.1, and uncertainty of ±0.3 from the uncertainty in the epicentre. Taking R_p as 119 km, ML(I) is 5.0.

The West Coast Earthquake, 0127 UT, 4 November 1911

This earthquake occurred at 11.27 am local time on 4 November 1911. The isoseismal map (Fig. 8) and description of the effects of the earthquake have been compiled from reports in the *Zeehan and Dundas Herald*, the *Mercury* (Hobart), the *Examiner* (Launceston), the *North West Post* (Devonport), the *Advocate and Times* (Devonport and Burnie), and the *Circular Head Chronicle*.

At Zeehan, the *Zeehan and Dundas Herald* described it as the

> 'most severe earth tremor felt... It was preceded by a peculiar rumbling, and as the movement passed by houses were considerably shaken, giving much alarm to residents, especially those in brick buildings... At Messrs W.T. York and Co's store a number of hat boxes were thrown from the shelves, at the School of Mines bottles were thrown to the ground and broken, and several other establishments suffered more or less in this direction'.

According to the *Examiner*, 'numbers of persons promptly found their way into the street'.

At Strahan, the shock was also regarded as being the heaviest for years. Articles were shaken violently and some people ran into the street. The *Zeehan and Dundas Herald* remarked that

> 'strange to say, the bank manager, who was busy in the chambers, did not notice anything unusual, whilst persons immediately outside observed it... As regards the harbour, boatmen say their crafts were visibly affected, and in some instances alarm was felt.'

In Queenstown, some people were alarmed, doors and windows rattled loudly, and loose objects either rattled noisily or fell down, while at Tullah, crockery was broken and the tremor was described as severe.

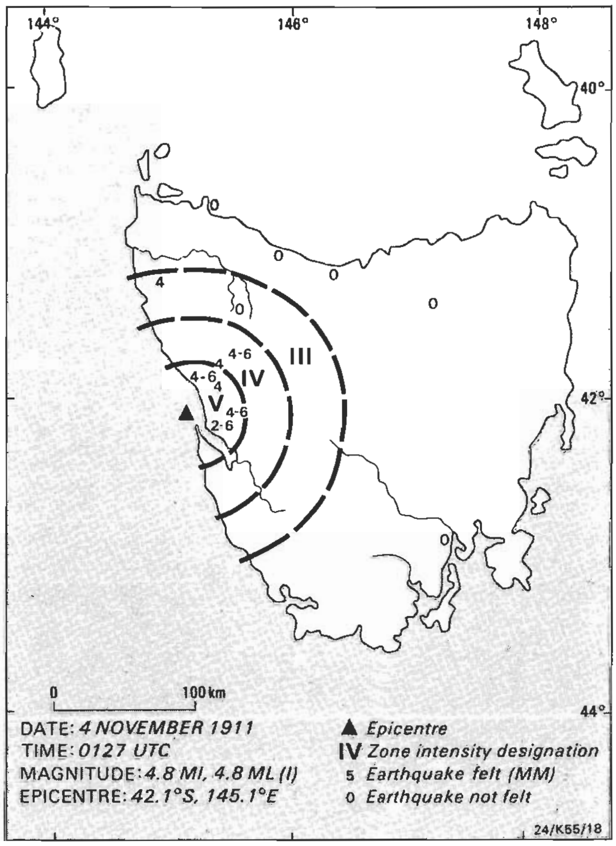

Figure 8. Isoseismal map of the West Coast earthquake of 4 November 1911.

The epicentre in Figure 8 is located at 42.1° S, 145.1° E with an uncertainty of up to 40 km, because no isoseismals are well-constrained, owing to the low population density of the area. The isoseismal radii are: MMV, 38 km; MMIV, 71 km; and MMIII, 106 km. These would give a magnitude, MI, of 4.8 with a standard deviation of 0.1. Taking R_p as 106 km gives ML(I) as 4.8 also. However, because of the uncertainty in the isoseismal contours, MI 4.8 may be an upper limit, and if the epicentre was under Zeehan, the magnitude would be MI 4.5.

The West Coast earthquake, 1155 UT, 1 March 1924

This earthquake, at 9.55 pm local time on Saturday, 1 March 1924, was felt widely over the northwestern part of Tasmania, but most strongly at Zeehan. The information for the isoseismal map (Fig. 9) and description of the effects of the earthquake have been compiled from the *Advocate* (Burnie), the *Mercury* (Hobart), the *Examiner* (Launceston), and the *Circular Head Chronicle*. The *Argus* (Melbourne) did not mention the tremor being felt in Victoria.

The *Mercury* states that 'Zeehan residents rushed out of their houses and places of entertainment on to the roads panic stricken. Picture frames and ornaments fell off walls of houses and were smashed. Two small huts collapsed, but no other damage was done'. The Examiner noted that the disturbance was in two parts; the first lasted five seconds when there was a heavy thump against buildings, and the second lasted three seconds and was much more acute. These 'two parts' could be the P and S waves. The epicentre in Figure 9 would give an (S-P) time of 6 s, corresponding to an epicentral distance of 40 km, which fits this estimated time quite well. Another less likely alternative would be that the first 'thump' was a foreshock. The *Examiner* goes on to say that the

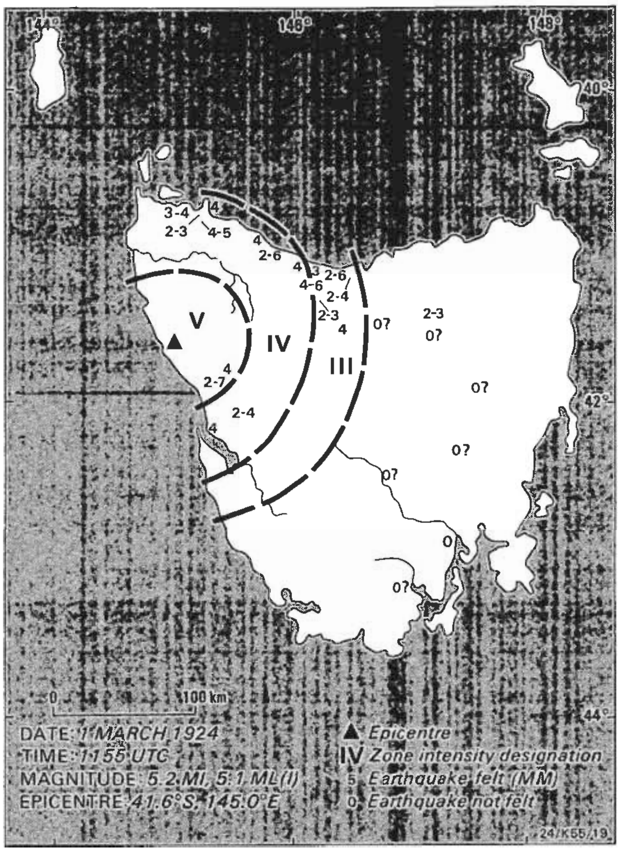

Figure 9. Isoseismal map of the West Coast earthquake of 1 March 1924.

earthquake was felt both indoors and outside and was noticed all over town, with very many people being momentarily alarmed. There was one case of wet cell batteries being shaken off a shelf. However, the tremor was not felt by people watching a movie at the Gaiety Theatre.

The other places where minor damage was reported were Devonport, Burnie and Sprent, all on or near the northwest coast. The Advocate states that

> 'at Devonport, the tremors were felt by many residents... when windows began to rattle, and crockery in some cases was thrown from shelves and broken.
>
> 'At Burnie some people became somewhat alarmed at the pronounced nature of the trembling, while others were not aware that any such disturbance had occurred. People in houses were generally the ones to observe the tremors by rattling windows and creaking walls. In one or two instances crockery was shaken from dresser shelves and broken.
>
> 'Sprent — A severe earth tremor was felt here ... causing quite a stir among the women folk. In several instances crockery and glassware were shaken from shelves and broken.'

The epicentral coordinates are 41.6°S, 145.0°E, with an estimated uncertainty of about 35 km. The isoseismal radii for MMV, IV and III are 50 km, 102 km, and 135 km respectively, giving a magnitude, MI, of 5.2 with a standard deviation of 0.1, and an uncertainty of about ±0.3 from uncertainty in the epicentre. If R_p is taken as 135 km, ML(I) = 5.1.

Conclusions

The study of contemporary newspaper reports has been invaluable in elucidating the seismic history of Tasmania over the last 130 years (Table 3). An estimate of the maximum possible magnitude is necessary for earthquake risk studies, and the maximum observed magnitude puts a lower bound on this. In the Western Tasmanian Zone, the maximum observed magnitude has been increased from 5.3 to 5.5, and this South West Tasmania earthquake may have been on the Lake Edgar fault. However, the uncertainty in the epicentre is too great to be sure of this. In the West Tasman Sea Zone, the maximum observed magnitude has been increased from 6.5 to 6.9. This MI 6.9 event occurred in 1892, east of Cape Barren Island.

The intensity-based magnitude, MI, is useful for determing magnitudes when the radius of perceptibility of the earthquake (McCue, 1980) cannot be measured accurately. For a well-constrained epicentre, it usually approximates ML with an accuracy of half a magnitude unit or better.

Table 3. Summary of parameters of the eight early Tasmanian earthquakes.

Earthquake	*Latitude (°S)*	*Longitude (°E)*	*I*[1]	*MI*	*Other magnitude*
Circular Head, 1805 UT, 21/11/1859	40.7	145.2	VII	5.4	5.4ML(I)
South West Tas, 0630 UT, 3/2/1880	43.0	146.4	VI	5.5	—
Cape Barren I., 0355 UT, 13/7/1884	40.5	148.5	VII	6.4	6.2ML
Tasman Sea, 2337 UT, 12/5/1885	39.9	148.9	VIII	6.8	6.5ML
Tasman Sea, 1648 UT, 26/1/1892	40.4	149.5	VII	6.9	-
Queenstown, 0950 UT, 4/5/1908	42.0	145.4	VII	4.8	5.0 ML(I)
West Coast, 0127 UT, 4/11/1911	42.1	145.1	VI	4.8	4.8 ML(I)
West Coast, 1155 UT, 1/3/1924	41.6	145.0	VII	5.2	5.1 ML(I)

[1] I is maximum intensity (Modified Mercalli Scale, 1956 version, Richter, 1958) assessed during the earthquake. It does not represent the average intensity at a locality.

Acknowledgements

I thank David Denham and Kevin McCue for helpful discussions, and David Denham, Kevin McCue, Jack Rynn and Rob Underwood for critically reading the manuscript and suggesting improvements, Pat Burrell and Helen Tozer for typing it, and Larry Hollands and Colin Johnson for drafting the figures.

References

Biggs, A.B., 1886 — The Tasmanian earth tremors, 1883-4-5. *Papers and Proceedings of the Royal Society of Tasmania*, 1886, 325-334.

Burke-Gaffney, T.N., 1952 — Seismicity of Australia. *Journal of the Proceedings of the Royal Society of New South Wales*, 85, 47-52.

Carey, S.W., 1960 — Tasmania University Seismic Net. *Publication 84, Geology Department, University of Tasmania.*

Committee on Seismological Phenomena in Australasia, 1892 — Seismological phenomena in Australasia. *Report of the Australasian Association for the Advancement of Science, IV.*

Denham, D., 1985 — The Tasman Sea earthquake of 25 November 1963 and stress in the Australian plate. *Tectonophysics*, 111, 329-338.

Everingham, I.B., McEwin, A.J., & Denham, D., 1982 — Atlas of isoseismal maps of Australian earthquakes. *Bureau of Mineral Resources, Australia, Bulletin* 214.

Gaull, B.A., Michael-Leiba, M.O. & Rynn, J.M.W., in press — Probabilistic earthquake risk maps of Australia. *Australian Journal of Earth Sciences*

Gibson, G., 1982 — Earthquakes. *In* Atlas of Victoria. *Victorian Government Printing Office, Melbourne.*

Greenhalgh, S.A., Denham, D., & Rynn, J.M.W., 1987 — Magnitude intensity relations for Australian earthquakes. *IUGG XIX General Assembly, Vancouver, Canada, Abstracts* 1, 283.

Hogben, G., 1898 — The Tasmanian earthquake of 27 January 1892. *Transactions New Zealand Institute*, XXXI, 594–601.

McCue, K.F., 1980 — Magnitude of some early earthquakes in southeastern Australia. *Search*, 11(3), 78–80.

McCue, K.F., Kennett, B.L.N., Gaull, B.A., Michael-Leiba, M., Weekes, J., & Krayshek, C., 1989 — A century of earthquakes in the Dalton-Gunning region of New South Wales. *BMR Journal of Australian Geology & Geophysics*, 11, (this issue).

McGregor, P.M., & Ripper, I.D., 1976 — Notes on earthquake magnitude scales. *Bureau of Mineral Resources, Australia, Record* 1976/56.

Michael-Leiba, M.O., & Denham, D., 1987 — The Lithgow earthquake of 13 February 1985: macroseismic effects. *BMR Journal of Australian Geology & Geophysics*, 10, 139–142.

Michael-Leiba, M.O., & Gaull, B.A., 1989 — Probabilistic earthquake risk maps of Tasmania. *BMR Journal of Australian Geology & Geophysics*, 11, (this issue).

Morris, P.H., Rynn, J.M.W., & Williams, D.J., 1987 — Engineering implications of linear regression of geotechnical data. *Australian Civil Engineering Transactions, November*, 239–247.

Richter, C.F., 1958 — Elementary Seismology. *Freeman & Co., San Francisco*, 137–138.

Ripper, I.D., 1963. Local and regional events recorded by the Tasmania seismic net. *Honours thesis, University of Tasmania.*

Rynn, J.M.W., Denham, D., Greenhalgh , S., Jones, T., Gregson, P.J., McCue, K.F., & Smith, R.S., 1987 — Atlas of isoseismal maps of Australian earthquakes Part 2. *Bureau of Mineral Resources, Australia, Bulletin* 222.

Shortt, J., 1885 — Summary of observations on earthquake phenomena made in Tasmania during 1883 and 1884. *Papers and Proceedings of the Royal Society of Tasmania*, 1885, 263–270.

Underwood, R., 1972 — Studies of Victorian seismicity. *Proceedings of the Royal Society of Victoria*, 85(1), 27–48.

A teleseismic travel time residual map of the Australian continent

B.J. Drummond[1], K.J. Muirhead[2], C. Wright[1] & Peter Wellman[2]

Teleseismic travel time residuals for 43 seismic observatories and 6 networks of portable seismographs have been combined to produce a contour map of residuals for the Australian continent. Travel times to the shield regions of central and western Australia are low compared with average global travel times, indicating relatively high velocities in the upper mantle. The lowest times occur in the Archaean shield regions of Western Australia, the Proterozoic terranes in central Australia and the Gawler Block in South Australia, where heat flow is generally below world average. The residuals become progressively higher (arrival times later) towards the southeast, and the largest residuals are in Tasmania. The positive residuals indicate low velocities in the upper mantle, consistent with the predicted low velocity layer in the upper mantle under southeastern Australia, and higher observed heat flow.

Introduction

Teleseismic travel time residuals indicate the time taken for vertically or near-vertically travelling seismic energy to propagate through the lithosphere, and are therefore useful for studying differences in the structure of the crust and upper mantle in adjacent geological provinces. They are usually calculated from an equation such as

$R = T_{obs} - T_{cal}$

where R is the residual, T_{obs} is the observed travel time from an earthquake or explosion to the seismograph, and T_{cal} is the time calculated for a laterally uniform, spherically stratified Earth model or derived from a reference travel time curve.

Several variations to this equation have been used (e.g. Dziewonski & Anderson, 1983; Lambeck & Penney, 1984), usually to account for errors in R arising from deviations of the real Earth from a simplified model, for example, to account for the effects of seismic anisotropy or errors in earthquake location.

Travel time residuals have now been calculated for many Australian seismic observatories and for a number of portable seismograph stations set up in temporary networks. In all cases, the seismic events used to measure the residuals were in the distance range 30° to 90°, so that the energy measured by the seismographs was travelling at angles of between 14° and 28° to the vertical when it reached the surface. This

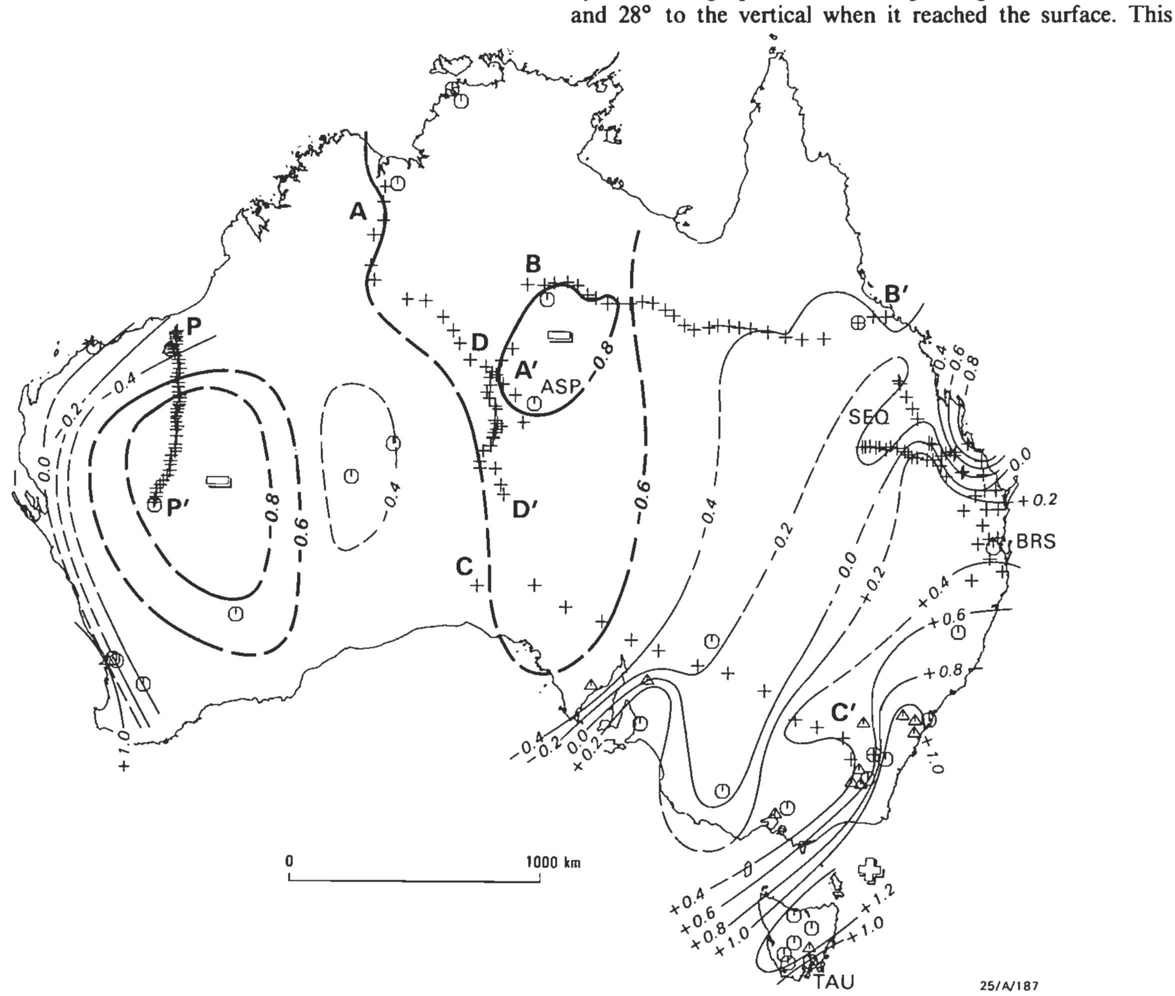

Figure 1. Teleseismic travel time residual map of the Australian continent.

Contour interval 0.2 s. Large circles indicate observatories for which Dziewonski & Anderson (1983) calculated residuals. Triangles are seismic observatories for which residuals were obtained from other sources. Crosses represent temporary seismograph stations. Contours are dashed in areas of few data.

[1]Division of Petrology & Geochemistry, Bureau of Mineral Resources, GPO Box 378, Canberra ACT 2601

[2]Division of Geophysics, Bureau of Mineral Resources, GPO Box 378, Canberra ACT 2601

Table 1. Teleseismic travel-time residuals for Australian stations. Standard deviations for some residuals are available in the original references.

Station mnemonic	*Station type*[1]	*Lat.* °S	*Long.* °E	*Reported residual(s)*	*Method of adjustment*[2]	*Station residual(s)*
ADE	O	34.969	138.709	0.38	1	0.38
ASP	O	23.683	133.897	-0.88	1	-0.88
BFD	O	37.176	142.544	-0.09	1	-0.09
BRS	O	27.392	152.775	-0.02	1	-0.02
CAN	O	35.321	148.999	0.42	1	0.42
COO	O	30.578	151.892	0.73	1	0.73
CTA	O	20.088	146.254	-0.31	1	-0.31
DAR	O	12.408	130.818	-0.47	1	-0.47
GLS	O	25.035	128.296	-0.43	1	-0.43
KAA	O	20.777	116.859	-0.14	1	-0.14
KLG	O	30.784	121.458	-0.75	1	-0.75
KNA	O	15.750	128.767	-0.62	1	-0.62
MBL[3]	O	21.160	119.833	-0.46	1	-0.46
MEK	O	26.613	118.545	-0.80	1	-0.80
MTN	O	12.846	131.130	-0.74	1	-0.74
MUN	O	31.978	116.208	-0.38	1	-0.38
NWA[4]	O	32.927	117.234	-0.43	1	-0.43
PMG	O	9.409	147.154	0.26	1	0.26
RIV	O	33.829	151.158	0.85	1	0.85
SAV	O	41.721	147.189	1.07	1	1.07
SBR	O	35.259	149.533	1.41	1	1.41
SFF	O	41.337	146.307	1.27	1	1.27
SPK	O	43.038	146.275	1.71	1	1.71
STG	O	42.848	146.207	1.20	1	1.20
STK	O	31.882	141.592	-0.23	1	-0.23
SWV	O	31.883	116.065	-0.11	1	-0.11
TAU	O	42.910	147.320	0.95	1	0.95
TOO	O	37.571	145.491	0.24	1	0.24
TRR	O	42.304	146.450	1.30	1	1.30
WAM	O	36.193	148.883	0.46	1	0.46
WBN	O	26.140	126.578	0.09	1	0.09
WRA[5]	O	19.944	134.364	-1.13	1	-1.13
YOU	O	34.278	148.382	0.47	1	0.47
MEL	O	37.832	144.973	0.26	2	0.26
PER	O	31.953	115.840	1.34	2	1.34
TNM01	T	24.349	133.450	-0.02	3	-0.72
TNM02	T	23.374	133.147	-0.12	3	-0.82
TNM03	T	22.998	132.664	-0.58	3	-1.28
TNM04	T	22.656	132.403	-0.20	3	-0.90
TNM05	T	22.369	131.996	-0.60	3	-0.11
TNM06	T	22.114	131.382	-0.09	3	-0.79
TNM07	T	21.515	131.986	0.01	3	-0.69
TNM08	T	21.055	130.743	-0.04	3	-0.74
TNM09	T	20.566	130.355	-0.09	3	-0.79
TNM11	T	19.967	129.708	-0.15	3	-0.85
TNM12	T	19.899	129.000	0.01	3	-0.69
TNM14	T	19.1745	127.790	-0.24	3	-0.94
TNM15	T	18.6422	127.672	0.08	3	0.62
TNM17	T	17.557	127.828	0.24	3	-0.46
TNM18	T	17.056	128.200	0.19	3	-0.51
TNM19	T	16.386	128.232	-0.05	3	-0.75
TNM20	T	15.842	128.300	0.01	3	-0.69
TCT01	T	19.434	134.227	-0.14	4	-0.68
TCT02	T	19.348	134.606	-0.28	4	-0.82
TCT03	T	19.314	134.116	-0.25	4	-0.79
TCT04	T	19.418	135.504	-0.19	4	-0.73
TCT05	T	19.754	135.889	0.01	4	-0.53
TCT06	T	19.852	136.202	-0.35	4	-0.89
TCT07	T	20.039	136.661	-0.36	4	-0.90
TCT08	T	20.027	137.068	-0.34	4	-0.88
TCT09	T	20.017	137.529	0.02	4	-0.52
TCT10	T	19.923	138.000	0.12	4	-0.42
TCT11	T	19.956	138.402	0.19	4	-0.35
TCT12	T	20.189	138.899	-0.23	4	-0.77
TCT14	T	20.693	139.665	-0.01	4	-0.55
TCT15	T	20.833	140.047	0.33	4	-0.21
TCT16	T	20.722	140.623	0.10	4	-0.44
TCT17	T	20.631	140.946	0.55	4	0.01
TCT18	T	20.627	141.378	0.20	4	-0.34
TCT19	T	20.651	141.773	0.14	4	-0.40
TCT20	T	20.663	142.214	0.21	4	-0.33
TCT21	T	19.420	133.581	0.12	4	-0.42
TCT22	T	20.739	142.882	0.19	4	-0.35
TCT23	T	20.856	143.569	0.08	4	-0.46
TCT24	T	20.895	144.198	0.21	4	-0.33
TCT25	T	20.791	145.024	0.22	4	-0.32
TCT27	T	20.088	146.254	0.23	4	-0.31
TCT28	T	19.819	146.807	0.04	4	-0.50
TCT29	T	19.770	147.284	-0.18	4	-0.70
MR	T	30.160	131.580	-0.58	5	-0.58
MU	T	30.150	133.990	-0.70	5	-0.70
KI	T	30.910	135.320	-1.02	5	-1.02
ILN	O	31.393	136.870	-0.23	5	-0.23
PNA	O	32.006	138.165	-0.78	5	-0.78
ME	T	32.330	139.350	-0.27	5	-0.27
MZ	T	32.790	141.070	-0.20	5	-0.20
HA	T	32.980	142.380	0.47	5	0.47
CU	T	33.500	144.000	-0.12	5	-0.12
CA	T	34.420	145.440	0.54	5	0.54
YA	T	34.610	146.410	0.45	5	0.45
WO	T	34.880	147.580	0.37	5	0.37
TAO	O	35.596	148.290	0.37	5	0.37
PIL01	T	20.523	120.140	0.64	6	-0.30
PIL02	T	20.568	120.073	0.64	6	-0.30
PIL05	T	20.810	120.073	0.59	6	-0.35
PIL06	T	20.892	120.070	0.56	6	-0.38
PIL07	T	20.997	120.060	0.55	6	-0.39
PIL08	T	21.068	119.967	0.48	6	-0.46
PIL09	T	21.167	119.928	0.49	6	-0.45
PIL10	T	21.272	119.980	0.47	6	-0.47
PIL11	T	21.412	120.067	0.39	6	-0.55
PIL13	T	21.693	120.065	0.42	6	-0.52
PIL14	T	21.878	120.108	0.52	6	-0.42
PIL15	T	22.037	120.047	0.44	6	-0.50
PIL16	T	22.160	119.945	0.01	6	-0.93
PIL17	T	22.370	119.975	0.14	6	-0.80
PIL18	T	22.523	119.977	0.03	6	-0.91
PIL19	T	22.710	119.948	0.03	6	-0.91
PIL22	T	23.063	119.967	0.35	6	-0.59
PIL23	T	23.163	119.933	0.05	6	-0.89
PIL24	T	23.225	119.913	0.09	6	-0.85
PIL25	T	23.312	119.847	0.00	6	-0.94
PIL26	T	23.428	119.805	0.01	6	-0.93
PIL27	T	23.567	119.760	0.08	6	-0.86
PIL29	T	23.767	119.718	-0.02	6	-0.96
PIL30	T	23.928	119.797	0.03	6	-0.91
PIL31	T	24.043	119.718	0.26	6	-0.68
PIL32	T	24.268	119.713	-0.38	6	-1.32
PIL33	T	24.538	119.633	0.05	6	-0.89
PIL34	T	24.677	119.620	0.30	6	-0.64
PIL35	T	24.787	119.593	-0.02	6	-0.96
PIL36	T	24.918	119.438	0.25	6	-0.69
PIL37	T	25.102	119.368	0.23	6	-0.71
PIL38	T	25.243	119.328	0.17	6	-0.77
PIL39	T	25.448	119.302	0.16	6	-0.78
PIL40	T	25.610	119.188	0.17	6	-0.77
PIL41	T	25.775	119.005	0.54	6	-0.40
PIL42	T	25.918	118.863	0.40	6	-0.54
PIL43	T	26.023	118.692	0.37	6	-0.57
PIL44	T	26.187	118.682	0.33	6	-0.61
PIL45	T	26.328	118.637	0.21	6	-0.73
PIL46	T	26.422	118.582	0.12	6	-0.82
PIL47	T	26.525	118.528	-0.32	6	-1.32
SMQ01	T	27.813	152.708	0.46	7	0.44
SMQ02	T	28.179	153.306	0.17	7	0.15
SEQ01	T	27.113	152.553	-0.05	7	-0.07
SEQ02	T	27.013	152.896	0.04	7	0.02
SEQ03	T	26.664	152.205	0.32	7	0.30
SEQ04	T	26.011	152.728	0.10	7	0.08
SEQ05	T	25.658	151.744	0.13	7	0.11
SEQ06	T	24.872	151.115	-0.17	7	-0.19
SEQ07	T	26.088	152.258	-0.01	7	-0.03
SEQ08	T	24.334	150.654	-0.64	7	-0.66
SEQ09	T	24.400	151.775	-0.60	7	-0.62
SEQ10	T	25.350	152.515	0.03	7	0.01
CBB03	T	28.672	152.119	0.31	7	0.29
CBB04	T	27.349	152.137	-0.08	7	-0.10
CBB05	T	26.247	151.368	0.06	7	0.04
CBB06	T	25.140	150.436	-0.64	7	-0.66
CBB07	T	24.046	149.554	0.28	7	0.26
CBB08	T	22.918	148.735	-0.28	7	-0.30
BBQ03	T	21.989	148.060	-0.17	7	-0.19
BBQ10	T	22.528	148.440	-0.24	7	-0.26
BBQ38	T	24.785	150.140	0.12	7	0.10
BBQ04	T	22.084	148.130	-0.02	7	-0.04
BBQ18	T	23.255	148.991	-0.25	7	-0.27
BBQ29	T	24.070	149.663	0.27	7	0.25
CBB07	T	24.046	149.554	0.31	7	0.29
CBB08	T	22.918	148.735	-0.16	7	-0.18
QHC02	T	23.869	151.133	-0.81	7	-0.83
QHC05	T	24.226	150.695	-0.58	7	-0.60
QHC06	T	24.241	150.458	-0.52	7	-0.54
QHC07	T	24.322	150.277	-0.30	7	-0.32
QHC08	T	24.426	150.110	-0.03	7	-0.05

Station mnemonic	Station type[1]	Lat. °S	Long. °E	Reported residual(s)	Method of adjustment[2]	Station residual(s)
QHC09	T	24.616	149.790	0.30	7	0.28
QHC10	T	24.639	149.563	0.37	7	0.35
QHC12	T	24.611	149.165	0.03	7	0.01
QHC13	T	24.609	148.963	0.13	7	0.11
QHC14	T	24.545	148.800	0.19	7	0.17
QHC15	T	24.458	148.642	0.08	7	0.06
QHC16	T	24.374	148.329	-0.30	7	-0.32
QHC17	T	24.361	148.062	-0.40	7	-0.42
QHC18	T	24.469	147.903	-0.37	7	-0.39
QHC19	T	24.414	147.644	-0.29	7	-0.31
QHC20	T	24.445	147.510	-0.16	7	-0.18
QHC21	T	24.420	147.260	-0.33	7	-0.35
QHC22	T	24.457	147.080	-0.23	7	-0.25
QHC23	T	24.476	146.965	-0.34	7	-0.36
MBQ01	T	24.914	151.054	-0.19	7	-0.21
MBQ02	T	24.875	151.924	-0.52	7	-0.54
MBQ03	T	25.350	152.515	-0.05	7	-0.07
MBQ04	T	25.423	152.073	-0.18	7	-0.20

Notes:

[1]O Seismic observatory. Not all observatories listed are still operating.

T Temporary station.

[2]1 Source is Dziewonski & Anderson (1983). Residuals listed are the azimuth independent values relative to their average global travel-time curve which agrees to within ±0.2 s with the Herrin (1968) times for the distance range 30° to 90°.

2 From Herrin & Taggart (1968). Residuals given are azimuth independent terms relative to the Herrin (1968) travel-time curves.

3 Unpublished data of Wright & Muirhead with a baseline adjustment to fit KNA and ASP. Residuals are for the azimuth range 85 to 125°.

4 Unpublished data of Wright & Muirhead with a baseline adjustment to fit WRA and CTA. Residuals are for the azimuth range 85 to 125°.

5 Source is Cleary & others (1972). Station coordinates are estimates only. Residuals listed are relative to the Herrin (1968) travel-time curves. No adjustment was necessary to make these values agree with those of observatories on or near the line of temporary stations.

6 Residuals are from Drummond (1979) with a baseline adjustment to fit MBL (near stations PIL08-PIL10) and MEK (near stations PIL46 and PIL47).

7 From Hearn & Webb (1984), whose original residual values were relative to BRS.

[3]Includes MBT

[4]Includes NWAO

[5]Includes WB2, WB3, WB4 & WCB

paper summarises the residuals now available by providing a contoured map (Fig. 1) of the residuals. Most of the residuals are listed in Table 1. The structures responsible for the residuals are briefly discussed.

Method of constructing the map

Several studies have produced seismic travel time residuals for Australian observatories. The most comprehensive and regional was that of Dziewonski & Anderson (1983), who used an iterative procedure to locate more than 3000 earthquakes, refine the P-wave residuals to 1000 seismic stations scattered worldwide, and calculate the residuals for the stations. Thirty-four of the stations were in Australia. Their study supersedes several that used similar procedures to determine residuals for Australian stations (eg. Cleary & Hales, 1966; Herrin & Taggart, 1968; Lilwall & Douglas, 1970), and extends other studies in which the residuals were calculated in relation to published global travel time curves. For example, Poupinet (1979) and Hearn & Webb (1984) used the curve of Jeffreys & Bullen (1940); and Cleary & others (1972) used the curves of Jeffreys & Bullen (1940) and Herrin (1968). The residuals for many of the stations studied by Dziewonski & Anderson exhibited azimuthal dependence. The mean residuals for the 34 Australian stations in the Dziewonski & Anderson study were used as a base to which residuals from all of the other studies were adjusted.

The residuals for several observatories not studied by Dziewonski & Anderson (1983) were available in Herrin & Taggart (1968) and Cleary (1967), which fortunately had several observatories in common with the Dziewonski & Anderson study, allowing the adjustment of the residuals to the Dziewonski & Anderson base. We have included the residuals from the regional study of Hearn & Webb (1984) in southeast Queensland (SEQ in Fig. 1) and the traverse of Cleary & others (1972) (the Cannikin line, C–C′). Unpublished residuals from Drummond (1979) (line P–P′) and from the studies of Wright and Muirhead, that include the results of Wright & others (1985) (lines A–A′ and B–B′), were adjusted until they generally agreed with the values for observatories at both ends of each line. The adjustments required only baseline shifts; no regional trends had to be removed from any of the lines. The results of Lambeck & Penney (1984) and Lambeck (1986) (P–P′, Fig. 1) were not tied to the observatory network, so they are not listed in Table 1. The baseline for their array of stations was adjusted until the northern stations agreed with the values for adjacent stations on line A–A′. Their residuals were useful for controlling the shape of the contours in central Australia. Lambeck (1986) showed that the residuals for several stations in central Australia have a strong azimuthal dependence. The values used in Figure 1 are the mean values for the stations.

Discussion

The contours represent a very smoothed picture of the residuals, because the data set is not large or evenly distributed. Intensive studies in small areas show that the residuals can vary by a large amount over small distances. Abrupt changes of more than 1.0 s correlate with known major changes in the upper crust, such as from granulite outcrop to areas of thick sediment in central Australia (Lambeck & Penny, 1984), and from the Perth Basin eastwards to the Yilgarn Block (Fig. 1). Smaller changes of more than 0.5 s occur over distances of tens to hundreds of kilometres in eastern Australia where the geophysical signature, especially the gravity field, does not indicate major structural changes (Hearn & Webb, 1984).

The residuals at many stations are azimuth dependent. Lambeck (1986) found that relative residuals at stations in central Australia vary by more than a second as the azimuth from earthquake sources varies from north through east to south. He attributes the azimuthal dependence to the effects of crust/upper mantle structure in the region. Dziewonski & Anderson (1983) identified two azimuthal components in some residuals. One they attributed to the effects of crust/upper mantle structure, and the other to possible seismic anisotropy in the upper mantle. Figure 2 shows their residuals for the stations BRS in eastern Australia, TAU in Tasmania and ASP in the region of central Australia where Lambeck (1986) observed azimuthal dependence of residuals. Two curves are shown for each station: the straight line indicates the mean residual, and the wavy line the azimuth-dependent solution. The bars indicate the rms deviations for the azimuth-dependent solutions. The curves show that, even when the azimuthal dependence of the residuals is considered, the residuals for central Australia (ASP) are different from those for Tasmania (TAU) and are likely to be different from eastern Australian residuals (e.g. BRS). Overlap of the wavy lines will occur only at a small range of azimuths and then only if the scatter of the data is considered.

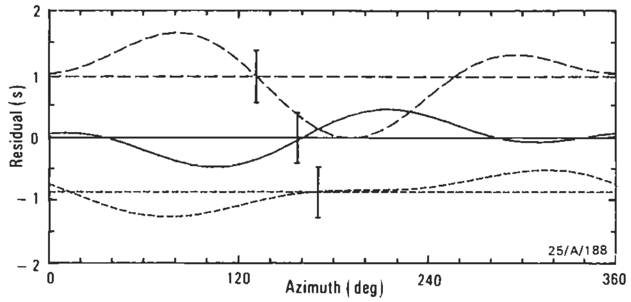

Figure 2. Variation of teleseismic travel time residual with azimuth for the observatories BRS (solid lines), TAU (dashed) and ASP (dotted).
For each station, the straight line shows the azimuth independent term of the residual, the curve shows the azimuth dependent term, and the bar shows the rms residual calculated when the azimuth-dependent residual was derived.

Most of the shield regions of central and western Australia have negative residuals, consistent with shield regions elsewhere in the world (Dziewonski & Anderson, 1983). The most negative residuals occur in the Archaean terranes of Western Australia, and in the Proterozoic terranes of central Australia and the Gawler Block. They are encompassed by the -0.6 s contour. Seismic velocity increases with decreasing temperature. The geothermal compilations of Cull (1982) and Cull & Conley (1983) show that heat flow over the shield (west of 136°E) is generally less than world average. The lowest values (half of the world average) occur over the Yilgarn Block in Western Australia where the residuals are the lowest (generally <-0.6 s). The negative travel time residuals are therefore consistent with lower geothermal gradients in the shield, low temperatures and high velocities in the upper mantle with no low velocity layer above a depth of 200 km (Hales & others, 1980).

Residuals become progressively higher and then positive towards the east, with a difference of more than 1.0 s between the shield in the west and the southeastern coast. The boundary between Phanerozoic eastern Australia and the older shield regions of central and western Australia corresponds approximately to the easternmost -0.4 s contour in Figure 1. The change from shield to non-shield basement correlates with an abrupt change of 0.44 s along line B-B′ (Wright & others, 1985). Along line C-C′, the change from west to east is more gradual. These changes cannot be explained in terms of crustal structure alone. Some, and perhaps most, of the effect must come from the mantle (cf. Finlayson, 1982). The residuals are consistent with a low velocity zone predicted in the upper mantle in the Phanerozoic regions of eastern Australia by Muirhead & others (1977). The low velocity zone probably results from high temperatures in the upper mantle. The region in which residuals exceed -0.5 s generally has higher than world average heat flow (Cull, 1982; Cull & Conley, 1983), indicating high geothermal gradients.

The largest positive residuals are observed in southeastern Australia including Tasmania. In southeastern Australia, they lie in a zone parallel to and near the coastline, and may be, at least partly, an effect of the continental margin. The large positive residuals in Tasmania are state-wide, and occur in several types of geological province including basement outcrop and igneous terranes. They are most probably caused by extremely low velocities in the mantle, probably associated with high temperatures associated with the mantle plume that caused the Cainozoic hot spot activity (Wellman, 1983).

Acknowledgements

We thank Kurt Lambeck for copies of his unpublished results from central Australia.

References

Cleary, J.R., 1967 — P times to Australian stations from nuclear explosions. *Seismological Society of America, Bulletin*, 57, 773-781.

Cleary, J., & Hales, A.L., 1966 — An analysis of the travel times of P waves to North American stations, in the distance range 32° to 100°. *Seismological Society of America, Bulletin*, 56, 467-489.

Cleary, J.R., Simpson, D.W., & Muirhead, K.J., 1972 — Variations in Australian upper mantle structure, from observations of the Cannikin explosion. *Nature*, 236, 111-112.

Cull, J.P., 1982 — An appraisal of Australian heat flow data. *BMR Journal of Australian Geology & Geophysics*, 7, 11-21.

Cull, J.P., & Conley, D., 1983 — Geothermal gradients and heat flow in Australian sedimentary basins. *BMR Journal of Australian Geology & Geophysics*, 8, 329-337.

Drummond, B.J., 1979 — Structural relations between the Archaean Pilbara and Yilgarn Cratons, Western Australia, from deep seismic sounding. *M.Sc. thesis, Australian National University, Canberra.*

Dziewonski, A.M., & Anderson, D.L., 1983 — Travel-times and station corrections for P waves at teleseismic distances. *Journal of Geophysical Research*, 88, 3295-3314.

Finlayson, D.M., 1982 — Geophysical differences in the lithosphere between Phanerozoic and Precambrian Australia. *Tectonophysics*, 84, 287-312.

Hales, A.L., Muirhead, K.J., & Rynn, J.M.W., 1980 — A compressional velocity distribution for the upper mantle, *Tectonophysics*, 63, 309-348.

Hearn, S.J., & Webb, J.P., 1984 — Relative teleseismic P residuals and upper mantle structure in eastern Queensland, Australia. *Seismological Society of America, Bulletin*, 74, 1661-1681.

Herrin, E., 1968 — Introduction to the '1968 seismological tables for *P* phases'. *Seismological Society of America, Bulletin*, 58, 1193-1195.

Herrin, E., & Taggart, J., 1968 — Regional variations in *P* travel-times. *Seismological Society America, Bulletin*, 58, 1325-1337.

Jeffreys, H., & Bullen, K.E., 1940 — Seismological tables. *British Association for the Advancement of Science, London*, 50 pp.

Lambeck, K., 1986 — Crustal structure and evolution of the central Australian basins. *In* Dawson, J.B., Carswell, D.A., Hall, J., & Wedepohl, K.H., (editors), The nature of the lower continental crust. *Geological Society of London, Special Publication*, 24, 133-145.

Lambeck, K., & Penney, C., 1984 — Teleseismic travel-time anomalies and crustal structure in central Australia. *Physics of the Earth and Planetary Interiors*, 34, 46-56.

Lilwall, R.C., & Douglas, A., 1970 — Estimation of P-wave travel times using the joint epicentre method. *Geophysical Journal of the Royal Astronomical Society*, 19, 165-181.

Muirhead, K.J., Cleary, J.R., & Finlayson, D.M., 1977 — A long-range seismic profile in south-eastern Australia. *Geophysical Journal of the Royal Astronomical Society*, 48, 509-520.

Poupinet, G., 1979 — On the relation between P-wave travel time residuals and the age of continental plates. *Earth and Planetary Science Letters*, 43, 149–161.

Wellman, P., 1983 — Hotspot volcanism in Australia and New Zealand: Cainozoic and mid-Mesozoic. *Tectonophysics*, 96, 225–243.

Wright, C., Muirhead, K.J., & Dixon, A.E., 1985 — The P wave velocity structure near the base of the mantle. *Journal of Geophysical Research*, 90, 623–634.

BMR Journal of Australian Geology & Geophysics, 11, 107–118

Upper Cambrian (Mindyallan) trilobites and stratigraphy of the Kayrunnera Group, western New South Wales

Wang Qizheng[1], K.J. Mills[2], B.D. Webby[2], & J.H. Shergold[3]

Nine species of trilobites are recorded from three localities within a restricted stratigraphic interval near the base of the newly defined Kayrunnera Group (previously Kayrunnera Beds) on Kayrunnera station, western New South Wales. These occurrences come from the Boshy Formation of the Kayrunnera Group. The trilobites described include species of *Ammagnostus, Meteoraspis, Biaverta, Blackwelderia, Bergeronites,* and *Placosema.* This assemblage is early Late Cambrian (Mindyallan), and most closely referable to the late Mindyallan zone of *Glyptagnostus stolidotus.* The steeply dipping, weakly cleaved Upper Cambrian–basal Ordovician Kayrunnera Group overlies, with a well-defined angular unconformity, a more deformed tightly folded and strongly cleaved, graded, turbidite sandstone sequence. The turbidite succession is considered to be Early to Middle Cambrian, by lithological correlation with similar rocks containing sponge spicules and trace fossils elsewhere in the Wonominta Block. The upright isoclinal folds of this sequence and the angular unconformity were produced during a major orogenic phase, probably an early expression of the Delamerian Orogeny, in late Middle Cambrian time. After uplift and erosion there followed a period of early–middle Late Cambrian marine transgression, during which the lower part of the Kayrunnera Group was deposited. The beds include the trilobite-bearing Boshy Formation, of shallow marine origin.

Introduction

In 1963, officers of the Geological Survey of New South Wales discovered and mapped a trilobite-bearing sequence near Kayrunnera homestead, and this sequence was observed to overlie an older basement (Rose & others, 1964; Rose, 1974). Trilobites collected from near the base of the sequence south of the homestead were identified by A.A. Öpik (1975) and found to be of Mindyallan (early Late Cambrian) age. The sequence was referred to informally as the Kayrunnera Beds (Brunker & others, 1971).

One of the authors (KJM) mapped the extent of the trilobite-bearing sequence in detail from a fault south of Kayrunnera homestead northwest to the southeastern flanks of Koonenberry Mountain, a distance of 28 km (Fig. 1). The unconformity at the base of the sequence can be traced from south of Kayrunnera homestead northwest to Morden Creek, a distance of 16 km. Throughout its length the unconformity surface appears remarkably smooth and eroded across an older tightly folded and cleaved, immature, graded, lithic sandstone sequence, which has undergone low grade regional metamorphism. The fossiliferous sequence is less-cleaved, but dips steeply, and the extent of its exposure is controlled by near-vertical faults, which curve southeast and east from the Koonenberry Fault System near Koonenberry Mountain. On Kayrunnera station only the lower part of the sequence is preserved, but southeast of Koonenberry Mountain, on Wonnaminta station, over 2000 m of section has been measured. The sequence has been formally renamed the Kayrunnera Group and divided into three formations — the basal Morden Formation, the Boshy Formation and the Watties Bore Formation (Webby & others, 1988).

The purpose of this paper is to record new observations on the Mindyallan (early Late Cambrian) trilobite fauna collected from three localities near the base of the Kayrunnera Group. The localities are defined by reference to the Australian Map Grid on 1:100 000 topographic sheets of the Central Mapping Authority, New South Wales, as follows:

Locality No. I (including BMR locality K333): Kayrunnera 7436; grid ref.476-041

Locality No. II: Wonnaminta 7336; grid ref. 409-089

Locality No. III: Wonnaminta 7336; grid ref. 409-088

All localities belong to a fairly restricted stratigraphic interval within the Boshy Formation (Fig. 2). The trilobites are preserved as moulds in a fine-grained silty calcareous sandstone.

The three localities have produced the following assemblages. From locality No.I, the association includes *Ammagnostus* sp. indet., *Meteoraspis* sp. cf. *M. bidens* Öpik, 1967, *Biaverta* sp. cf. *B. reineri* Öpik, 1967, *Blackwelderia* sp. cf. *B. repanda* Öpik, 1967, *Bergeronites italops* (Öpik, 1967) and *Bergeronites* sp. indet. At locality No.II the assemblage comprises *M.* cf. *bidens, Biaverta* cf. *reineri, Blackwelderia* cf. *repanda* and *Placosema* cf. *adnatum* Öpik, 1967. A third assemblage has been recorded from locality No. III, and it includes *Biaverta* cf. *reineri, Biaverta* sp. indet. and *Blackwelderia* cf. *repanda.*

Compared with the distribution of trilobites in the Mindyallan successions of western Queensland (Öpik, 1963; 1967), these New South Wales assemblages seem most closely comparable with those of the Zones of *Acmarhachis quasivespa* and *Glyptagnostus stolidotus.* The agnostid genus *Ammagnostus* ranges through these Mindyallan Zones in Queensland. Of the polymeroid species, *Blackwelderia repanda* and the genus *Meteoraspis* are restricted to the Zone of *Glyptagnostus stolidotus,* while *Bergeronites italops* and *Placosema adnatum* are known from both the *A. quasivespa* and *G. stolidotus* Zones. *Biaverta reineri* is recorded only from the early Mindyallan *Erediaspis eretes* and *Acmarhachis quasivespa* Zones (Öpik, 1967). Over all, it seems that the ranges of the New South Wales assemblages are best regarded as belonging to the Zone of *Glyptagnostus stolidotus,* or, less likely, to a position near the boundary between the Zones of *Acmarhachis quasivespa* and *G. stolidotus.*

Structural and stratigraphical relationships

The steeply dipping Koonenberry Fault is a major tectonic feature developed parallel to the structural grain of the older basement rocks. This fault may be traced throughout the length of the Wonominta Block, either by surface expression (brecciated and sheared rocks) or by means of aeromagnetic maps, which reveal a marked contrast in magnetic signature across the fault trace (Leitch & others, 1987). Rocks as young as Late Palaeozoic age are cut by the fault, and Upper

[1] Department of Geology, Hebei Institute of Geology, Xuanhua County, Hebei Province, The Peoples Republic of China

[2] Department of Geology and Geophysics, University of Sydney, New South Wales, 2006

[3] Division of Continental Geology, Bureau of Mineral Resources, GPO Box 378, Canberra, ACT 2601

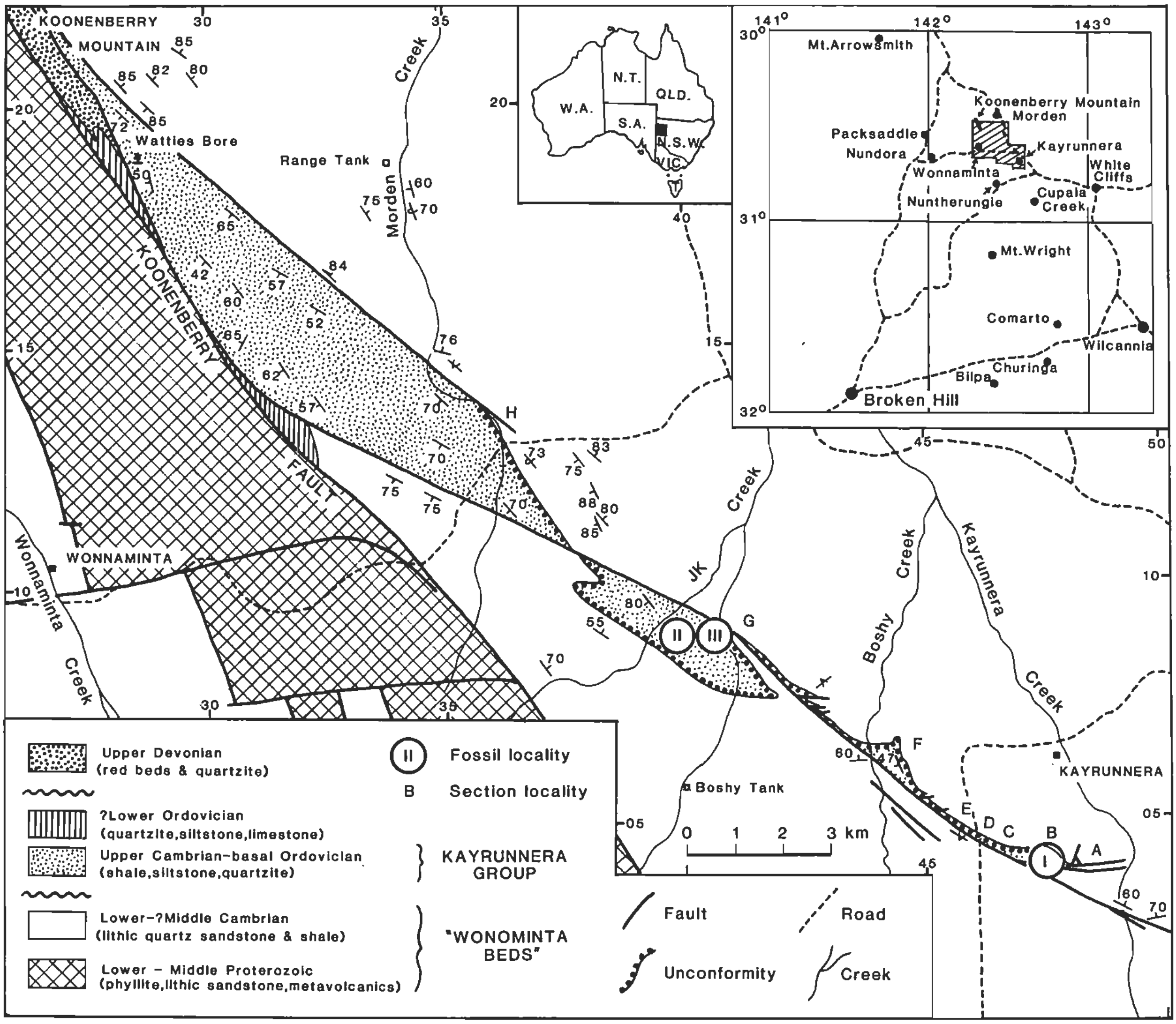

Figure 1. Geological map of the Kayrunnera-Wonnaminta area and inset locality maps of far western New South Wales to show location of the trilobite collecting localities Nos.I, II and III, and the positions of the sections shown in Fig.2.

Devonian quartzite is commonly preserved as upended or downfaulted slivers caught within the fault zone. Whereas in some places the fault is a simple planar structure, in others it branches into a number of sub-parallel surfaces, such as those which define the flanks of Koonenberry Mountain, an elongate upended blade of Upper Devonian quartzite and other Palaeozoic rocks several hundred metres wide and up to 10 km long (Fig. 1). Several near-vertical faults branch off from the Koonenberry Fault on the eastern side and trend towards the southeast and east. In the region between Koonenberry Mountain and Kayrunnera these branch faults control the distribution of the Kayrunnera Group, so that it is bounded either by these faults or by the basal unconformity. Movement on the Koonenberry Fault System is undoubtedly large, but evidence of the sense of movement is equivocal. From the curvature of some of the branch faults it may be suggested that they had a large component of dip-slip movement (northeast side down) through the Palaeozoic.

The Kayrunnera Group occurs as a series of steeply dipping fault-bounded wedges and is known only east of the Koonenberry Fault in the Koonenberry-Kayrunnera region, where it overlies a monotonous sequence of tight to isoclinally folded and well-cleaved, immature, feldspathic lithic sandstone of turbidite aspect. However, correlatives of the Kayrunnera Group may occur at Cupala Creek, Comarto and Churinga (east of the Koonenberry Fault), and at Mt Arrowsmith, Mt Wright and near Bilpa (west of the Koonenberry Fault).

Both the Kayrunnera Group and the underlying sequence tend to weather very readily, leading to subdued topography and poor exposure east of the Koonenberry Fault. Higher ground to the west of the Koonenberry Fault shows better exposures of Precambrian Wonominta Beds, a more thoroughly deformed sequence dominated by wide belts of phyllite and fine-grained lithic sandstone metamorphosed to the biotite zone of regional metamorphism. Within this older sequence are a number of magnetitic phyllite horizons and basic rock units, which define an interesting pattern on aeromagnetic maps (Stevens, 1985). To the west of the older rocks is a further belt of lithic sandstone, like that exposed east of the Koonenberry Fault. This belt passes through Wonnaminta and Nuntherungie homesteads. Slaty units within this belt near Wonnaminta homestead contain sponge spicules. Sponge spicules, along with trace fossils, are also found in the Copper Mine Range Beds (Webby, 1984), which unconformably underlie the Upper Cambrian Cupala Creek Formation (Powell & others, 1982) near Cupala Creek (30 km SSE of Kayrunnera homestead). No fossils have so far been found in the lithic sandstone or rarer slate beds that

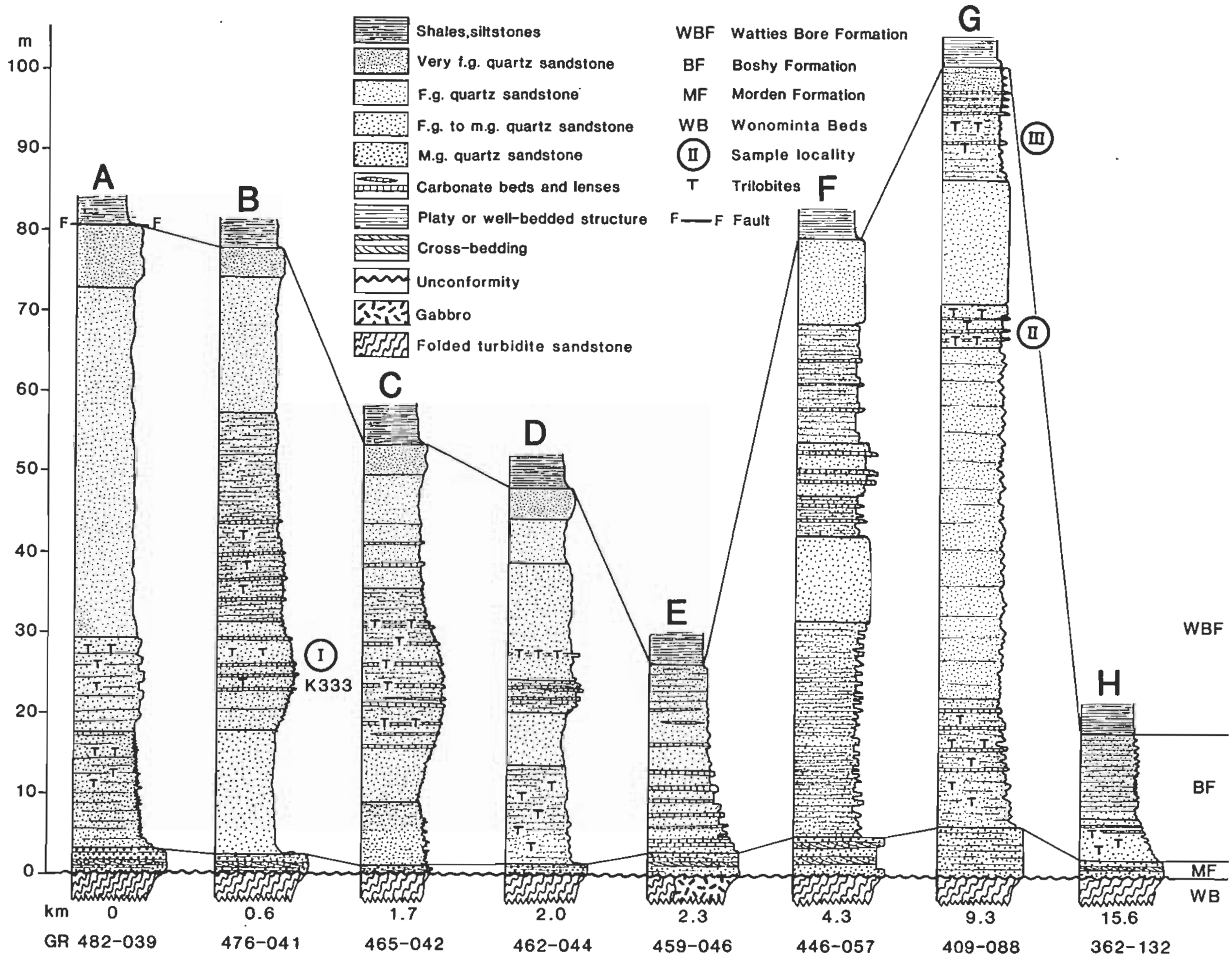

Figure 2. Stratigraphic columns of sections through the lower part of the Kayrunnera Group in the Kayrunnera-Wonnaminta area. For location of these columns see Fig. 1.

Note the stratigraphic positions of the trilobite collecting localities Nos. I (including BMR locality K333), II and III in the lower Upper Cambrian Boshy Formation of the Kayrunnera Group. The other horizons shown as exhibiting trilobites in the columns are either too fragmentary or too poorly preserved to be worthy of further detailed study. WB Wonominta Beds; MF Morden Formation; BF Boshy Formation; WBF Watties Bore Formation.

underlie the Kayrunnera Group, but, by lithological correlation with some sections of the Copper Mine Range Beds and the lithic sandstone and slate beds around Wonnaminta homestead, an Early to Middle Cambrian age is considered likely.

The greatest thickness of the Kayrunnera Group (over 2000 m) is preserved in the Koonenberry-Wonnaminta region, where most of the section is composed of weakly cleaved shaly slate and siltstone of the Watties Bore Formation. The best exposures of the lower part of the sequence (Morden and Boshy Formations) and the basal unconformity occur to the southeast on Kayrunnera Station. Eight stratigraphic sections, A to H (Fig. 2), have been measured from the unconformity through the Morden and Boshy Formations.

The sections illustrate wide variation in thickness and lithological character of the lower part of the succession, and also show the stratigraphic position of the sampled localities.

Where the Kayrunnera Group shows well-preserved lamination or bedding, it characteristically dips very steeply to the west and is, for the most part, west facing. Silty and shaly rocks within the sequence may show a weak to moderate sub-vertical cleavage trending 120°, which initiates pencil slate weathering in finely laminated shales. The degree of metamorphism is slight (chlorite zone), and narrow quartz veins are only rarely encountered. White quartz veins and pods are a prominent feature of the older basement rocks, especially in the multiply deformed phyllites west of the Koonenberry Fault. The unconformity at the base of section E (Fig. 2) appears to overlie a weathered gabbro intrusion into the older basement. No basic intrusions penetrate the Kayrunnera Group.

The basal unit of the Kayrunnera Group is the Morden Formation, consisting of a distinctive hard white medium-grained quartzite, 1–6 m thick, forming prominent exposed outcrops over much of its strike length. Within the unit, bedding is often defined by fine silty laminations or partings. Small to medium scale cross-bedded units are not uncommon (Fig. 2, Sections A,B,E,F) and, based on 6 measurements, suggest a southeasterly current source. Thin limestone lenses and a calcareous cement may be found in places (e.g. section E, Fig. 2).

The overlying Boshy Formation consists of interbedded fine-grained quartz sandstone, feldspathic quartz sandstone, siltstone, and some calcarenite and impure limestone beds and lenses. The measured sections A to H show considerable variation in thickness of this formation (from 15.7 m in section H to 94.3 m in section G, 6.3 km south). The base of the formation is defined by a sharp contact with the hard medium-grained quartzite of the Morden Formation, and the top is sharply defined by the incoming of soft recessive yellow-weathering shale of the Watties Bore Formation. The lithological variation within the sections makes it difficult to correlate units from one section to another. Some tentative correlations can be made where the sections are closer together (e.g. sections A to D, Fig. 2). A very fine-grained angular weathering pale-pink to buff-cream coloured sandstone at the top of the section can be correlated from A to D. Some sections are more richly fossiliferous than others, and trilobites, usually associated with carbonate-rich beds and lenses, may be found in one or more horizons in a column (e.g. section G). No particular age distinctions were made between specimens recovered at localities 4 and 5 within section G. Further sampling may eventually reveal subtle age differences.

The Morden and Boshy Formations together represent a progression of nearshore to shallow marine facies, accumulated during a Late Cambrian marine transgression across eroded rocks of the earlier, pre-Middle Cambrian fold belt succession. Exposed in the creek channel at grid ref. 410-076 (Wonnaminta sheet 7336) is a local lens of lithic conglomerate, reminiscent of that at the base of the Cupala Creek Formation, but preserved here at the base of the Morden Formation. This conglomerate contains rounded pebbles and cobbles of lithic arenite, up to 50 mm across, and may represent a localised fluvial deposit that formed immediately before the main marine transgression. Elsewhere, the unconformity surface at the base of the Kayrunnera Group appears remarkably smooth, with the eroded debris being composed of a blanket of medium-grained quartz sand. Above the Boshy Formation is a thick sequence (>2000 m) of finely laminated siltstone and shale of the Watties Bore Formation. These rocks represent a deeper marine facies and contain species of trilobites more representative of an 'outer detrital facies' (Webby & others, 1988). This shaly sequence continues upward into the lowermost Ordovician with the appearance of *Hysterolenus* sp.

Correlation of Upper Cambrian sequences in the Wonominta Block

Figure 3 presents a tentative correlation of the Kayrunnera Group with some other Upper Cambrian and Lower Ordovician units within the Wonominta Block. The figure shows an almost two-dimensional section from Mt Wright to Koonenberry Mountain by way of Cupala Creek and Kayrunnera. Middle Upper Cambrian (Idamean) trilobites have been described from shale and shaly limestone near the top of the Cupala Creek Formation (Jell, in Powell & others, 1982), and trilobites of latest Cambrian–early Ordovician ages have been recorded from a number of levels through the Mootwingee Group (Shergold, 1971).

A gap of at least 10 Ma is inferred in the upper part of the Middle Cambrian succession, representing the major

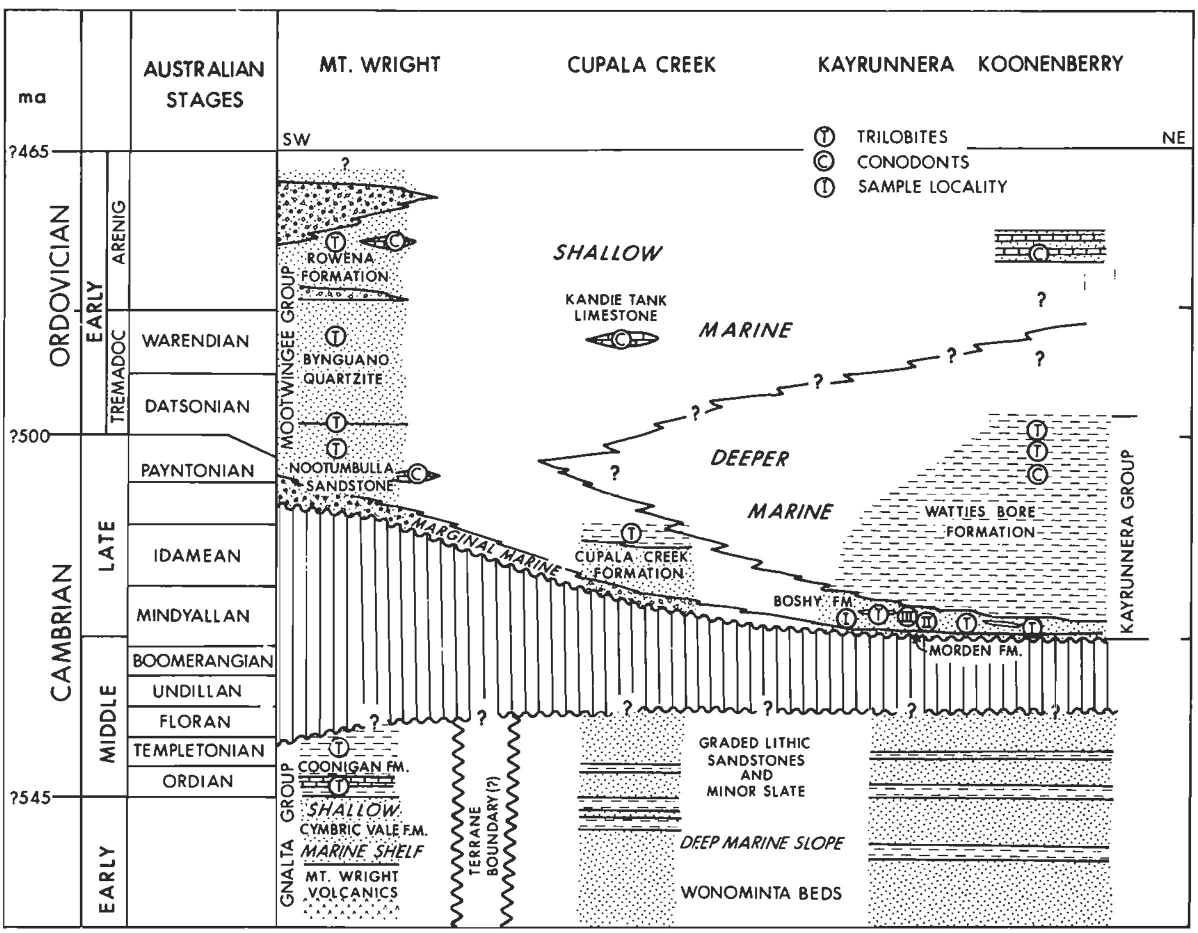

Figure 3. Diagram showing the inferred stratigraphical age and environmental relationships of the Cambrian–Early Ordovician deposits in Western New South Wales.
Note the major late Middle–Late Cambrian break (Mootwingee Movement of the Delamerian Orogeny) shown by the vertical lines.

orogenic phase, probably the main expression of the Delamerian Orogeny, in western New South Wales. This was a time of intense, upright, tight to isoclinal folding of the previously deposited, deeper marine turbidite facies, lithic sandstone of Early to early Middle Cambrian age in the central and eastern parts of the Wonominta Block. These intensely deformed rocks are separated from the less intensely folded and metamorphosed western shallow shelf facies at Mt Arrowsmith and Mt Wright (Gnalta Group) by one and two terrane boundaries, respectively (Leitch & others, 1987).

The stratigraphic break that developed above these Early-early Middle Cambrian deposits existed through the late Middle Cambrian of the Kayrunnera and Wonnaminta areas, a little longer, to early Late Cambrian, at Cupala Creek, and until the mid-late Late Cambrian in the Mt Wright area. This break was previously identified near Mt Wright as representing an important orogenic pulse (Mootwingee Movement) of the Delamerian Orogeny (Webby, 1978). The major break in the Amadeus Basin is, by comparison, also identified as reflecting the Delamerian Orogeny, but only extends through the Late Cambrian (post-Mindyallan to pre-Payntonian) interval (Shergold, 1986). In the Flinders Ranges of South Australia, Jago & Daily (in Cooper & Grindley, 1982, p.11) noted that at least part of the Lake Frome Group is late Middle Cambrian age, but then sedimentation was 'halted by the Late Cambrian-Ordovician Delamerian Orogeny'. Most of the evidence of age of the Delamerian Orogeny as near the Cambrian-Ordovician boundary in the Adelaide Fold Belt seems to come from radiometric dates of granites (Preiss, 1987), but these probably reflect the cooling history rather than the timing of major folding and uplift events in the fold belt. In western New South Wales, the break seems to have been established a little earlier than elsewhere, and it may be interpreted as suggesting a slightly earlier start to the major orogeny in this most easterly part of the Precambrian-Early Palaeozoic fold belt.

The markedly diachronous overlying Late Cambrian-Early Ordovician sequences formed part of a depositional system with common provenance, facies and faunal relationships, and a consistent palaeogeography. They have linkages across a region formerly divided into three terranes (Leitch & others, 1987). In terms of generalised palaeogeography, most of the area of the Wonominta Block had a shelf-like configuration, and has been referred to the Gnalta Shelf (Webby, 1978; 1983). It represented a part of the Gondwana continental shelf, and was dominated by a large delta complex with successive influxes of siliciclastic material being transported across the shelf from the south and west. Gross facies variations and cross-bedding directions support this interpretation. A major Late Cambrian-Early Ordovician transgressive-regressive cycle is depicted in Fig. 3, with sandy, trilobite-bearing, on-shelf facies moving slowly southwards through Mindyallan (Boshy Formation) to Payntonian (Nootumbulla Sandstone) time, during the initial transgression. By latest Cambrian-earliest Ordovician (Payntonian-Datsonian) time, near the maximum of the transgression, a deeper, silty, trilobite-bearing, off-shelf (slope or basinal) facies (Watties Bore Formation) developed in the Koonenberry-Kayrunnera area (Webby & others, 1988), while contemporaneous deposits to the south at Mt Wright were marginal to shallow marine, and still farther south at Bilpa, fluvial to marginal marine (Webby, 1983). In the succeeding Warendian to younger regressive phase, there are records of isolated occurrences of shallow-water carbonate (Kandie Tank Limestone of Pogson & Scheibner, 1971) near Cupala Creek, and thin-bedded shelf-type carbonate, shale and quartzite at Koonenberry Gap, these latter closely analogous to Early Ordovician (Arenig) sequences (Yandaminta Quartzite and Tabita Formation) at Mt Arrowsmith (Webby & others, 1981).

Systematic descriptions

Specimens bearing the prefix SUP are deposited in the collection of the Department of Geology and Geophysics, University of Sydney; those bearing the prefix CPC are housed in the Commonwealth Palaeontological Collection of the Bureau of Mineral Resources, Canberra. References to suprageneric taxa erected before 1959 may be found in the *Treatise on Invertebrate Paleontology,* part O (Moore, 1959).

All the material described here is rather poorly preserved as moulds in siltstone or sandstone, and all has been deformed to some degree. It is clearly referable taxonomically to elements of the lower Upper Cambrian (Mindyallan) fauna of western Queensland (Öpik, 1967), but the preservation generally does not allow us to be categoric in our determinations. Accordingly, we have made full use of the confer (cf.). Since this Mindyallan fauna has been described at length by Öpik (1967), minimal description is given here unless significant new information is available as in the case of *Blackwelderia* cf. *repanda,* a practice again dictated by preservation. We do, however, comment at some length on the distribution of the main faunal components, to give some idea of the age limits and geographic spread of this characteristic Asian/Australian biofacies.

Order **Agnostida** Salter, 1864
Suborder **Agnostina** Salter, 1864
Family **Diplagnostidae** Whitehouse, 1936
Subfamily **Ammagnostinae** Öpik, 1967
Genus ***Ammagnostus*** Öpik, 1967

Type species. *Ammagnostus psammius* Öpik, 1967

Ammagnostus sp. indet.
Fig. 4A-D

Material. Two cephalic internal moulds (CPC 26515 & 26516), one of which is incomplete, and two pygidial internal mounds (CPC 26517 & 26518), all from locality No. I.

Remarks. Originally, it was thought that the agnostoid material described here represented two distinct genera. Both cephala are laterally compressed to some extent, and thus the distinctiveness of the second glabellar lobe and the configuration of the furrow separating it from the posterior lobe is emphasised to resemble the situation found commonly in *Idolagnostus* Öpik, 1967. In the pygidium, the effaced elongate axis, deliquiate border furrows, wide borders and acrolobe constriction all resemble conditions seen in early Mindyallan species of *Agnostoglossa* Öpik, 1967; already reported from Kayrunnera by Öpik (1975, p.7).

Allowing for preservation and deformation, however, the combination of cephalon and pygidium found at Kayrunnera seems more likely to represent a single species of *Ammagnostus.* Öpik (1967) described four species of this genus from the Mindyallan *Acmarhachis quasivespa* and *Glyptagnostus stolidotus* Zones in western Queensland, and other material has been described from Lesser Karatau, southern Kazakhstan (Ergaliev, 1980) that is of similar age. The genus possibly also occurs in Liaoning Province,

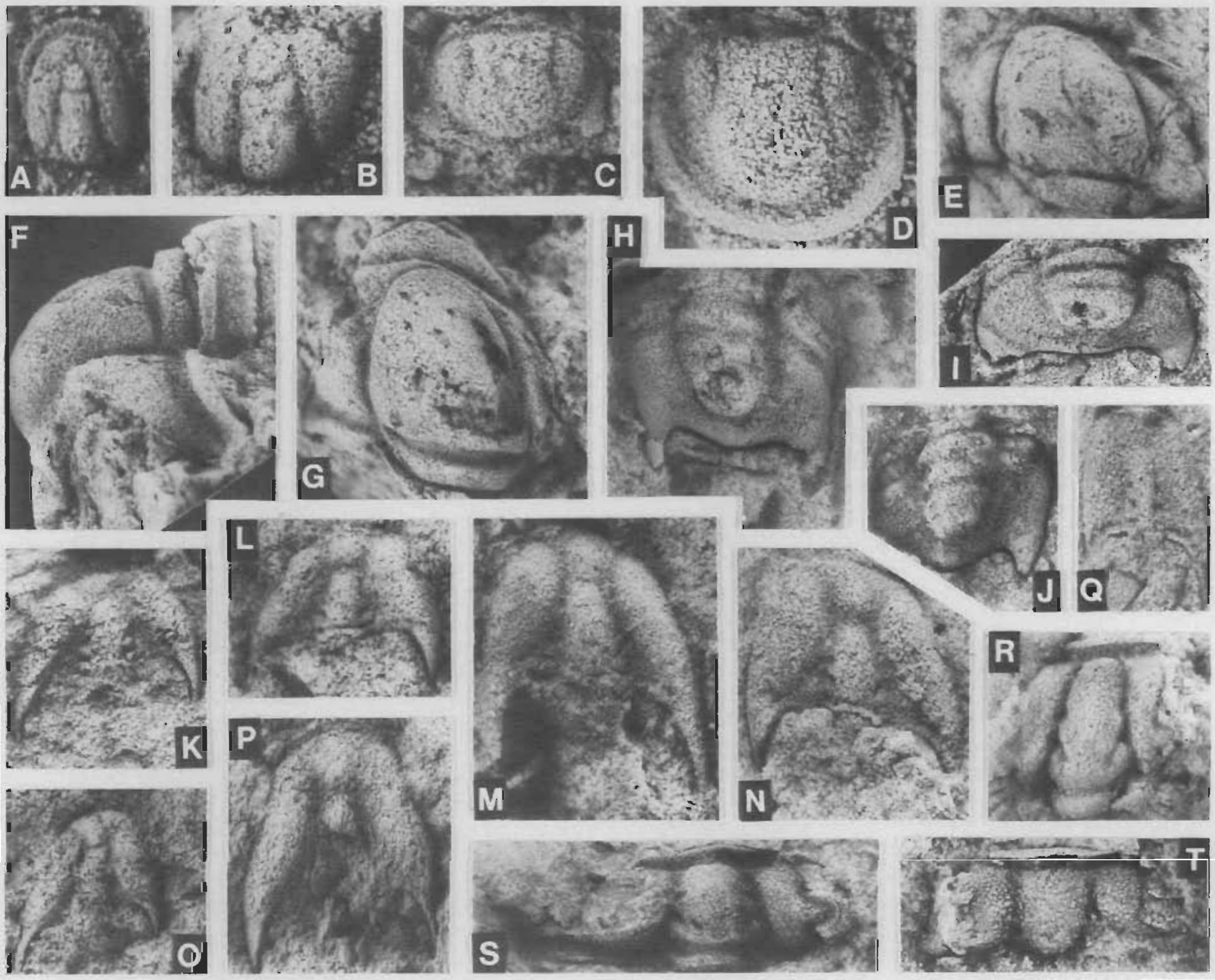

Figure 4. Late Cambrian (Mindyallan) trilobites from the Boshy Formation (Kayrunnera Group) at Kayrunnera.
A-D *Ammagnostus* sp. indet., x10; locality No. I. A, internal mould of cephalon, CPC 26515. B, internal mould of incomplete cephalon, CPC 26516. C, internal mould of incomplete pygidium, CPC 26517. D, internal mould of pygidium, CPC 26518. **E–J *Meteoraspis* sp. cf. *M. bidens*, Öpik, 1967,** x3; E–G from locality No. II, H–J from locality No. I. E, external mould of cranidium of paratype, SUP 54901. F–G, lateral and dorsal views of internal mould of holotype cranidium, SUP 54900. G, internal mould of holotype cranidium, SUP 54900. H, internal mould of paratype pygidium CPC 26519. I, internal mould of paratype pygidium CPC 26520. J, internal mould of paratype pygidium SUP 54902. **K-P *Biaverta* sp. cf. *B. reineri* Öpik, 1967,** x5; locality No. I. K, internal mould of cranidium, CPC 26521. L, internal mould of cranidium, SUP 54903. M, external mould of cranidium, CPC 26522. N, internal mould of cranidium, SUP 54904. O, internal mould of cranidium, SUP 54905. P, internal mould of incomplete cranidium CPC 26523. Q ***Biaverta* sp. indet.**, x5, internal mould of cranidium SUP 54906 from locality No. III. **R-T *Blackwelderia* sp. cf. *B repanda* Öpik, 1967,** x2; locality No. I. R, external mould of cranidium, CPC 26524. S, internal mould of cranidium, CPC 26525. T, internal mould of incomplete cranidium, CPC 26526.

northeastern China (Schrank, 1975) and in the southeast of the Altai Mountains, Siberia (Romanenko *in* Zhuravleva & Rozova, 1977).

The material from Kayrunnera seems most closely to resemble the type species, *A. psammius* Öpik, 1967, from the O'Hara Shale of western Queensland, particularly in glabellar and pygidial axis characteristics, even though the third anterior ring of the latter is not visible. Nevertheless, the general construction of the pygidium, with its constricted acrolobes, broad borders and deliquiate border furrow, and possession of a long (sag.) laterally expanded saccate posterior axial lobe, which extends to the posterior border furrow, seems quite typical. Since the original cephalic shape cannot be determined, and because sufficient comparative material is unavailable, the species from western New South Wales is left under open nomenclature.

Order **Ptychopariida** Swinnerton, 1915
Suborder **Ptychopariina** Richter, 1933
Family **Tricrepicephalidae** Palmer, 1954
Genus ***Meteoraspis*** Resser, 1935

Type species. *Ptychoparia? metra* Walcott, 1890

Meteoraspis sp. cf. ***M. bidens*** Öpik, 1967
Fig. 4E–J

cf. 1967 *Meteoraspis bidens* sp. nov.; Öpik, 1967, pp. 195-198, pl. 5, figs 4–9.

Material. Two cranidia, SUP 54900, an internal mould, and SUP 54901, an external mould; and three pygidial internal moulds, CPC 26519 & 26520 and SUP 54902. Material is from both localities I and II.

Remarks. The genus *Meteoraspis* is widely distributed in North America, Asia and Australia. Up to now, twenty species (apart from uncertain and questionable forms) have been assigned to the genus, among which are the Australian species *M. bidens* Öpik, 1967 and *M.* aff. *bidens* Öpik, 1967 from the early Late Cambrian (Mindyallan) Georgina Limestone, Mungerebar Limestone and O'Hara Shale of western Queensland. A Chinese species of *Meteoraspis* occurs in the Upper Cambrian Lindagogou Group, Nidaogou, Hualong, Qinghai Province (see Xiang & others, 1981, p.62).

Most species of *Meteoraspis*, however, have been described from North America: *M. laticephalus* Kobayashi, 1938, *M. banffensis* Resser, 1942, *M. borealis* Lochman, 1938, *M. spinosa* Lochman, *in* Lochman & Duncan, 1944, *M. robusta* Lochman, *in* Lochman & Duncan, 1944, *M. elongata* Lochman, *in* Lochman & Duncan, 1944, *M. keeganensis* Duncan, *in* Lochman & Duncan, 1944, *M. boulderensis* DeLand, *in* DeLand & Shaw, 1956, *M. globosa* (Miller, 1936), *M. intermedia* Lochman & Hu, 1961, *M. metra* (Walcott, 1890), *M. bipunctata* Lochman, 1938, *M. delia* Lochman, 1940, *M. mutica* Rasetti, 1961, *M. brevispinosa* Rasetti, 1965, and *M. minuta* (Raymond, 1937). One additional species, *M. tinguirensis* Rusconi, 1954 has been reported from Argentina.

The above-listed species are restricted to sequences of the Late Cambrian Mindyallan Zone of *Glyptagnostus stolidotus* in Australia and the *Cedaria* to *Crepicephalus* Zones of North and South America. It is too difficult to analyse all the relationships between these described species because the recorded material is so incomplete: in some, for example, the pygidium is unknown. Nevertheless, the species as a whole may be divided into groups depending on the presence or absence of pygidial spines. The first is typified by *M. brevispinosa* Resetti which has short pygidial spines. The second, characterised by *M. mutica* Rasetti, from the Dresbachian Conococheague Formation of Virginia, has a broad median notch on the posterior margin and lacks pygidial spines. Most species, including all those from Australia, belong to the first group. They are differentiated by cranidial convexity, geometry and organisation of the preglabellar area, size and position of the palpebral lobes, segmentation of the pygidium, and size, shape and orientation of the spines and posterior margin.

Kayrunnera material is quite similar to *Meteoraspis bidens* Öpik, from the Late Cambrian Mindyallan Zone of *Glyptagnostus stolidotus* in western Queensland, but even allowing for indifferent preservation, there are discrete differences. In particular, the cranidium seems more convex (sag., tr.), the glabella proportionately longer (sag.), the preglabellar area slopes adventrally, and the palpebral areas may be narrower (tr.). The pygidium appears to have only two well-defined axial rings, whereas in *M. bidens* there are three, with a fourth indicated, but less distinct. The posterolateral spines are distally incurved (adaxially), whereas in *M. bidens* they are directed straight backwards. There is also cranidial similarity with *Meteoraspis brevispinosa* described by Rasetti (1965) from the late Cambrian *Crepicephalus* Zone of the Lower Limestone Member of the Nolichucky Formation of Tennessee, but again the pygidium assigned to this species has three, rather than two, distinctive axial rings. The American species additionally possesses a straight posterior pygidial margin between the spine bases, whereas on the Australian ones it is always curved.

Family **Menomoniidae** Walcott, 1916
Genus ***Biaverta*** Öpik, 1967

Type species. *Biaverta biaverta* Öpik, 1967

Biaverta sp. cf. ***B. reineri*** Öpik, 1967
Fig. 4K–P

cf. 1967 *Biaverta reineri* Öpik, 1967, pp. 371–372, pl. 39, Figs. 1–5

?1967 *Ascionepea anitys* Öpik, 1967, p. 366, pl. 40, figs. 4–6; pl. 46, fig. 4.

Material. Öpik's original type specimens of *Biaverta reineri* from the Mindyallan Mungerebar Limestone of western Queensland are deposited in the collections of the Bureau of Mineral Resources, Canberra, CPC 5660–5664. The New South Wales material described herein includes a large number of cranidial internal moulds and a few cranidial external moulds CPC 26521–26523 and SUP 54903–54905. These specimens come from all the localities described herein. All the New South Wales material has to a certain degree been compressed or tectonically distorted, and affected by preservation in the sandstone lithology.

Age. In western Queensland the species ranges from the Mindyallan Zone of *Erediaspis eretes* to low in the Zone of *Glyptagnostus stolidotus.*

Remarks. Specimens from New South Wales are essentially similar to *Biaverta reineri* as described by Öpik (1967) from western Queensland. They are, however, larger, have a more strongly convex preglabellar field, and better defined lateral glabellar lobes and furrows. They also have posterolateral limbs which are larger and more strongly retrally directed. Their observed lack of prosopon is probably a function of their preservation in sandstone. *Biaverta* cf. *reineri* is also very similar to *Ascionepea anitys* Öpik, 1967, which is also from the *Erediaspis eretes* Zone in western Queensland. Both, for example, have ill-developed ocular ridges which are in line with the front of the glabella, and bear no anterior border or border furrow. According to Öpik's descriptions, *A. anitys* differs from *Biaverta reineri* Öpik, mainly in being smaller and having minute palpebral lobes (0.2 of the glabellar length), although the latter cannot be seen on Öpik's figures 4–6. *A. anitys* is better considered an early representative of the genus *Biaverta* Öpik, perhaps even a synonym of *Biaverta reineri.* The type species of *Ascionepea* Öpik, *A. janitrix* Öpik, is distinctly different from *Biaverta* in having prominent eyes and a glabella projecting forward beyond the ocular ridges.

Biaverta sp. indet.
Fig. 4Q

Material. One reasonably well-preserved internal cranidial mould (SUP 54906), from locality No. 111.

Remarks. This single specimen of *Biaverta* Öpik is related to the type species, *B. biaverta,* but has a shorter glabella, a shorter (sag.) anterior border, and a longer (sag.) depressed preglabellar field. There is insufficient material to diagnose this species accurately and consequently it is left in open nomenclature.

Family **Damesellidae** Kobayashi, 1935
Subfamily **Damesellinae** Kobayashi, 1935
Genus ***Blackwelderia*** Walcott, 1905

Type species. *Calymene? sinensis* Bergeron, 1899

Age and distribution. Although *Blackwelderia* is known from the late Middle to early Late Cambrian in parts of Asia, in Australia it is confined to the Late Cambrian, Mindyallan Zones of *Erediaspis eretes* through *Glyptagnostus stolidotus* (Öpik, 1967) where its representatives are *B. sabulosa* Öpik, 1967, *B. gibberina* Öpik, 1967 and *B. repanda* Öpik, 1967.

In the Soviet Union, the genus occurs in the late Middle to early Late Cambrian. It is represented by *B.? florens* Lazarenko, 1966 from the Late Cambrian of northern Siberia, and *B. sinensis* (Bergeron, 1899), *B.* cf. *repanda* Öpik, 1967 and *Blackwelderia* sp. from the late Mayan and Ayusokkanian Stages (*Lejopyge laevigata* to *Glyptagnostus* *stolidotus* Zones) of Maly Karatau, southern Kazakhstan (Ergaliev, 1980, 1981).

In the Himalaya, a probable species of *Blackwelderia* has been reported from the Trahagam Formation, Hundwara Tehsil, Kashmir (Jell, 1986).

In China, *Blackwelderia* occurs mainly in the early Late Cambrian Gushan Stage, and has been found in such regions as the North China Platform, the Kunlun-Qiling subprovince, the Yangzi Platform and the Jiangnan geological subprovince. On the North China Platform the Gushan Stage is divided into two zones, the *Blackwelderia* Zone (below) and the *Drepanura* Zone (above). However, *Blackwelderia* is usually found in both zones, even in the type section and locality of the stage, at Gushan County, Shandong Province. Many species of *Blackwelderia* have been described from the North China Platform, including: *B. sinensis* (Bergeron, 1899), *B. sinensis lingchengensis* Sun, 1924, *B. chiawangensis* Chu, 1959, *B. gigas* Sun, 1924, *B. granosa* Endo, *in* Endo & Resser, 1937, *B. liaoningensis* Chu, 1959, *B. longispina* Endo & Resser, 1937, *B. mui* Chu, 1959, *B. octaspina* (Kobayashi, 1935), *B. paronai* (Airaghi, 1902), *B. paronai* var. *penchiensis* Chu, 1959, *B. paronai tieni* Sun, 1924, *B. pingluensis* Zhang & Wang, 1986, *B. shenhi* Chu, 1959, *B. similis* Endo, *in* Endo & Resser, 1937, *B. spectabilis* (Resser & Endo, *in* Endo & Resser, 1937) *B. triangularis* Chu, 1959, *B. disticha* Zhang *in* Qiu & others, 1983, *B. tenuicarina* Zhang *in* Qiu & others, 1983, *B. fengshanensis* Kuo, 1965, and *B. minuta* Zhang & Wang, 1985. Older species have been recently revised by Zhang & Jell (1987).

In the Oulongbuluke area of the Kulun-Qiling geological subprovince, stable platform-type lithological sequences of Cambrian age contain North China-type trilobites, although the Kulun-Qiling subprovince was strictly part of a transitional (intermediate depth) region at that time (Chang, 1988). *Blackwelderia* sp. is often found in the upper portion of the Middle-Upper Cambrian Oulongbuluke Formation, at Oulongbuluke in Qinghai Province, and it has also been reported from the Late Cambrian Wugongy Formation of Xinzigou and Caigou, Xichuan, Henan Province, in the eastern part of the Qiling Mountains (Xiang & others, 1981, pp. 63, 68). On the Yangzi Platform, which was mainly a hypersaline shallow sea during the Middle-Late Cambrian, *Blackwelderia* is rather rare, and only found in some local intercalations of normal shallow marine beds. Species include *B. quangxiensis* Zhou *in* Zhou & others, 1977 from the Upper Cambrian at Shechang, Longlin Ge Autonomous County of Guangxi Province, *B. sinensis* Bergeron, 1899 and *B. paronai* (Airaghi, 1902) from the early Late Cambrian sequences near the border between Yunnan Province and Vietnam; *Blackwelderia* sp. from the lower portion of the Upper Cambrian of Dingyan, Xianfeng (Zhou & others, 1977), and *B. nodosaria* Zhu, 1987 from Xijiadian, Junxian, both in Hubei Province.

The transitional Jiangnan geological subprovince contains a probable species of *Blackwelderia* in the *Paradamesopsis jimaensis-Cyclolorenzella tuma* Zone of Guizhou Province. This zone predates the Gushan Stage and contains *Lejopyge laevigata*, regarded as indicating the uppermost Middle Cambrian in Europe (Yin & Li, 1978). *Blackwelderia* therefore mainly has a normal shallow marine occurrence in the early Late Cambrian of China. However it probably appeared earlier during late Middle Cambrian times, in the transitional regions.

Blackwelderia sp. cf. ***B. repanda*** Öpik, 1967

Fig. 4R–T; Fig. 5A–I

cf. 1967 *Blackwelderia repanda* Öpik, pp. 315-316; pl. 32, fig. 2, pl. 47, fig. 10.

Material. Öpik's previously described type specimens of *Blackwelderia repanda* from the O'Hara Shale of western Queensland are deposited in the collections of the Bureau of Mineral Resources, Canberra, CPC 5736 & 5605. The presently described New South Wales material includes a large number of specimens (cranidia, pygidia and free cheeks) from all localities at Kayrunnera. The best-preserved specimens, though still to a certain degree affected by tectonic distortion, are described herein because they contribute new information on this species. They are referred to specimen numbers CPC 26524–25631 and SUP 54907–54910.

Age. In western Queensland this species is restricted to the early Late Cambrian Mindyallan Zone of *Glyptagnostus stolidotus*.

Description. Cranidium trapezoidal, moderately to strongly convex. Glabella long, forwards tapering, anteriorly truncated, strongly elevated, with three pairs of lateral glabellar furrows and deep well-defined axial furrows; first and second pairs of glabellar furrows (counting from the rear) long, deep, extending inwards and rearwards; third anteriormost pair shorter, sometimes imperceptible, nearly transverse. Occipital ring longer (sag.) at middle, gently narrowing and backwardly curved laterally; occipital furrow broad (sag.) and deep. Preglabellar area consists of broad (sag.), deep and extended anterior border furrow and straight, ridge-like, upturned border; no preglabellar field; pair of indistinct pits (fossulae) located at anterolateral corners of glabella, at intersection of axial and anterior border furrows. Fixed cheeks strongly convex, about two-thirds of glabellar width at level of anterior margins of palpebral lobes; palpebral lobe about 50–60% the glabellar length, crescentic, highly elevated and with deep palpebral furrow on adaxial side; ocular ridge weakly developed extending from anterior end of the palpebral lobe towards anterolateral corner of glabella. Posterolateral limbs narrow (exsag.) and long (tr.), steeply downturned posteriorly; posterior border furrow deep, broad, widening gently laterally; posterior border narrow (exsag.), ridge-like. Anterior branches of facial suture gently convex and forwards converging; posterior branches run nearly transversely and slightly posteriorly, cutting posterior border at a considerable distance (about maximum width of glabella) out from the axial furrow. Dorsal surface of cranidium covered with coarse granules set in a matrix of closely spaced fine granules.

Lateral border of free cheek broad, slightly convex, well-defined by shallow and broad furrow that is continuous with posterior border furrow, but somewhat deeper at genal angle; genal spines long, narrowing from a thickened base, but not in continuity with curvature of outer margin of free cheeks; base of spine situated well in front of posterolateral corner of cephalon; free cheeks also show on their broad, moderately convex external surface a covering of fine and coarse granules.

Pygidium (except for spines) is reversed trapezoidal in dorsal outline, and moderately convex. Axis as wide as the pleural field anteriorly, strongly convex, tapering backwards, consisting of four to five axial rings with semicircular terminal piece; four moderately to strongly convex pleurae divided by deep and broad interpleural grooves. Seven pairs of backwardly and outwardly directed marginal spines developed; fifth pair (from front) more prolonged and robust, but first to fourth (especially the first) also relatively long; sixth and seventh presented as short, dentate extensions of posterior border; base of each spine bears a more or less

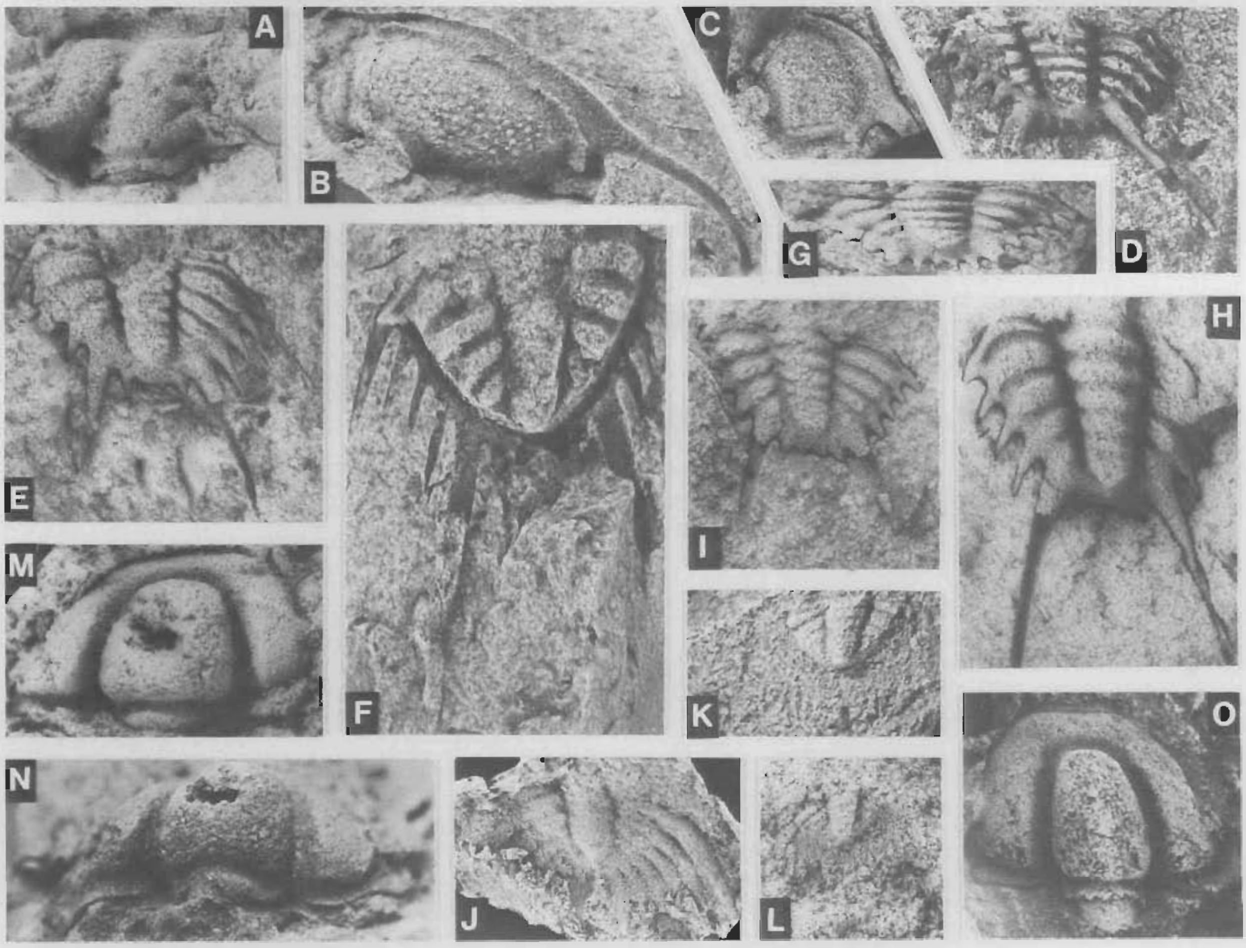

Figure 5. Late Cambrian (Mindyallan) trilobites from the Boshy Formation(Kayrunnera Group) at Kayrunnera.
A–I *Blackwelderia* sp. cf. *B. repanda* Öpik, 1967, x2. A–E & I, locality No. I, F & H, locality No. II. G, locality No. III. A, internal mould of cranidium, CPC 26527. B, internal mould of free cheek, CPC 26528. C, internal mould of free cheek, CPC 26529. D, internal mould of pygidium, CPC 26530. E, internal mould of pygidium, CPC 26531. F, internal mould of pygidium, SUP 54907. G, internal mould of pygidium, SUP 54908. H, internal mould of pygidium, SUP 54909. I, internal mould of pygidium, SUP 54910. J ***Bergeronites italops*** (Öpik, 1967), x2, external mould of pygidium, CPC 26532, locality No. I. **K–L *Bergeronites* sp. indet.,** x2; locality No. I. K, internal mould of pygidium, SUP 54911. L, internal mould of pygidium, CPC 26533. **M–O *Placosema adnatum* Öpik, 1967,** x5; locality No. II. M–N, dorsal and posterodorsal views of internal mould of cranidium, SUP 54912. O, internal mould of cranidium, SUP 54913.

clearly defined granule, only seen on well-preserved specimens (see Fig. 5 D). Surface of pygidium bigranulate.

Remarks. The illustrated cranidia and pygidia have the basic characteristics of *Blackwelderia repanda* Öpik. They have, for example, a straight, upturned and ridge-like anterior border, an extended cephalic marginal furrow, crescentic palpebral lobe, faint ocular ridges, strongly developed pygidial spines, especially the fifth pair, and a granule on the base of each pygidial spine. The only difference between the New South Wales material and that from western Queensland is that the former are a little larger. They also seem to have more closely spaced granulation and a better developed, longer, fifth pair of pygidial spines, but these are comparatively minor distinctions, probably in part reflecting differences in preservation.

Subfamily **Drepanurinae** Hupé, 1953
Genus ***Bergeronites*** Sun *in* Kuo, 1965
[= ***Palaeodotes*** Öpik, 1967, = ***Drepanura*** (***Spinopanura***) Kushan, 1973, = ***Bergeronites*** (***Palaeodotes***) Öpik, 1967 ***sensu*** Peng, 1987]

Type species. *Bergeronites ketteleri* (Monke, 1903)

Remarks: Daily & Jago (1976) first indicated the synonymy of *Palaeodotes* Öpik, 1967 (containing *P. dissidens* Öpik, *P.* aff. *dissidens* Öpik and *P. italops* Öpik) with *Bergeronites* Kuo, 1965. This synonymy was confirmed by Zhou & others (1977) who also suggested the synonymy of *Drepanura (Spinapanura)* Kushan, 1973 (containing *D. (S.) erbeni* Kushan and D. *(Spinapanura)* sp.). Peng (1987) has recently regarded *Palaeodotes* as a subgenus of *Bergeronites* but his justification is not convincing. The type species, *B. ketteleri* (Monke), has recently been reviewed by Zhang & Jell (1987).

Age and distribution. *Bergeronites* is widely distributed in Europe, Asia, Australia and Antarctica and, until now, 33 species have been assigned to the genus. Australian species are *B. dissidens* (Öpik, 1967), *B.* aff. *dissidens* (Öpik, 1967) and *B. italops* (Öpik, 1967) from the Mindyallan *Acmarhachis quasivespa* to *Glyptagnostus stolidotus* Zones of western Queensland. *B.* cf. *italops* (Öpik, 1967) has been identified from the Bowers Group, Mariner Glacier sequence, North Victoria Land (Cooper & others, 1976). *B. eremita* (Westergård, 1947) has been recorded from the *Agnostus pisiformis* Zone of Sweden, and *B. erbeni* (Kushan, 1973) and *Bergeronites* sp. from the early Late Cambrian of northern Iran.

In the Soviet Union *B. ingens* (Poletaeva, 1960) occurs in the Upper Cambrian of West Siberia; *B. acutisulcatus* (Ergaliev, 1980), *B.* cf. *italops* (Öpik, 1967), *B. angustus* (Ergaliev, 1980) and *Bergeronites* sp. occur in the late Middle to early Late Cambrian Mayan to Ayusokkanian Stages (*Lejopyge laevigata* to *Kormagnostus simplex* Zones) of Maly Karatau, southern Kazakhstan; and *B. latus* (Romanenko, 1977) has been found in the Upper Cambrian of the North-East Altai.

In China, *Bergeronites* has been reported from the North China Platform, the Jiangnan transitional region, the Yangzi Platform, and the Talimu, North Tibet–West Yunnan and Qilian geological subprovinces. *B. ketteleri* (Monke, 1903), *B. minus* (Resser & Endo, *in* Endo & Resser, 1937), *B. transversus* (Chu, 1959; = *B. yanshanensis*, Guo & Duan, 1978), *B. huoshanensis* Zhang & Wang, 1985, and *B. wuanensis* Zhang & Wang, 1985 have been described from the early Late Cambrian Gushan Stage of the North China Platform. Other species have been recorded from the upper Middle to lower Upper Cambrian sequences of southern Anhui, western Hunan and eastern Guizhou Provinces in the Jiangnan transitional region, including *B. hunanensis* Yang, 1978, *B. hunanensis minocollus* Qiu, *in* Qiu & others, 1983, *B. austricus* Yang, 1978, *B. major* Zhou, *in* Zhou & others, 1977, *B. augustus* Zhang *in* Qiu & others, 1983, *B bellus* Qiu, *in* Qiu & others, 1983, *B. changdeensis* Peng, 1987, *B. guichiensis* Qiu, *in* Qiu & others, 1983, *B. taoyuanensis* Peng, 1987, *B. transversus* Qiu, *in* Qiu & others, 1983, *B. wannanensis* Qiu, *in* Qiu & others, 1983, *B. wulingensis* Peng, 1987, *B. dissidens* (Öpik, 1967) and *Bergeronites* sp. Additionally, in the eastern part of the Yangzi Platform, specifically in the Langyashan area, Jiangnan-type transitional sediments have yielded *B. langyashanensis* Lu & Zhu, 1980, and *Bergeronites* sp. has been reported from the Upper Cambrian Longpen Formation of the Chuxian-Quangjiao region, Anhui Province. Near the border between Yunnan Province and Vietnam, *B. ketteleri* (Monke) has been recorded, and *Bergeronites* sp. has been reported from the lower Upper Cambrian Hetaoping Formation of Baoshan County, Yunnan Province, as well as in the North Tibet-West Yunnan geological subprovince (Xiang & others, 1981, p.70) and from the Upper Cambrian Lindaogou Group, Liangzui, Yuedu, Qinghai Province from a basinal sequence in the Qilian geological subprovince (Xiang & others, 1981, pp. 60–61). Jiangnan-type deposits and fauna also accumulated during the Middle–Late Cambrian boundary interval of the Kuruktag (formerly called Kulukoshan, in Geelan and Twitchett, 1974) area of the Talimu geological subprovince, where the Mokeershan Formation contains *B.* cf. *hunanensis* Yang, 1978.

In summary, *Bergeronites*, like *Blackwelderia*, has a late Middle Cambrian to early Late Cambrian age, and is found both in platform and basinal deposits, apparently occurring earlier in the latter.

Bergeronites italops (Öpik, 1967)
Fig. 5J

1967 *Palaeodotus italops* Öpik, pp. 345–347, text-figs 132, 133; pl. 16, fig. 2; pl. 50, figs. 9–12; pl. 51, figs. 1–4.

Material. The type specimens of *Bergeronites italops* (Öpik, 1967) from the O'Hara Shale of western Queensland are deposited in the collections of the Bureau of Mineral Resources, Canberra, CPC 5757–5764 and CPC 5486. The presently described New South Wales material comprises only one incomplete external mould of a pygidium (CPC 26532), and comes from locality No.I at Kayrunnera.

Age. In western Queensland this species is recorded from the Mindyallan Zones of *Acmarhachis quasivespa* and *Glyptagnostus stolidotus.*

Remarks. Although the material is poorly preserved, it is larger, and shows the essential features of *Bergeronites italops* (Öpik). In common with that species, the axis consists of four rings, a terminal piece and a short postaxial ridge; the seventh pair of spines is short and close together; and a broad and slightly concave border is present.

Bergeronites sp. indet.
Fig. 5K–L

Material. Two poorly preserved pygidia are recorded from locality No.I. One is an internal mould and the other exhibits both internal and external moulds (CPC 26533 and SUP 54911).

Remarks. Although these pygidia have a more convex axis and pleural fields, they also show the basic features of *Bergeronites italops* (Öpik, 1967). For example, they have an axis consisting of four rings and a terminal piece, a relatively broad and flattened border, and seven pairs of marginal spines, of which the anterior ones are the longer and stronger, and the seventh pair the strongest. The specimens are, however, too poorly preserved to establish whether the material is conspecific with *Bergeronites italops* (Öpik, 1967).

Family **Placosematidae** Öpik, 1967
Genus ***Placosema*** Öpik, 1967

Type species. *Placosema caelatum* Öpik, 1967

Placosema sp. cf. ***P. adnatum*** Öpik, 1967
Fig. 5M–O

cf. 1967 *Placosema adnatum* Öpik, p. 382, pl. 19, fig. 6, pl. 20, fig. 1

cf. 1971 *Placosema adnatum* Hill, Playford & Woods, p. 14, pl. VII, fig. 5.

Material. Öpik's types of *Placosema adnatum* from the Georgina Limestone of western Queensland are deposited in the collections of the Bureau of Mineral Resources, Canberra, CPC 5516 & 5517. The New South Wales material recorded here includes two cranidial internal moulds (SUP 54912 & 54913) and comes from locality No. II.

Age. In western Queensland the species is recognised in the Mindyallan Zones of *Acmarhachis quasivespa* and *Glyptagnostus stolidotus.*

Remarks. The genus Placosema Öpik contains only two species, *P. caelatum* Öpik, 1967 and *P. adnatum* Öpik, 1967. The former is reported by Öpik from the Mungerebar Limestone of western Queensland, and the latter from the Georgina Limestone as well. In addition, the genus is reported by Xiang & others (1981, p.62) from the Upper Cambrian Lindaogou Group, Nidangou, Hualong, Qinghai province.

The two cranidia from the Kayrunnera area of western New South Wales are very similar to *P. adnatum* Öpik, showing the same type of preglabellar border furrow and anteriorly slightly constricted though well-rounded glabella. The only difference between the New South Wales material and Öpik's types of *Placosema adnatum* is the presence of somewhat narrower (tr.) fixed cheeks (about 50 per cent of the glabellar width) but this may be merely an artefact of the tectonic distortion of the former specimens, hence the confer (cf.) used in the determination.

Acknowledgements

This study has been supported by funds from the Australian Research Grants Committee (ARGS grant no. E82/15297). We thank Dr J.R. Laurie, BMR, for comments on an earlier draft of this paper, and Drs R.A. Henderson (James Cook University) and J.B. Jago (S.A. Institute of Technology) for helpful suggestions on a later draft.

References

Airaghi, C., 1902 — Di alcuni trilobiti della Cina. *Atti della Società italiana di scienze naturali,* 41(1), 2–27.

Bergeron, M.J., 1899 — Étude de quelques trilobites du Chine. *Bulletin de la Société Géologique de France,* 27, 499–519.

Brunker, R.L., Offenberg, A., & Rose, L., 1971 — Koonenberry 1:500 000 *Geological Sheet. Geological Survey of New South Wales, Sydney.*

Chang, W.T., 1988 - The Cambrian System in eastern Asia. *Union of Geological Sciences, Publication* 24, 81 pp., 4 correlation charts.

Chu Chaoling, 1959 — Trilobites from the Kushan Formation of North and Northeastern China. *Memoir of the Nanjing Institute of Geology and Palaeontology,* 2, 44–128, pls I-VII.

Cooper, R.A., & Grindley, G.W., 1982 — Late Proterozoic to Devonian sequences of southeastern Australia, Antarctica and New Zealand and their correlation. *Geological Society of Australia, Special Publication* 9, 1–103.

Cooper, R.A., Jago, J.B., Mackinnon, D.I., Simes, J.E., & Braddock, P.E., 1976 — Cambrian fossils from the Bowers Group, Northern Victoria Land, Antarctica. *New Zealand Journal of Geology and Geophysics,* 19(2), 283–288.

Deland, C.R., & Shaw, A.B., 1956 — Upper Cambrian trilobites from western Wyoming. *Journal of Paleontology,* 30(3), 542–562.

Endo, R., & Resser, C.E., 1937 — The Sinian and Cambrian and fossils of southern Manchukuo. *Bulletin of the Manchurian Science Museum,* 1, 1–474, pls. 14–73.

Ergaliev, G. Kh., 1980 — Middle and Upper Cambrian trilobites of the Maly Karatau Range. *Academy of Sciences of the Kazakh SSR, Order of the Red Banner of Labour K.I. Satpaev Institute of Geological Sciences,* 1–211. Nauka, Kazakh Publishing House, Alma-Ata.

Ergaliev, G. Kh., 1981 — Upper Cambrian biostratigraphy of the Kyrshabakty section, Maly Karatau, southern Kazakhstan. *In* Taylor, M.E. (editor), Short papers for the second international symposium on the Cambrian System. *United States Geological Survey, Open File Report* 81-743, 82–88.

Geelan, P.J.M., & Twitchett, D.C. (editors), 1974 — *The Times Atlas of China.* Time Books, London, 144 pp.

Guo Hongjun & Duan Jiye, 1978 — Cambrian and Early Ordovician trilobites from northeastern Hebei and western Liaoning. *Acta Palaeontologica Sinica,* 17(4), 445–458, 3 pls. [In Chinese with English abstract].

Hill, D., Playford, G., & Woods, J.T. (editors), 1971 — Cambrian fossils of Queensland. *Queensland Palaeontographical Society, Brisbane,* 1–32.

Jell, P.A., 1986 — An early Late Cambrian trilobite faunule from Kashmir. *Geological Magazine,* 123(5), 487–492.

Kobayashi, T., 1935 — The Cambro-Ordovician formations and faunas of South Chosen. Paleontology, Pt. III. Cambrian faunas of South Chosen with special study on the Cambrian trilobite genera and families. *Journal of the Faculty of Science, Imperial University of Tokyo, series 2,* 4(2), 49–344.

Kobayashi, T., 1938 — Upper Cambrian fossils from British Columbia. *Japanese Journal of Geology and Geography,* 15(3–4), 149–192.

Kuo Zhenming, 1965 — New material of Late Cambrian trilobite fauna from the Yehli area, Kaiping Basin, Hopei. *Acta Palaeontologica Sinica,* 13(4), 629–637, 3 pls. [In Chinese with English summary].

Kushan, B., 1973 — Stratigraphie und Trilobitenfauna der Mila-formation (Mittelkambrium-Tremadoc) in Alborz-Gebirge (N-Iran). *Palaeontographica, [A],* 144, 113–165, pls. 26-34.

Lazarenko, N.P., 1966 — Biostratigraphy and some new trilobites from the Upper Cambrian of the Olenek Uplift and Kharaulakh Mountain. *Research Work, Institute of Geology of the Arctic, Learned Papers in Palaeontology and Biostratigraphy,* 2, 33–78, 8 pls. [In Russian].

Leitch, E.C., Webby, B.D., Mills, K.J., & Kolbe, P., 1987 — Terranes of the Wonominta Block, far western New South Wales. *In* Leitch, E.C., & Scheibner, E. (editors), Terrane accretion and orogenic belts. *American Geophysical Union, Geodynamics Series,* 19, 31–37.

Lochman, C., 1938 — Upper Cambrian faunas of the Cap Mountain Formation of Texas. *Journal of Paleontology,* 12(1), 72–85.

Lochman, C., 1940 — Fauna of the basal Bonneterre Dolomite (Upper Cambrian) of southeastern Missouri. *Journal of Paleontology,* 14(1), 1–53.

Lochman, C., & Duncan, D., 1944 — Early Upper Cambrian faunas of central Montana. *Special Papers of the Geological Society of America,* 54, i–ix, 1–81.

Lochman, C., & Hu Chunghung, 1961 — Upper Cambrian faunas from the Northwest Wind River Mountains, Wyoming, Part II. *Journal of Paleontology,* 35(1), 125–146.

Lu Yanhao & Zhu Zhaoling, 1980 — Cambrian trilobites from Chuxian-Quanjiao Region, Anhui. *Memoir of the Nanjing Institute of Geology and Palaeontology,* 16, 1–30, pls. I-VI [In Chinese with English abstract].

Miller, B.M., 1936 — Cambrian trilobites from northwestern Wyoming. *Journal of Paleontology,* 10(1), 23–34.

Monke, H., 1903 — Beitrage zur Geologie von Schantung. 1: oberkambrische trilobiten von Yen-tsy-yai. *Jahrbuch der Preussischen Geologischen Landesanstalt,* 22, 103–151.

Moore, R.C. (editor), 1959 — Treatise on Invertebrate Paleontology, Part O, Arthropoda 1. *Geological Society of America and University of Kansas Press, Lawrence, Kansas.* xix + 560 pp.

Öpik, A.A., 1963 - Early Upper Cambrian fossils from Queensland. *Bureau of Mineral Resources, Australia, Bulletin,* 64, 1–133.

Öpik, A.A., 1967 — The Mindyallan fauna of Northwestern Queensland. *Bureau of Mineral Resources, Australia, Bulletin,* 74, vol. 1, 1–404; vol.2, 1–166, 67 pls.

Öpik, A.A., 1975 — Cymbric Vale fauna of New South Wales and early Cambrian biostratigraphy. *Bureau of Mineral Resources, Australia, Bulletin,* 159, 1–78.

Peng Shan-chi, 1987 — Early Late Cambrian stratigraphy and trilobite fauna of Taoyuan and Cili, Hunan. *Collection of Postgraduate Theses Nanjing Institute of Geology and Palaeontology, Academia Sinica* 1, 53–134, pls 1–13 [In Chinese with English summary].

Pogson, D.J., & Scheibner, E., 1971 — Pre-Upper Cambrian sediments east of Copper Mine Range, New South Wales. *Quarterly Notes of the Geological Survey of New South Wales,* 4, 3–10.

Poletaeva, O.K., 1960 — New genera and species of Cambrian trilobites of western Siberia. *Trudy Sibirskogo nauchnoisseldo-vatl'skogo instituta geologii geofiziki i mineral'nogo Syr'ja,* 8, 50–76, pls. i–iii [In Russian].

Powell, C. McA., Neef, G., Crane, D., Jell, P., & Percival, I.G. 1982 — Significance of Late Cambrian (Idamean) fossils in the Cupala Creek Formation, northwestern New South Wales. *Proceedings of the Linnean Society of New South Wales,* 106(2), 127–150.

Preiss, W.V., 1987 — The Adelaide Geosyncline. Late Proterozoic stratigraphy, sedimentation, palaeontology and tectonics. *Geological Survey of South Australia, Bulletin,* 53, 1–438.

Qiu Hongan, Lu Yanhao, Zhu Zhaoling, Bi Dechang, Lin Tianrui, Zhou Zhiyi, Zhang Quanzhong, Qian Yiyuan, Ju Tianyin, Han Hairen, & Wei Xiuxi, 1983 — Trilobita. *In* Paleontological Atlas of East China. Part I (Early Paleozoic Era); chiefly edited by Nanjing Institute of Geology and Mineral Resources, 28-352, pls. 11-88 *Geological Publishing House, Beijing, China.* [In Chinese].

Rasetti, F., 1961 — Dresbachian and Franconian trilobites of the Conococheague and Frederick Limestones of the central Appalachians. *Journal of Paleontology,* 35(1), 104-124.

Rasetti, F., 1965 — Upper Cambrian trilobite faunas of northeastern Tennessee. *Smithsonian Miscellaneous Collections,* 148(3), 1-127.

Raymond, P.E., 1937 — Upper Cambrian and Lower Ordovician Trilobita and Ostracoda from Vermont. *Bulletin of the Geological Society of America,* 48, 1079-1146.

Resser, C.E., 1935 — Nomenclature of some Cambrian trilobites. *Smithsonian Miscellaneous Collections,* 93(5), 1-46.

Resser, C.E., 1942 — New Upper Cambrian trilobites. *Smithsonian Miscellaneous Collections,* 103(5), 1-136, 21 pls.

Romanenko, E.V., 1977 — Cambrian trilobites from sections on the River Bolshaya Ishe (Northeast Altai). *Trudy Instituta Geologii i Geofiziki, Akademiya Nauk, Sibirskoe Otdelenie,* 313, 161-183 [In Russian].

Rose, G., 1974 — Explanatory notes on the White Cliffs 1:250 000 Geological Sheet. *Geological Survey of New South Wales, Sydney,* 1-48.

Rose, G., Louden, A.G., & O'Connell, P., 1964 — White Cliffs Sheet SH 54-12, 1:250 000 Geological Series (1st Edn.), *Geological Survey of New South Wales, Sydney.*

Rusconi, C., 1954 — Trilobitas Cambricos de la quebrada Oblicua, Sud del Cerro Aspero. *Revista Museo Historia Natural de Mendoza.* 7, 3-59.

Schrank, E., 1975 — Kambrische Trilobiten der China Kollektion v. Richthofen, 2. Die Fauna mit *Kaolishania? quadriceps* von Saimaki. *Zeitschrift für geologische Wissenschaften,* 3(5), 591-619, pls 1-8.

Shergold, J.H., 1971 — Résumé of data on the base of the Ordovician in northern and central Australia. *In* Colloque Ordovicien — Silurien, Brest, Sept. 1971. *Bureau de Recherches Géologiques et Minières, Mémoire,* 73, 391-402.

Shergold, J.H., 1986. Review of the Cambrian and Ordovician palaeontology of the Amadeus Basin, central Australia. *Bureau of Mineral Resources, Australia, Report,* 276, 1-21.

Stevens, B.P.J., 1985 — Preliminary interpretation of regional basement geology in northwestern New South Wales. *Quarterly Notes, Geological Survey of New South Wales,* 61, 9-22.

Sun, Yunchu, 1924 — Contributions to the Cambrian faunas of North China. *Palaeontologica Sinica,* B, 1(4), 1-109, pls. I-V.

Walcott, C.D., 1890 — Fauna of the Lower Cambrian or Olenellus Zone. *United States Geological Survey* (Washington), *10th Annual Report,* 1, 509-760, pl. 43-98.

Walcott, C.D., 1905 — Cambrian faunas of China. *Proceedings of the United States National Museum,* 291, 1-106.

Webby, B.D., 1978 — History of the Ordovician continental and shelf margin of Australia. *Journal of the Geological Society of Australia,* 25, 41-63.

Webby, B.D., 1983 — Lower Ordovician arthropod trace fossils from western New South Wales. *Proceedings of the Linnean Society of New South Wales,* 107, 61-76.

Webby, B.D., 1984 — Precambrian-Cambrian trace fossils from western New South Wales. *Australian Journal of Earth Sciences,* 31, 427-437.

Webby, B.D., VandenBerg A.H.M., Cooper, R.A., Banks, M.R., Burrett, C.F., Henderson, R.A., Clarkson, P.D., Hughes, C.P., Laurie, J., Stait, B., Thomson, M.R.A., & Webers, G.F., 1981 — The Ordovician System in Australia, New Zealand and Antarctica. Correlation chart and explanatory notes. *International Union of Geological Sciences, Publication,* 6, 1-64.

Webby, B.D., Wang Qizheng, & Mills, K.J., 1988 — Upper Cambrian-basal Ordovician trilobites from western New South Wales, Australia. *Palaeontology,* 31, 905-938.

Westergård, A.H., 1947 — Supplementary notes on the Upper Cambrian trilobites of Sweden. *Sveriges Geologiska, Undersökning, Ser.* C, 489, 1-34.

Xiang Liwen, Nan Runshan, Guo Zhenmin, Li Shanji, Yang Jialu, Zhou Guoqiang, Sheng Xinfu, Qian Yi, An Taixiang, Yuan Kexing & Zhang Sengui, 1981 — *Stratigraphy of China No. 4. The Cambrian System of China,* 210 pp., 12 pls. Geological Publishing House, Beijing China. [In Chinese].

Yang Jialu, 1978 — Middle and Upper Cambrian trilobites of Hunan and eastern Guizhou. *Professional Papers of Stratigraphy and Paleontology,* 4, 1-82, 13 pls. [In Chinese with English abstract].

Yin Gongzheng & Li Shanji, 1978 — Trilobites. *In* Stratigraphic and Paleontological Team of Guizhou (editors) Paleontological Atlas of Southwest China, Guizhou Volume, Part I (Cambrian-Devonian), pp. 385-395, pls. 144-192. *Geological Publishing House, Beijing.* [In Chinese].

Zhang Jinlin, 1985 — New materials of the early Gushanian trilobites in Zhuozishan district, Nei Monggol Zizhigu (Autonomous Region). *Bulletin Jianjin Institute of Geology and Mineral Resources,* 12, 111-120, 2 pls.

Zhang Jinlin & Liu Yu, 1986 — On the Cambrian trilobites in the region of Dashetai, Inner Mongolia. *Journal of Hebei College of Geology,* 9(1), 11-18, pls 1-3. [Chinese with English abstract].

Zhang Jinlin & Wang Shaoxing, 1985 — Trilobita. *In* Paleontological Atlas of North China. Vol. 1 Paleozoic, pp. 327-487. *Geological Publishing House, Beijing.* [In Chinese].

Zhang Jinlin & Wang Shaoxing, 1986 — Some Late Cambrian Kushanian trilobites from Pinglu, Shanxi. *Acta Palaeontologica Sinica,* 25(6), 663-669 [Chinese], 670 [English], pls. 1-2.

Zhang Wentang & Jell, P.A., 1987 — Cambrian trilobites of North China. Chinese Cambrian trilobites housed in the Smithsonian Institution. i-xvi + 459 pp., 125 pls, *Science Press, Beijing, China.*

Zhou Tianmei, Liu Yireng, Mong Siensung & Sun Zhenghua, 1977 — Trilobita. *In* Hubei Institute of Geological Sciences and others (editors), Paleontological Atlas of Central and Southern China. Part I (Early Palaeozoic Era), pp. 104-266, pls. 38-81. *Geological Publishing House, Beijing.* [In Chinese].

Zhu Hongyuan, 1987 — Cambrian trilobites from Xijiadian, Junxian, Hubei. *Acta Palaeontologica Sinica,* 26(1), 86-95 [Chinese with English summary], pls. 1-3.

Zhuravleva, I.T., & Rozova, A.V. (editors), 1977 — Biostratigraphy and fauna of the Upper Cambrian boundary beds (new data from asiatic regions of the USSR). *Trudy Instituta Geologii i Geofiziki, Akademiya Nauk, Sibirskoe Otdelenie,* 313, 355 pp., 31 pls. [In Russian].

BMR Journal of Australian Geology & Geophysics, 11, 119-121

DISCUSSION: The elusive Cook volcano and other submarine forearc volcanoes in the Solomon Islands

L.H.Hall[1]

A recent paper (Exon & Johnson, 1986) in this journal concluded that activity attributed in the past to the Cook submarine volcano, in the forearc region of the New Georgia Group of the Solomon Islands, was probably largely hydrothermal blowouts from a sea floor vent (or vents) 1300 m below sea level, rather than volcanic activity.

Surveys of the three research vessels *Vulcanolog*, *Machias*, and *Moana Wave* show nothing resembling a volcanic feature at the position (approximately 8°25′ S, 157°06′ E) reported by HMS *Cook* in 1963, where that ship found a shoal depth of 36 m and sulphurous fumes. I suggest that an error was made in the original report of the volcano's position, and that it might lie outside the area surveyed either by R/V *Vulcanolog* or *Machias*. (The area surveyed by R/V *Moana Wave* is not known to the writer).

I have recently examined a copy of the *Cook*'s bridge log for the night of 14/15 December 1963, when the volcanic activity was first reported. I have spoken to and corresponded with *Cook*'s Commander at the time, Commander Hunt. All quotations in this discussion are his.

There are some inaccuracies in Exon & Johnson's paper which need to be corrected, for they affect the issue of the 36 m sounding. First, a submarine sentry is not an acoustic device but a 'practical old fashioned warning device used in early survey ships until echo sounding was established as reliable'. In essence, it is an underwater kite towed behind a ship — in *Cook*'s case 'at about 35 fathoms' (65 m) — with an arming lever protruding down. When this lever strikes the bottom a catch is released, and the kite no longer tows horizontally but at a large angle to the water flow. It then rises to the surface where it causes a plume of spray, visible to a man posted on the quarterdeck for that purpose. It is improbable that a turbulent column of gas and water could have triggered the sentry, although *Cook* had difficulty preventing false alarms caused by incorrect lengths of the kite's tow slings.

Secondly, it is not true that the sailors on *Cook* were inexpert in the use of the lead line. The Commander of *Cook* was 'one of the few really experienced men in the Surveying Service', with extensive experience in its use since 1942. Although he is not certain after all these years, he thinks that he himself felt the hand lead. The lead (weighing 6.4 kg), seemed 'to be sliding down something soft, or into it', and he assessed the beginning of the slide as the shoalest sounding. He is certain that there was sand stuck to the tallow in the heel of the lead. There can be little doubt that the lead line found the bottom. It is worth recording that the Commander of *Cook* was not unfamiliar with volcanoes. His previous posting was as Oceanographer to the Hydrographer of the Royal Navy, and in that capacity he served on the Royal Society Committee on Volcanology.

The bridge log of *Cook* records that, early in the evening of 14 December (all times are local), the ship was in Blanche Channel with courses (unrecorded) as required to land a two-man geological party at Munda Bar. Between 2230 and 2240 the ship was stopped (at a position not logged) while these two men were transferred to a launch from Munda. Although Grover (Grover, 1968) wrote that the rendezvous took place half a mile off Munda Bar, it is not uncommon for the first of two vessels at a rendezvous to move towards the second vessel. There was no compelling reason for the transfer to have taken place off Munda Bar, and the principal assumption in what follows is that the transfer took place between Roviana Island and the islets to the north of Rendova Island. The bridge log recorded that the wind was between 5 and 10 knots (2.5-5 m/s) and that the waves were 0.3 to 0.6 m high. It is reasonable to assume that a launch was at sea about 15 km from Munda Bar, but about 2 km from the fringing reefs and islets south of Munda, through which it may have been possible to pass, even at night.

From 2250, *Cook* steered 240° by gyro compass or 238° True, and no further course alterations were logged before 2325, when the submarine sentry was tripped. Two hundred and forty degrees is a typical course for clearing the confined waters between New Georgia Island and Rendova Island, if the next port is via Vitiaz Strait.

Cook's speed as it left the rendezvous was not logged, although at 2300 the log recorded a mean shaft revolution rate corresponding to normal cruising speed, and this is what would be expected for a ship on passage. During 14 and 15 December, cruising speed was 11.7-12.5 knots. It is reasonable to assume that *Cook* made good an average ground speed of 12 knots in the 45 minutes between getting underway and when the sentry tripped, and so travelled about 9 nautical miles or about 17 km.

Figure 1 shows the estimated position of the 36 m sounding under the two assumptions of disembarkation point and ship's speed. This position lies just outside the area surveyed by *Vulcanolog* and *Machias*. Interpretation of the sounding traces is likely to have been made more difficult by the Vulcanolog's change of course and the underlying irregular, shoaling bathymetry. Figure 3 of Exon & Johnson indicates a water depth here of about 850 m. The circle with 1.5 km radius centred on the estimated position includes other possible locations for the volcano, given the uncertainties in rendezvous location, ship's speed and course made good.

Grover put the volcano at a bearing of 241° True, 6.7 nautical miles from Unda Point. This is not the position 8°24.9′ S, 159°06′ E that he also quotes. The location now proposed bears 241° from Kosianae Point, the southeastern extremity of Roviana Island. Another prominent radar feature, Hofovo Point (formerly known as Baniata Point), the western extremity of Rendova Island, lies 6.7 nautical miles away. It is possible that, in the confusion caused by an 'eerie and alarming... occasion', when the prime concern of the ship's Commander was to avoid grounding on what he considered to be an active volcano, the ranges and bearings of the various radar features became exchanged.

[1] Defence Scientific Establishment, Ministry of Defence, Auckland Naval Base, Auckland, New Zealand

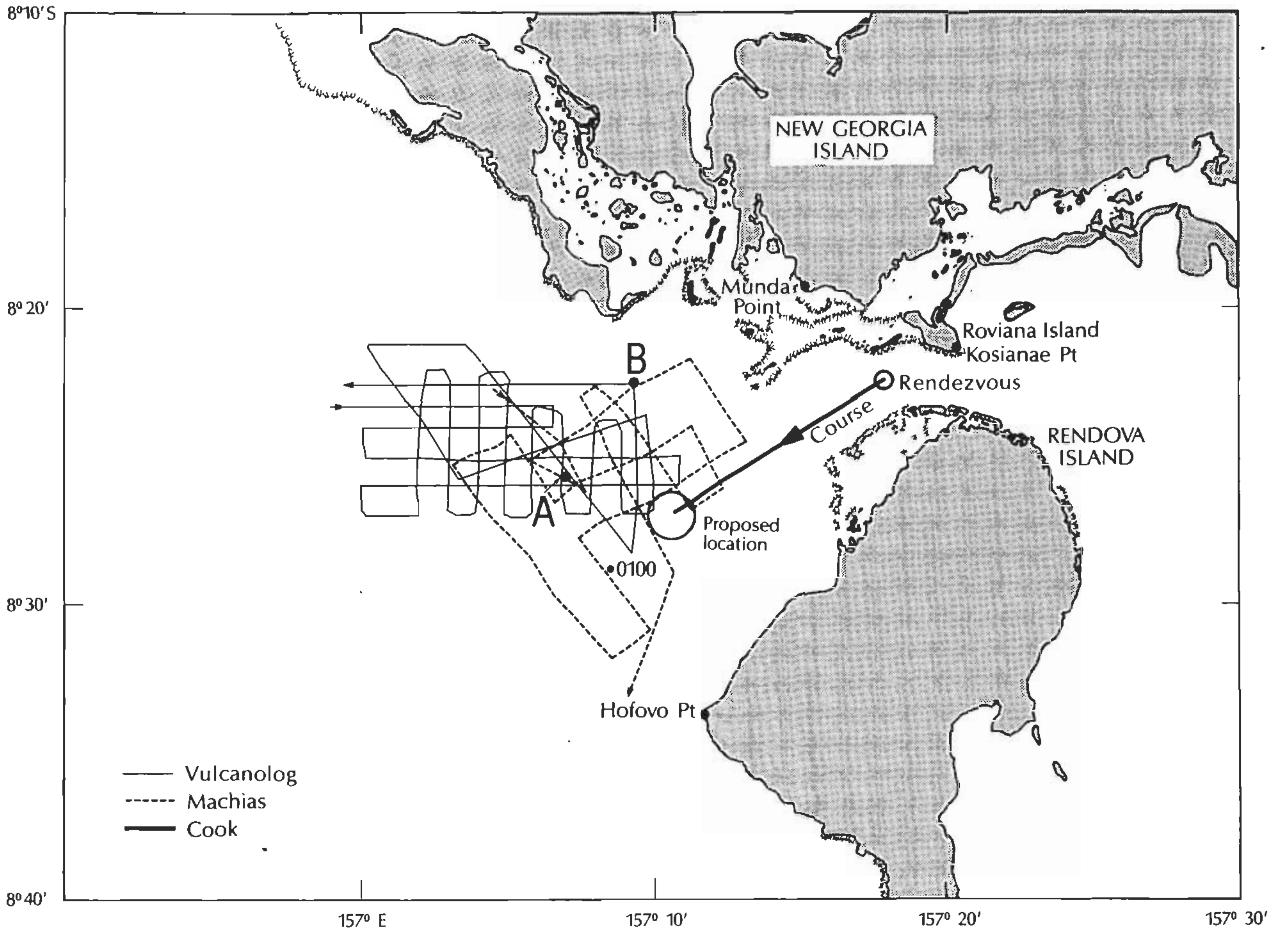

Figure 1. Tracing of Admiralty Chart 3995 showing the new estimated position of the 36 m sounding (surrounded by a circle of radius 1.5 km), *Cook's* assumed track between 2240 and 2325 (local time) and *Cook's* 0100 position (from *Cook's* bridge log).
The earlier reported position of the volcano is marked A and the position also reported by Grover (Munda Point 241°, 6.7 nautical miles) is marked B.

There is surely the need for yet another survey before the Cook submarine volcano can be confidently removed from the list of volcanoes active in recent time.

I gratefully acknowledge the cooperation of Commander (H) F.W. Hunt, MBE, RN (Retd), who was in command of HMS *Cook* in 1963. The responsibility for the inferences drawn from the available data, however, is mine.

References

Exon, N.F., & Johnson, R.W., 1986 — The elusive Cook volcano and other submarine forearc volcanoes in the Solomon Islands. *BMR Journal of Australian Geology & Geophysics*, 10(1), 77–83.

Grover, J.C., 1968 — Submarine volcanoes and oceanographic observations in the New Georgia Group, 1963–64. *British Solomon Islands Geological Record*, 3-1963-67. Report 96, 116–125.

REPLY

N.F.Exon[1] & R.W.Johnson[2]

We welcome Hall's discussion of our paper. The first point raised by Hall deals with the evidence of a shoal provided by the 'submarine sentry' used from HMS *Cook*. The sentry triggered when streamed in about 65 m of water. We are grateful for Hall's description of how the sentry operated. We accept that a mechanical device of that type, if rigged properly, probably was less likely to be triggered by a turbulent column of gas, water, and sediment than would be an acoustic device. However, we note Hall's statement that on the *Cook* there had been 'a continuing difficulty in preventing false alarms caused by incorrect lengths of the tow slings to the kites' on the sentry, which casts doubts on the general reliability of the equipment. Furthermore, we remain unclear whether triggering could have been caused by contact with a turbulent column, either by the sentry being tossed around, or by its contact with sediment or even rocks in the water column, and particularly if the sentry was rigged incorrectly as well.

The second point deals with the soundings taken with the lead line, and their meaning. The evidence presented by Hall strengthens the case that the soundings were meaningful, and that bottom really was struck. The *Cook*'s commander, unlike his crew, was experienced with the hand lead, and he believes it contacted bottom, and is certain it had sand stuck in the tallow in its heel. However, major turbulence from a deepwater hydrothermal vent conceivably could have confused the lead men (if they, rather than the commander, took the soundings) and the sand could have been carried up in a turbulent plume.

Hall's arguments about the possible location of HMS Cook on the evening of 14-15 December form a logical, but as yet unproven, basis for accepting the position of the vent that he proposes (that is, south and east of the other possible locations, A and B, and just outside the grids of the R/V *Machias* and R/V *Vulcanolog* surveys) as a possible alternative to the ones claimed by J.C. Grover. This new position is also east of the area surveyed by R/V *Kana Keoki* using the Sea-MARC II side-scan sonar system in December 1985.

If a volcano had come almost to the surface at the location suggested by Hall (about 8°27′ S, 157° 10.5′ E) and had slopes of 25° like those of Kavachi submarine volcano, it would have had a base diameter of about 3.5 km in water 800 m deep, the prevalent water depth in that general locality. A structure even of that size could conceivably have been missed by the surveys carried out. Frustratingly, the proposed position is perfectly positioned immediately outside the existing data grid! Alternatively, post-volcanic mass wasting could have removed all or most of the volcano since activity stopped in 1964. Kavachi volcano, presumably representing the sort of structure Cook volcano might be, has been above sea level seven times since 1952 (Johnson & Tuni, 1987), but has also in that period been as deep as 180 m below sea level (Okrugin, 1985). Karua volcano, in Vanuatu, is another similar volcano. It was above sea level in 1974, but there was no evidence of it near the surface in 1981 (Exon & Cronan, 1983).

We conclude that Hall is right when he says that yet another survey is needed before Cook submarine volcano can be confidently removed from the list of volcanoes active in recent times. Nevertheless, we still doubt that the current evidence for its existence as a major subsea cone in 1983 is strong. Furthermore, if the volcano existed at all, mass-wasting since 1964 may well have eroded it to a depth where it is no longer a hazard to shipping.

References

Exon, N.F., & Cronan, D.S., 1983 — Hydrothermal iron deposits and associated sediments from submarine volcanoes off Vanuatu, southwest Pacific. *Marine Geology*, 52, M43-52.

Johnson, R.W., & Tuni, D., 1987 — Kavachi, an active forearc volcano in the western Solomon Islands: reported eruptions between 1950 and 1982. *Circum-Pacific Council for Energy and Mineral Resources, Earth Science Series*, 7, 89-112.

Okrugin, V.M., 1985 — Information note on the results of the 7th cruise of the R/V *Vulcanolog* in the vicinity of the *Solomon Islands. Solomon Islands Geological Division File Report* (unpublished).

[1]Division of Marine Geosciences & Petroleum Geology, Bureau of Mineral Resources, GPO Box 378, Canberra, ACT 2601

[2]Division of Petrology & Geochemistry, Bureau of Mineral Resources, GPO Box 378, Canberra, ACT 2601

BMR Journal of Australian Geology & Geophysics, 11, 123-125

DISCUSSION: Major geomorphic features of the Kosciusko–Bega region

G. Taylor[1], I.McQueen[1], & M.C. Brown[1]

Ollier & Taylor (1988) are correct when they write that the Kosciusko–Bega region has long been of interest to geomorphologists. They also point out that there has been debate over its geomorphic evolution since the early 1900s and, after reviewing some of this, develop a hypothesis of landscape evolution for the area. We wish to examine the data underlying their hypothesis, and comment on other aspects of their paper.

The geomorphic arguments of Ollier & Taylor suppose (1) that the pre-basaltic drainage of the Monaro was to the north, and (2) that the basalts derive from a single large shield volcano centred on Brown Mountain. There is little evidence for either idea.

We know of no data which show that the major pre-basaltic drainage of the Monaro was northwards. Taylor & others (1985) showed that the pre-basaltic drainage north of the present Great Divide between Berridale and Nimmitabel was to the north. They also argued, however, that the divide has not shifted since the early Eocene, because they could show southwards drainage into Wullwye Creek then. No published data confirm pre-basaltic drainage directions further south. Ollier & Taylor's evidence for north-flowing pre-basaltic rivers is that, south of their postulated shield volcano, the present drainage is northwards. Veitch (1986) showed palaeodrainage on the highlands above the Towamba River to the southeast, in line with the present Towamba valley. We suggest that the palaeo-Towamba was a major drainage outlet for the southern Monaro, because here the basalts are at their lowest elevation. Recent field mapping of the Bombala 1:100 000 sheet area, by staff and students of the Geology group at the Canberra College of Advanced Education, has revealed palaeocurrent directions in pre-basaltic sediments, which show palaeoslopes to the north, west, west-northwest and south.

The only evidence in Ollier & Taylor for the existence of a large shield volcano, their 'Monaro volcano', is a radial drainage pattern around Brown Mountain. While we recognise the radial pattern, it might have other causes. Brown Mountain has a basalt capping and is the highest point on the escarpment in the region. It is not surprising that some streams drain off this feature. Most of the major drainage around Brown Mountain is in basement rock, and drainage to the north and south largely follows a north–south structural grain. Drainage to the east runs generally east, off the existing escarpment and mostly through massive granites. It is also partly controlled by northwest-trending fracture zones in the basement. To the west, drainage is west, mostly off basalts on the broad, west-sloping Monaro plateau. Ollier & Taylor argue that the drainage might be superimposed, but any earlier drainage pattern would need to be inherited through a considerable amount of basement erosion (>750 m, east of the escarpment). It should also be noted that, in the northwestern part of the Monaro, there is a major drainage system which does not conform to a radial pattern related to Brown Mountain (e.g. Wullwye, Cooma Back, Slack's and Bridle Creeks).

[1]Geology, School of Applied Science, Canberra College of Advanced Education, PO Box 1, Belconnen, ACT 2616

Field observations at Brown Mountain show a sequence (<240 m thick) of horizontal basalt flows. This thin sequence of flows is inconsistent with nearness to the centre of a shield volcano 80–100 km wide (by Ollier & Taylor's reckoning). At the trig station there is a small area (150 m across) of basalt containing crustal xenoliths which might be part of a small volcanic plug, like the many others we have found across the southern Monaro. There is certainly no surface evidence for a major volcanic plug or central intrusive complex which is usually developed in large shield volcanoes, such as Tweed Volcano, Barrington, and others, (Wellman, 1986), and Mt Dromedary (Eggleton, 1987). No significant magnetic or gravity anomalies suggest a hidden feeder or central complex in the area (Department of National Development, 1978; Bureau of Mineral Resources, 1976).

In contrast with this lack of evidence for a large shield volcano, there is good field evidence that the Monaro basalts erupted from many vents over a wide area of the southern Monaro (Brown & others, 1988). We have located 23 plugs and eruption points, scattered basaltic tuffs and a maar structure (Fig. 1). Evidence for flow directions, including

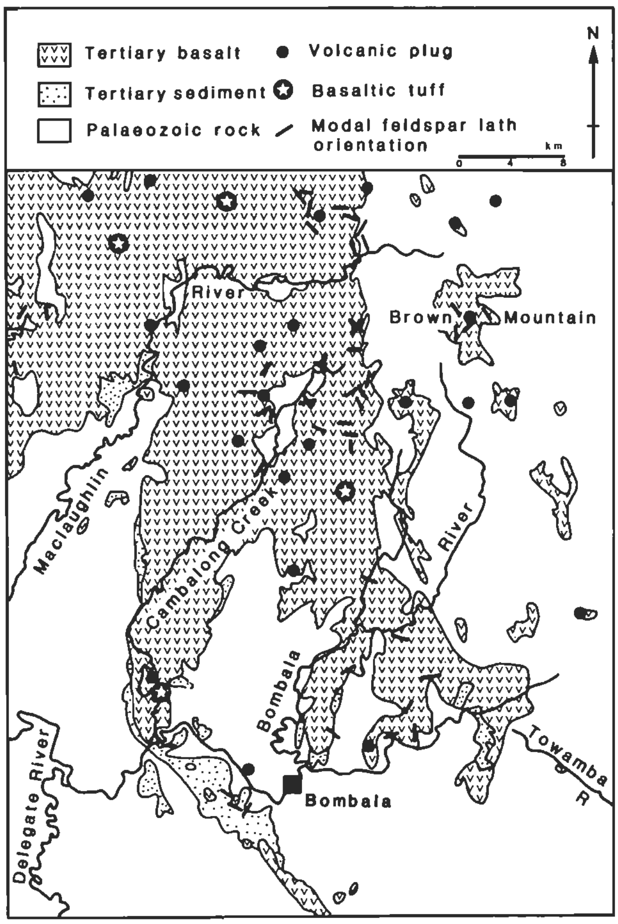

Figure 1. Distribution of early Tertiary sediments and basalt, volcanic plugs and/or eruption centres for the basalt field, basaltic tuffs, and modal feldspar lath orientations in the Bombala 1:100 000 sheet area.

Lath orientations measured from oriented thin sections of the basalts.

plagioclase lath orientations, directions of vesicle alignment and palaeoslope information, is consistent with basalt eruption from many vents into predominently north-south trending major valley systems. We therefore believe that the Monaro basalts are the remnants of a lava field rather than a shield volcano (see also Wellman & McDougall, 1974), and we propose the term Monaro Lava Field to describe more accurately the volcanic province.

Since there is no unequivocal evidence for the former existence of a large shield volcano, and even less evidence for its shape and extent, it is hard to see how Ollier & Taylor can claim that about half of it has been eroded away. If the 'Monaro volcano' did not exist as a circular or sub-circular pile, then Ollier & Taylor's arguments on the age of uplift and hence the Great Escarpment are not supported. Their argument that most of the uplift (and the escarpment) post-dates 50 Ma is based on removal of the eastern part of the hypothetical volcano and their view that the present regional relief is much greater than that of the pre-basalt surface (about 10 times, on their Fig. 3). Near the Towamba River, the pre-basaltic relief was at least 400 m and perhaps as much as 800 m (Veitch, 1986), which is half to all the present relief. In other areas of the Monaro, the sub-basaltic relief is up to 300 m. Some palaeovalleys are deeply incised, and have very steep sides (from 50° to near vertical). Such relief suggests substantial enough pre-basaltic uplift for the development of an escarpment.

In arguing against an early Tertiary escarpment, Ollier & Taylor draw an analogy with an area near Innisfail, where basalt 2 Ma old drapes the escarpment, showing that the scarp was there before 2 Ma ago. They then claim that, because this situation cannot be found on the Monaro, a scarp did not exist 'near' its present position before basalt eruption. Since the basalts of the Monaro date from the Paleocene, and have been subjected to at least 30 Ma of erosion, we suggest that the analogy with Innisfail is inappropriate and misleading.

Some major geomorphic features in the Kosciusko-Bega region have not been covered by Ollier & Taylor. Notable among these is Mt Dromedary, a large mid-Cretaceous volcano (Eggleton, 1987; Smith & others, 1988), which must have been a significant geomorphic feature during the late Mesozoic and probably also the early Tertiary. Remnants of its volcanic pile crop out near sea level, suggesting that it erupted east of any existing escarpment and/or highlands, or that the base of the volcano has subsided (relative to the highlands) since the Late Mesozoic.

We also point out the following errors and/or drafting mistakes in the paper of Ollier & Taylor. The average elevation of the Monaro is about 850 m, and not 2000 m as they state. On Ollier & Taylor's Figure 2, the Bago Plateau has been labelled the Bega Plateau and the Coolumbooka River the Bombala River. Their Figure 5 shows the lower Murrumbidgee River draining south, implying that Lake Bunyan was the centre of an internal drainage system. This was never implied by Taylor & Walker (1986).

Much work is needed to resolve the geomorphic history of the Kosciusko-Bega region. We make a strong plea for more detailed field studies, rather than the erection of hypothetical models based on inadequate or erroneous data.

References

Brown, M.C., Clarke, I., McQueen, K.G., & Taylor, G., 1988 — Early Tertiary volcanism in the southern Monaro region, New South Wales. *Ninth Australian Geological Convention, Abstracts, Geological Society of Australia*, 21, 70-71.

Bureau of Mineral Resources, 1976 — Bega 1:250 000 Bouguer Anomaly Map. File No. J55/B2-4. *Bureau of Mineral Resources, Australia.*

Department of National Development, 1978 — Bega 1:250 000 Total Magnetic Intensity Map. File No. J55/B1-55.

Eggleton, T., 1987 — Mt Dromedary, the Golden Volcano. A field guide to the geology of the Tilba region, N.S.W. *Geology Department, Australian National University, Canberra.*

Ollier, C.D., & Taylor, D., 1988 — Major geomorphic features of the Kosciusko-Bega region. *BMR Journal of Australian Geology & Geophysics*, 10, 357-362.

Smith, I.E.M., White, A.J.R., Chappell, B.W., & Eggleton, R.A., 1988 — Fractionation in a zoned monzonite pluton: Mount Dromedary, southeastern Australia. *Geological Magazine*, 125, 273-284.

Taylor, G., Taylor, G.R., Bink, M., Foudoulis, C., Gordon, I., Hedstrom, J., Minello, J., & Whippy, F., 1985 — Pre-basaltic topography of the Northern Monaro and its implications. *Australian Journal of Earth Sciences*, 32, 65-71.

Taylor, G., & Walker, P.H., 1986 — Tertiary Lake Bunyan, Northern Monaro, NSW, Part 1: geological setting and landscape history. *Australian Journal of Earth Sciences*, 33, 219-229.

Veitch, S. M., 1986 — Landscape evolution of the Cathcart area, NSW. *Grad. Dip. Sci. thesis (unpublished), Australian National University, Canberra.*

Wellman, P., 1986 — Intrusions beneath large intraplate volcanoes. *Exploration Geophysics*, 17, 135-139.

Wellman, P., & McDougall, I., 1974 — Cainozoic igneous activity in Eastern Australia. *Tectonophysics*, 23, 49-65.

REPLY

C.D. Ollier[1] & D. Taylor[2]

Taylor & others correctly state that we envisage a large volcano, centred on Brown Mountain.

They mistakenly conclude that the presence of many eruption points shows that there was no major volcano with radial drainage. In fact, many large volcanoes with radial drainage have numerous parasitic cones on their flanks. Well known examples are Mt Etna (Romano, 1982), shown in Figure 1, and Tristan da Cunha (Baker & others, 1964; Ollier, 1988, fig. 3.0).

In analysing drainage patterns around volcanoes one looks for radial drainage on the volcano, pre-volcanic drainage lines and their possible continuations, and drainage flowing around the volcano or otherwise diverted. All these we have described from the postulated Monaro Volcano. Radial drainage is a major indicator of volcanic drainage, even when much of the original volcano has been removed. This is described, with examples from New South Wales, by Ollier (1985). A particularly fine example is that of the Ebor Volcano (Ollier, 1982), where about half the original volcano has been destroyed by erosion. The radial drainage, however, is reserved, even though the valleys are now superimposed on underlying bedrock with structural directions different from the drainage lines.Napak Volcano in Uganda retains a radial drainage pattern even though only an estimated 3% of the original volcano is preserved (King, 1949).

Interpretation of buried and diverted drainage may be illustrated by using the modern Mt Etna as an analogue (Fig. 1). Pre-volcanic rivers there flowed southeast, but after being blocked by the volcano, the drainage is now via the River Alcantara in the north and the River Simeto in the south. Details of the blocking and the interaction of fluvial and volcanic features over the past 300 000 years are given by Chester & Duncan (1932). Our interpretation of the original northerly direction of rivers in the Monaro region is not based on Taylor & others (1985), but on an analysis by D. Taylor of Cretaceous drainage of this and a larger region. A map of this drainage will be published in Ollier and Wyborn (in press).

The evidence of Veitch is a matter of detail. In the case of Mt Etna, some younger lava flows occupy valleys formed long after the original valleys were buried, and follow prior courses of the Alcantara and Simeto rivers (Fig. 1), but they do not affect the large scale interpretation of earlier events.

Detailed mapping of the whole Monaro area will eventually lead to a fuller understanding of the landscape history of the region, but the few points of detail provided by Taylor & others do not persuade us that our general view is incorrect.

[1]Department of Geography, University of New England, Armidale, NSW 2351

[2]C.R.A. Exploration Pty Ltd, 826 Whitehorse Rd, Box Hill, Victoria 3128

References

Baker, P.E., Gass, T.G., Harris, P.G. & Le Maitre, R.W., 1964 — The volcanological report of the Royal Society expedition to Tristan da Cunha, 1962. *Philosophical Transactions of the Royal Society of London, Series* A No. 1073, 439–578.

Chester, D.K., & Duncan, A.M., 1982 — The interaction of volcanic activity in Quaternary times upon the evolution of the Alcantara and Simeto Rivers, Mount Etna, Sicily. *Catena*, 9, 319–42.

King, B.C., 1949 — The Napak area of southern Karamoja, Uganda. *Memoirs of the Geological Survey of Uganda*, 5.

Ollier, C.D., 1982 — Geomorphology and tectonics of the Dorrigo Plateau, New South Wales. *Journal of the Geological Society of Australia*, 29, 431–435.

Ollier, C.D., 1985 — Geomorphology and volcanism in Eastern Australia. *In* Sutherland, F.I., Franklin, B.J., & Waltho, A.E. (editors), Volcanism in Eastern Australia. *Geological Society of Australia, New South Wales Division, Publication* No. 1, 1–12.

Ollier, C.D., 1988 — Volcanoes. *Basil Blackwell, Oxford.*

Ollier, C.D., & Wyborn, D., in press — Geology of Alpine Australia. *In* R. Good (editor), The Scientific Significance of the Australian Alps. Chapter V. *Australian Alps Liaison Committee and Australian Academy of Science*, Canberra.

Romano, R. (editor), 1982 — Mount Etna Volcano. *Memoria Della Societa Geologica Italiana*, 23.

Taylor, G., Taylor, G.R., Bink, M., Foudoulis, C., Gordon, I., Hedstrom, J., Minelo, J., & Whippy, F., 1905 — Pre-basaltic topography of the Northern Monaro and its implications. *Australian Journal of Earth Sciences*, 32, 65–71.

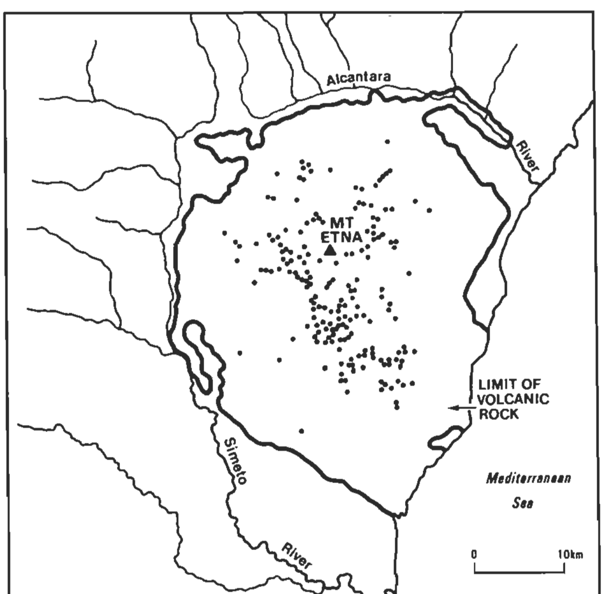

Figure 1. Drainage diversion around Mt Etna, Sicily, and the distribution of points of eruption.